HYDRATION OF PORTLAND CEMENT MODIFIED BY CARBON NANOTUBES/SURFACTANT DISPERSIONS

Oscar Aurelio Mendoza Reales

Tese de Doutorado apresentada ao Programa de Pós-graduação em Engenharia Civil, COPPE, da Universidade Federal do Rio de Janeiro, como parte dos requisitos necessários à obtenção do título de Doutor em Engenharia Civil.

Orientador: Romildo Dias Toledo Filho

Rio de Janeiro
Setembro de 2017

HYDRATION OF PORTLAND CEMENT MODIFIED BY CARBON NANOTUBES/SURFACTANT DISPERSIONS

Oscar Aurelio Mendoza Reales

TESE SUBMETIDA AO CORPO DOCENTE DO INSTITUTO ALBERTO LUIZ COIMBRA DE PÓS-GRADUAÇÃO E PESQUISA DE ENGENHARIA (COPPE) DA UNIVERSIDADE FEDERAL DO RIO DE JANEIRO COMO PARTE DOS REQUISITOS NECESSÁRIOS PARA A OBTENÇÃO DO GRAU DE DOUTOR EM CIÊNCIAS EM ENGENHARIA CIVIL

Examinada por:

_____
Prof. Romildo Dias Toledo Filho, D.Sc.

_____
Prof. Jordi Payá Bernabeu, Ph.D.

_____
Prof. Jorge Iván Tobón, Ph.D.

_____
Prof. Eduardo de Moraes Rego Fairbairn, Dr.Ing.

_____
Dr. Emilio Cesar Melo da Silva, Ph.D.

RIO DE JANEIRO, RJ - BRASIL
SETEMBRO DE 2017

Reales, Oscar Aurelio Mendoza

Hydration of Portland cement modified by carbon nanotubes/surfactant dispersions / Oscar Aurelio Mendoza Reales. – Rio de Janeiro: UFRJ/COPPE, 2017.

XIX, 226 p.: il.; 29,7 cm.

Orientador: Romildo Dias Toledo Filho

Tese (doutorado) – UFRJ/ COPPE/ Programa de Engenharia Civil, 2017.

Referências Bibliográficas: p. 209-226.

1. Cement hydration. 2. Carbon nanotubes. 3. Surfactants. I. Toledo Filho, Romildo Dias. II. Universidade Federal do Rio de Janeiro, COPPE, Programa de Engenharia Civil. III. Titulo

To my loving family

AGKNOLEDGEMENTS

I would like to express my gratitude to all the persons and institutions involved in the successful development of this work, especially to professor Romildo Dias Toledo Filho for welcoming me at the "Núcleo de Tecnologias e Materiais Sustentáveis" (NUMATS) and giving invaluable advice and orientation. I would like to thank also the "Conselho Nacional de Desenvolvimento Científico e Tecnológico" (CNPq) and Hallliburton for providing financial support, and the "Instituto Nacional de Metrologia, Calidad y Tecnología" (INMETRO), "Nucleo de Catalise" (NUCAT), "Instituto de Macromolécuas" (IMA), "Centro de Pesquisas da Petrobras" (CENPES), Universidad de Medellín and Universidad Nacional de Colombia for providing technical support and access to their facilities.

To my parents Oscar and Marlene, whose lifetime effort and example allowed me become who I am today. To my friends Carlos, Katlin and Manuel, who encouraged me all this time from the distance. To my friends Esoly, Emanuel, Sandra, Francisco, Barbara, Karyne, Javier, Aline, Nina and Emilio, whose kind support was invaluable during these years in Brazil. To my students Pedro, Clarice, Carol, Carmen, Caterin and Brayhner, and professors Yhan Paul Arias and Jorge Hernan Quintero, whose hard work and constant curiosity allowed this work to be successfully completed. To professors Sergio Camargo de Souza and Eduardo Fairbairn, who were the first to open the doors of UFRJ for me.

Thank you

Resumo da Tese apresentada à COPPE/UFRJ como parte dos requisitos necessários para a obtenção do grau de Doutor em Ciências (D.Sc.)

HIDRATAÇÃO DO CIMENTO PORTLAND MODIFICADA POR DISPERSÕES DE NANOTUBOS DE CARBONO/SURFACTANTE

Oscar Aurelio Mendoza Reales

Setembro/2017

Orientador: Romildo Dias Toledo Filho

Programa: Engenharia Civil

Este trabalho apresenta um estudo abrangente sobre a influência dos nanotubos de carbono de parede múltipla (MWCNT) no desempenho de matrizes a base de cimento, usando surfactantes como agentes dispersantes para os MWCNT. Uma campanha experimental de duas fases foi desenvolvida para avaliar o efeito de dispersões de MWCNT/surfactante disponíveis comercialmente e as preparadas no laboratório, nas propriedades mineralógicas, reológicas, microestruturais e mecânicas de pastas de cimento. A primeira fase focou-se em entender os efeitos globais nas propriedades da pasta de cimento da dispersão de MWCT/surfactante disponível comercialmente. Um processo de mistura de dois passos foi proposto para mitigar os efeitos negativos do surfactante por meio da adição de uma área superficial adicional. A segunda fase focou-se em desacoplar os efeitos individuais nas propriedades da pasta de cimento do surfactante e dos MWCNT, buscando identificar o efeito neto dos MWCNT. De forma global foi concluído que a interação surfactante/cimento é prejudicial para o desempenho compósito, mascarando os efeitos positivos da incorporação dos MWCNT. Não obstante, os mecanismos pelos quais os nanotubos modificam o comportamento reológico e mecânico da matriz foram claramente identificados.

Abstract of Thesis presented to COPPE/UFRJ as a partial fulfillment of the requirements for the degree of Doctor of Science (D.Sc.)

HYDRATION OF PORTLAND CEMENT MODIFIED BY CARBON NANOTUBES/SURFACTANT DISPERSIONS

Oscar Aurelio Mendoza Reales

September/2017

Advisor: Romildo Dias Toledo Filho

Department: Civil Engineering

This work presents a comprehensive study of the influence of multi walled carbon nanotubes (MWCNT) on the performance of cement based matrices, using surfactants as a chemical dispersing aid for nanotubes. A two phase experimental campaign was carried out to measure the effect of commercially available and in-house prepared MWCNT/surfactant aqueous dispersions on the mineralogical, rheological microstructural and mechanical properties of cement paste. The first phase focused on understanding the global effects on cement paste of a commercially available MWCNT/surfactant dispersion. A two-step mixing process was proposed in this phase to mitigate the negative effects of surfactants by introducing an additional free surface area in the paste. The second phase focused on decoupling the individual effects of surfactants and MWCNT on the properties of cement paste, aiming to identify the net effect of MWCNT. Overall, it was concluded that the surfactant/cement interaction was detrimental for the performance of the composite, masking the positive effects of MWCNT; nevertheless, the mechanisms by which nanotubes modify the rheological and mechanical behavior of the matrix were clearly identified.

CONTENTS

LIST OF FIGURES

LIST OF TABLES

1. Introduction

The challenge of writing in the smallest scale possible, using lines one atom thick, was first presented by Richard Feynman more than fifty years ago [1]. This challenge made evident a series of technological limitations that had to be surpassed in order to miniaturize the writing process and manipulate atoms, giving a kick start to a new field in science. But it was not until fifteen years later that the term nanotechnology was used for the first time to make reference to the processing of materials atom by atom [2], taking advantage of the fact that the properties of the materials change at the nanoscale due to surface area and quantum effects.

The nanoscale is in within units and tens of billionths of meters (10^{-9}m). Particles within this range of size can be considered nanoparticles and have a very interesting set of properties that their homologous microparticles, with the same chemical composition and mineralogical structure, do not have. The specific surface area of nanoparticles is extremely high when compared to microparticles, causing that a high fraction of their atoms is located on their surface, giving them a very high chemical reactivity [3]. There are two approaches to produce nanoparticles, top-down and bottom-up. The top-down approach takes a bulk material in the macro or micro scale, and by mechanical processes reduces its size to the nanoscale. The bottom-up approach uses chemical or physicochemical processes to assembly atoms and molecules to build nanoparticles [4]. Top-down methods usually require high amounts of energy to obtain nanoparticles, and parameters such as the shape of the particles are not controllable. Bottom-up methods are able to control not only size but also shape and structural organization of the nanoparticles, being the most used methodology to produce nanoparticles both in laboratory as in industrial scale.

Given the exceptional chemical and physical properties of nanoparticles, they became natural candidates to produce the next generation of construction materials, less polluting and with high chemical and mechanical performance and novel electromagnetic properties [5]. The particle size versus the specific surface area of the components of different generations of concretes is presented in Figure 1-1. In the figure it can be seen how from conventional concrete, passing through high-performance concrete and to nano-engineered concrete there is a clear evolution towards components with smaller particle size and higher specific surface area.

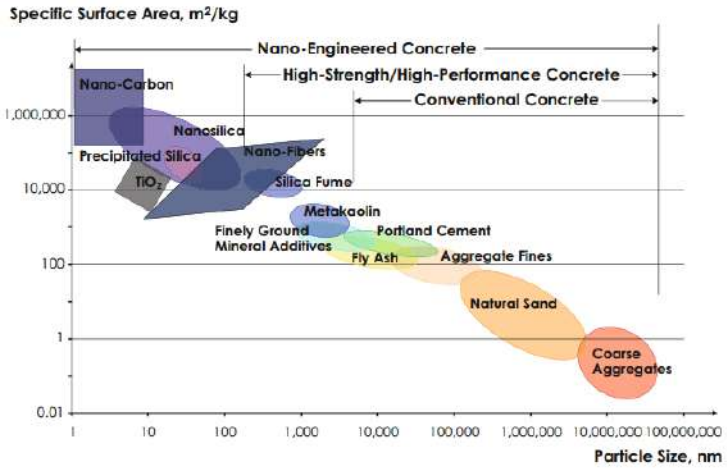

Figure 1.1. Particle size and specific surface area related to concrete materials [6]

Some of the challenges that the construction industry faces today that can be addressed using nanotechnology are: decreasing the emissions associated with the fabrication and usage of concrete, decreasing the amount of energy used to control the temperature of indoor spaces, optimizing the soil usage by vertical construction in densely populated urban areas, producing slender structural elements to optimize usage of space, and decreasing the use of non-renewable natural resources and produce smart construction materials. In this last aspect nanoparticles have shown the best promise by generating cement based composites with novel properties such as self-sensing, self-cleaning, decontaminating, bactericide, sub micrometric crack propagation control and electromagnetic shielding.

The most commonly used nanoparticles in cement based composites are nanosilica [7], nanoalumina [8], nano-Fe_2O_3 [9], nanoclay [10], carbon nanotubes [11], carbon nanofibers [12], graphene [13], nano-TiO2 [14] and nanocellulose [15]. Each one of these nanoparticles has a different effect on the properties of the cement matrix and different mechanisms by which those properties are modified. Some of those mechanisms are nucleation or seeding effect, pozzolanic activity, filler effect, nano-reinforcement, submicrometric crack control, photo catalysis and piezoresistivity.

Nucleation or seeding effect is as consequence of the size and surface area of the nanoparticles, and depends on the calcium concentration and temperature [16]. Cement hydration is a nucleation reaction, where hydrates are nucleated around a nucleation site to later precipitate [17]. Nanoparticles include additional nucleation sites into the system in a highly efficient manner, due to their high surface area. This accelerates the hydration kinetics, and depending on the chemical affinity of the nanoparticles with the

hydration reaction, might increase the amount of hydration product precipitated during the first hours.

Pozzolanic activity is a widely studied reaction between the $Ca(OH)_2$ produced during the formation of calcium silicate hydrate (C-S-H) and amorphous material rich in SiO_2 or Al_2O_3. Nanoparticles with pozzolanic activity such as nanosilica [18] are very efficient pozzolans since their high surface area gives them a high chemical reactivity, and at the same time work as nucleation points, accelerating the hydration reaction and generating extra C-S-H at early ages, which increases the compressive strength of the matrix [19].

Nanoparticles are also able to work as fillers of the mesopores, refining the pore structure of the matrix and increasing its durability. Clay nanoparticles have been found to have such filler effect in the pores; additionally, their double layered structure is capable of retaining water and modifying the mobility regime of water inside the matrix [20]. Additionally nucleation effects are also found due to their size and surface area.

Nanoreinforcement and submicrometric crack control are properties of nanofibers and nanotubes. Traditional fibers in the scale of millimeters and micrometers are able to reinforce and control crack propagation at their own scale, and have been found to be ineffective to control the propagation of cracks of submicrometric width [21]. Due to their diameter in the scale of nanometers and length in the scale of micrometers, i.e. very high aspect ratio, nanotubes and nanofibers are able to work as bridges for load through the cracks, enhancing the load distribution and controlling their propagation [22].

Photocatalysis is a property of nano TiO_2 among others, which when excited by light of the appropriate wavelength produce reactive oxygen species that convert organic pollutants into CO_2 and water, resulting in the cleaning of the surface containing the nanoparticles [14]. This self-cleaning effect can be used in concrete exposed to direct sunlight and rain to produce self-cleaning facades that require minimum maintenance. White concrete takes de most benefit from this photocatalytic effect, since the durability of the color becomes widely enhanced.

Piezoresistivity completes the set of effects that nanoparticles can have over the properties of cement matrixes. Cement paste is electrically conductive by nature, and its resistivity is increased slightly by the addition of silica fume or latex [23]. This electrical conductivity can be enhanced with an electrical conductive admixture such as carbon or metallic fibers that touch each other to form a conductive path [24]. In this

case the electrical conductivity of the composite is governed by the intrinsic resistivity of the conductive phase and the contacting conduction between fibers. This resistivity is sensitive to load, decreasing proportionally to the increase of load in the matrix; therefore, a correlation between deformation and electrical resistivity can be obtained, generating a composite with self-sensing capabilities.

Nanotechnology is currently emerging from fundamental research to the industrial floor; thus, its full-scale applications are currently very limited. However, the tremendous potential for nanotechnology to improve the performance of conventional materials and processes is extremely promising [6]. Some of real scale applications that can already be found in the world are for example the facade of the Dives in Misericordia church in Rome, which was built using photocatalytic white concrete supplied. The photocatalytic effect was obtained with nano-TiO_2 particles. Another application that is being built in several locations around the world is strips of self-sensing rigid pavement to control speed, weight and flow of vehicles through highways.

Vast progress in construction materials, especially concrete, is expected in coming years by the adaptation of new knowledge generated from the rapidly growing field of nanotechnology [6]. For this to happen is necessary to advance furthermore in the knowledge of the mechanisms of interaction between the nanoparticles and the cement matrix, both in fresh and hardened state.

This work is focused on the effects of blending multi walled carbon nanotubes (MWCNT) in cement based matrices. First, a comprehensive literature review on nanotube-cement composites is presented (chapter 2), followed by a state of the art on the characterization techniques currently used to measure the effects of MWCNT on chemical, mineralogical, rheological and mechanical properties of cement based matrices (chapter 3). This literature revision serves as a motivation for the development of a research problem and a methodology (chapter 4) to approach the study of the effect of MWCNT/surfactant aqueous dispersions on the properties of cement paste. The experimental campaign was divided in two phases, one using commercially available MWCNT/surfactant dispersions (chapters 5 to 9), and one using in-house prepared MWCNT/surfactant dispersions (chapters 10 to 12). The first phase focused on understanding the global effect of a commercial MWCNT/surfactant dispersion, while the second phase developed a process to obtain dispersions and decouple the individual effects of surfactants and MWCNT on the properties of cement paste. Finally, a

summary and conclusions (chapter 13) finalizes the work with a holistic view of the problem and future research perspectives.

Each chapter was built as a self-contained document, following a typical paper structure; nevertheless, they all revolve around the MWCNT/surfactants main topic, and follow a conducting line which is presented in the methodology section. Citations are presented using a continuous numeration throughout the document and a full bibliography is presented at the end of the document (chapter 14).

2. Literature Review

Nanotube-Cement Composites

Abstract

This chapter presents a comprehensive review of the properties of carbon nanotubes (CNT)/cement composites. A general picture of the advances in the manipulation of cement matrixes in the scale of the nanometers is provided, discussing the role of CNT in the development of a new generation of construction materials with superior performance. The review covers all the modifications induced by the CNT in the properties of the cementitious matrix, and how these modifications affect the performance of the composite in both fresh and hardened state, and at the nano, micro and macro scales.

Special interest is given to the dispersion of the CNT in the matrix and how it affects the effectiveness of the nanoparticle and the final properties of the composite. Interactions of CNT with other nano- and micro- particles such as nanosilica, metakaolin and fly ash are also presented.

2.1 Introduction

Nanotechnology is not usually associated with the cement and construction industries, but today more than ever there is a growing interest in a next generation construction materials, and nanotechnology has shown a great potential to deliver them. Two factors have influenced the growth of interest of these industries in the use of nanomaterials; first the industrial scale production of nanoparticles, which has lowered considerably their cost, and second the growing body of knowledge about the properties of hydrated cement matrixes at the nanoscale, which has helped to understand how to nano-engineer construction materials with improved properties, lower cost and lower polluting emissions associated.

It has been recognized that different nanoparticles can improve the properties of hydrated cement matrixes, whether it is due to their chemical affinity and high reactivity with cement, or to their exceptional mechanical properties. Additionally, some of these nanoparticles also have electromagnetic, photocatalitic, bactericide, hydrophilic or hydrophobic properties among others; these properties can be exploited to develop smart construction materials with decontaminating, self-healing, self-cleaning and self-

sensing capabilities. Within this group of nanoparticles, a special interest has been given to the carbon nanotubes (CNT). Their mechanical properties and high aspect ratio put them as a potential nano-reinforcement to generate cement composites with high flexural strength, capable of crack propagation control and increased strain; also, their electromagnetic properties can be used to generate composites with novel properties such as self-sensing and electromagnetic shielding.

Several challenges have to be addressed in order to obtain cement/CNT composites suitable for a mass production process that guarantees repeatable properties and homogeneous performance. Effective dispersion and surface interactions of the CNT within the hydrated cement matrix stand out as the key issues. Different chemical treatments and dispersion mechanisms have been studied to maximize the effect of the CNT on the properties of cement composites, but in most of the cases it has been found that they are too aggressive for the integrity of the nanotubes, and additionally the final result is sensitive to the alkaline environment generated by the hydration of cement, causing reagglomeration of the previously dispersed particles.

This chapter presents a comprehensive review of the properties of CNT/cement composites. A general picture of the advances in the manipulation of cement matrixes in the scale of the nanometers is provided, discussing the role of CNT in the development of a new generation of construction materials with superior performance. The review covers all the modifications induced by the CNT in the properties of the cementitious matrix, and how these modifications affect the performance of the composite in both fresh and hardened state. First a general overview of the properties of the cement matrixes at the nanoscale is presented, then it is discussed how the CNT can modify these properties, and how the dispersion and surface interaction issues are related to these modifications. Combinations of CNT with other nano and micro particles such as nanosilica, metakaolin and fly ash in cement matrixes are also presented. Finally, novel electromagnetic properties conferred to the cement matrix by the CNT are presented.

2.2 Nanostructures of the hydrated cement

Calcium-Silicate-Hidrate (C-S-H) is the main hydration product of Portland cement, comprising approximately 50% to 60% of the total volume of product [25], and also responsible for the cohesion and mechanical response of the hydrated matrix at the micro and macro scale. Transmission Electronic Microscopy images [26],

crystallographic models [27], molecular simulations [28], nuclear magnetic resonance spectra [29] and nanomechanical results [30] all agree in the fact that C-S-H can be considered of nanometric nature with a short range crystalline structure. Therefore, hydrated cement can be considered a naturally nanostructured material, and the nanoscale considered as the most adequate scale to induce modifications that enhance its performance, and consequently the performance of the whole matrix.

Portland cement is composed of calcium silicates, calcium aluminates and calcium ferroaluminates, which are formed by solid solution reactions during the burning of SiO_2, CaO, Al_2O_3 and Fe_2O_3 approximately at 1450°C; these silicates are rapidly cooled down to ambient temperature to maintain its crystalline structures, and then grounded together with gypsum and some inert material that act as filler, such as $CaCO_3$ or $CaMg(CO_3)_2$ [31]. Of all of these components, only the calcium silicates alite (Ca_3SiO_5) and belite (Ca_2SiO_4), which are approximately 75% of the mass of cement, form C-S-H and $Ca(OH)_2$ in presence of water. The reactions are as follows:

$$Ca_3SiO_5 + (1.3 + x)H_2O \rightarrow (CaO)_{1.7}SiO(H_2O)_x + 1.3Ca(OH)_2 \qquad (2.1)$$

$$Ca_2SiO_4 + (0.3 + x)H_2O \rightarrow (CaO)_{1.7}SiO(H_2O)_x + 0.3Ca(OH)_2 \qquad (2.2)$$

The water content, the Ca/Si ratio and structure of C-S-H is still a matter of discussion. The empirical formula $(CaO)_{1.7}SiO(H_2O)_{1.8}$ [32] is currently the most accepted one. Regarding its structure, different models have evolved since Taylor first proposed that the C-S-H was composed of layers of linear silicate chains or "Dreierkette" chains, constructed of silica tetrahedra coordinated with a central Ca-O layer [33] as presented in Figure 2.1. Currently the tobermorite/jennite and tobermorite/calcium hydroxide-based models [34] are the ones that agree better with the experimental Ca/Si ratios reported in the literature. The continuity of the silicate chain is usually interrupted by the absence of some silicate tetrahedra; this is why the C-S-H crystalline structure is considered of short range and difficult to identify in X-ray diffraction patterns.

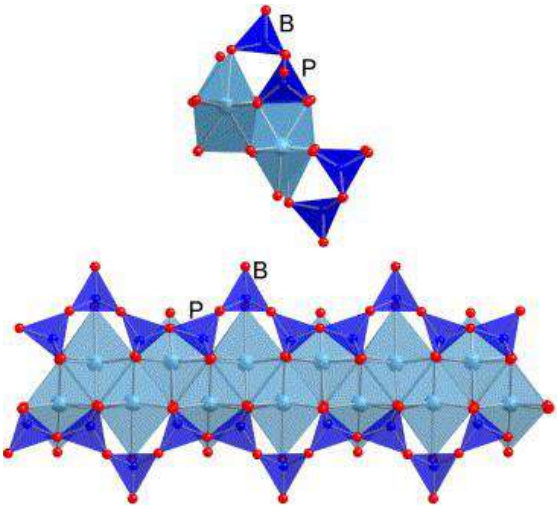

Figure 2.1 - Schematic representation of Dreierkette chains present in C-S-H [34]

The formation of C-S-H is divided in three stages: dissolution, saturation and precipitation. When in contact with water, the surface of the anhydrous grains suffers protonolysis and dissolution, which releases Ca^{2+} and SiO_4^{4-} into the liquid surrounding the grains. This process occurs until the liquid becomes locally oversaturated and C-S-H starts to precipitate at the surface of the grain [31]. The precipitation process generates individual C-S-H particles of approximately 5 nm and CaO/SiO_2 ratios between 1.2 and 2.3. If the C-S-H precipitates from the original surface to the inside of the grain, it is called inner product (Ip), which has a foil-like texture; if it precipitates to the outside of the grain is called outer product (Op), which has a fibrilar texture [26]; and example of this is presented in Figure 2.2, showing Ip at the left and Op at the right side of the figure. Individual C-S-H particles form agglomerations, which have different elastic response depending on its packing density. The more densely packed the agglomerations, the higher its elastic moduli. Three different kinds of C-S-H agglomerations have been identified: low density (LD), high density (HD) and ultra-high density (UHD) [30].

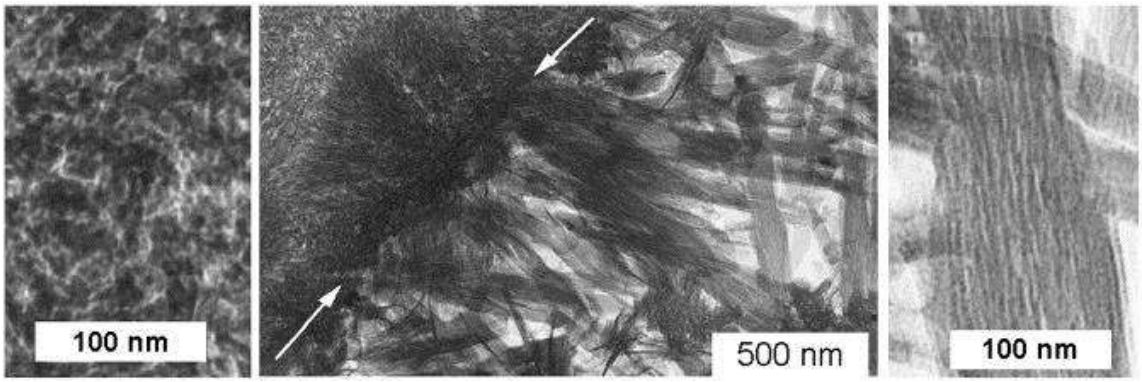

Figure 2.2 - TEM micrograph showing inner product (left) and outer product (right) in hardened C_3S [35]

As presented in equations (1) and (2), crystalline $Ca(OH)_2$ is precipitated as a byproduct of the C-S-H, and is the second constituent of hydrated phase in volume. It is formed as hexagonal platelets of approximately 10μm and is responsible for the elevated pH value of the matrixes. $Ca(OH)_2$ can be easily lixiviated by water, or transformed in $CaCO_3$ by any CO_2 present in the atmosphere. This carbonation process, as will be seen later, is a source of noise in the study of the properties of C-S-H at the nanoscale [36].

2.3 Relations among nano, micro and macro scales of hydrated cement

The hydrated matrix has intrinsic properties at the nano, micro and macro scales. The processes that modify the intrinsic properties of the matrix at the nano scale will have an effect in the properties at the micro scale, and these in turn will modify the properties at the macro scale. Therefore, all the modifications that occur at the nanoscale, affect the behavior of the bulk material with a certain level of proportionality [4]. To better understand these scaling relations, multi scale models ranging from 10^{-8} to 10^{1} m have been developed. The distinction of scales is made in function of the size of its fundamental components, rather than using decimal orders of magnitude. A four level model [37] starts at Level I, in the scale of the nanometers, with C-S-H particles and gel porosity. Follows at Level II, in the micro scale, including C-S-H agglomerations, $Ca(OH)_2$ platelets, capillary pores and air voids. Continues at Level III, in the scale of micrometers and millimeters, with microcracks, sand particles and the Interfacial Transition Zone (ITZ), which is a zone of higher porosity around the aggregates. And finally ends at Level IV, in the scale of millimeters to meters, with the coarse aggregates and the bulk properties of the material. This multi scale approach can

be applied to the porosity of the hydrated matrix to show how all its properties, in all scales are somehow related to porosity [25].

Porosity is one of the properties of the matrix that exists in all the scales, from the gel pores of 0.5 to 10 nm, which are considered to be in the structure of the C-S-H, passing through the capillary pores of 10 nm to 10 μm, up to the air voids, ITZ and microcracks. The size distribution of the pores is continuous throughout the length scale, but each size classification has a different origin and functionality, which at the end are correlated. The volume of pores within the matrix is controlled the by the amount of water present in the mixture. The water that is not chemically bound to the hydrates is called evaporable water; gel and capillary pores are originated by the evaporable water, and bigger pores by the intentional or unintentional inclusion of air voids in the matrix [38]. Additional porosity is induced by the aggregates at the ITZ, which can later become interconnected by microcracks [39]. Using the multi scale approach of four levels, the inter level relations can be characterized as follows:

Level I – Gel pores: The small size of gel pores inside the C-S-H generates and electrical unbalance on their inside surface, which causes an alignment of the water molecules inside the pore. This alignment modifies the properties and reduces the mobility of the water. A direct consequence of this decrease in mobility is a modification of the creep behavior of the matrix when a steady load is applied [40].

Level II – Capillary pores: The water inside the capillary pores is not oriented, but due to the high surface area in comparison to their diameter, it is influenced by the surface tension at the interfaces between water and C-S-H. If the capillary water evaporates or desiccates, differential pressures will be generated inside the pore; to relax this internal stresses, the C-S-H goes into compression and causes shrinkage. The shrinkage process is also highly influenced by the gel pores from level I [40].

Level III – Permeability: The permeability of the matrix is not only controlled by the porosity, but also by the characteristics of the ITZ, and any possible microcracks induced in the material. Among other factors, microcracks can be induced by the creep and shrinkage processes, originated in levels I and II. When the cracks become interconnected with each other, with the ITZ and with the capillary pores, continuous channels are generated and the permeability of the matrix is dramatically increased [31].

Level IV – Strength and durability: The porous structure from level III, whether it is filled with air or liquid, is not capable of supporting the same load as the solid phase; therefore, porosity is a fundamental factor for the strength of the material. Most of the

aggressive agents that penetrate the cement matrix come within the water that is absorbed through the porosity. Two consequences arise from these degradation processes, the formation of higher volume products that generate internal pressures which generate microcracks, and the dissolution or lixiviation of hydrated phases, which increases the amount of voids in the matrix. Both processes have one common consequence, the increase of porosity that reduces the strength of the matrix [25].

2.4 Interaction of CNT with cement matrix in fresh state

Fresh state can be defined as the state at which the matrix is plastic and can be molded. This state has a limited time span, starting from the moment that cement comes in contact with water, and lasting approximately 300 minutes for ordinary Portland cement. During this period the matrix goes through a series of chemical reactions and physical transformations which are part of the hydration reaction of cement. At the end of this period the matrix has already gained some of its final strength and is capable of bearing load; it is only at this point when the nanotubes start to work as nanoreinforcement. The reinforcing effectiveness of the CNT will depend not only on their properties, but also on how well dispersed through the matrix they are. It is of vital importance to understand how the alkaline environment generated by the hydration of cement influences the CNT, and also how the presence of CNT influences the physical and chemical processes that lead to the hardening of the matrix. This section presents all the interactions that occur among the CNT and the cement in fresh state, focusing on the dispersion as the fundamental parameter to be controlled to obtain a good quality composite.

2.4.1 Dispersion of CNT in the cement matrix

The main role of the CNT when working as reinforcement in cement composites is to control the propagation of submicrometric cracks by modifying the load transmission through bridging effects. It has been demonstrated that micro and macro fibers are ineffective to arrest the propagation of this kind of cracks [21], therefore nanotubes or nanofibers are a viable solution to control them. When the composite is exposed to a flexural stress that the cement matrix is not capable of bare, the cracking process begins; at this stage the CNT which are in the path of the submicrometric cracks will work as a bridge, redistributing the load and arresting the propagation of the

opening [41]. The formation of the cracks is a random process that can only be predicted to some extent, therefore uniform dispersion of the CNT throughout the entire matrix will ensure that the majority of the microcracks formed will have nanotubes in their path to bridge them and redistribute the load.

Dispersion methods

The most straight forward method to incorporate CNT in the cement matrix is through the mixing water. CNT are dispersed in water using a combination of mechanical waves and chemical dispersing agents, which together aim to produce a colloid of individual nanotubes, stable over time and not sensitive to alkaline environments. Some authors have attempted to disperse the CNT together with cement using acetone [42], or growing them directly on the anhydrous grains [43], which has proven to be effective but also more expensive if not made on an industrial scale. Thus, this section will be focused in the dispersion methods of CNT in water.

Due to their size, the interaction among CNT is mainly governed by Van der Waals attractions; hence, a tendency to agglomerate is intrinsic to them [44]. These agglomerates are usually difficult to separate to obtain individual CNT; mechanical waves from different sources are used to overcome the Van der Waals forces and disperse the nanotubes. Ultrasonic processors are used to transform a vibration of ultrasonic frequency into a mechanical wave that propagates through water by the generation of cavitation bubbles, which implode and transfer their energy to the CNT bundles, exfoliating individual nanotubes [45]. High shear mixers are also used to disperse CNT in water [46]. The high shear mixer first exerts suction that draws solid and liquid material from the bottom of the container into the rotor-stator pair, where the solids are subjected to milling and hydraulic shear, which expels the material to the sides of the container and draws more material to the rotor-stator pair.

Chemical dispersing agents adsorb onto the surface of the CNT due to hydrophobic interactions [47], this effect is used to maintain individual CNT separated by electrostatic repulsion among the electric charges of the dispersant molecules. Different dispersing agents such as surfactants [45], superplasticizers [48], Sodium Dodecil Sulfate (SDS) [49], and Polyvinylpyrrolidona (PVP) [50] have been tested in nanotubes/cement composites. Besides the adsorption capacity, the dispersing agent also has to be compatible with the hydration reaction and the highly alkaline conditions generated by it. It has been found that for pH values higher than 8 the adsorption of

dispersants onto the surface of the CNT is not significant [47]; it has also been found that for pH values near to12 the dispersion of CNT in water become unstable and tends to reagglomerate [51], and that high concentrations of surfactants hamper the cement hydration reaction due to steric hindrance caused by the molecules of surfactant adsorbed onto the surface of the anhydrous cement grains[52], retarding the heat release during the first hours [53].

Chemical dispersing agents are also used in combination with mechanical waves to optimize the dispersion process. The molecules of dispersant propagate through the gaps in the CNT bundles generated by the mechanical waves, these gaps are free surfaces for the dispersing agents to adsorb onto and prevent the reattachment of the surface to the bundle; this process continues through the length of the CNT until it is completely separated from the bundle. This exfoliation mechanism is called "unzippering" [54]. If the CNT are functionalized, the additional electric charge of the functional groups on the surface of the nanotube has an influence on the electrostatic equilibrium of the dispersion. An example of the use of chemical dispersion in combination with mechanical waves is presented in Figure 2.3. Parts (a) and (c) of the figure present an aqueous dispersion of CNT without and with a chemical dispersing agent, immediately after being exposed to 40.000J of ultrasonic energy; parts (b) and (d) present the same dispersions but after 24 hours of rest. It can be clearly seen that a much higher degree of dispersion is achieved with the help of a chemical dispersing agent, due to the "unzzipering" effect; additionally, after 24 hours of rest, the dispersion with a chemical dispersing agent remained stable, while the one without dispersing agent did not remained stable.

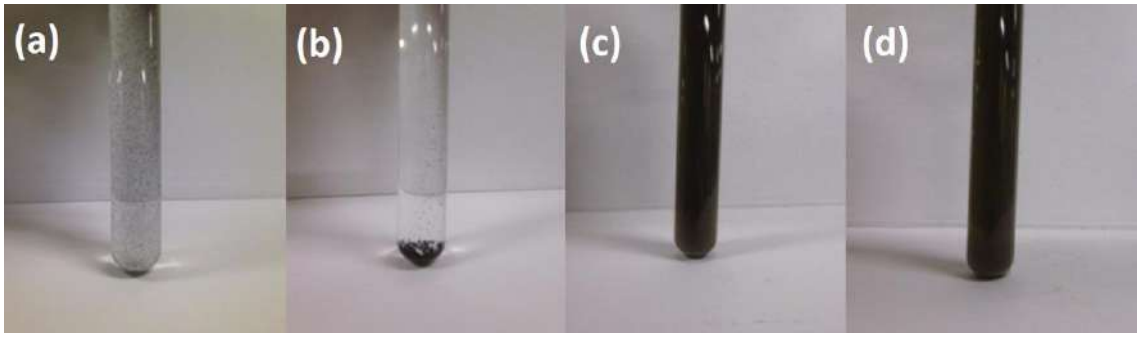

Figure 2.3 - Stability of aqueous dispersions of CNT dispersed using 40.000 J of ultrasonic energy. (a) dispersion without chemical dispersant immediately after sonication; (b) dispersion without chemical dispersant after 24 hours of rest; (c) CNT dispersion with chemical dispersant immediately after sonication; (d) CNT dispersion with chemical dispersant after 24 hours of rest [51]

Functionalization and damage induced by the dispersion process

Functional groups are of vital importance to improve the surface interactions between the nanotubes and the matrix. Since plain CNT have no chemical affinity with the hydrated and non-hydrated phases of the matrix, functional groups work as an anchor between surfaces to improve the load transmission [55] and avoid any "pull out" effects of the nanotubes when the matrix is loaded. Different kinds of structures can be grafted on the surface of the CNT via physical or chemical treatments to be used as functional groups; many tailored functionalization techniques have been developed depending on specific applications [56], for cement composites applications it has been found that the –OH (carboxylic) functional groups have chemical affinity to form bonds with the C-S-H and $Ca(OH)_2$ and transmit load [55]. A schematic representation of how the CNT interact with the hydration products of cement through the OH- functional groups is presented in Figure 2.4.

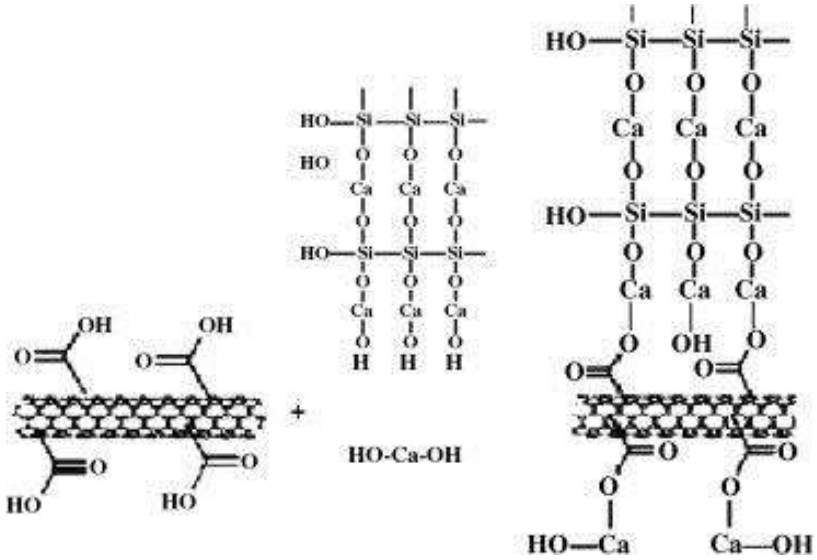

Figure 2.4 - Schematic representation of interaction between OH- functionalized CNT and hydration products ($Ca(OH)_2$ and C-S-H) [55]

Carboxylic groups are generated on the surface of the CNT using a mixture of sulfuric acid and nitric acid, as an adaptation of a methodology originally proposed for the application of CNT in polymeric matrixes [57] and [58]. Acid treatments generate defects in the organized structure of the CNT during the functionalization process, affecting their performance [59]. The presence of defects in the structure, in combination with a highly energetic dispersion process using mechanical waves, can lead to breakage of the CNT [60], thus decreasing their aspect ratio. Using RAMAN spectroscopy, a direct relation between sonication energy and organization of the

structure of the CNT has been found; typical RAMAN spectra of CNT dispersed in water with different ultrasonic energies are presented in Figure 2.5. D and G bands, associated with disorganized and organized carbon structures are clearly identified. A decrease in the intensity of the G band, proportional to the amount of sonication energy is evidenced; this has been associated with a loss of organization in the structure of the CNT as consequence of the mechanical damage caused by the sonication process [51]. In general, for applications where the CNT will work as reinforcement, high aspect ratio CNT are desirable since they have a higher reinforcing efficiency; but in practice, the longer the CNT the higher their tendency to agglomerate [61] since their surface area is directly proportional to their length, and the attraction phenomena between nanotubes that leads to agglomeration are surface phenomena. This tendency to agglomerate reduces the reinforcing efficiency of longer CNT in comparison to shorter CNT in a cement matrix [62]. In contrast, to generate composites with piezo-electric or piezo-resistive properties, the CNT must form an efficient conductive network through the cement matrix, and for this the highest possible aspect ratio is desirable [49].

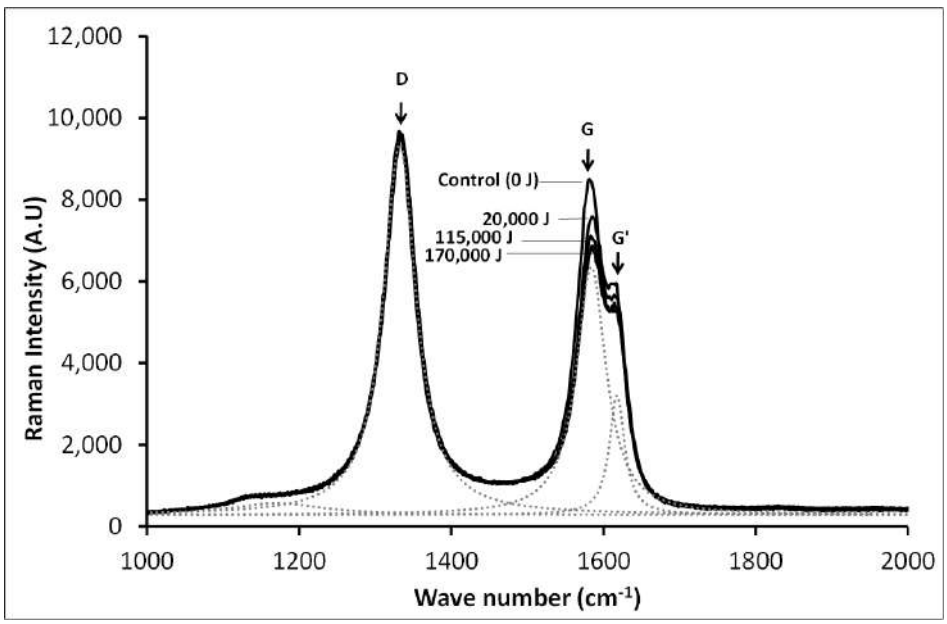

Figure 2.5 - Evolution of RAMAN spectra of CNT after different sonication energies. [51]

Different solutions have been proposed to minimize the amount of damage induced on the CNT after the dispersion and functionalization process. It has been proposed that the acid treatments must be controlled not only to obtain functional groups, but also to obtain CNT of a specific aspect ratio, according to the specific application at which the nanotubes will be used [61]. Pre-treatments with supercritical

CO_2 on the already functionalized CNT have been proposed to minimize the amount of mechanical energy necessary to disperse them, therefore decreasing the amount of damage induced during the dispersion process [60]. Modifications of the functionalization process to eliminate the acid treatments have also been proposed; alternative treatments with O_3 and short wave UV radiation [63] or hydrogen peroxide and UV radiation [64] generate the same carboxylic functional groups and eliminate the need to expose the CNT to highly aggressive environments.

Maximum amount dispersible

The maximum amount of nanotubes dispersible in the matrix is limited not only by the technical aspects of the dispersion process as it was previously show, but also by the geometry of the space available for the CNT. For additions that can be modeled as spheres, the best dispersion scenario is a fully uniform dispersion, where all the particles are evenly distributed and equidistant in the matrix. The worst dispersion scenario is a fully non-uniform dispersion, where all the particles are in contact. A more realistic approach is a random distribution of the particles in all the available space, but the space available is limited by the geometry of the matrix. In the anhydrous state, the matrix is composed mainly of finite size and non-porous particles of angular shapes; this means that the additions are able to occupy only the space left available between particles, and that a fully uniform dispersion is impossible to achieve. When the particles of the matrix are much bigger than the particles of addition (in this case nanoparticles) a clustering dependent on the geometry of the space available appears, causing a low homogeneity in the dispersion of the nanoparticles [65].

In the case of fiber shaped additions, which is the case of the CNT, the geometry dependent clustering will also depend on the amount of fibers included in the empty space of the matrix. For low concentrations of fibers their distribution on the matrix can be considered approximately random, but as the concentration increases, the fibers will start to align following the direction of the borders between particles [66]; this is schematically represented in Figure 2.6 using a ceramic matrix composed of non-porous particles. The distribution of the available space for the CNT between particles is presented in the part (a) of the figure; the distribution of CNT in a low concentration and a high concentration are presented in parts (b) and (c) of the figure respectively. For a low concentration of CNT the distribution of the nanotubes can be considered random; whilst, for a high concentration of CNT the distribution is strongly influenced by the

geometry of the matrix. Cement matrixes are usually designed to maximize their packing density in anhydrous state, consequently minimizing the space between particles, making them more sensitive to the geometry dependent clustering. Therefore, it is important to keep in mind that a higher inclusion of CNT in the matrix does not necessarily means and improvement in the properties of the composite.

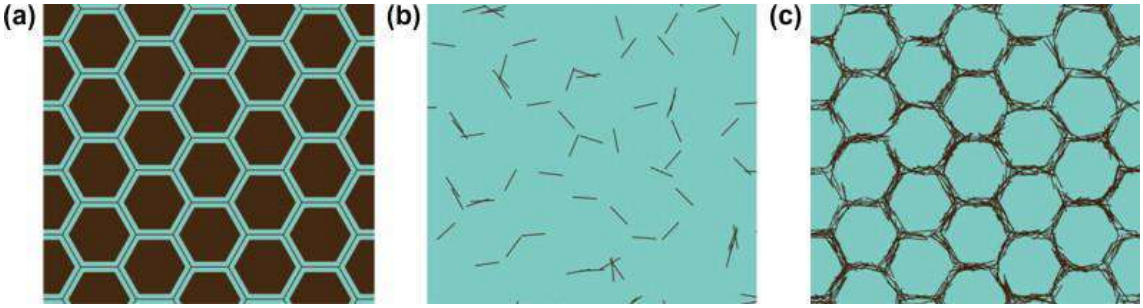

Figure 2.6 - Schematic representation of carbon nanotubes distributed in a ceramic composite of non-porous particles. (a) distribution of the available space for the CNT between particles; (b) distribution of a low concentration of CNT; (c) distribution of a high concentration of CNT [65]

2.4.2 Reagglomeration of CNT and its consequences in the properties of the composite

Despite all efforts made to obtain uniform and stable dispersions of CNT in water, it has been found that this state is hardly maintained when the matrix reaches hardened state [67], the most common result is to find some individual CNT bridging cracks, and the rest as agglomerations throughout the matrix, whether inside the pores or surrounding specific phases. Two main phenomena have been identified as the cause of reagglomeration of CNT dispersions in cementing matrixes: the release of Ca^{2+} cations in the media during the dissolution of cement, and the alkaline environment generated during the precipitation of C-S-H and $Ca(OH)_2$ as consequence of the hydration reaction of C_3S and C_2S. The first occurs during the first hours of the hydration reaction, when the cement is undergoing dissolution and Ca^{2+} cations are released into the media; these cations are capable of interacting with the –OH functional groups generated by the acid treatments, affecting the electrostatic equilibrium of the colloid [51]. The second occurs when the mixing water becomes locally saturated in Ca^{2+} and the pH of the media becomes highly alkaline due to the precipitation of C-S-H and $Ca(OH)_2$. For polymeric dispersing agents with hydrophobic properties, such as

surfactants or SDS, it has been found that at elevated pH values the adsorption of the polymeric molecules on the surface of the CNT is not significant and the dispersions will have the same stability regardless of the presence of a dispersant molecule [47]. Also, the nanotubes agglomerates can reach a critical mass where the gravitational forces overcome the electrostatic repulsions and the agglomerations start to precipitate and segregate from the matrix.

After reagglomeration the CNT are found in form of bundles similar to those found prior to dispersion. These bundles can be of micrometric size, with lower surface area and aspect ratio than the individual nanotubes. A lower surface area implies that there will be a lower load transmission between the matrix and the CNT, since this interaction is done through the outer wall and surface functional groups of the nanotubes. A lower aspect ratio as consequence of twisting and curling of the CNT will prevent that the nanotubes work as bridges between neighboring C-S-H clusters and across submicrometric cracks [68]. Thus, it can be said that the reagglomeration process decreases the effectiveness of CNT as reinforcement because only a portion of the nanotubes work as reinforcement and the other portion remains in the matrix as filler, due to the lack of chemical affinity between the CNT bundles and the components of the matrix.

2.4.3 Effect of the CNT in the kinetics of the hydration reaction

Even though the CNT do not have chemical affinity with the anhydrous or hydrated phases of the cement matrix, it has been demonstrated that they have an influence on the kinetics of the hydration reaction, acting as extra nucleation spots [69]. In a normal hydration reaction, the hydration products are formed by precipitation from nucleation spots, which are located on the surface of the anhydrous grains or on the hydrated phases themselves. The kinetics of this nucleation process depends on the calcium concentration (Thomas 2007), the surface area available for nucleation (Garrault and Nonat 2001), and the temperature (Thomas, Jennings, and Chen 2009). Due to their high surface area CNT work as nucleation spots, occupying all the relevant nucleation sites and promoting the formation of hydration products, with preference for C-S-H [69]. Additionally to their surface area, it has been found that the electromagnetic properties of the CNT also influence the nucleation process. CNT are capable of attracting metallic ions to their surface [70], and polarize water molecules

[71]; therefore, the Ca^{2+} cations and water necessary for the precipitation of hydrates are drawn to the surface of the CNT, enhancing the nucleation process.

When the CNT are functionalized by acid treatments there is an additional enhancement to the nucleation process, this because the –OH functional groups have the ability to adsorb metallic ions [72], increasing the amount of Ca^{2+} on the surface of the CNT. It should be noticed that the nucleation effect of the CNT is not limited to the hydration of cement, evidences of nucleation have been identified for example in polymers [56] and many other materials. Also, the effects of nucleation in cementing matrixes is not limited to CNT, on the contrary, this effect has been found in many different nanoparticles regardless of its pozzolanic activity or chemical affinity with cement [4].

A direct consequence of the presence of additional nucleation spots is the acceleration of the kinetics of the hydration reaction during the first hours. Therefore, the hydration products are formed faster during the first hours of the reaction, releasing a higher amount of heat in a shorter time. This does not mean that the total amount of hydration products is increased but only that its rate of production accelerated, since there is no chemical affinity between the CNT and the hydration products [69]. The accelerating effect takes place only during the first hours of the reaction until the CNT stop working as nucleation spots, whether it is because all the effective surface area available for nucleation has been used, or because the surface area has decreased due to reagglomeration phenomena of the dispersed CNT. After the accelerating effect of the CNT has ceased, the hydration reaction take back its normal course. These phenomena will have a direct impact in the initial and final setting time of the cementing matrix.

Not only the CNT, but also the dispersing agent used in combination with the CNT will have an effect on the kinetics of the reaction; a dispersant compatible with cement should be used to obtain optimal results. Positive results have been found using sodium dodecyl sulfate (SDS) [49], polyvinylpyrrolidone (PVP) [50], ether polycarboxilates also commonly known as superplasticizers [73], and surfactants [74]. For the specific case of surfactants, relatively high surfactant to CNT ratios have been identified as an effective dispersing agent for [45]; however, it is known that high concentrations of surfactants hamper the cement hydration reaction due to steric hindrance caused by the molecules of surfactant adsorbed onto the surface of the anhydrous cement grains [53], retarding the heat release during the first hours [52].

2.4.4 Effect of the CNT on the rheology and shrinkage

Some nanoparticles, such as nanosilica and nanoclay, have a direct influence on the rheology of cement matrixes [75]. Whether it is due to water adsorption or flocculation phenomena, their surface properties or chemical compatibility with the hydration reaction decrease the workability of pastes, mortars and concretes, increasing the water and superplasticizer demands. In the case of CNT, the variations in rheology of the matrixes are not caused by the properties of the CNT themselves [76], but depend mainly on the type and amount of dispersant used [77], and on the type of functional groups present on their surface. A valid approach is to use commercial chemical admixtures with proven compatibility with cement as dispersing agents. Some of the most commonly used are sulfonic acid, polycarboxilates, and sulphonates among others; these admixtures have specific functions in the mix, such as air entraining agents, surface tension modifiers, defoamers, retardants or accelerants, and also have the potential to work as a dispersing agent for the CNT. Usually, high amounts of chemical admixtures are required to obtain an adequate dispersion of CNT [45], and also maintain its function in the mixture.

The rheological properties of the mixture can be measured directly using a rheometer or viscosimeter, to calculate yield stress and viscosity, or using flow measurements, which give quantitative information about the rheology of the mixture in an easier manner, and work as indicators for viscosity. The most commonly used flow tests used in the industry are the marsh cone and mini slump for pastes, the flow table for mortars and the slump cone for concretes. Due to the great variety of chemicals admixtures that can be used, a single effect of the CNT on the rheology of the mix cannot be identified, for example, while CNT mixed with air entraining agents decrease the fluidity of thee mixture, CNT mixed with polycarboxilates increase it [77], therefore this should be studied for each particular case.

Regarding the shrinkage process of the cementing matrix, it has been found that the CNT have a beneficial role [78]. The magnitude of the shrinkage that a cement matrix undergoes has been found to be proportional to the fraction of gel and capillary pores. Due to their size, the CNT promote the decrease of this fraction of pores through two mechanisms, the nucleation of C-S-H and the filling of the pores. This modification in the pore structure modifies the transport of water inside the matrix and the internal pressure inside the pores after drying, decreasing the overall amount of shrinkage [79].

A direct consequence of this decrease in shrinkage is a lower formation of submicrometric and micrometric cracks, which decreases the permeability and increases the durability of the matrix. This effect is not exclusive of the CNT, and other nanoparticles present it due to their size and surface area [4].

2.5 Interaction of the CNT with cement matrix in hardened state

Hardened state can be defined as the state at which the matrix is no longer plastic and cannot be molded. The cement matrix is constantly developing its strength and is capable of bearing the service load for which it was designed. At this point the matrix behaves as a quasi-brittle material, capable of sustaining high compressive and not so high tensile and flexural loads. Is at this point that the CNT start to work as nanoreinforcement, enhancing the load transmission thorough the matrix and modifying the cracking behavior of the material in the nano and micro scales. These modifications in the cracking behavior have an effect on the porosity of the matrix, increasing its durability and the overall performance of the material over time. This section is focused on the surface interactions between the CNT and the hydration products of cement at hardened state, and how these interactions modify the mechanical behavior of the matrix. The dispersion issues presented in the previous section have a direct consequence on the reinforcing effectiveness of the CNT in hardened state, generating non uniform reports in the literature; this is also discussed.

2.5.1 Bridge effect and cracking control

It has been previously discussed that pure CNT do not bond chemically with the components of the cement matrix; this ensures that the CNT maintain their structure and properties, but at the same time possess a challenge: the lack of interaction between surfaces to transmit tensile load. Due to the high tensile strength of the CNT, it is likely that a CNT/cement composite will fail by fiber pull-out, rather than by fracture of CNT [80]. The lack of surface interaction between the CNT and the hydration products causes an easier pull-out of CNT from the matrix. Therefore, the reinforcing efficiency of the CNT is limited by the amount of tensile load that the interfaces are capable of transmitting, rather than by the tensile strength of the nanotubes. Acid treatments, which generate -OH functional groups on the surface of the CNT, are a method to enhance the tensile load transmission and take advantage of additional reinforcing potential of the

CNT. It has been found that -OH functional groups are capable of bonding with calcium hydroxide and C-S-H [55], this interaction enhances the tensile load transmission and increases the efficiency of the CNT as reinforcement. In samples with treated CNT, both pull-out and breakage of CNT was observed; the presence of breakage implies that the tensile load transmission between the matrix and the nanotubes was significantly improved, to the point that a portion of the CNT was stressed until its tensile limit [62]. The pull-out and breakage of CNT modify the fracture energy stored in the composite; this can be seen as a multi-peak behavior in a stress-strain curve, increasing the total strain capacity and toughness of the material [62].

Another mechanism by which the CNT modify the load transmission within the composite, and enhance its mechanical properties is the "bridge effect". Individual CNT act as a network of bridges that transmit the tensile load across cracks and pores [81]; an example of this bridge effect is presented in Figure 2.7, where two agglomerations of C-S-H are bridged by CNT, some of which suffered pull-out and others breakage after the crack opening. Due to their diameter in the scale of the nanometers, CNT are capable of bridging submicron sized cracks, for which larger fibers are not effective [21]; and due to their length in the scale of the micrometers, CNT are capable of bridging micron sized cracks [12]. The aspect ratio of the CNT also plays an important role, since it has been demonstrated that lower amounts of long CNT have the same effect on the properties of the matrix than a higher amount of shorter CNT [62]. Finite element analyses of beams reinforced with CNT have proposed that CNT bridging the cracks prevented sudden failure by transferring the tensile load across the cracks and controlling the crack propagation, allowing substantial strain of the matrix until complete pull out of the nanotubes was reached. The cracks develop upwards, generating sequential pull out of nanotubes until the capacity of the beam drops abruptly at the maximum strain [50].

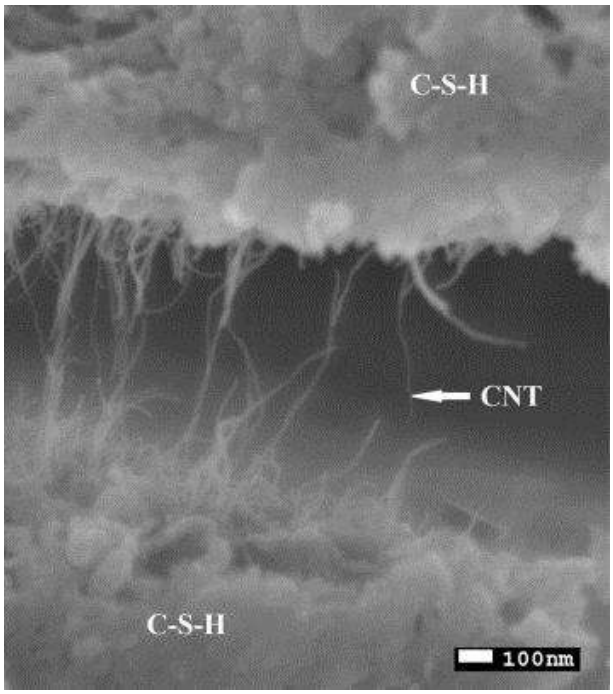

Figure 2.7 - Scanning electron microscopy of bridge effect of CNT [62].

For an effective crack propagation control CNT must be not only well dispersed, but also bridging the appropriate phases. C-S-H is usually formed in agglomerations, with a variable spacing among them from nanometers to micrometers; CNT must reach across these spaces and bridge the C-S-H agglomerations. If the CNT become agglomerated inside or around individual C-S-H agglomerations, they will not help in the tensile load distribution and will not have any effect on the mechanical properties of the matrix [68]. This is presented schematically in Figure 2.8 for long and short CNT. Parts (a) and (c) of the figure present short and long CNT bridging individual agglomerations of C-S-H, while parts (b) and (d) present short and long CNT agglomerated in the individual C-S-H agglomerations.

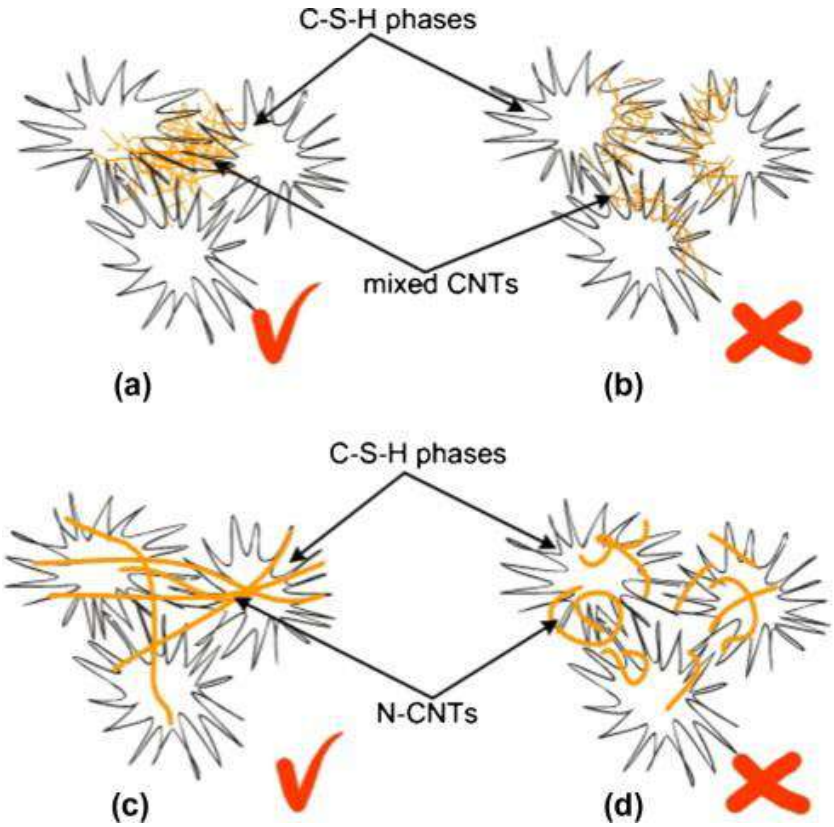

Figure 2.8 - Representation of the arrangement of CNTs in a cement matrix: advantageous (a and c) and disadvantageous (b and d) distribution of the mixed CNTs [68]

An extremely high load transmission was found between CNT and a matrix of geopolymeric cement [82]. The experimental results showed that most of the CNT were found normal to the cracks, with no evidence of pull-out from the matrix or breakage of the CNT; the authors proposed that a slippage occurred between the inner and outer shells of the nanotubes, allowing the opening of the crack without the full pull-out of the nanotubes from the matrix. This slippage had been previously predicted by molecular dynamics simulations and some evidence of it found by transmission electron microscopy [83]. The mechanism proposed for the reinforcing activity of the CNT in a geopolymeric matrix is based in the fact that the bond strength between surfaces is high enough to cause a failure of the CNT instead of a pull-out. When load is applied and a crack opens, first a small interfacial de-bonding between the CNT and the matrix happens, followed by the failure of only some of the outer shells of the nanotubes; these shells remain in its original position, allowing the inner shells to slip a be pulled away [82]; a representation of this mechanism is presented in Figure 2.9. So far this behavior has not been reported for ordinary Portland cement matrixes.

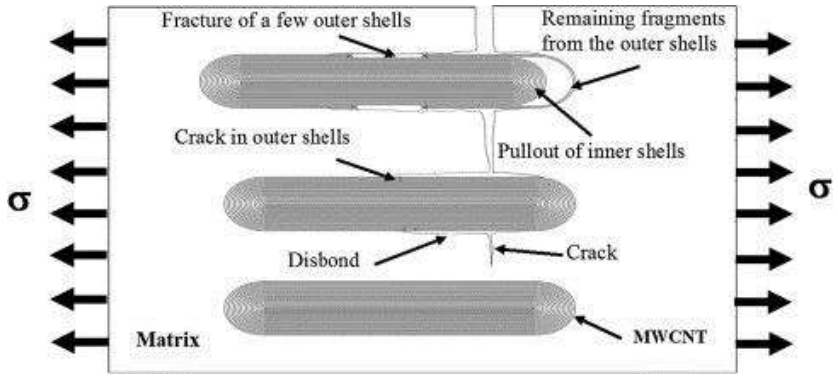

Figure 2.9 - Proposed mechanism for crack bridging in geopolymeric composites [82]

2.5.2 Modification of mechanical properties

The mechanical response of cement composites is most usually studied in terms of compressive and flexural strengths, whether it is in pastes, mortars or concretes. The interactions of CNT with the cement matrix, both in fresh and hardened state, modify this mechanical response not always in a positive manner. This has been found to depend on many factors, such as amount of water, type, aspect ratio and amount of CNT, dispersion and mixing procedures, dispersing agent and presence of functional groups on the CNT. Additions of CNT have been studied in amounts as high as 2.0 or as low as 0.01% by weight of cement, finding that higher amounts of CNT do not mean better reinforcing efficiency, since they are more sensitive to reagglomeration phenomena [84]. Also, acid treatments have been found to improve the reinforcing efficiency of the CNT [85], but at the same time if the acid treatment is not sufficiently controlled, and are combined with sonication, the CNT will break and an excess of defects will be induced on their structure, degrading their properties [51]. Finally, the electrostatic interactions among the functional groups on the CNT, the dispersing agents and the ionic components of cement will also play an important role in the stability of the dispersion of CNT, determining if the nanotubes will work as reinforcement [11]. All of this has led to non-uniform reports in the literature, and has kept the research community from reaching a general consensus about the beneficial role of the CNT in cement composites.

Regarding compressive strength, mixed results have been reported. While some authors have reported a steady loss of compressive strength with additions between 0.5% and 2.0% of CNT by weight of cement [77], others have found and optimum amount of addition at 0.02%, associated to an increase of compressive strength of 30%

[86]. At low contents of water, it has been found that modifications in the amount of water have a higher impact on the compressive strength than modifications in the amount of CNT [48]; and that the hydrophilic behavior of functionalized CNT is capable of adsorbing enough water to hamper the hydration of cement at early ages, requiring high water contents to reach a full hydration [42]. In contrast, after 28 days of hydration, composites presented a better compressive strength [55], and functionalized CNT generated a higher compressive strength than untreated CNT [85].

Regarding flexural strength there is a higher uniformity of results and a consensus in the fact that CNT do increase the performance of the composites when exposed to tensional and flexural loads. Small amounts of long CNT have been found to increase significantly the flexural strength of the composites [22], confirming the correlation between aspect ratio and reinforcing efficiency [79]. This has been directly correlated with the dispersion of the CNT and the bond strength between CNT and cement. A dispersant to CNT ratio of 4.0 was identified as the optimum dispersant amount which generated enough degree of dispersion to increase substantially the fracture load of the composite [45]. In three point bending tests it has been found that the CNT/cement composites are capable of sustaining a higher load and a higher deflection when compared to plain cement samples; numerical simulations based on these experimental results concluded that it is necessary to increase drastically the bond strength between the CNT and the cement matrix to reach the full potential of the CNT as reinforcing material [50]. At early ages, specifically during the first hours of hydration, the CNT have been found to improve the early train capacity of the composites, this associated to a reduction of capillary stresses, which lead to a smaller drying shrinkage [79]. Other evidences that indicate the enhancement of flexural strength of the composites are increases in the modulus of rupture [42], higher fracture energy and higher fracture toughness [87].

Finally, statistical nanoindentation technique has been used to characterize the nanomechanical response of CNT/cement composites. This technique measures a grid of load versus penetration curves in the scale of mN and nm, and from these results calculates the frequency distribution of elastic moduli of the different phases in the composite. The fundamental principle of the technique is the fact that each phase present in the composite, whether it is hydrated or anhydrous, has an intrinsic modulus of elasticity that does not depends on the proportioning of raw materials used to produce the composite [37]. It has been found that the inclusion of CNT increases the frequency

of higher elasticity moduli and decreases the amount of nano porosity. Higher presence of high density and ultra-high density C-S-H has been associated to a better mechanical performance of composites in the macro scale [88]. Some authors have interpreted this an enhancement in the production of high density and ultra-high density C-S-H [4], coupled with an increase in elastic moduli as consequence of a decrease in nano porosity. Since CNT do not have any chemical affinity with the hydration reaction, and the nano mechanical response of C-S-H has been proposed to be of nanogranular nature, meaning that the particle-to-particle contact has a greater influence on the mechanical behavior than the intrinsic properties of the phase [30], the mechanism by which the CNT increase the elastic moduli of C-S-H has to be of physical nature, rather than chemical. This is still a matter of discussion.

2.6 Hybrids of CNT with other nano and micro particles in cement composites

CNT have been combined with other nanoparticles with the goal of maximizing their positive effects and complementing the weak aspects of the other nanoparticles. A complementarity of effects is considered successful when the individual effects of each nanoparticle are enhanced, or when a new effect is generated. For this complementarity of effects to happen, chemical and scale compatibility between CNT and the other nanoparticles has to be guaranteed. In other areas of knowledge, the potential of combinations of CNT with other particles has already been recognized; CNT have been coated with silicon oxide and gold nanoparticles to fabricate coaxial wires that work as markers for carcinoembryonic biological fluids [89], also silica nanotubes have been produced using CNT as molds through the decomposition of chlorosilanes [90], only to cite some of the many possibilities that have been studied.

The combination of CNT with other nanoparticles can be thought from different approaches: combinations with micro and nano fibers to control the crack propagation at different scales simultaneously, combinations with pozzolanic micro and nano particles to enhance tensile and compressive strengths at the same time, functionalization of the CNT with other nanoparticles to enhance the bond strength and load transmission efficiency between CNT and the matrix, and growth of CNT on the surface of particles or fibers to modify their surface properties. These combinations, among many others that are possible, can be tailored to solve a specific problem or

enhance a specific property of a CNT/cement composite, not only regarding its mechanical response, but also its electromagnetic properties.

One of the most promising combinations is CNT with silica micro and nano particles. Two approaches, each with a different objective, are used for this combination: a simple combination of CNT and silica in the mixing water, and a coating of silica particles onto the surface of the CNT. The goal of the simple combination is to take advantage of the pozzolanic activity of the silica, and guarantee an increase both in compressive strength as consequence of the pozzolanic activity, as in flexural and tensile strength as consequence of the reinforcing effect of the CNT; as it was presented before, the effect of CNT on the compressive strength of the composites is not always beneficial, and this would be a solution to this issue. This combination has been tested with micrometric [91] and nanometric [11] silica particles, and has been found to be partially effective with high levels of substitution of cement by micrometric silica and nanometric silica. The main issues of this type of combination is the scale incompatibility between the micrometric silica and the CNT, and the reagglomeration phenomena that occur in the aqueous dispersions of CNT and nanosilica; these issues cause a loss of surface area of the particles, generating a lower reactivity of the silica and, and the accumulation of CNT as agglomerations inside the pores, which limits their reinforcing capability.

The goal of the coating of CNT with silica is the improvement of the bond strength between the surface of the CNT and the cement matrix; this by inducing the growth of C-S-H from the silica on the surface of the CNT [92]. Higher bond strength between reinforcement and matrix means higher reinforcing efficiency of the CNT, since they would be able to withstand more load before suffering pull-out from the matrix, even to the point of reaching their maximum tensile strength, point at which the CNT reach their maximum reinforcing efficiency. The coating of silica is obtained by sol-gel reaction, and individual nanotubes coated with a thin layer of silica on their surface is the final result; the silica structure is stable enough to withstand the calcination of the internal nanotube, maintaining its shape and internal structure [93]. Other method to induce the growth of C-S-H on the surface of CNT is by pre treating them with $Ca(OH)_2$ and nanosilica particles [85]; the main goal of this treatment was to differentiate the morphology of CNT from ettringie crystals. A marginal gain in compressive and flexural strenght of the composites was obtained with this treatment.

Besides silica, the simple combination approach has also been tested with nano kaolin clay, obtaining similar results [86]. Some authors claim that the presence of nanometric clay particles, or even nanometric and micrometric silica particles help to disperse and maintain stable the CNT; this as an extrapolation of results from micrometric fibers, where the additional particles help to mechanically separate the individual fibers taking advantage of the gaps between them [94]. Unfortunately, there are no dispersion studies that directly measure the dispersing effect of these particles on CNT agglomerations; therefore, the affirmation that clay and silica particles as dispersing agents for CNT has to be carefully used, taking into account that the most important condition for this to happen is a compatibility of scale, meaning that the particles have to be small enough to enter the gaps in between agglomerated nanotubes [95].

CNT have also been combined with other fibers with the goal of increasing flexural and tensile strength of the composites. As for the combinations with pozzolanic particles, the combinations of CNT with other fibers can be made by simple mixing or by coating, but in this case the other fibers are coated with nanotubes. The coating of CNT can be achieved by growing them onto the surface of other fibers, using a chemical vapor deposition technique; in this case the CNT act as elements of interaction between the fiber and the matrix, and its function is to enhance the load transmission and bonding strength between surfaces. CNT have been mixed with hemp [96] and bagasse fibers [97], finding a significant increase in flexural strength and a modification in the water absorption dynamics of the natural fibers.

2.7 Novel properties of CNT/Cement composites

Besides modifying the known properties of the cement composites, CNT can also confer new electromagnetic functionalities to the matrix; these functionalities have opened a new range of potential applications for smart structures. If the CNT are in an adequate volume fraction and properly dispersed throughout the matrix, they form a conductive network. This network has piezoelectric [64] and piezoresistive [49] properties, which can be used to generate matrixes with with self-sensing or self-monitoring capabilities, i.e. that are capable of sensing its own state of strain, stress, damage and temperature [98]. The self-sensing properties of a CNT/cement composite are widely governed by the amount of nanotubes present in the matrix; if they are

present in a volume fraction at which the fibers touch each other, they form a continuous conductive path and the electric response is governed by the effect of strain on the contact between nanotubes [99]. This volume fraction, at which the matrix exhibits an increase in conductivity, is called the electrical percolation threshold [100]. The percolation volume in cement based composites has been found to be dependent on the conductivity and geometry of the conductive phase, rather than on the composite composition [101].

Two pressure sensitive responses have been found in the CNT/MWCNT composites, piezoelectricity and piezoresistivity. The piezoelectric response consists on the generation of a voltage when load is applied to the matrix [64]; this voltage is originated in the pores of the matrix, which are filled with a conductive electrolytic solution. When a compressive load is applied, additional ions are transported from the matric to the electrolyte solution, causing a difference of potential [102]. CNT enhance the transmission of this voltage throughout the matrix, working as a conductive network. The piezoresistive response consists on the decrease of the electric resistivity of the matrix when load is applied [103]; this drop in resistivity has been attributed to two sources, to the intrinsic piezoresistivity of the CNT and to a higher contact among CNT due to deformations of the matrix [49]. The electric charges have been found to be conducted mainly by the network of CNT, and the effect of adsorbed water has been found to be minimum [104]. An example of piezoresistive behavior of a CNT/cement composite is presented in Figure 2.10.

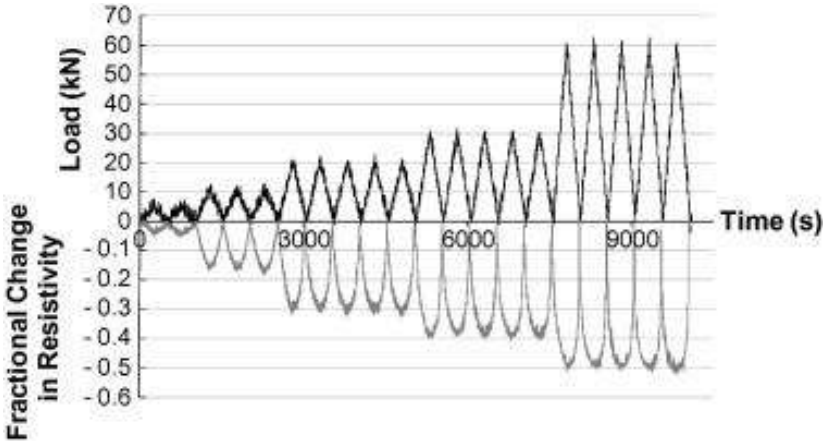

Figure 2.10 - Piezoresistive response of a CNT/cement composite in cyclic load [105]

The piezoresistive effect of the CNT/cement has shown the most potential to generate strain sensors. Not only carbon nanotubes, but also carbon nanofibers have

proven to be an effective conductive phase in the composites [103], exhibiting not only piezoresistivity but also capacitance characteristics, this last not sensitive to load [106]. The strain sensors developed with CNT/cement composites can be of small volume and embedded in structural elements, minimizing the consumption of conductive phase and therefore their cost [99]. Some of the requisites that have to be fulfilled to design an effective fiber based sensor are that the fibers have to be more conductive than the matrix, their diameters smaller than the crack length, well dispersed and randomly oriented [107]. The water content of the mixture, i.e. the water/cement ratio, is one of the key factors to tailor a strain sensor, since a non-linear relationship between the water content and the electric resistivity of the matrix has been found [74]. This nonlinear response is caused by a polarization of the water molecules in the matrix, which increases the electrical resistance of the composite during measurement [103], this increase is non-linear a dependent on the load application rate [105]. Solutions to this issue go from using dry specimens, to measurements with AC current or the use of nonlinear calibration curves.

A direct consequence of the addition of CNT, or any other conductive fiber to the composite, is the increase of the electric conductivity of the matrix, regardless of the presence of compressive or tension loads. Electrically conductive cement matrixes are useful for electrical grounding, lighting protection, resistance heating, static charge dissipation, electromagnetic interference shielding, cathodic protection, and thermoelectric energy generation [24]. The high electrical conductivity of the CNT has generated an additional application in cement composites as electromagnetic interference shielding, specifically in the frequency range used for mobile phones communication [94]. It has been found that CNT/cement composite have potential as an alternative shielding material, but this property is also limited by the adequate dispersion of the CNT in the matrix, as is also by the amount of conductive phase in the composite and the thickness of the shielding wall [108]. These non-structural applications have become interesting over time, since they allow a traditionally structural material to be multifunctional, saving costs and increasing its durability [23].

2.8 Present challenges and future perspective

Until recent past, the price and scale of production of nanoparticles made them prohibitive for industrial scale applications, but as the price of nanoparticles has been

increasingly dropping over time [109], they have become affordable for general construction applications. The full development of all the potential applications for CNT/cement composites is not being held back any more by their price, but by two main technical issues: the effective dispersion of CNT and their interfacial bond strength with the cement based matrix. The research community has recurrently reported that all the improvements obtained in the known and novel properties of the cement matrix, are in some way limited by these two issues; therefore, they should become the main focus of the research carried out in the field.

As a conclusion for this chapter, it can be said that so far the exceptional properties of the individual CNT are being widely underused in cement matrixes. This is clearly evidenced in the fact that the beneficial effects of CNT over the mechanical properties of cement composites are comparable with the effects obtained with traditional fibers and pozzolanic particles. Novel functionalization and dispersion methods, specifically designed to target the dispersion and bond strength issues would provide the leap forward in knowledge necessary to exploit at its full the strengths of CNT. The use of the scale compatibility criteria is one of the tools that should be used to better understand the effects of the CNT; this means that the CNT must be used to target specific issues at their own scale, and not be expected to widely enhance the properties of the composite in all scales. The combined used of CNT with other larger fibers or pozzolanic particles will help to bring the effects of the CNT from the nanosacale, to the micro and macro scale, generating synergies of individual effects that bridge the scales as a cascade.

3. State of the art

A review on the chemical, mechanical and microstructural characterization of carbon nanotubes-cement based composites

Abstract

It is known that carbon nanotubes (CNT) modify the properties of cement based composites in fresh and hardened state; it is also known that these modifications are positive when appropriate dispersion of CNT within the matrix is achieved. Traditional experimental approaches used for fiber reinforced composites have been widely applied to study CNT-cement composites; nevertheless, high statistical dispersions and conflicting reports have been found to be a common issue due to the nanometric nature of CNT. This review presents a critical analysis of the most commonly used techniques to produce and test CNT-cement composites. Topics such as CNT dispersion and measurement of mechanical performance, electromagnetic properties and durability of CNT-cement composites are addressed.

It is concluded that the benefits of CNT in cement composites have been fairly identified, but the mechanisms by which nanotubes maintain dispersion within the matrix, interact with hydrating cement, and modify properties of composites are not yet fully understood. Understanding these mechanisms is considered of most importance to identify the limitations of CNT-cement composites and define which applications are achievable with the use of CNT. Better characterization of the interaction between CNT and hydration products at the nanoscale is required to develop more efficient composites, targeting the enhancement of multiple properties at the same time.

3.1 Introduction

The development of more efficient characterization techniques has allowed a better understanding of the principles and mechanisms by which carbon nanotubes (CNT) modify the properties of cement matrixes in multiple scales [110]. This better understanding led to the first steps in the development of the CNT-cement based

composites technology, finding some consensus within the literature regarding the most adequate methodologies to produce composites. Additionally, identification of the challenges inherent to the usage of CNT has cleared the view regarding the expected impact of CNT over the mechanical and electromagnetic properties of CNT-cement composites. It is important to understand the potential and limitations of CNT-cement composites to think the future applications accordingly. This will help to filter which applications can be obtained with micro and macro fibers, and which are only achievable with the use of CNT.

Standardization of the properties of CNT-cement composites is a necessary step towards mass production processes that guarantee reliable products. Existing technical regulations for Portland cement matrixes must be carefully adapted for this nano-structured composite; therefore, it is important to identify the key properties of the composite to be measured, and which techniques should be used to obtain repeatable results. In general, most of the current techniques used to measure mechanical properties and durability of cement matrixes can be adapted to CNT-cement composites without substantial modifications, but an additional effort must be made to find the most adequate techniques to measure novel electromagnetic properties of the composites.

Production of CNT-cement composites requires the application of a set of characterization techniques covering a range of scales from nano to macro. Aspects such as dispersion degree and integrity of CNT must be evaluated at the nanoscale, while the performance of the composite is usually evaluated at the micro and macro scales. A combination of spectroscopic techniques, microscopy imaging, mechanical testing, electromagnetic measurements, and durability evaluations, among others, represent the minimum body knowledge required from a CNT-cement composite to predict its performance. This review presents a state of the art of the CNT-cement composites technology. First the characterization techniques used to measure the dispersion degree of CNT are presented; then, the different methodologies used to produce such composites and test their mechanical and electromagnetic properties are reviewed. Finally, the potential of CNT to improve the durability of cement composites is discussed.

3.2 Basic characterization of CNT

A basic set of features must be known prior to the application of CNT in a cement-based composite; these include diameter, length, multi wall or single wall character, degree of structural organization and surface functionalities. Diameter and length are used to calculate the aspect ratio of CNT, which has been found to be a key parameter that controls the reinforcing efficiency [62] and strain sensing [111] capabilities of the composites. These values are usually obtained using transmission electron microscopy (TEM) [112] or scanning electron microscopy (SEM) [61]. Drawing conclusions from a single microscopy image can be misleading; image processing methods that identify variations in gray intensities to isolate individual CNT must be applied to large groups of images to obtain a statistical analysis of length and diameter. This kind of analysis is time consuming, but allows a more reliable quantification of the dimensions of CNT in terms of a size distribution, rather than in terms of a nominal value [113]. Particle size distribution techniques such as Dynamic Light Scattering (DLS) should not be used to characterize individual CNT, since it has been demonstrated that the results obtained from these techniques are representative of agglomerations rather than individual nanotubes. Additionally, these results depend on the presence of a dispersing agent and the application of dispersion energy such as ultrasonic waves [114]. A similar issue occurs with the specific surface area measured by BET adsorption isotherms [61], bulk densities measured by traditional powder methods, and specific masses measured by pycnometer, are also dependent on the dispersion degree of CNT agglomerations.

Structural characteristics of CNT can be defined by their crystalline organization [115], chiral vector [116] and single wall or multi wall character [109]. The crystalline organization of CNT can be characterized by the I_D/I_G ratio determined from RAMAN spectroscopy results. I_D/I_G represents the proportion between the organized and disorganized carbon structures in the CNT, and uses the intensities of D (defective carbon) and G (graphitic carbon) bands located at high wave numbers in the RAMAN absorption spectrum [117]. I_D/I_G is a good quality indicator for CNT, low I_D/I_G ratios are characteristic of highly graphitized structures [115]; with reports in the literature ranging from 0.65 for laboratory quality MWCNT [118], to 2.04 for industrial grade MWCNT [119].

The chiral vector of CNT indicates the geometric organization of the hexagonal arrays of carbon atoms, and can be determined by electron diffraction [120]. The chiral vector is mostly relevant for single wall carbon nanotubes (SWCNT), since it defines if they behave as metallic conductor or semi-conductors [116]. Electric and thermoelectric properties of individual CNT can be measured using standard lithographic practices [121]. Multi walled or single walled character of the CNT can also be determined using RAMAN spectroscopy by the radial breathing mode absorption bands, which are located at low wave numbers, and are characteristic of SWCNT [122]. SWCNT and MWCNT differ in many properties such as Young´s modulus [123]–[125], electrical conductivity, thermoelectric properties and optical properties [121]. Nevertheless, there are no reports in the literature indicating if the reinforcing efficiency or self-sensing capabilities of the cement-based composites are noticeably modified by differences in I_D/I_G, chiral vector, electric resistivity or single wall or multi wall character. A vast majority of the literature reports use MWCNT as reinforcement in CNT-cement based composites [110]. Higher availability and lower cost seem to be the main criteria to select MWCNT over SWCNT.

Finally, the presence of functional groups on the surface of CNT can be determined by Fourier Transform Infrared (FTIR) spectroscopy [126], through the vibrational modes of chemical bonds [63]. Physicochemical treatments are able to induce –OH or –COOH groups on the surface of the CNT, these groups can be used to improve the interfacial bond between nanotubes and the cement matrix [55], or use this groups to graft different molecules on the surface of the nanotubes, which are capable of chemically interacting with the cement matrix [127].The main goal of this treatment is to increase the load transmission efficiency, but some studies have shown negative effects due to agglomeration phenomena caused by the negatively charged surface of functionalized CNT [51].A summary of the techniques discussed in this section is presented in Table 3.1.

Table 3.1. Summary of techniques used to determine basic properties of CNT

Parameter	Technique	References
Specific surface area*	BET adsorption isotherms	[61]
Crystalline organization	RAMAN spectroscopy	[109], [115], [117]–[119], [122]
Chiral vector	Electron diffraction	[116], [120]
Diameter and length	Microscopy and image processing	[61], [112], [113]
Surface functionalities	Fourier Transformed Infrared spectroscopy (FTIR)	[55], [63], [126], [127]

*Properties of agglomerates or bundles

3.3 Measuring dispersion and integrity of CNT

The dispersion degree of CNT and their stability over time have been identified as key issues to produce quality CNT-cement composites [110]. For aqueous CNT dispersions, the most straight forward technique to follow the dispersion process in a qualitative manner is visual inspection; the more advanced the dispersion process, the darker the color of the suspension [128]. Evolution of the color of a suspension containing 0.33% CNT by mass after different sonication times is presented in Figure 3.1. It can be seen that the higher the sonication time, the darker the color of the sample due to the exfoliation of individual CNT from agglomerations. The general effectiveness of a dispersing agent can be qualified by the presence of visible agglomerations [129], and its stability over time by the appearance of flocculation or segregation of solids [130]. Visual inspection is qualitative in nature and limited by the human eye; thus, quantitative techniques are required for a rigorous control.

Figure 3.1 - Evolution of a dispersion of 0.33% CNT in water and surfactant after different sonication energies

More reliable techniques to follow the dispersion process of CNT in water are UV-Visible (UV-Vis) spectroscopy, dynamic light scattering (DLS) and microscopic imaging. It has been found that CNT have absorption bands in the UV-Vis wavelength

region, and that this absorption can be related to their degree of dispersion [126]. When CNT become agglomerated, the intensity of the absorption band decreases; therefore, the intensity of the absorption band can be directly correlated with the degree of dispersion, allowing the determination of the optimal dispersion parameters for each case [131]. An example of the UV-Vis absorption spectra obtained for a suspension of CNT in water after different sonication times is presented in Figure 3.2. Many authors have adopted this methodology because it is time and cost effective. Some authors have proposed that the use of the absorbance value at an specific wavelength is enough to characterize the phenomena [132], while others have proposed a refinement of this by calculating a solids concentration proportional to the absorbance value [47], and the use of the ratio between the non-resonant background and the resonant band [133]. Also, to account for the variability of power output of the equipment used to mechanically disperse CNT, it has been proposed that the process should not be controlled in terms of dispersing time, but in terms of the amount of energy applied to the system normalized by the mass of CNT in the dispersion.

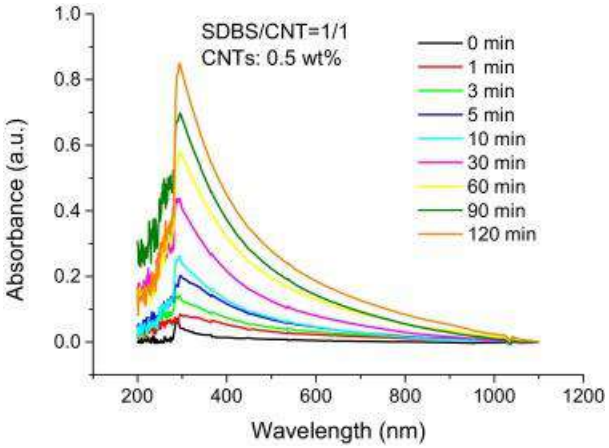

Figure 3.2 - UV-Vis absorbance spectra of CNT dispersed in water and exposed to different sonication times [134]

Scanning electron microscopy (SEM) and transmission electron microscopy (TEM) have been used to qualify the state of CNT before and after a dispersion process [131], or to verify the effectiveness of adsorption of a dispersing agent [59]. Image processing techniques can be applied study statistically the changes in length of the CNT and size of agglomerations [113]. Dynamic Light Scattering (DLS) and Centrifugal Separation Analysis (CSA) have been used to calculate the hydrodynamic particle size, which can be correlated to the degree of dispersion of CNT [114]. A great

advantage of these techniques is that they measure particle size distributions instead of a single average particle size, allowing a better understanding of the dynamics of the dispersion process. The great disadvantage is that they do not give access to the real diameter and length of the CNT, since the hydrodynamic diameter of CNT is governed by the size of the agglomerations; this is reflected in wide particle size distributions, ranging from tens to hundreds of nanometers.

The dispersion degree of CNT is variable with time, this variation is called stability. The stability of a dispersion of CNT is affected in a lesser extent by gravity, but in greater extent by electrostatic interactions among its components [135]. UV-Vis techniques can be used in combination with centrifugal forces to study the stability of a dispersion of CNT, simulating a sedimentation process caused by gravity over time, with high speed centrifugation [114]. Electrostatic interactions among components of the dispersion can be studied using electrophoretic ζ-potential measurements. The magnitude of the surface charges are correlated to how prone to agglomeration the dispersion is. It has been found through ζ-potential that the presence of substances such as $Ca(OH)_2$ [51], NaCl, $CaCl_2$ and $AlCl_3$ [130] in the dispersion cause a partial or total agglomeration of the CNT, with or without the presence of a dispersing agent. This agglomeration effect is caused by the combined effect of changes in pH of the media and an interaction between cations in the substances and the surface charges of the CNT.

Dispersion and functionalization methods that use mechanical waves or chemical routes generally are too aggressive for CNT, causing damage in their structure in the form of defects or amorphization. RAMAN spectroscopy can be used to determine the amount of damage induced to the CNT and monitor the dispersion or functionalization process using the I_G/I_D ratio [60]. RAMAN spectra of an aqueous CNT dispersion measured after different sonication times are presented in Figure 3.3. It can be seen that the intensity of the band associated with organized C-C bonds (around 1600 cm^{-1}) decreases proportionally to the sonication time. This indicates that the sonication is damaging the nanotubes by inducing disorganization in their structure or by breaking them. UV-Vis techniques combined with RAMAN spectroscopy can be used to follow a dispersion process and determine the point at which CNT are sufficiently dispersed and have not suffered significant damage to their structure [51]. A summary of the techniques discussed in this section is presented in Table 3.2.

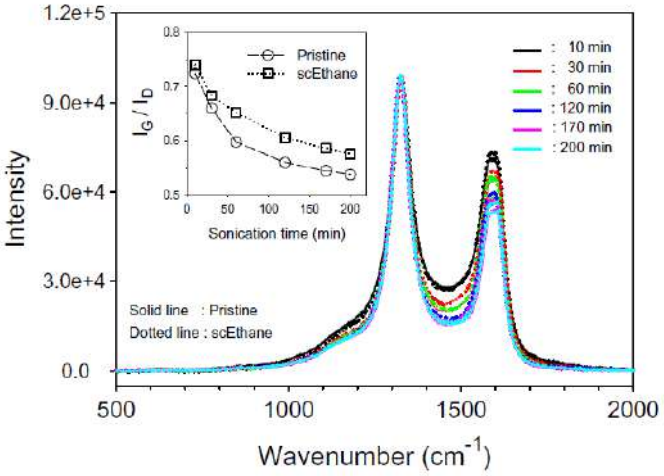

Figure 3.3 - D ang G absorption bands in RAMAN spectra of CNT dispersed in water after different sonication times [60]

Table 3.2. Summary of techniques to measure dispersion and stability of CNT

Parameter	**Technique**	**References**
Dispersion degree in water	UV-Vis spectroscopy, Microscopy and image processing, Dynamic Light Scattering	[47], [110], [113], [126], [128]–[134]
Stability	UV-Vis spectroscopy, ζ-potential	[51], [114], [130]
Integrity	RAMAN spectroscopy	[51], [60]

3.4 CNT-cement composites fabrication

Two basic steps are required to fabricate CNT-cement based composites, first dispersion of agglomerated CNT in a media, and then mixture of the dispersed CNT into the cement matrix. This approach is called the first admixing method [136]. Synchronous admixing and later admixing, which consists on adding CNT during or after the mixing of the components of the matrix, are not expected to yield better results than first admixing, and have been little studied. Different approaches have been proposed to complete the two steps of the first admixing method, all seeking homogeneous distribution of individual CNT throughout the cement matrix, maximizing the beneficial effects of the nanotubes, and minimizing the amount of CNT required to obtain a specific performance. The most used technique to disperse the CNT in a media is a combination of mechanical waves and chemical dispersing agents in water. Ultrasonic pulses during prolonged periods of time [137], and high shear stresses [63] can be considered the most effective mechanical methods to disperse CNT in

water; nevertheless, it has been clearly identified that they are too aggressive for the nanotubes, and the resulting dispersions are not stable over time. Covalent or non-covalent functionalization of CNT is a tool to improve the efficiency of mechanical dispersion, minimizing the damage induced to the CNT. Covalent functionalization consist of the induction of free radicals species on the surface of the CNT, whether it is by acid treatments [12] or UV treatments [64]; electric charges of the free radicals will cause a natural repulsion between individual CNT when immersed in water, improving the dispersion degree and stability over time of the colloid. Non-covalent functionalization consists of the adsorption of polymers on the surface of the CNT. These polymers have electric charge and hydrophilic or hydrophobic properties, which in combination with the mechanical waves, improve drastically the dispersion degree, and help to maintain the stability of the colloid over long periods of time [50].

Some alternative dispersion methods have been explored obtaining similar results. CNT have been dispersed in acetone using ultrasonic pulses for long periods of time (up to 4 hours), then left to dry at room temperature [42]. This decreases the size of the CNT bundles and allows homogeneous dispersion throughout the cement matrix in dry state. A similar approach has been tested using water and surfactants instead of acetone [48]. Another method to guarantee that there are no CNT bundles in the dispersion is to use centrifugation. After dispersing CNT using mechanical waves and dispersing agents, the obtained colloid is centrifuged at high speeds until all the bundles sediment and only individual CNT remain in the supernatant [138]. Although these methods increase the amount of individual CNT in the dispersion, they are considered time consuming and of low efficiency.

The second step in the fabrication process of CNT-cement composites is to incorporate CNT in the cement matrix. Dry mixing powdered CNT together with cement [86] by mechanical means such as ball mills is the simplest method, but also the less efficient. The most used is the addition of pre-dispersed CNT in a portion [91] or the total [137] of the mixing water, and then adding cement and any other solid constituents. The use of methyl cellulose and defoamers has also been studied to guarantee adequate dispersion without affecting the properties in fresh state of the composites [55]. More elaborated methods such as ultrasonic pulses to disperse cement and CNT together in acetone and dried before adding water [69], and growing CNT directly on cement grains by chemical vapor deposition [139], have been proposed. Even though these methods obtain good dispersion of CNT when the matrix is in dry

state, results obtained after adding water are not particularly better than those obtained by pre dispersing CNT in the mixing water. A summary of the techniques discussed in this section is presented in Table 3.3.

Table 3.3. Summary of techniques used in the fabrication of CNT-cement composites

Parameter	Technique	References
Dispersion of CNT by Covalent functionalization	Acid treatments and mechanical waves	[12], [41], [61], [92], [112], [130], [140]–[143]
Dispersion of CNT by non-covalent functionalization	Chemical dispersing agents and mechanical waves	[11], [44], [48], [50], [51], [142], [144]–[147]
Mixing CNT in the cement matrix	Dry mixing, dispersion in mixing water, in situ growth of CNT, dispersion in acetone	[42], [48], [69], [86], [91], [137], [139]

3.5 Characterization and performance of CNT-cement composites in fresh and hardening state

CNT do not have chemical affinity with the reactions that occur during the hydration of cement, but do have the capacity of modifying the kinetics of some of these reactions by nucleation effects. Heat flow curves of Portland cement pastes from isothermal calorimetry experiments, with and without CNT, are presented in Figure 3.4. It can be seen that the paste blended with CNT released a higher amount of heat in a shorter time. In the same study, it was shown that for similar heat release values, i.e. when the reactions with and without CNT are comparable, the same amount of calcium hydroxide was formed. This evidence indicates that even though the hydration is accelerated by the nucleation effect, no additional hydration products are formed due to the lack of chemical affinity between CNT and the hydration reactions [69]. No reports on the direct effect of CNT on the setting time of composites were found. This can be related to the nucleation effect of CNT, which is only relevant at very early stages of the hydration reaction, and also to the fact that the chemical dispersing agents used to disperse CNT in water can also have accelerating or retarding effects on the hydration reaction [119], which makes difficult to separate the individual effect of CNT from the effect of dispersants.

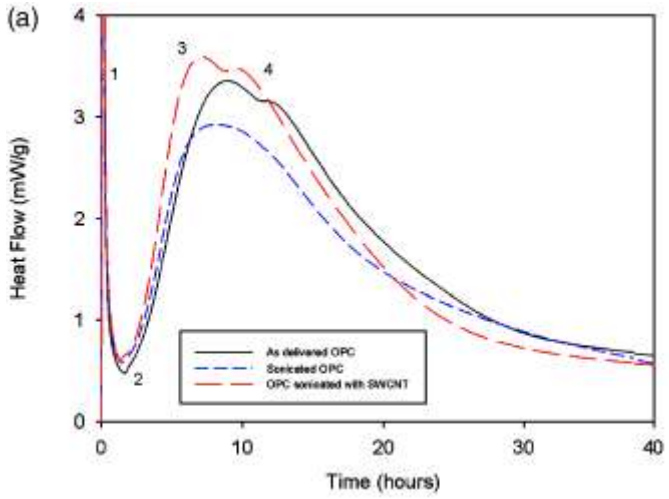

Figure 3.4 - Isothermal calorimetry heat flow results of Portland cement pastes with and without CNT [69]

The interaction between functional groups on the CNT and some hydration products of cement can be identified by FTIR spectroscopy. Studies have found that the absorption band at 3643 cm^{-1}, which is characteristic of the vibrational mode of (OH) from $Ca(OH)_2$, disappears in pastes blended with –OH functionalized CNT. This indicates that an interaction between the COOH or C-OH groups on CNT and $Ca(OH)_2$ occurred [55]. This interaction has the potential to improve the bond strenght between CNT and matrix; therefore, increasing the amount of tension load that the composite can withstand before CNT are pulled-out from the matrix. The disappearance of the 3643 cm^{-1} band is a potential indicator of an interaction between –OH groups and calcium-silicate-hydrates (C-S-H), but so far there is no conclusive experimental evidence that confirms this hypothesis.

Rheology of the composites can be measured by simple means such as mini-slump cone [148], or by more sophisticated means such as a rheometer equipped with concentric cylinders [45] or parallel plates geometries [145]. Regarding the rheology of matrices in fresh state, it is expected that both CNT and dispersing agents control the viscosity of the suspensions. At lower dispersant levels, less polymer molecules are adsorbed onto the CNT surface and the protection from agglomeration is reduced. At higher dispersant levels, bridging flocculation can occur between polymer chains [149]. Therefore, suspensions with larger scale agglomerates exhibit higher viscosity [45]. Also, due to their high surface area, they have potential to adsorb any additives destined to control the rheology of the mixture. Mini-slump spread of pastes blended with CNT and superplasticizer are presented in Figure 3.5. CNT were sonicated with a fixed

amount of superplasticizer and after different ultrasonic energies cement was added and the mini-slump spread measured. It can be seen that the higher the ultrasonic energy applied, the lower the spread. This because the dispersing process of CNT bundles leaves more surface area available for the superplasticizer to adsorb onto, leaving less free superplasticizer to control the rheology of the paste [148]. This type of phenomena creates a scenario similar to that of setting time, where rheological parameters of the composite in fluid state are mostly governed by the dispersing agent used for the CNT, instead of the CNT themselves.

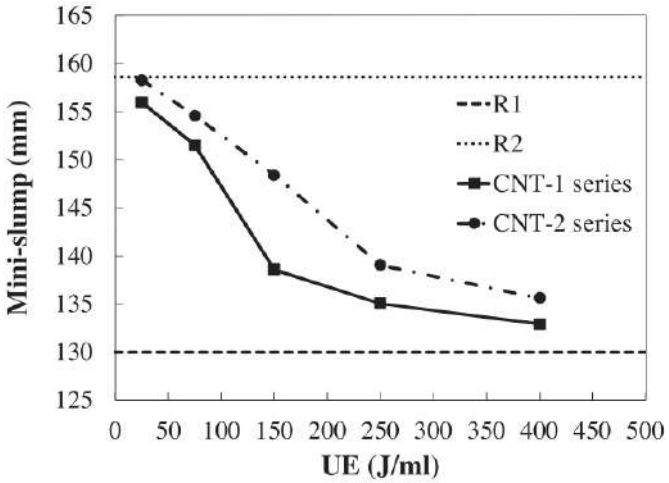

Figure 3.5 - Mini slump spread of Portland cement pastes with superplasticizer and CNT after different sonication energies [148]

Only one report of shrinkage measurements has been found in the literature. CNT have been found to decrease the porosity of cement-based composites at the nanoscale, probably due to filler effects. This decrease in the amount of pores under 40 nm has a direct impact in the water mobility inside the matrix, reducing capillary stresses, which in turn affects the amount of autogenous shrinkage suffered by the composite [79]. This was studied at early ages by longitudinal change measurements, finding a decrease in shrinkage proportional to the amount of CNT in the composite. A summary of the techniques discussed in this section is presented in Table 3.4 -

Table 3.4 - Summary of the techniques used to characterize CNT-cement composites in fresh and hardening state

Parameter	Technique	References
Hydration reaction	Isothermal calorimetry	[69], [119]
Interaction of CNT with hydration products	Fourier Transformed Infrared spectroscopy (FTIR)	[55]
Rheology	Mini slump, flow curves	[45], [145], [148]
Shrinkage	Autogenous shrinkage	[79]

3.6 Characterization and performance of CNT-cement composites in hardened state

Several parameters can be measured to characterize the performance of a CNT-cement composite in hardened state. Mineralogical composition, morphology, microstructure, mechanical properties, electromagnetic properties and durability are some of the properties that control the performance of the composites. A deep understanding of how modifications of these properties affect the overall performance of the composites, will guarantee tailored solutions for each application scenario.

Since CNT are generally used in small amounts, qualitative X-ray diffraction (XRD) patterns from composites with and without CNT will not show significant differences due to the limitations of the technique, and will be useful only to perform a general identification of the mineralogical components of the composite [150]. In the other hand, Thermogravimetric Analysis (TGA) [42] is a more useful tool, because it allows quantifying the influence of CNT over the amount of hydration products due nucleation effects. Some authors have found through TGA that the inclusion of CNT with hydrophilic groups on their surface adsorbed enough water to hamper de hydration of cement and decrease the amount of C-S-H formed [42].

SEM imaging allows a qualitative and quantitative characterization of the dispersion state of CNT within the cement matrix. Through visual inspection or by the application of image processing techniques, it can be identified if CNT are agglomerated around a specific phase or filling the pores [91], or even if they are working as reinforcement. An example of this is presented in Figure 3.6, where CNT can be identified across a micro-crack, acting as “bridges” for the load, enhancing the load transmission through the composite. In Figure 3.7 is shown how identification of

the spatial distribution of CNT throughout the cement composite is constructed using digital image processing techniques. TEM imaging is less commonly used to characterize CNT-cement composites; this because the preparation required for a thin section adequate for electron transmission will remove most of the CNT from the sample. If hydration is arrested at very early ages using cryogenic techniques, samples will not have to undergo through such an extensive preparation, and information such as the distribution of CNT around the anhydrous cement grains can be obtained.

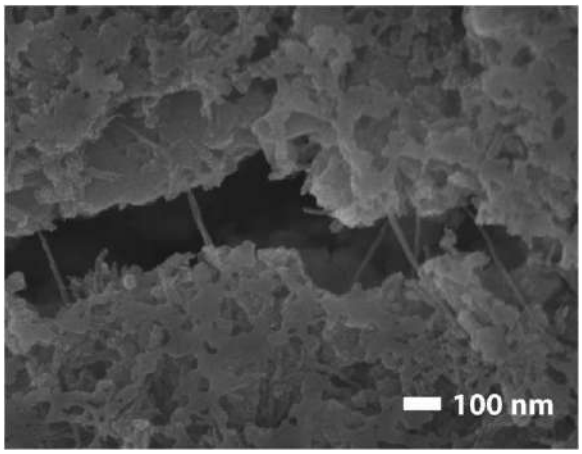

Figure 3.6 - SEM micrograph of CNT bridging a crack in a CNT/cement composite [12]

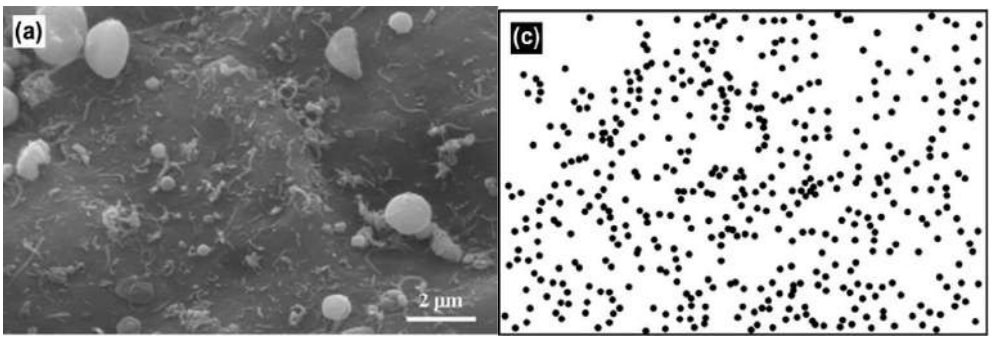

Figure 3.7 - SEM micrograph and distribution of CNT in a cement composite [65]

Due to nucleation and filler effects of CNT, porosity of CNT-cement composites is also modified. This modification generally occurs in the scale of mesopores, i.e. under 50 nm of diameter [55]. Mercury Intrusion Porosimetry (MIP) is capable of identifying these modifications. An example of this is presented in Figure 3.8, where pore size distribution curves from MIP experiments show that cement pastes with CNT have a smaller amount of mesopores than plain cement pastes.

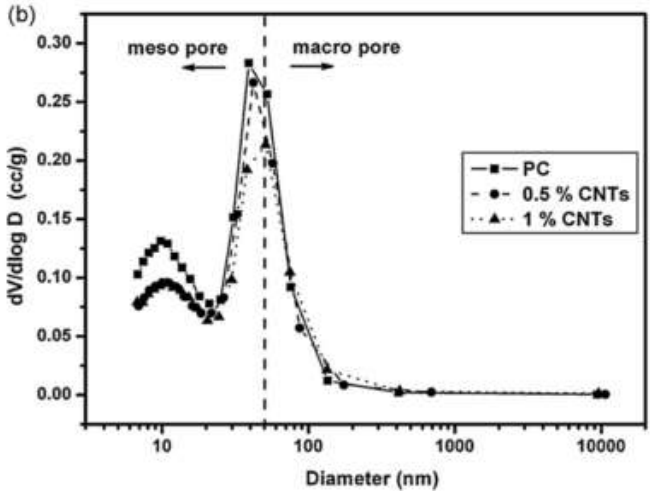

Figure 3.8 - Pore size distribution form MIP results of Portland cement pastes with and without CNT [137]

Mixed reports regarding mechanical performance of CNT-cement composites can be found in the literature. This high variability in performance can be traced back to many extrinsic and intrinsic factors, which have to be carefully taken into account when comparing different studies to define the real effect of CNT. Extrinsic factors causing variability between studies are related to experimental procedures used to fabricate and test CNT-cement composites, while intrinsic factor are related to basic characteristics of CNT and their interaction with the hydration reaction and cement matrix.

The extrinsic factors identified in this review are sample size, sample preparation, testing geometry, testing speed, and type of deformation control. A summary of the different mechanical parameters that have been determined so far for CNT-cement composites, and the type of test employed for each case are presented in Table 3.5. It can be seen that most studies have focused on compressive and flexural strength testing, while very few have reported elastic or fracture mechanics parameters. The most commonly used sample geometries to determine compressive strength of the composites are cubes and half-prisms, while beams and prisms are used to measure flexural strength and elastic or fracture mechanics parameters.

Table 3.5. Summary of measured mechanical properties add testing methods for CNT-cement composites

Parameter	Technique	References
Compressive strength	Cubes	[86], [151]–[155]
	Cylinders	[77], [95]
	Half-prisms	[42], [139], [144], [156]–[159]
Flexural strength	Notched beam in three-point bending	[45], [148]
	Unnotched beam/prism in three-point bending	[42], [62], [79], [96], [139], [144], [151], [152], [155], [157], [159]
	Unnotched beam/prism in four point bending	[156]
Tensile strength	Round bars	[147]
Young´s modulus	Notched beam in three-point bending	[148], [160]–[162]
	Unnotched beam in three-point bending	[79]
Fracture toughness	Unnotched beam/prism in three-point bending	[145], [163]
Ductility	Unnotched beam in three-point bending	[62]
	Direct tension in round bars	[147]
Fracture energy	Notched beam in three-point bending	[148]
Modulus of toughness	Unnotched beam/prism in three-point bending	[62]
Fracture modulus	Unnotched beam/prism in three-point bending	[42]

Regarding sample preparation, three strategies have been identified. The first is to cast 40x40x160 mm^3 prisms from the ASTM C348 standard for mortars or similar [42], [96], [139], [152], [155], [157], [158], [163], which is the most widespread due to high availability of standardized molds. The second is to cast small size beams with lengths under 100 mm, and rectangular or square transversal sections with 10 to 30 mm sides [42], [45], [62], [79], [144], [145], [148], [151], [162], [164]; this reduces the amount of material required for the study without compromising the quality of the results due to the small sized of CNT. The third strategy is to cast a big specimen, which then will be cut into smaller beams using a diamond saw [161]. This strategy is supported on the fact that casting and vibration of small amounts of material is ineffective, and the quality of specimens is significantly worse than the quality reached by cutting from larger bodies [161]; nevertheless, this process might induce micro cracking into the samples, and would not be recommended for samples at early ages.

Three point bending tests in notched and unnotched beams are the most commonly testing geometries used to measure flexural strength and fracture mechanic parameters of CNT-cement composites. Testing speeds reported in the literature were found to be inhomogeneous, varying from 0.5 mm/min [151] to 0.009 mm/min [79], with few studies using any type of deformation control for their bending tests. Crack mouth opening displacement (CMOD) has been used as deformation measurement tool [45], requiring notched beams at mid span. An example of this type of testing setup is presented in Figure 3.9. Four-point bending test in unnotched beams with deformation control by LVDT is an alternative testing setup that has good potential to deliver interesting results and has been little explored. This setup with load application controlled by vertical deformation at mid span allows studying the post-cracking behavior of CNT reinforcement, which is still an open discussion topic. An example of this type of testing setup is presented in Figure 3.10.

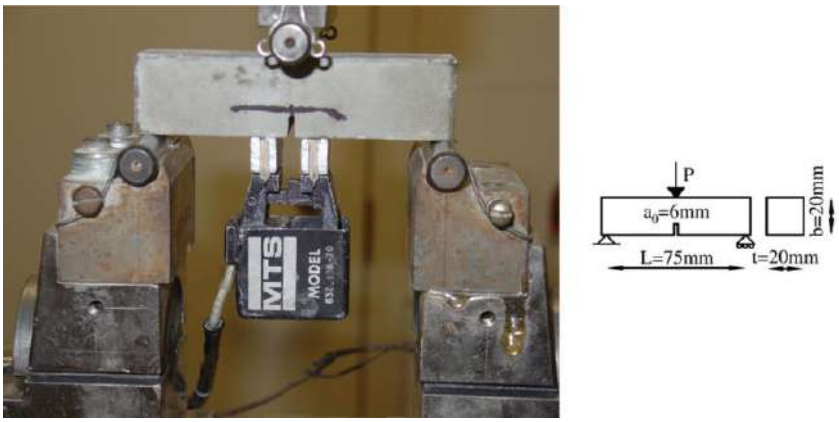

Figure 3.9- Three-point bending test of notched beams (20x20x80mm) with deformation control by CMOD [45]

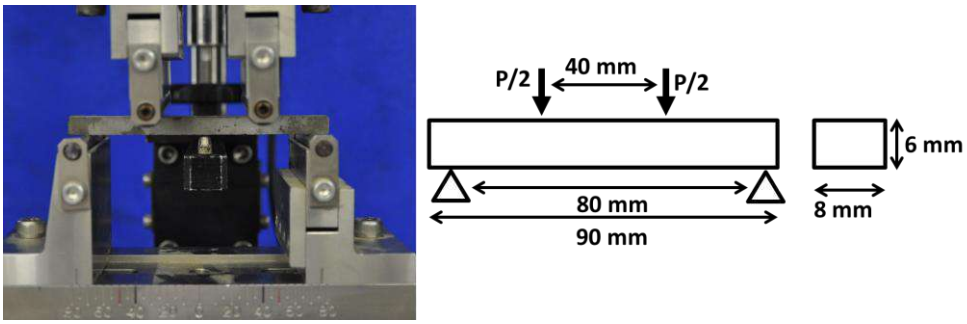

Figure 3.10- Four-point bending test of unnotched beams (6x8x90mm) with deformation control by LVDT

Regardless of the type of geometry used to measure mechanical properties of CNT-cement composites, rigorous mechanical testing procedures are necessary to

obtain accurate and reproducible results. In the initial section of this review, it was identified that highly specialized techniques have been adapted to measure the basic properties and dispersion degree of CNT before and after their inclusion in the cement matrix, due to the complexity of the phenomena involved. However, the techniques used to determine their mechanical performance do not reflect the complexity of this type of nanoreinforcement. Appropriate testing speeds and load control by deformation, whether it is by CMOD, stain gauges, or LVDT, are required to identify potential impacts of CNT beyond ultimate load in flexural strength. Multiple cracking or strain-hardening behaviors of CNT-cement composites still have not been clearly identified nor dismissed as a direct effect of CNT, and further refinement of the testing techniques is required to do so.

The intrinsic factors causing variability between studies identified in this review are nucleation of CNT, competition for additives between CNT and cement, amount of CNT, dispersion degree, aspect ratio, and surface functionalities. These factors are consequence of a combination between the properties of CNT and the dispersant used to guarantee a minimum dispersion degree, and have led to situations where some authors have found increases in compressive strength up to 200% [164], while some others have found decreases down to four times less when compared to a plain cement composite [77]. Increases in compressive strength are usually explained by nucleation effects of CNT [86]. Decreases have been attributed, among other factors, to a competition between CNT and cement for plasticizing additives, which modifies the consistency of the composite in fluid state [148], to agglomerations of CNT that act as stress concentration points [77], and to adsorption of the water contained in the cement mixture by hydrophilic groups on the surface of CNT [42]. Another factor that contributes to the heterogeneity of results is the type of dispersing agent used, which might affect the hydration reaction of cement depending on the amount of CNT and dispersant used [145].

The amount of CNT used is also an important factor. As with other nanoparticles, high amounts of nanotubes have negative effects, while the optimum value of addition is very small [4]. Some authors have studied additions between 0.5% and 2.0% of CNT by mass of cement, finding a deterioration in compressive strength proportional to the amount of CNT [77]. On the contrary, authors studying additions under 0.1% of CNT by mass of cement have found optimum additions, almost doubling the compressive strength of the composite [86].

Reports regarding flexural strength are more homogeneous, most of them showing improvements in both maximum load and maximum deformation. An example of increase in maximum load in a three point bending test on notched beam is presented in Figure 3.11. The maximum load to failure was increased due to the reinforcing effect of the CNT, i.e. due to the bridging effect, but at the same time no increase in deformation was found. This means that the Young´s modulus of the composite increased substantially, obtaining a more brittle material.

The ductility of the composite has been found to be sensitive to the length of CNT; this is presented in Figure 3.12. For all studied cases, the maximum strain was modified by the aspect ratio of CNT and the curing age. Composites with low concentrations of long CNT give a mechanical performance comparable to composites with higher concentration of short MWCNT [62]. This confirms the fact that the aspect ratio of CNT is a key factor to optimize the amount of nanotubes required to obtain a desired performance, and that this parameter must be carefully studied during the dispersion process.

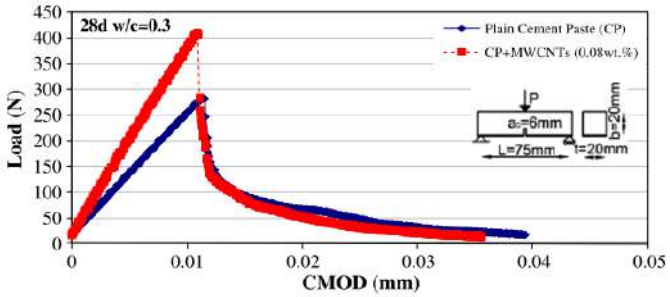

Figure 3.11 - Mechanical behavior of 28 day plain cement paste and cement paste reinforced with 0.08 wt.% MWCNT (w/c = 0.3) [79]

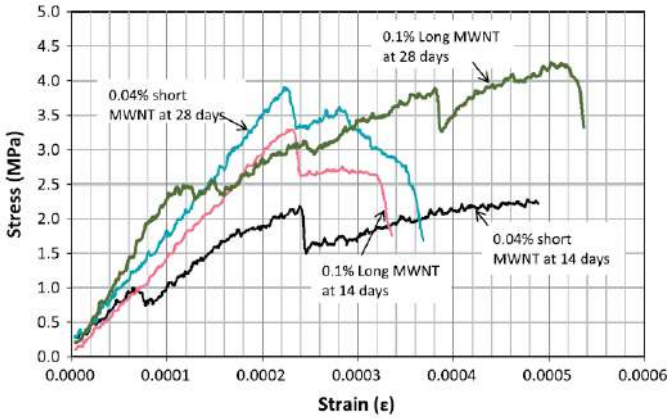

Figure 3.12- Stress–strain diagrams for some samples of the 0.04% short MWCNT and 0.1% long MWCNT at ages of 14 and 28 days [62]

Aspec ratio of CNT is affected by the amount of mechanical energy used to disperse them, consequently decreasing their reinforcing efficency. To illustrate this, a correlation between reinforcing index and dispersion degree is presented in Figure 3.13. In the left of the figure it can be seen how two different amounts of CNT (0.094 wt% and 0.188 wt%) have a similar reinforcing index of flexural strenght, and that this index reaches a maximum at the dispersion plateau. The dispersion plateau was identified using UV-Vis absorbance measurements and is presented in the right of the figure. The onset of the plateau indicates the point at which maximum dispersion has been achieved and beyond this point any energy applied to the system will have only an adverse effect, breaking the CNT and decreasing their aspect ratio. After the dispersion plateau is reached, the reinforcing index starts to decrease as consequence of a shortening process of CNT [148].

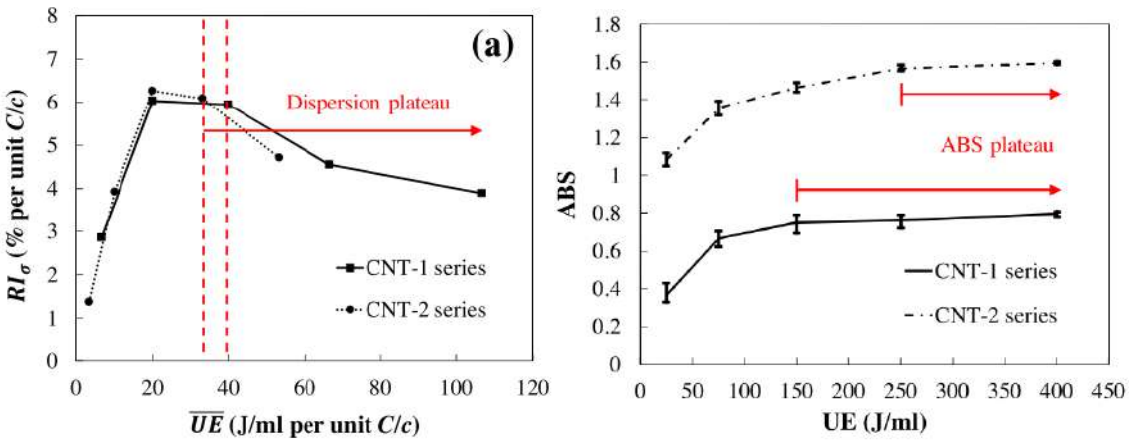

Figure 3.13 - Left: Reinforcing index of flexural strength (RI_σ) of CNT/cement composites per unit of CNT; Right: Absorbance of CNT dispersions with concentration of 0.094 wt% and 0.188 wt% at five different sonication energies [148]

Nanomechanical response of cement composites is also influenced by the presence of CNT, as evidenced by Young´s modulus probability plots of cement pastes with and without CNT, obtained by statistical nanoindentation. The effects of CNT on the porosity of the matrix and kinetics of hydration are reflected in the nanoindentation results, where it can be seen that the probability of Young's modulus below 10 GPa, which corresponds to the porous phase, is significantly reduced for samples with CNT. Also, the maximum of the probability distribution, which fell into the typical Young´s modulus values for low stiffness C-S-H for the plain cement paste, shifted to a higher Young´s modulus zone, characteristic of high stiffness C-S-H. This suggests that the

nucleation effect of CNT favors the formation of high density C-S-H [79]. The actual mechanism by which this shift in density of C-S-H occurs has not yet been identified. Molecular dynamics simulations have identified increases in tensile strength up to 6GPa of C-S-H due to CNT reinforcement in their structure [165]. Probability plots obtained from nanoindentation experiments can be interpreted using deconvolution, which fits a set of Gaussian functions to the experimental results to identify the elastic properties and volumetric fractions of individual phases [30]. The validity of this approach has been questioned by some authors, who found that depending on the experimental parameters, multiple sets of Gaussian functions can be fitted to the same probability plot different results for each individual phase [166], [167]. A summary of the techniques discussed in this section is presented in Table 3.5 and Table 3.6.

Table 3.6. Summary of techniques to characterize CNT-cement composites in hardened state

Parameter	**Technique**	**References**
Mineralogy and phase composition	X-ray diffraction, Thermogravimetric Analysis (TGA)	[42], [150]
CNT distribution in the matrix	Scanning Electron Microscopy, Transmission Electron Microscopy	[12], [62], [65], [91], [137]
Nano-porosity	Mercury intrusion porosimetry	[137][22]
Nano-mechanics	Nanoindentation	[79], [168]

3.7 Durability

CNT have been found to contribute to the durability of cement matrices through different mechanisms. Bridge effect and reduction of capillary porosity help to control crack propagation and reduce autogenous shrinkage. This has a direct effect on durability, since the amount of pathways for aggressive agents to penetrate the matrix are decreased [169]. Most of the traditional techniques to study durability of cement matrixes have been applied to nanocomposites, having evaluated parameters such as capillary water absorption, sulfate expansion, acid attack, freeze-thaw cycles, chloride penetration and ASR. Unfortunately, there are few reports of these techniques having been applied to CNT-cement composites. Need of further work in this area has been identified before, not only for CNT, but in general for nanoparticles used in cement-based nanocomposites [169].

Literature reports on durability of CNT-cement composites have focused on three parameters, transport properties of the matrix, thermal stability and corrosion of reinforcement. Regarding the transport properties of the cement matrix, water permeability, water sorptivity, gas permeability [170] and chloride penetration [171] are the parameters currently studied. In all cases, durability improvements of the composites have been associated to enhancements in the porous structure at the sub-micron and nano scales [22]. Regarding corrosion of reinforcing rebars in CNT-cement composites, it has been found that addition of CNT to the cement matrix could imply the development of higher levels of corrosion in aggressive conditions [159]. This has been related to a lower resistivity of the matrix induced by the presence of CNT [172], which contributes to the corrosion cell, and to the presence of a galvanic couple between the reinforcing steel and CNT [159]. Regarding thermal stability, a study in autoclaved aerated concretes blended with CNT has identified an increase in crystallinity in CNT-cement composites, which lead to an improvement in thermal stability of hydration products and decrease in shrinkage due to heating [143]. A summary of the techniques discussed in this section is presented in Table 3.7.

Several durability parameters have not been reported yet, mostly those related to chemical stability of the matrix and long term deformation, i.e. creep. Nanoindentation studies have indicated potential improvements in durability associated to modifications in Young´s modulus of C-S-H at the nanoscale [79]. This coupled with improvements in the transport properties of the matrix, has the potential to generate composites with higher chemical durability. Sulfate attack, acid attack, accelerated carbonation, freeze-thaw, alkali-silica reaction and calcium leaching are some of the tests that should be performed more extensively in CNT-cement composites.

Table 3.7. Summary of techniques used to study durability of CNT-cement composites

Parameter	Technique	References
Transport properties	Water permeability, water sorptivity of, gas permeability	[170]
	Chloride penetration	[171]
	Mercury intrusion porosimetry	[22], [137]
Electrochemical properties of reinforcement	Carbonation of cement matrix and corrosion by polarization resistance of reinforcement rebar	[159]
	Chloride penetration of cement matrix and corrosion by polarization resistance of reinforcement rebar	[159]
Thermal stability	Thermogravimetric analysis and dilatometry	[143]

3.8 Novel properties and smart materials

An interesting aspect of CNT-cement composites is the use of the electromagnetic properties of CNT to generate smart materials, with elevated mechanical and chemical performance, and also novel properties such as piezoresistivity and electromagnetic shielding. To obtain such properties, CNT must work as a conductive network for electrons throughout the low conductivity cement matrix. Two conditions have to be fulfilled to obtain an adequate conductive network, CNT must be uniformly dispersed and also in a concentration above the electric percolation threshold. When the concentration of conductive fibers increases the composites goes from non-conductive to conductive, and there is a critical amount of fiber concentration where the conductivity of the composite increases drastically several orders of magnitude, this point is known as the percolation threshold [56]. Well dispersed CNT have a very low percolation threshold due to the high aspect ratio, this because they are capable of forming longer continuous conductive paths [173].

Cement paste is electrically conductive by nature, and its resistivity is increased slightly by the addition of silica fume or latex [23]. This electrical conductivity can be enhanced with an electrical conductive admixture such as carbon or metallic fibers that touch each other to form a conductive path, i.e. above the percolation threshold [24]. In this case the electrical conductivity of the composite is governed by the intrinsic

resistivity of the conductive phase and the contacting conduction between fibers. At the scale of CNT, besides contacting conduction it also exists electron tunneling between neighboring nanotubes. This means that electrons are able to flow through the conductive matrix without the need for the CNT to be in contact, given that the layer of material separating them allows tunneling. This layer is called the tunneling gap and is defined not only by the distance between CNT but also by the electrical properties of the material separating them [82]. When a CNT-cement composite is deformed due to compressive load, the overall tunneling gap is decreased and the electrical resistivity of the composite decreases consequently [74], obtaining piezo-resistive behavior.

A typical experimental set-up to measure piezo-resistive properties of a CNT-cement composite is presented in Figure 3.14. There it can be seen that two or four electrodes must be embedded in the matrix, two to measure current intensity and voltage difference, which is called the two-pole method, and four to measure voltage drop and current intensity, which is called the four-pole method [103]. Compressive cyclic load is applied to the sample and resistivity change and deformation are recorded to later construct load versus resistivity and load versus deformation curves. These curves can be used as calibration curves to obtain a self-strain sensing of the composite by increase in piezo-resistivity.

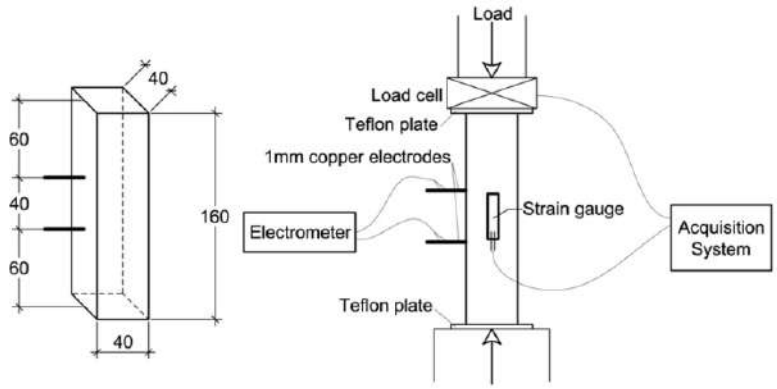

Figure 3.14 - Experimental set-up typically used to measure piezo-resistive behavior of CNT-cement composites in compression using two poles [174]

When using direct current (DC) to measure the piezo-resistivity response of a CNT-cement composite, the capacitance properties of the composite must be taken into account to avoid biasing the results. It has been demonstrated that CNT-cement composites behave as capacitors, storing charge inside them. Even though capacitance is insensitive to compressive loading, it causes an increase in resistivity when measuring it using DC. This can be corrected by subtracting the linear increase of resistivity caused

by the increase of charge, or by using alternate current (AC), which is not sensitive to the effect of capacitor charging of the composite [106]. High values of resistivity in the composite can be consequence of a poor state of dispersion or a low concentration of conductive phase that has not yet reached the electric percolation threshold. AC-impedance spectroscopy is able to differentiate these two states by differentiating changes in the resistivity of the matrix from changes in the resistivity of the composite, discriminating percolation issues from agglomeration effects [73].

Another property exhibited by most cement based composites with carbonaceous inerts is electromagnetic shielding. Two possible mechanisms are capable of generating an electromagnetic shielding effect, reflection or absorption of the waves [175]. For CNT it has been found that shielding effect is mainly caused by wave absorption, and reflection and multiple reflections are negligible [94]. Shielding effect has been studied in a wide range of microwave frequencies, from 0.9 GHz up to 10.0 GHz [176], but the range of frequencies that has generated more interest is from 0.75 GHz to 1.2 GHz, which is used by mobile phone radio access networks [108]. A summary of the techniques discussed in this section is presented in Table 3.8.

Piezo-resistive response has also been identified for other conductive fibers in three-point bending [98], compression and tension, in monotonic, cyclic and impact loading modes [136]. Some of these tests have been replicated for CNT-cement composites, finding promising results. Nevertheless, further work is required to understanding how deterioration of the cement matrix affects the resistivity of the composites and the accuracy of the measurement.

Table 3.8. Summary of techniques used to measure electromagnetic properties of CNT-cement composites

Parameter	**Technique**	**References**
Self-sensing	Piezo-resistivity in compression using two or four poles	[49], [103]–[105], [111], [174], [177]–[179]
	Piezo-resistivity in direct tension using two poles	[180]
	AC-impedance spectroscopy	[73]
	Capacitance	[106]
Electromagnetic shielding	Reflection and absorption loss	[94], [108]

3.9 Conclusions and future perspective

CNT are able to modify many properties of a CNT-cement composite in fresh and hardened state, when an appropriate dispersion of nanotubes is achieved. These multiple effects classify CNT as a multifunctional addition, and its effectiveness should not be judged only in terms of the enhancement of one property, but as a combination of beneficial effects. In fresh state CNT are able to accelerate the hydration reactions by nucleation effect, but in some cases hamper the precipitation of hydrates and worsen the rheology of the fresh composite due to water or superplasticizer adsorption. Also, through the refinement of the porous structure, CNT increase the volumetric stability of the composites by reducing autogenous shrinkage. Compressive strength, flexural strength, ductility and durability are also enhanced due to nucleation and crack bridging effects, but in magnitudes comparable to those obtained by traditional microfibers and pozzolanic microparticles. At the nanoscale, CNT are capable of modifying the nanomechanical response of C-S-H, promoting the formation of more high density C-S-H, which is beneficial for the overall mechanical behavior of the composite. An additional benefit is the enhancement of electromagnetic properties of the cement composites, which are almost nonexistent for plain cement composites, and reach significant levels with the incorporation of nanotubes. Low electrical resistivity, load sensitivity, and electromagnetic shielding in a broad range of microwave frequencies are benefits not exclusive of CNT, but that can be obtained with very low additions of conductive material in comparison with traditional conductive fibers. While many intrinsic factors related to basic characteristics of CNT are harder to control, those related to the dispersion process of CNT and to the dispersing agent used in the fabrication process of composites can be easily addressed, as has been demonstrated in the literature. It is necessary to differentiate the effects of dispersants on cement from the effects of CNT, both in fresh and hardened state.

Even though direct benefits of CNT in composites have been identified, the mechanisms by which they interact with the hydration reaction to modify properties of the cement matrix are not yet fully understood. Better understanding of the interactions between CNT and C-S-H at the nanoscale will allow the development of more efficient composites, targeting the enhancement of multiple properties at the same time. The CNT-cement composite technology must adapt advanced characterization techniques from other areas, and apply rigorously those traditionally used in cement-based

composites, to understand these interactions at the nanoscale and the scaling relations to bring benefits from the nanoscale to the macroscale. Many of the aspects discussed in this review are still matter of open discussion, and require more profound work. Dispersion, stability, mixing, hydration reaction, mechanical properties, durability and piezo-resistivity are some of them.

4. Research problem and methodology

4.1 Conclusions from the literature revision

After a comprehensive literature revision it can be concluded that MWCNT are able to positively modify most of the properties of a MWCNT/cement composite in fresh and hardened state, when an appropriate dispersion of the nanotubes is achieved. Nevertheless, the following gaps in the knowledge were identified:

- It is known that most of the improvements obtained with MWCNT in the known and novel properties of cement based composites are in some way limited by the effective dispersion of MWCNT and their interfacial bond strength with the matrix. A dispersion methodology that guarantees a homogeneous dispersion of CNT throughout the matrix has not been yet found.
- The exceptional properties of the individual MWCNT are being widely underused, making the beneficial effects obtained with them comparable to those obtained with traditional micro and macro fibers. It is not yet clear if simple combinations or functionalization of MWCNT with pozzolanic nano- or micro- particles are able to generate a synergy of positive effects in cement based composites, complementing the weaknesses of MWCNT with the other nanoparticle's strengths.
- Even though the direct benefits of MWCNT in the cement composites have been characterized, the mechanisms by which they interact with the hydration reaction to modify the properties of the cement matrix are not yet fully understood. Better understanding of the interactions of MWCNT with C-S-H at the nanoscale will allow the development of more efficient composites, targeting the enhancement of multiple properties at the same time.
- It is already known that through modification of the physicochemical properties of the cement matrix, MWCNT are able to modify the porosity of cement based composites. Nevertheless, the effect of these modifications on the durability of the composites has not been studied.
- Before advancing in the study of the effects of MWCNT on parameters such as nanomechanics, creep and durability, it is necessary to fully understand the interaction mechanisms between cement, MWCNT and dispersing agents.

4.2 Problem definition

Despite of the exceptional properties of individual MWCNT, there is a gap between the potential benefits expected from numerical simulations and those obtained experimentally. It is not yet clear if the source of this gap is the use of dispersing agents for MWCNT, nor if it can be surpassed with novel dispersion techniques, functionalization methods, or combinations with other nanoparticles.

4.3 Research question

Taking into account the conclusions drawn from the literature revision, the gaps identified in the knowledge, and problem definition, answering the following question will be attempted through this doctoral research:

What are the effects of the triple interaction MWCNT/surfactant/cement on the performance of a cement paste?

4.4 Hypothesis

If surfactants are used as chemical dispersing agents for MWCNT in water, any excess of surfactant will adsorb onto the surface of the anhydrous grains when in contact with cement. This cement/surfactant interaction affects negatively the performance of a cement-based composite, masking the beneficial effects of MWCNT.

4.5 Objectives

- General

  Understand the effects of the triple interaction MWCNT/surfactant/cement on the performance of a cement paste.

- Specific

  - Evaluate the individual and combined effects of MWCNT and surfactants on the mineralogical, rheological and mechanical properties of cement pastes.

- Identify the mechanisms by which MWCNT are able to work as reinforcement in cement pastes.
- Propose a method to mitigate the negative effects of MWCNT/surfactant dispersions on the hydration kinetics of cement paste.

4.6 Reach

This work intends to study the influence of MWCNT, surfactants and pozzolanic micro- and nano- particles on the performance of a cement paste. Three groups of properties will be studied: mineralogical, rheological and mechanical. This will be done using both a commercially available and an in-house prepared MWCNT/surfactant dispersion.

4.7 Methodology

The study of the effect of the MWCNT/surfactant dispersions on the performance of a cement paste was divided in two phases: using a commercially available MWCNT/surfactant dispersion, and preparing MWCNT/surfactant dispersions in-house. The study was divided in two phases because each phase was aimed to fulfil a distinct objective. Phase one focused on understanding the global effect of a commercial MWCNT/surfactant dispersion on the hydration process (Chapter 5), rheology (Chapter 6), mechanical properties and microstructure of a cement paste (Chapter 7); additionally, a methodology to mitigate the negative effects of the dispersion on the hydration kinetics of cement (Chapters 8 and 9) was proposed. Even though the approach used in this phase has the potential to yield very interesting results, the lack of control over the characteristics of the MWCNT/surfactant dispersion is a limiting factor. Thus, the second phase developed a process to obtain dispersions and decouple the individual effects of MWCNT and surfactants on the hydration reaction (Chapter 10), rheology (Chapter 11), and mechanical properties (Chapter 12) of cement paste. This structure is presented as a flow chart in Figure 4.1.

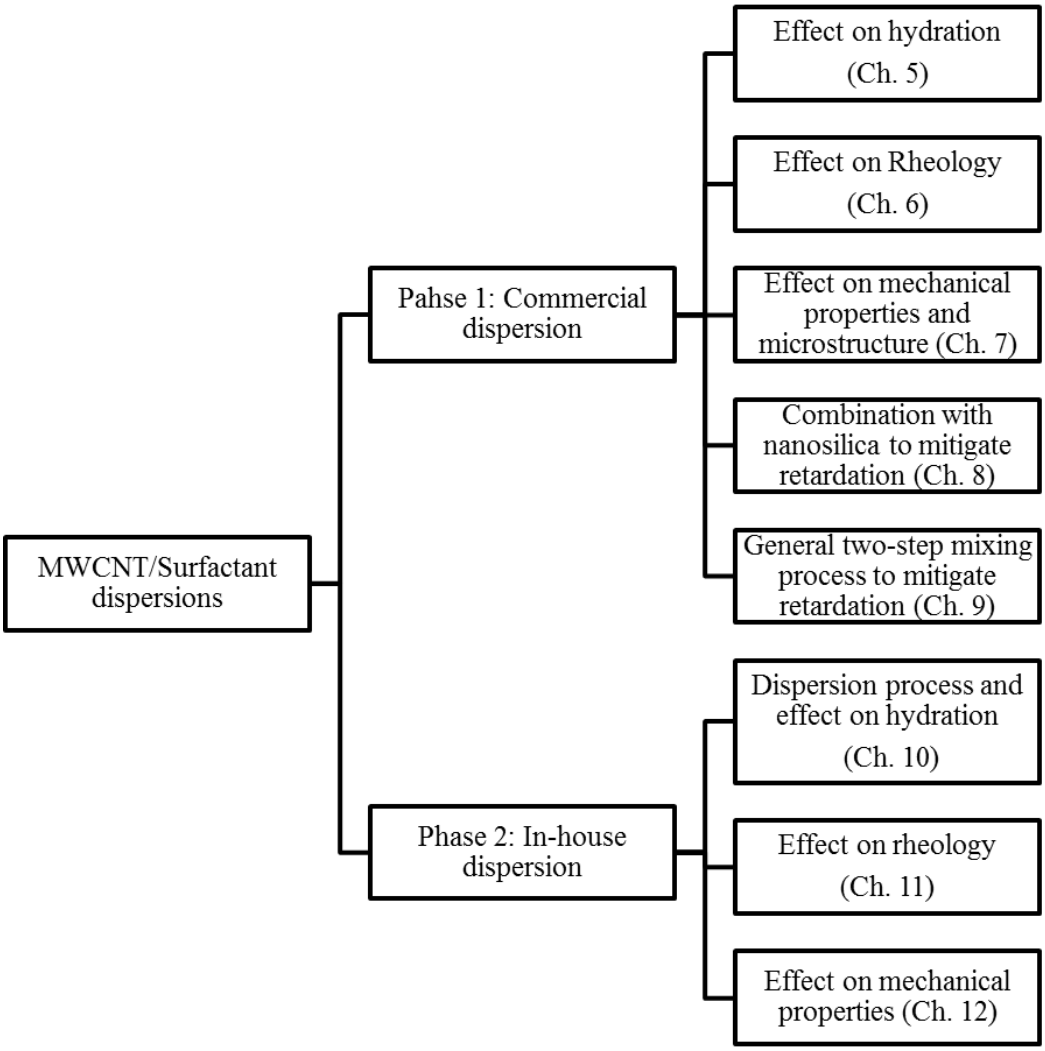

Figure 4.1 – Flow chart of the methodology used in this work

The following is a brief description of the methodologies adopted in each one of the six chapters presented in the flow chart. Specific details of the samples analyzed and experiments carried out can be found within each chapter, since they are self-contained.

Phase 1: Commercial dispersion

- Chapter 5: Commercial dispersion - Effect on hydration

  This chapter presents the first approach to identify the influence of a commercial MWCNT/surfactant dispersion on the hydration process of cement during the first hours of hydration. Different amounts of MWCNT were blended in a

cement paste; isothermal calorimetry and thermogravimetric analysis experiments were performed to identify changes in the heat release kinetics of cement and the amount of hydration products formed. These experiments were carried out at 23 °C and 60 °C to verify the sensibility of the MWCNT effect to temperature.

- Chapter 6: Commercial dispersion – Effect on rheology

  This chapter focuses in understanding the effect of the commercial MWCNT/surfactant dispersion on the rheology of a cement paste by comparing it to other types of micro- and nano- particles. Different amounts of MWCNT, micro silica, nanosilica, metakaolin and nanoclay aqueous dispersions were blended in a cement paste and their effects on the rheological parameters were studied. The roles of compacity and specific surface area of the micro- and nano- particles are discussed in an attempt to find an adequate comparison basis for all particles studied.

- Chapter 7: Commercial dispersion - Effect on mechanical properties an microstructure

  This chapter studies the effect of the commercial MWCNT/surfactant dispersion on the compressive and flexural strength of cement paste. Different amounts of MWCNT were blended in a paste, and their compressive and flexural strengths were measured after 1, 3 and 9 days of hydration. Rheology and microstructural imaging are used to explain the observed effects of MWCNT on the mechanical performance of the paste.

- Chapter 8 - Commercial dispersion – Combination with nanosilica to mitigate retardation

  This chapter proposes a methodology to mitigate the negative effects of the MWCNT/surfactant dispersion on the hydration kinetics of a cement paste. Nanosilica particles were combined with MWCNT before mixing with cement

with the goal of introducing an additional surface onto which the excess of surfactant can adsorb, preventing it from adsorbing onto the surface of the cement grains. The effects of this two-step mixing process on the hydration kinetics and hydration products are evaluated with isothermal calorimetry and thermogravimetric analysis.

- Chapter 9 - Commercial dispersion – General two-step mixing process to mitigate retardation

  This chapter extends the two-step mixing process proposed in the previous chapter to other types of micro- and nano- particles. Nanosilica, microsilica, metakaolin and nanoclay were combined with the MWCNT/surfactant dispersion prior to their mixture with cement. Isothermal calorimetry and ultrasonic pulse velocity test were used to identify the effect of the different combinations tested over the hydration kinetics and setting time of cement paste. Specific surface area of the micro- and nano- particles is used to obtain an adequate comparison basis or all the results.

Phase 2: In-house dispersion

- Chapter 10 - In-house dispersion – Dispersion process and effect on hydration kinetics

  This chapter presents the development of an experimental process to obtain in-house MWCNT/surfactant dispersions, and characterizes their effect on the hydration reaction of cement paste. Three types of surfactants were used in three different concentrations as chemical dispersing aids for MWCNT in a sonication process. UV-Vis spectroscopy and total organic carbon test were used to find the best sonication energy and surfactant concentration. Hydration kinetics and setting time of the paste were measured with isothermal calorimetry and Vicat´s neddle respectively. The individual and combined effects of surfactants and MWCNT on the performance of the paste are presented and discussed.

- Chapter 11 - In-house dispersion – Effect on rheology

  This chapter focuses on understanding the individual and combined effects of MWCNT and surfactants on the rheology of cement paste. The same MWCNT/dispersions developed in the previous chapter were blended into a paste, and their effect on the rheological parameters of the paste was measured. Changes in density and heat release during the first hour of hydration were used to propose a mechanism by which MWCNT/surfactant dispersions affect the rheology of cement paste.

- Chapter 12 - In house dispersion – Effect on mechanical properties

  This chapter is focused in identifying the mechanisms by which MWCNT act as reinforcement in a cement paste. Three-point bending test were carried out in pastes with surfactants and with MWCNT/surfactant dispersions. Linear elastic fracture mechanics and finite elements simulations were used to isolate the real effect of MWCNT on the mechanical behavior of the paste and understand the limitations of their reinforcing effect.

4.8 Materials

The materials to be used in this research were chosen from those available commercially. A summary is presented in Table 4.1.

Table 4.1 - Summary of selected raw materials

Material	Commercial Brand	Manufacturer
Cement	Class G	Holcim
Cement	Class HE	Cementos Argos
MWCNT	AQUACYL 3010 aqueous dispersion of multi walled carbon nanotubes	Nanocyl
MWCNT	NC7000 industrial grade MWCNT in powder	Nanocyl
Nanosilica	Cembinder W50 aqueous dispersion	Akzonobel
Nanoclay	Nanoclay powder hydrophilic bentonite	Sigma Aldrich
Microsilica	Micrometric silica in powder	Camargo Correia
Metakaolin	Metakaolinite powder	Metacaulim do Brasil
TX-100	Laboratory grade triton X 100 of 98% purity	Sigma Aldrich
SDS	Laboratory grade Sodium Dodecyl Sulfate of 96% purity	J.T. Baker
CPC	Laboratory grade cetylpyridinium chloride 100% pure	Sigma Aldrich
VMA	Rheomac UW 410 viscosity modifying agent	BASF Chemicals

4.9 Equipment

The following is a summary of the equipment used throughout this work. Specific experimental conditions can be found in the “materials and methods” section of each chapter presenting experimental results.

Sample preparation

- All mixing of pastes was carried out in a 600mL Chandler constant speed mixer.
- Temperature of the paste was stabilized prior to rheological testing in a 1200 atmospheric consistometer from Chandler.
- Hydration was stopped using liquid nitrogen and a freeze dryer from Liotop.

- Ultrapure water for total organic carbon experiments was obtained from a Milli-Q purification system.
- Dispersions were sonicated using a 500 W ultrasonic processor from Sonics with variable amplitude and programmable on/off cycles.

Chemical and mineralogical characterization

- RAMAN spectra of MWCNT were acquired in a Horiba spectrometer, using a He/Ne laser with a wave length of 632.85 nm and a power output of 3.0 mW.
- FTIR spectra were acquired in an ABB Bomen MB series infrared spectrometer capable of measuring absorption from 400 cm^{-1} to 4000 cm^{-1} with a resolution of 2 cm^{-1} in KBr pills.
- X-Ray Diffraction patterns were obtained using a Θ-2Θ D8 Focus diffractometer from Bruker. The radiation source used was copper (Kα, λ = 1,5418 Å).
- Chemical composition was obtained from EDX spectra using an EDX – 720 Energy Dispersive X-ray Fluorescence Spectrometer from Shimadzu. The equipment is capable of identifying elements from Na to U.
- Thermogravimetric analyses were carried out in a Q500 TGA analyzer from TA Instruments, using a platinum crucible in a N_2 inert atmosphere with a gas flow of 100 ml/min, measured up to 900 °C with a heating rate of 10 °C/min.
- Calorimetry experiments were carried out in a TAM Air isothermal calorimeter, using water as reference material.
- Total Organic Carbon experiments were performed in a TOC-VCSH equipment from Shimadzu with a linear measuring range from 0.2 to 100 mg/l.
- UV-Vis absorbance spectra were acquired with a Genesys 10S UV-Vis spectrophotometer from Thermo Scientific, capable of measuring absorbance from 200 to 800 nm in 0.2 nm steps. A 1.5 mL PMMA cuvette with a 10 mm optical pathway was used as sample holder.

Physical characterization

- Specific surface area was measured using N_2 adsorption isotherms and BET theory in an ASAP 2020 Physisorption Analyzer from Micrometrics.

- Specific gravity was measured in a Helium Pycnometer from Micrometrics.
- Particle size distribution of microparticles was measured by laser diffraction in a Mastersizer 3000 instrument from Malvern Instruments.
- Particle size distribution of nanoparticles was measured by dynamic light scattering in a Zetasizer Nano ZS instrument from Malvern Instruments.
- Surface tension of water was measured using the pendant drop method in a Dataphysics OCA 15EC equipment.
- Ultrasonic pulse velocity of pastes was measured in a 4262 Ultrasonic Cement Analyzer (UCA) from Chandler.
- Electrophoretic ζ-potential measurements were performed in a Zetasizer nanoseries nanoZS from Malvern.
- Density of pastes was measured using a mud balance.

Morphological Characterization

- Low magnification imaging was obtained using a TM-3000 tabletop scanning electron microscopy from Hitachi, equipped with primary and backscattered electron detectors.
- High magnification SEM and TEM imaging was obtained using a scanning transmission electron microscope from FEI and #300 Fomvar copper meshes.

Mechanical characterization

- Compressive strength was measured in a Wykeham Farrance axial testing machine equipped with a 100 kN load cell and a LVDT to measure stroke.
- Flexural strength was measured in a Shimadzu AGX 100 universal testing machine equipped with a 100 kN load cell, capable of measuring stroke, beam deflection by LVDT and crack mouth opening displacement by clip gauge.

Rheological characterization

- Rheology of the pastes was tested using a DV-III Ultra rheometer from Brookfield equipped with a Vane spindle.

PHASE 1: COMMERCIAL MWCNT DISPERSION

5. Commercial dispersion - Effect on hydration

Effect of a commercial dispersion of multi walled carbon nanotubes on the hydration of a cement paste

Abstract

This work studies the influence of a commercial dispersion of multi wall carbon nanotubes (MWCNT) on the hydration of a class G cement paste, at room and elevated temperatures. The MWCNT dispersion is industrially produced with a solid concentration of 3.0 % by mass and an anionic surfactant as dispersing agent. Cement pastes with water to cement ratio of 0.45 and additions of MWCNT by mass of cement up to 0.50 % were produced. Isothermal calorimetry results showed a clear retardation of the hydration of cement caused by the surfactant contained in the MWCNT dispersion. Nevertheless, thermogravimetric evaluations showed that once the hydration reaction resumed, the retardation effect of the surfactant did not have a negative impact on the amount of hydration products precipitated.

Key words: Carbon nanotubes, surfactant, retardation, combined water, C-S-H

5.1 Introduction

Uniform dispersion of multi walled carbon nanotubes (MWCNT) in a cement matrix is one of the key factors to maximize their effect on the matrix properties [45]. MWCNT are usually dispersed in the mixing water of a cement/MWCNT composite, using sonication as the dispersion method. Nevertheless, the effectiveness of sonication has been found to be reversible in time due to reagglomeration phenomena [181]; dispersing agents such as surfactants are used to improve the stability of MWCNT dispersions in water. Relatively high surfactant to MWCNT ratios have been identified as an effective dispersing agent for MWCNT [45]. However, it is known that surfactant molecules adsorb on the surface of anhydrous cement grains [182], and in high

concentrations, lignosulfonates or polyacrilates among others, can hamper the hydration reaction of cement due to steric hindrance caused by the adsorbed molecules of surfactant, generating a retardation in the heat release of the exothermic hydration reaction during the first hours [183]. This work studies how the retardation effect of a commercial dispersion of MWCNT with surfactant as a dispersing agent modifies the kinetics and amount of hydrates produced in a cement paste.

5.2 Materials and methods

The materials used in the experimental campaign were class G and commercial MWCNT pre-dispersed in water with a solids concentration of 3 % by weight. Chemical composition of cement is presented in Table 1. MWCNT were produced using an anionic surfactant as dispersing agent; the specific type of surfactant was not disclosed by the manufacturer of the dispersion. MWCNT had an average diameter of 9.5 nm, and an average length of 1.5 µm according to the manufacturer. MWCNT were characterized using RAMAN, FTIR and energy dispersive X-ray (EDX) spectroscopy and transmission electron microscopy (TEM). RAMAN spectrum was acquired using a He/Ne laser with a wave length of 632.85 nm and a power output of 3.0 mW. FTIR spectrum was acquired from 400 cm^{-1} to 4000 cm^{-1} with a resolution of 2 cm^{-1}, using 0.1 mg of MWCNT and 100 mg of KBr. TEM images were obtained from a 5 µl aliquot of the dispersion that was dropped in a #300 copper mesh and left to dry at room temperature.

A reference sample of plain cement was prepared using a water to cement ratio of 0.45, hand mixing until a homogeneous paste was obtained. Cement/MWCNT pastes were prepared by first combining the MWCNT dispersion with the mixing water, maintaining the same water to cement ratio (w/c: 0.45), then adding cement and hand mixing. A portion of 5 g of each paste was sealed in a glass ampoule and used immediately for isothermal calorimetry at 23 °C and 65 °C. A second portion was cured in 50 ml plastic airtight containers at room temperature or in a 65 °C water bath. When testing age was reached the hydration was stopped using a freeze dryer. Thermogravimetric analyses (TGA) were carried out using a platinum crucible in a N_2 inert atmosphere with a gas flow of 100 ml/min, measured up to 900 °C with a heating rate of 10 °C/min. Calorimetry results were obtained using a TAM Air isothermal calorimeter, using water as reference material.

5.3 Results and discussion

5.3.1 Characterization of the MWCNT

TEM imaging of the MWCNT is presented in Figure 5.1. It can be seen that the length of the MWCNT is in the scale of the micrometers and its width in the scale of the nanometers. Chemical composition obtained by EDX is presented in Table 5.1, results were corrected by loss on ignition, which corresponded to carbon (91.18 %). Al_2O_3 was detected in a proportion that indicates its use as a catalyst during the production of the MWCNT. RAMAN spectrum is presented in Figure 5.2, D and G bands (I_D/I_G = 2.04) characteristic of highly graphitized carbon were identified, additionally the radial breathing mode confirmed that the nanotubes were multi wall. FTIR spectrum of the dispersion is presented in Figure 5.3, absorption bands characteristic of C-C bonds from the MWCNT structure were identified; additionally a group of C-H, -OH and C-O bonds was identified, which correspond to the anionic surfactant used as a dispersing agent. According to the manufacturer the concentration of surfactant was 5.0 % of the total mas of dispersion.

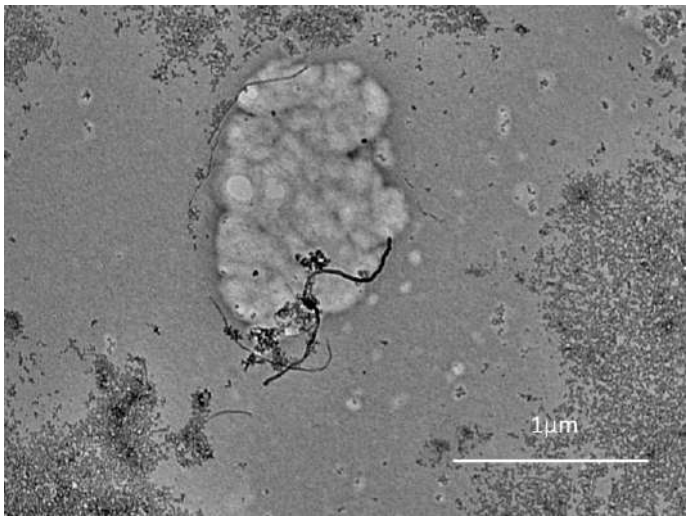

Figure 5.1 - TEM imaging of MWCNT

Table 5.1 - Chemical composition (EDX) and specific surface area of MWCNT and Class G cement

Compound	MWCNT (%)	Cement (%)
Al_2O_3	7.013	3.274
SiO_2	0.532	14.787
SO_3	0.456	4.492
P_2O_5	0.441	-
Fe_2O_3	0.175	5.758
CaO	0.111	70.287
Co_2O_3	0.087	-
Tm_2O_3	0.003	-
K_2O	-	0.585
TiO_2	-	0.296
LOI[a]	91.18	0.521
SSA[b]	250 – 300 m^2/g	300 – 500 m^2/kg

[a]LOI: loss on ignition; [b]SSA: BET Specific Surface Area (according to manufacturer)

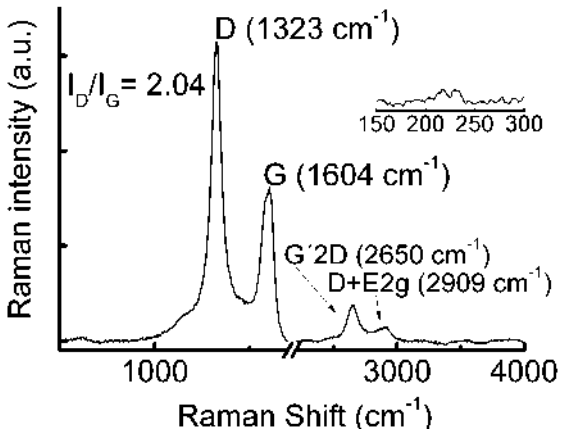

Figure 5.2- RAMAN spectra of MWCNT

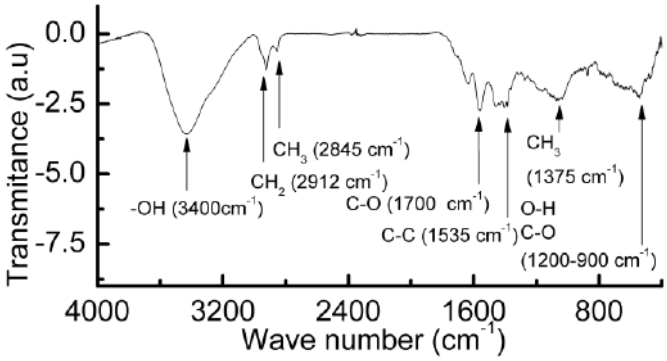

Figure 5.3 - FTIR spectra of MWCNT

5.3.2 Isothermal calorimetry results

Heat flow curves measured at 23 °C (Figure 5.4 (a)) showed that the MWCNT dispersion retarded the hydration reaction, prolonging the induction period up to 15

hours, and delaying the maximum of the main peak of hydration up to 25 hours. This effect was found to be proportional to the amount of MWCNT present in the sample and can be attributed to the surfactant used as a dispersing agent. Additionally, in the heat flow curves it was found that after 50 hours of hydration the peak associated to the formation of AFm was increased in the samples blended with MWCNT; this could be attributed to Al_2O_3 or SO_3 contents of the MWCNT, but still requires further work to confirm.

Heat flow curves obtained at 65 °C (Figure 5.4 (b)) showed a general acceleration of the hydration reaction due to the effect of the temperature, both in the plain cement and in the samples blended with MWCNT. The retardation effect of the surfactant was minimized but still present, indicating that the adsorption/desorption process of the surfactant on the surface of the anhydrous surfaces still occurs, but is accelerated by the temperature. This indicates that the elevated temperature conditions by themselves can partially solve the retardation issue.

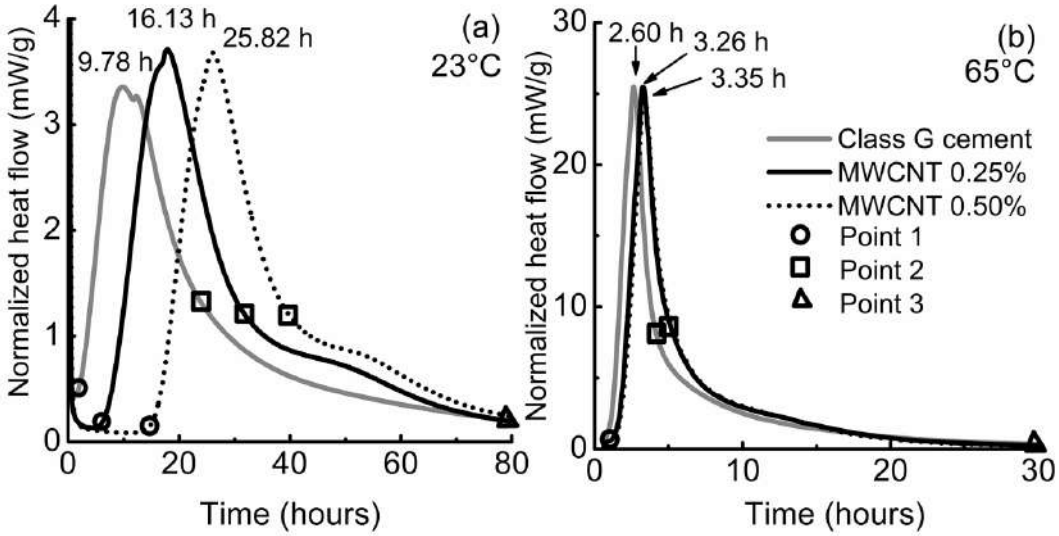

Figure 5.4 - Normalized heat flow curves of cement/MWCNT pastes at (a) 23 °C and (b) 65 °C

Cumulative heat curves measured at 23 °C (Figure 5.5 (a)) showed that even though the hydration reaction was retarded, the total amount of energy released by the samples blended with MWCNT was higher than the one from plain cement. This indicates that when the surfactant´s desorption from the anhydrous surfaces occurs, the hydration reaction is resumed (end of induction period) and accelerated. This can be attributed to a nucleation effect of the MWCNT [51] or to the extension of the induction period [184].

Cumulative heat curves at 65 °C (Figure 5.5 (b)) showed that samples blended with 0.25% MWCNT and 0.50%MWCNT presented approximately the same amount of total heat release as the plain cement sample during the 140 hours of hydration measured, and also reached a heat release plateau quicker than the samples studied at 23 °C. This indicates that the acceleration of the hydration reaction caused by the MWCNT nucleation or the increase of induction period at 23 °C is not significant enough at 65 °C to generate a visible change in the cumulative heat curves.

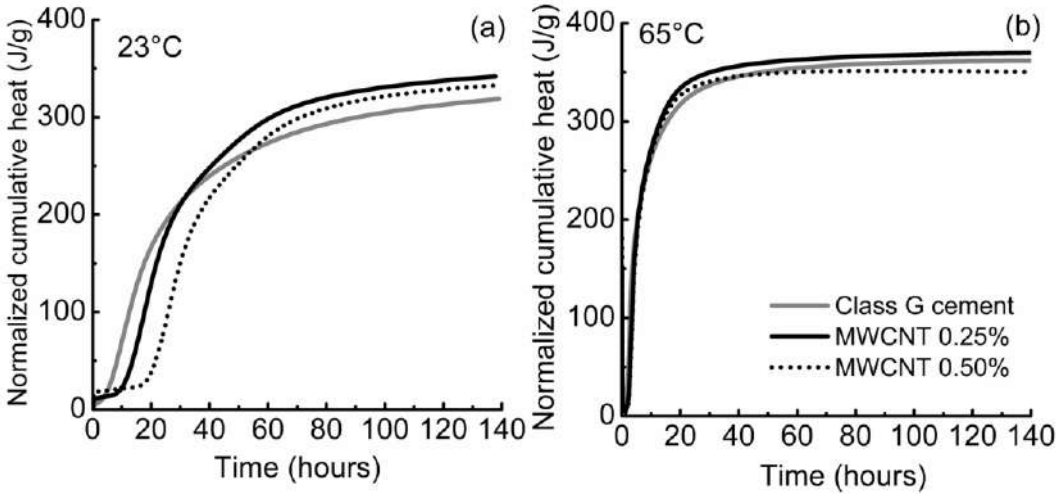

Figure 5.5 - Normalized cumulative heat curves of cement/MWCNT pastes at (a) 23 °C and (b) 65 °C

5.3.3 Thermogravimetric analyses results

TGA were used to confirm the effect of the MWCNT dispersion on the amount of hydration products precipitated during the hydration of the paste. Three points were chosen in each heat flow curve to stop the hydration of the samples: (1) at the end of the induction period, (2) at the end of the main hydration peak, and (3) after the formation of AFm, when all three samples reached a similar heat flow value. This assured that at each point all three samples were in a similar stage of hydration, and helped in the interpretation by decoupling the influence of the dispersant from the influence of the MWCNT. Localization of the points is presented in Figure 5.4.

Two typical TG/DTG curves were obtained, one for samples with hydration stopped before the main hydration peak (point 1) and one for samples with hydration stopped after the main hydration peak (points 2 and 3). Figure 5.6 presents the typical curves obtained and the decomposition reactions associated to each event. Weight fractions for $CaCO_3$ and $Ca(OH)_2$ were calculated. Due to the non-stoichiometric nature

of the C-S-H and the impossibility of separating the individual mass loss associated to the dehydration of gypsum, C-S-H, AFt, AFm and aluminate calcium hydrates (ACH), the weight fraction of these components was not calculated but presented as a mass loss of Total Combined Water (TCW). The $CaCO_3$ weight fraction calculations were corrected by the initial carbonate content of the cement before hydration, and the $Ca(OH)_2$ weight fraction calculations were corrected by the $CaCO_3$ content. Results obtained are presented in Figure 5.7 to Figure 5.9.

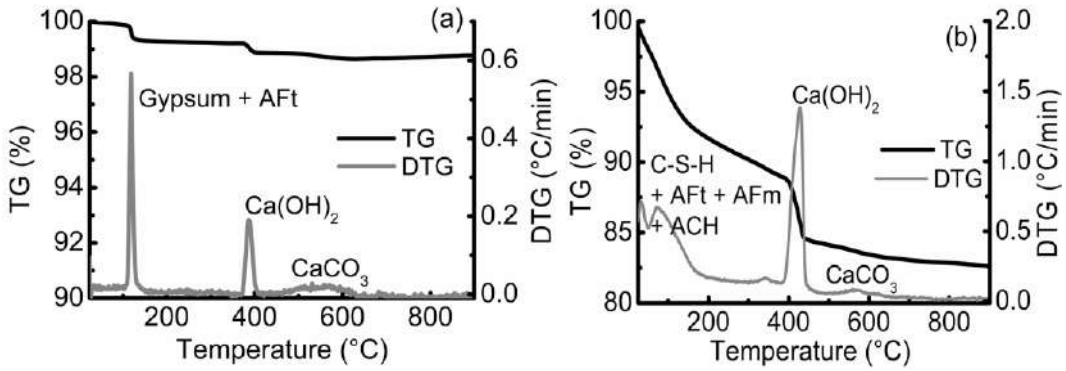

Figure 5.6 - Typical TG/DTG curves obtained for samples (a) point 1 and (b) points 2 and 3

Results from point 1 (Figure 5.7) showed an increase in the amount of $Ca(OH)_2$ both at 23 °C and 65 °C, proportional to the content of MWCNT dispersion and not affected by the temperature. This can be associated with the increase of the induction period caused by the surfactant. The positive slope of the induction period of the different samples presented Figure 5.5 indicates that even though the hydration is retarded, it is not completely hampered, and during this extra time the additional $Ca(OH)_2$ is produced. Results from points 2 and 3 (Figure 5.8 and Figure 5.9) showed that the addition of the MWCNT dispersion did not have a significant effect over the amount of $Ca(OH)_2$ and TCW precipitated, and that these amounts were not modified by the temperature. Additionally, in all three points and at both temperatures, an increase of the weight fraction of $CaCO_3$ proportional to the MWCNT content was found. All samples were stored in similar conditions; therefore, there is no reason to suspect of a differentiated carbonation due to environmental causes. Further work is required to identify the cause of this differentiated carbonation.

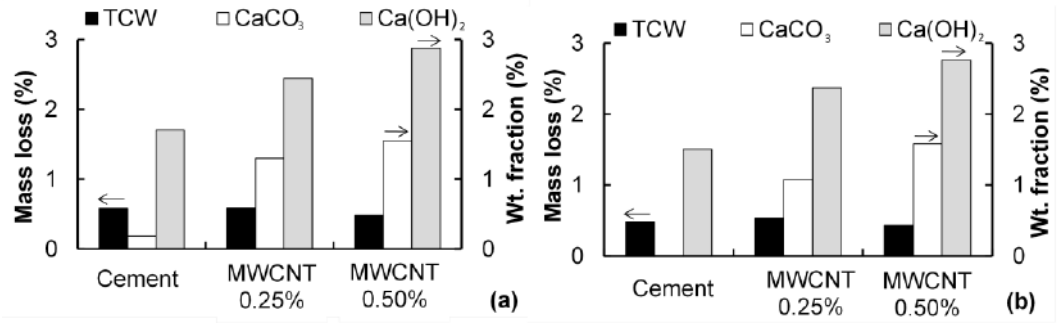

Figure 5.7 - TGA results obtained at the end of the induction period (point 1) of samples cured at (a) 23 °C and (b) 65 °C. (TWC: Total Combined Water)

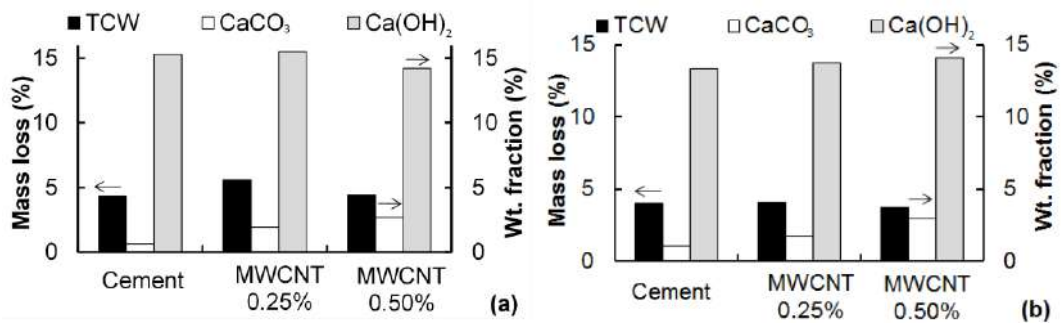

Figure 5.8 - TGA results curves obtained after the main hydration peak (point 2) of samples cured at (a) 23 °C and (b) 65 °C. (TWC: Total Combined Water)

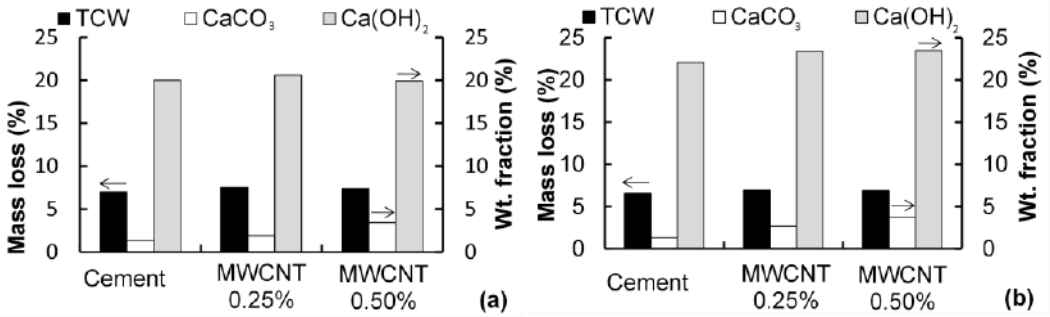

Figure 5.9 - TGA results obtained after the main hydration peak (point 3) of samples cured at (a) 23 °C and (b) 65 °C. (TWC: Total Combined Water)

5.4 Conclusions

The retardation effect of the surfactant did not have a negative impact on the amount of hydration products precipitated, neither at 23 °C nor at 65 °C. This combined with the fact that the retardation was minimized by the elevated temperature, and that the MWCNT maintained its integrity due to a lack of chemical affinity with the cement matrix, allows concluding that the commercial MWCNT dispersion presents a good potential to be applied in cement pastes. Elevating the temperature of the paste can be considered a simple solution for the retardation effect of the surfactant used to disperse MWCNT. The specific type of anionic surfactant used by the manufacturer of the

MWCNT dispersion was not disclosed; some of the behaviors found in this research could be better explained if the specific type of dispersant molecule was known. Further work is required to characterize the effect of this MWCNT dispersion over the rheology, microstructure and mechanical properties of the cement pastes.

6. Commercial dispersion – Effect on rheology

The role of surface area and compacity of nanoparticles on the rheology of cement paste

Abstract

Nanoparticles have a great influence on the rheology of cement matrices due to their inherent physical and chemical properties. This work quantifies the relation between matrix rheology and surface area of nanoparticles (carbon nanotubes, nanosilica and nanoclay), by comparing them with the effects of some equivalent microparticles (microsilica and metakaolin). Class G cement pastes blended with micro- or nano- particles were prepared using a water-to-cementitious material ratio of 0.45 and a viscosity modifying agent to prevent segregation and settlement. Static yield stress, dynamic yield stress, and plastic viscosity were determined to characterize the rheology. The first was measured directly, while the other two were obtained by fitting a Bingham model to the descending portion of a flow curve. It was found that micro- and nano- particle substitutions of similar composition and surface area have similar effects on the rheological parameters, indicating that the influence of nanoparticles is mainly governed by their specific surface area.

Keywords: nanoparticles; rheology; surface area; viscosity; yield stress.

6.1 Introduction

Rheological behavior of cement based matrices is a key parameter for their successful industrial application. Processes such as pumping, pouring, injection, spraying, spreading, and consolidation, among many others, are strongly affected by the rheology of the material [185]. Matrices can be characterized by the particle size distribution of their solid fraction, which ranges from millimeters to micrometers in apparent diameter. The compressive packing model [186] defines the compacity (Φ^*) as the maximum volume fraction of solids (Φ) that can obtained for a given material. The

normalized solid concentration (Φ/Φ*) has been correlated to rheological properties such as plastic viscosity [186], since it reflects how water is distributed around solids and thus modifies the flow properties of the material and affects internal friction due to modifications in solids concentration. The effect on rheology of cement matrices of different nanoparticles, such as TiO_2 [187], Al_2O_3 [188], ZnO_2 [189], cellulose nanofibers [190], graphene nanoplatelets [190], nanosilica [191], [192], nanoclay [193] and carbon nanotubes [145] has been studied to some extent. In most cases significant modifications of viscosity, yield stress and thixotropic behaviors can be encountered. However, changes in compacity and solid concentration are not sufficient to explain those effects.

Due to their small particle size and high specific surface area, nanoparticles have their interactions mainly governed by surface forces [194], such as electrostatic interactions and van der Waals forces, rather than gravity. Specifically, for carbon nanotubes it is not clear by which mechanisms they modify the rheology of a cement matrix, nor if they can be considered a strong modifier of the rheological parameters describing the flow of the material. This work focuses on characterizing the role of surface area and compacity of different micro- and nano- particles on the rheology of cement paste. Additionally, the effect of carbon nanotubes is characterized and compared to the effect of nanosilica, microsilica, metakaolin and nanoclay.

6.2 Research significance

It is not clear (i) if the rheological behavior of cement paste incorporating carbon nanotubes can be fully or partially correlated to the compacity of the solids, (ii) if nanotubes have effects that are comparable to other nanoparticles, and (iii) which role is played by the high specific surface area of nanoparticles in describing their influence on the rheology of the matrix. This work presents an approach to identify the key properties that describe the rheology of cement pastes blended with nanoparticles.

6.3 Experimental procedure

The methodology to understand the rheological behavior of multi walled carbon nanotubes (MWCNT) blended pastes was divided in three stages: (i) production and characterization of aqueous dispersions, (ii) characterization of the rheological behavior of cement pastes, and (iii) characterization of the granular fraction of cement pastes by

compacity measurements. In the first stage, aqueous dispersions of the different types of micro- and nano- particles were produced (nanosilica – NS, nanoclay – NC, metakaolin – MK and microsilica – MS) for comparison with MWCNT. Their basic characteristics (particle size distribution, specific surface area, specific gravity and crystalline structure) were measured. In the second stage, cement pastes blended with different amounts of micro- and nano- particles were mixed, and their rheological parameters were determined by rheometry. In the third stage, the compacities of the raw materials and of the granular fraction of pastes blended with micro- and nano- particles were measured. The final goal was to identify the relationship between rheological behavior of the paste, compacity of the granular fraction and surface area of the blended micro- and nano- particles.

6.4 Materials

The materials used in this work were Class G cement, a commercial aqueous dispersion of Multi Walled Carbon Nanotubes (MWCNT) with an anionic surfactant as dispersing agent, nanosilica (NS), hydrophilic bentonite nanoclay (NC), metakaolin (MK), microsilica (MS) and a cellulose based viscosity modifying agent (VMA).

6.5 Specimens

MWCNT and NS were acquired as aqueous dispersions and were used as received. MS, MK and NC were received as powders and had to be dispersed in deionized water using a 500W ultrasonic processor set to 20% amplitude in 20 second on/off cycles to avoid overheating the samples. The concentration of the dispersions and the amount of energy applied by the ultrasonic tip by mass of particles is presented in Table 6.1. Cement pastes were prepared with a fixed water-to-cementitious material (w/c) ratio of 0.45 and incorporated 0.6% of VMA by mass of cement (bwoc) to prevent segregation or settlement. It is known that a vertical gradient of solids within the paste can cause overestimation of yield stress and viscosity [185]; thus, the most adequate VMA dosage was determined for the reference paste from free fluid and sedimentation tests according to API Recommended Practice 10B-2. Since VMA is capable of modifying the rheological parameters of the cement matrix, its dosage was kept constant throughout all experiments, regardless of the amount of nano- or micro-

particles blended, guaranteeing that the rheological results for all pastes are in the same comparable base.

Table 6.1 – Specific surface area and average particle size of dispersed micro and nano particles (N/A: Not applicable)

Particle	Solid concentration (%)	Dispersion energy (J/g)	Specific surface area (m^2/g)	Average particle size D_{50} (*µm - ** nm)	Specific mass, (g/cm^3)
MS	21.3	440	18.1	9.6*	2.28
MK	21.3	440	18.7	23.1*	2.80
NS	15.0	Pre-dispersed	219.9	32.6**	2.50
NC	2.6	5320	71.7	238.8**	2.28
MWCNT	3.0	Pre-dispersed	208.0	N/A	1.50
CPG	N/A	N/A	0.84	17.4*	3.26

Mixing was carried out in a 600ml constant speed mixer by adding water, VMA and the nano- or micro- particle dispersion and mixing at 500 rpm for 1 minute, then cement was added, and the speed was increased to 2070 rpm during 1 minute and maintained constant for 5 more minutes. After this, pastes were transferred to an atmospheric consistometer set to room temperature and were conditioned for 20 minutes. A summary of the formulations studied for each type of particle is presented in Table 6.2. The solid fraction of the same formulation was used for compacity determination.

Table 6.2 – Summary of formulations studied

Particle	Cement (%)	Solid substitution (%)	VMA (% bwoc)	w/c
Ref	100	0	0.60	0.45
MS	99.39	0.61		
	96.96	3.04		
	93.92	6.08		
	87.80	12.20		
MK	99.81	0.19		
	99.04	0.96		
	98.08	1.92		
	96.17	3.83		
NS	99.95	0.05		
	99.75	0.25		
	99.50	0.50		
	99.00	1.00		
NC	99.95	0.05		
	99.75	0.25		
	99.50	0.50		
	99.00	1.00		
MWCNT	99.90	0.01		
	99.95	0.05		
	99.85	0.15		
	99.75	0.25		

6.6 Items of investigation

Particle size distribution of the dispersions was measured immediately after sonication by dynamic light scattering for the NS and NC dispersions, and by laser diffraction for the MS and MK dispersions. Afterwards, the dispersions were submerged in liquid nitrogen and dried using a freeze dryer in order to obtain powders with similar characteristics to the particles in dispersed state. BET specific surface area of the dried powders was measured using N_2 adsorption isotherms. Specific gravity was measured in a helium pycnometer. X-Ray Diffraction (XRD) patterns were obtained at a 2Θ angle range from 8° to 60°, with a step of 0.01° and an accumulation time of 1 second. The radiation source used was copper (Cu Kα, λ = 1,5418 Å).

Rheology of the pastes was tested at room temperature using a rheometer equipped with a Vane spindle. Four rheological parameters were obtained for each paste: static yield stress (τ_s), yield stress (τ_0), viscosity (μ_0) and hysteresis of the flow curve (H). First, samples were sheared from rest to $0.2s^{-1}$ in 180 seconds, from which τ_d was determined; then, a constant 0.2 s^{-1} shear rate was maintained for 60 seconds to ensure homogeneity of the sample, and finally a flow curve was obtained by increasing the shear rate from 0.2 s^{-1} to 45.2 s^{-1} and back to 0.2 s^{-1} in 20 steps of 30 seconds each. The τ_0 and μ_0 values were determined for each sample by fitting a Bingham model to the descending portion of the flow curve. The H was computed as the difference of area under the ascending and descending portions of the flow curves. H was used as an indicative of thixotropic phenomena induced by the nano- or micro- particles during the time between the beginning and end of the flow curve measurement. It should be highlighted that since this approach to characterize thixotropy is sensible to accelerations in setting time induced by nanoparticles, a fraction of the H value can be related to setting rather than to pure thixotropy. This testing method has been successfully applied before, in a similar equipment, for micro concrete [195] to measure similar parameters.

Experimental compacity (Φ*) of the granular fractions of the samples was measured by water demand tests suggested by DeLarrard [186]. For each sample, solids in a proportion equivalent to 40.0 g of paste were placed in a ceramic bowl. VMA was dissolved in a portion of the mixing water by hand mixing, and then the dispersions and cement were added and mixed with a silicone spatula. Water was added by drops using a syringe, until a funicular state was reached, i.e. when the interparticle spaces begin to

fill with water. The amount of water necessary to reach this state was added to the amount of water in the particle dispersions to compute Φ*, which is the maximum compacity achievable by the granular mix.

6.7 Experimental results and discussion

6.7.1 Particle dispersion characterization

Specific surface area, average particle size and specific mass results for the different dispersions produced are presented in Table 6.1, and the particle size distributions are shown in Figure 6.1. As expected, nanoparticles presented a much higher surface area than microparticles due to their nanometric nature. Particle size distribution was not measured for the MWCNT because results would be representative of their micrometric length instead of their nanometric diameter due to their fiber-like geometry. Results for cement and VMA are also presented for comparison purposes. NC was found to be bigger and to have less surface area than NS. This is due to its platelet geometry, which has two of the three dimensions much larger than the other.

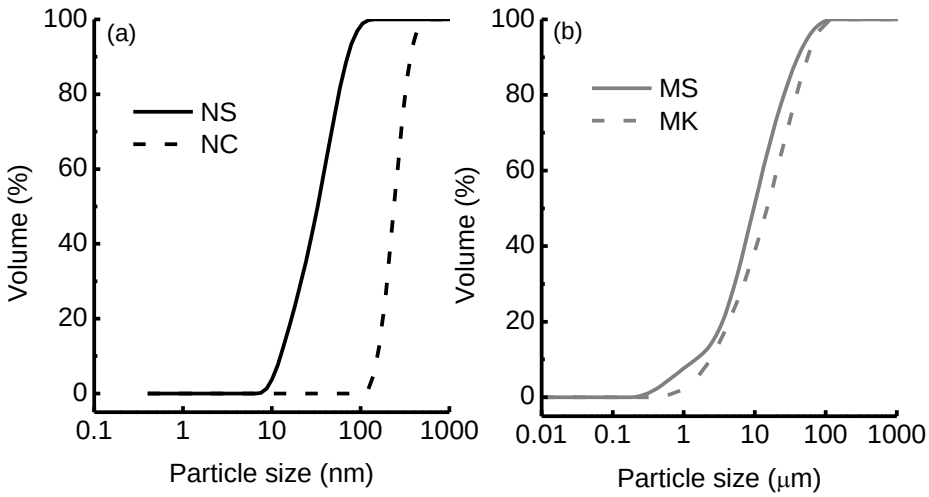

Figure 6.1 – Particle size distribution of (a) NS and NC, and (b) MS and MK

Since the effect of surface area is one of the variables of interest of this study, two pairs of micro- and nano-particles of similar chemical composition (NS with MS, and NC with MK) were coupled through it, i.e. the solid substitutions of MS and MK have equivalent surface areas to the solid substitutions of NS and NC, respectively. XRD patterns of NS, MS, NC and MK are presented in Figure 6.2. NS and MS were

found to be of amorphous nature, characteristic of silica-based pozzolanic materials. MK was found to have an amorphous fraction with presence of some crystalline clay minerals and quartz. NC was found to be composed mainly of montmorillonite, and the low intensity and broad base of the diffraction peaks can be related more with its nanometric size and not with the presence of amorphous material.

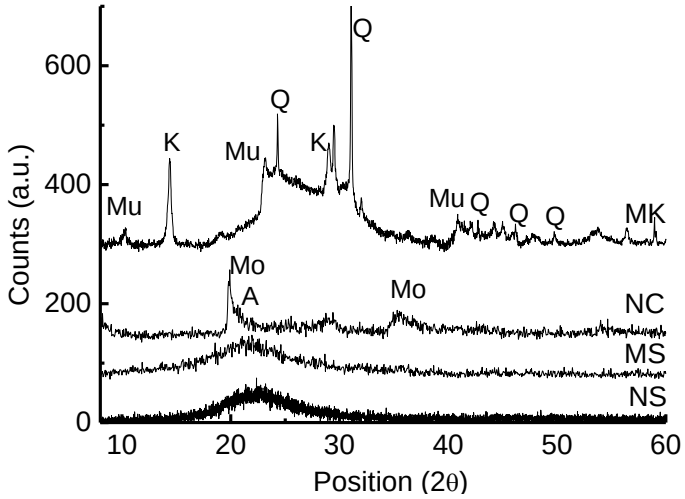

Figure 6.2 – XRD patterns of NS, NC, MS and MK (a.u: arbitrary units). (Mo: Montmorillonite, A: Aluminum silicate, Q: QuartzK: Kaolinite,Mu: Muscovite)

6.7.2 Rheological characterization

A summary of the rheological parameters versus solid substitution of particles for all the tested formulations is presented in Figure 6.3. It was found that both types of particles modify the rheological parameters of the pastes, but small amounts of nanoparticles had a much more pronounced effect than larger amounts of microparticles. In general, increasing the amount of nano- and micro- particles increased $\tau_{s,}$ τ_0 and H; while μ_0 was found to decrease for smaller quantities, before increasing for larger ones. The following is a detailed discussion of the results obtained for each particle type.

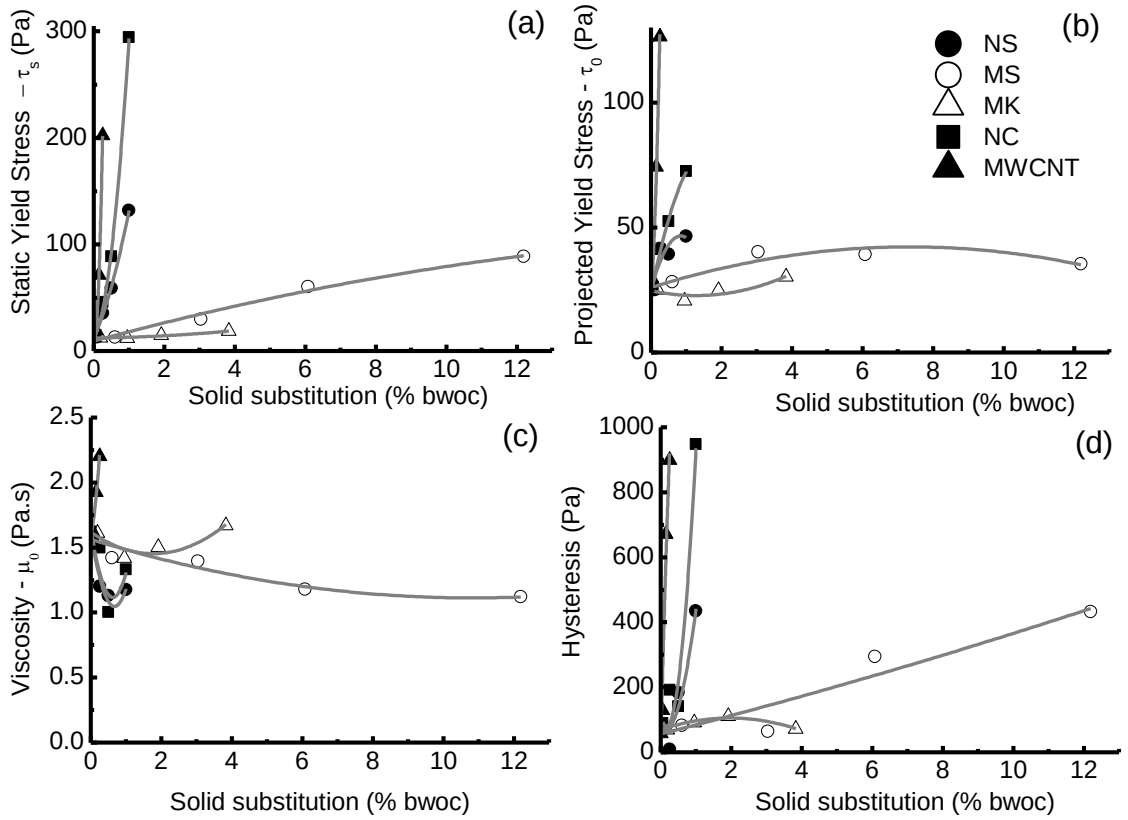

Figure 6.3 – (a) Static yield stress, (b) yield stress, (c) viscosity and (d) hysteresis of cement pastes blended with micro and nano particles versus percentage of solid substitution

MWCNT blended formulations

Static yield stress and flow curves for the MWCNT blended pastes are presented in Figure 6.4. It was found that MWCNT increased all the rheological parameters proportionally to the amount of nanotubes blended in the paste. Additionally, they had the strongest effect in τ_0, μ_0 and H among all particles studied. It should be noticed that MWCNT were purchased as an aqueous dispersion containing an anionic surfactant as dispersing agent of specific nature not disclosed by the manufacturer. It is known that to obtain an adequate dispersion degree of nanotubes it is necessary the use of chemical dispersing agents [196]. Surfactants used as dispersing agents can influence the rheological properties of cement pastes at some extent [145] by adsorbing on the surface of cement grains [182]; thus, a portion of the observed effects should be associated with the nanotubes, and other portion with the surfactant used as dispersing agent.

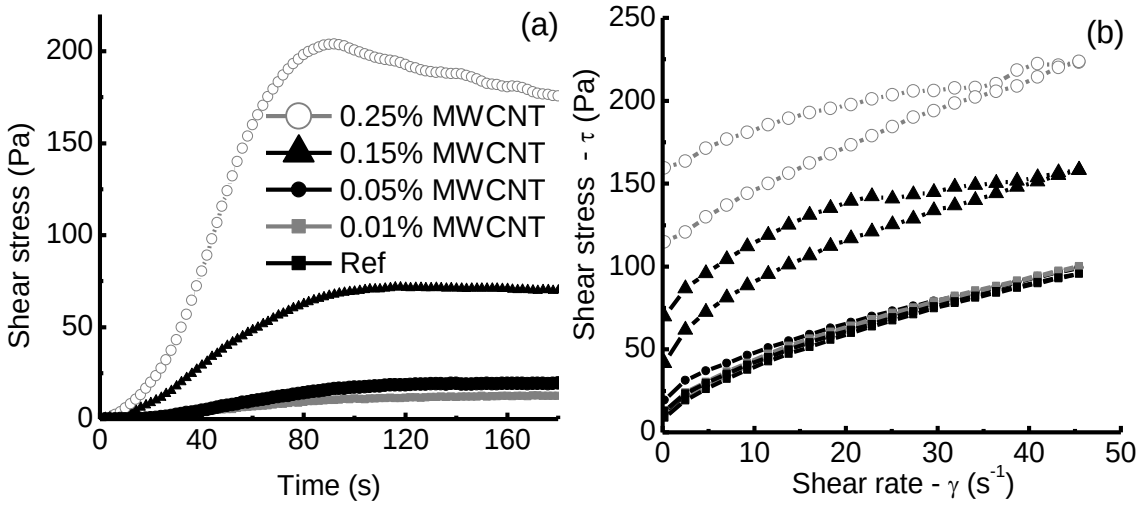

Figure 6.4 – (a) Static yield stress and (b) flow curves of cement pastes blended with MWCNT

MK blended formulations

Static yield stress and flow curves for the MK blended pastes are presented in Figure 6.5. MK was found to have almost no effect on the rheology of the paste when compared to the other investigated systems; only marginal changes in τ_s, τ_0, μ_0 and H were found. MK has a high surface area compared to cement, and is expected to increase the water demand and packing density of cement based matrices [197]. This can lead to viscosity increases and thixotropic behavior [198]. Nevertheless, the amounts of MK used in this work can be considered small to induce sensible changes in the rheology of the pastes [199]. It is worth noticing a decrease in viscosity induced by the lower MK substitutions, which is compatible with literature reports for other types of cement based matrices blended with MK [200].

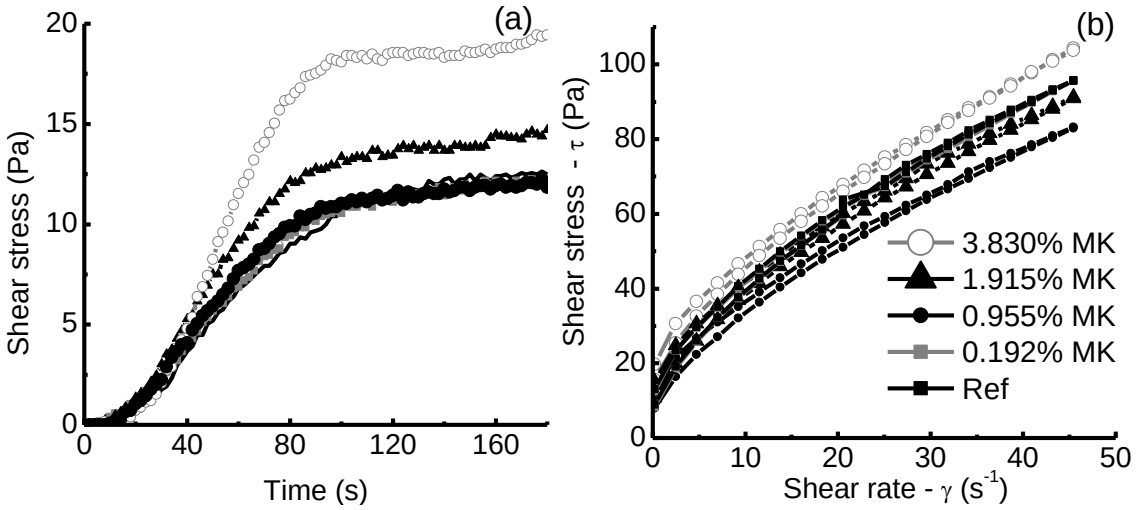

Figure 6.5 – (a) Static yield stress and (b) flow curves of cement pastes blended with MK

MS blended formulations

Static yield stress and flow curves for the MS blended pastes are presented in Figure 6.6. MS was the particle with the broadest solid substitution range studied, going up to 12.30%. The effect of MS was found to be more significant the one from MK, but still was lower than the effect of nanoparticles. Increases in τ_s, τ_0, and H proportional to the MS substitution were identified, while μ_0 decreased consistently throughout the range of MS blends. This fluidification effect has been widely reported in the literature as a consequence of the spherical shape of the silica particles [197] that causes a ball-bearing effect, and to increases in the packing density of the granular fraction [201]. The increases in τ_s, τ_0, and H have been associated with the porosity, surface roughness and surface area of the particles that increase water demand [202].

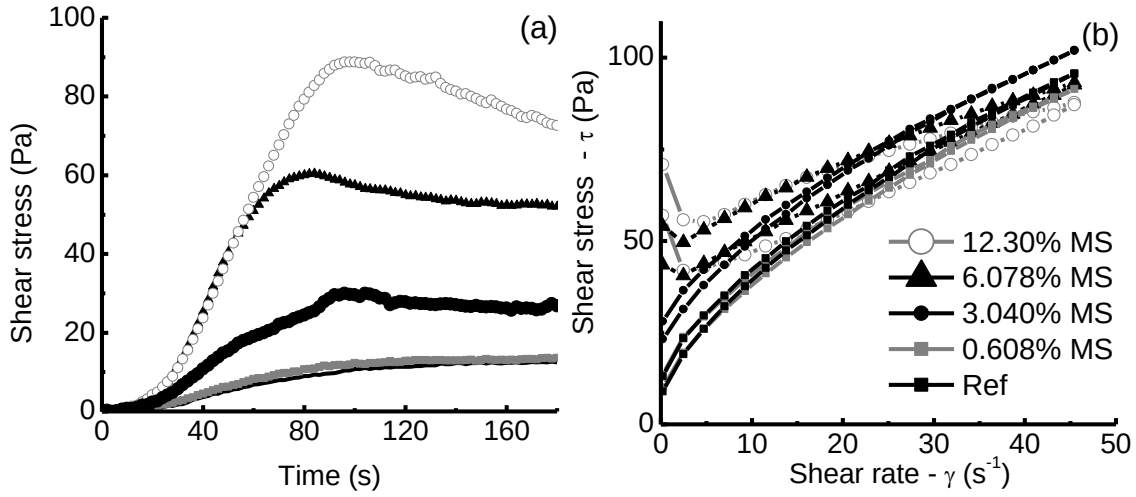

Figure 6.6 – (a) Static yield stress and (b) flow curves of cement pastes blended with MS

NC blended formulations

Static yield stress and flow curves for the NC blended pastes are presented in Figure 6.7. NC was found to have the highest impact on τ_s and H among all particles studied. Literature reports have shown similar behaviors attributed to flocculation of the clay particles [203], high water adsorption, or possible interaction between the clays and ettringite [204]. It has also been found that some clays lower the maximum packing fraction of the granular fraction [205].

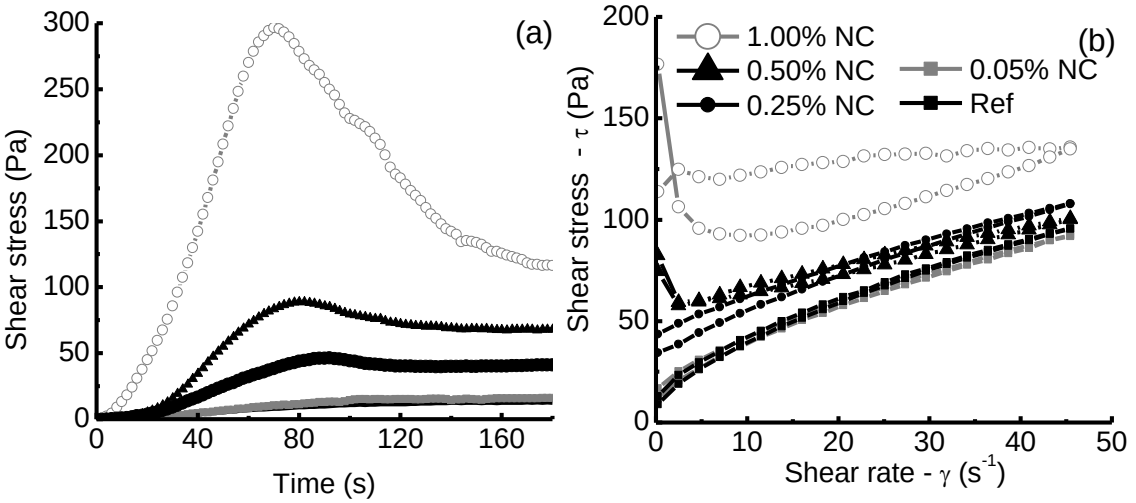

Figure 6.7 – (a) Static yield stress and (b) flow curves of cement paste blended with NC

NS blended formulations

Static yield stress and flow curves for the NS blended pastes are presented in Figure 6.8. The effect of NS was found to be similar to the effect of MS but of much

higher magnitude. Increases in τ_s, τ_0, and H were proportional to the amount of NS substitution, and a concave behavior in μ_0 was identified. Similar behaviors have been reported for cement mortars blended with NS [192], and have been related to a reduction of water demand by NS due to improvement of the voids fraction [206], i.e. increase in compacity and reduction of solids concentration. Due to its nanometric nature, the surface energy of the NS particles (ζ-potential) must also play an important role in how it interacts with cement grains and how effectively it fills voids, or even if it generates a ball-bearing effect.

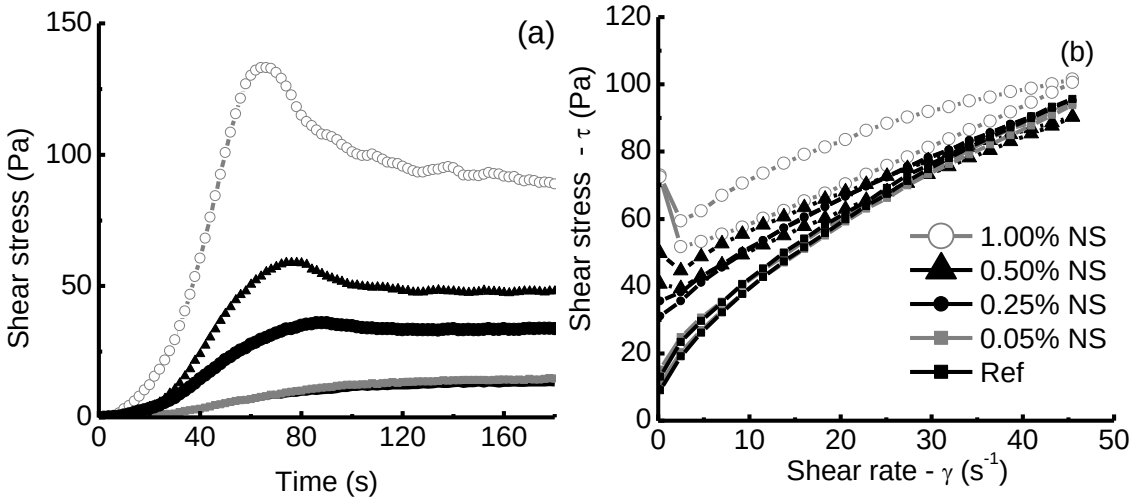

Figure 6.8 – (a) Static yield stress and (b) flow curves of cement pastes blended with NS

6.7.3 The role of surface area

To understand the role of the surface area of micro- and nano- particles on the rheological behavior of cement pastes, specific surface area results were used to calculate the available surface area of blended particles in 300 cm^3 of paste. This was plotted versus τ_s, τ_0, μ_0 and H, and is presented in Figure 6.9. Since cement has such a low surface area compared to the blended particles, the effect of removing some surface area by the solid substitution was considered negligible. Remember that the pairs of particles NS/MS and NC/MK are coupled through their surface area, i.e. the solid substitutions of MS and MK have equivalent surface area to the solid substitutions of NS and NC, respectively. It was found that when compared by surface area, the effect of MS and NS in all the rheological parameters overlapped. X-Ray diffraction results showed that MS and NS were both completely amorphous, and since they are silica-based materials, the only difference between them appears to be their particle size and

specific surface area. The MK and NC effects on rheology showed similar tendencies but did not overlap, regardless of the compatible surface areas of the amounts blended. This may be related to the fact that, even though MK and NC are both mainly clays, they presented different mineralogy and different degrees of crystallinity, leading to distinct surface properties. MWCNT were found to have an effect on the rheological parameters similar to NC, which has its interaction with cement governed by flocculation [203] and presents high water adsorption.

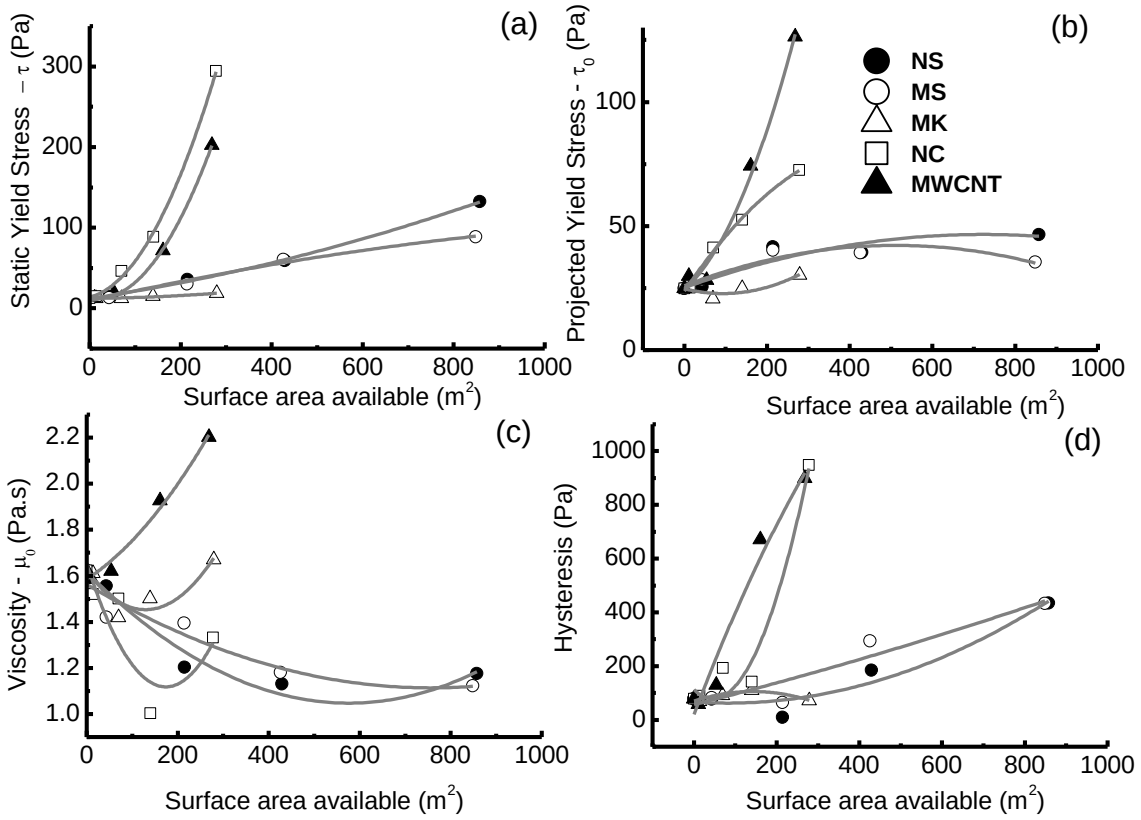

Figure 6.9 – (a) Static yield stress, (b) yield stress, (c) viscosity and (d) hysteresis of cement pastes blended with micro and nano particles versus surface area available

6.7.4 The role of compacity

To verify if the experimental compacity (Φ*) is able to explain the influence of micro- and nano- particles on the rheology of the pastes, water demand tests were first carried out for the raw materials; results are presented in Table 6.3. MWCNT and NS were found to have a much lower Φ* than the others. This means that they are able to fill only a small fraction of a unitary volume due to their nanometric nature and strong inter-particle interactions. NC was found to have Φ* that was closer to microparticles than nanoparticles. This may be interpreted as an evidence of agglomeration. MS, MK

and cement presented typical Φ* values for the respective classes of materials. The interaction of blended micro- and nano- particles with cement was also studied thorough measurement of Φ*; results are presented in Figure 6.10. In all cases, the reference sample was cement with 0.60% VMA by mass of cement. Different volumetric additions of each particle were blended to determine their influence on Φ*. As expected, MS and MK increased Φ* proportionally to the volume blended into the sample. For a constant amount of water, this can result in more water available to coat the grains and the viscosity should decrease. NS, NC and MWCNT did not induce significant changes of Φ* in the range studied, since the amounts used were minimal. On the other hand, these nanoparticles have the most influence on the rheological behavior of paste. This demonstrates that compacity does not fully describe the rheology of cement pastes blended with nanoparticles.

Table 6.3 – Compacity results of raw materials

Particle	Compacity (Φ*)
MS	0.37
MK	0.40
NS	0.15
NC	0.37
MWCNT	0.07
CPG	0.54
VMA	0.19

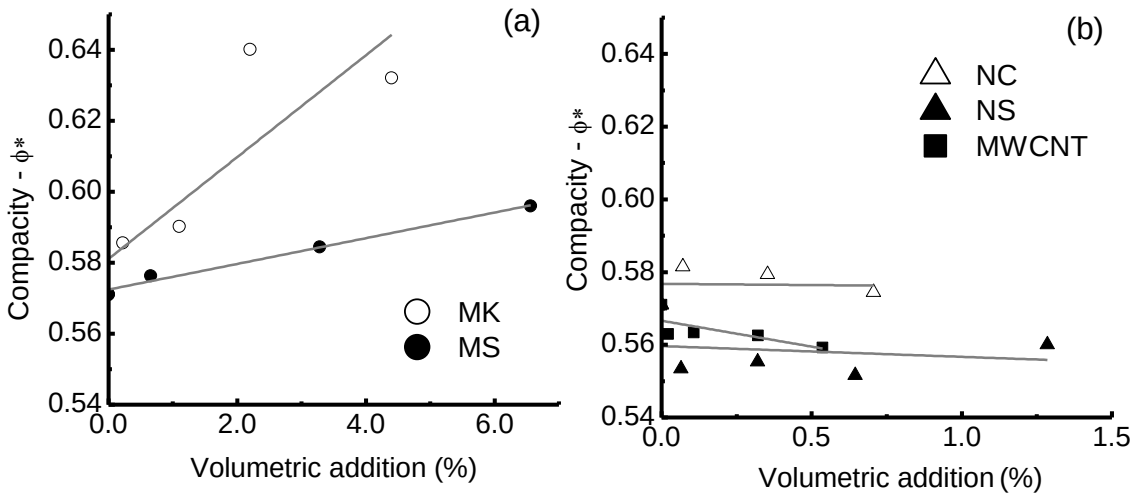

Figure 6.10 – Experimental **c**ompacity (Φ*) of cement blended with different volumetric additions of (a) MS and MK, and (b) NC, NS and MWCNT

The normalized solids concentration Φ/Φ* is presented in Figure 6.11. This ratio represents how close the sample is to the maximum compacity of the solid fraction. If Φ/Φ* increases, viscosity should also increase, until no flow is possible when Φ/Φ* is one. MS, MK and NC decreased Φ/Φ*, while NS and MWCNT increased it. This is not consistent with rheological observations of this work, further suggesting that other factors such as morphology and surface wetting govern the rheology, besides compacity.

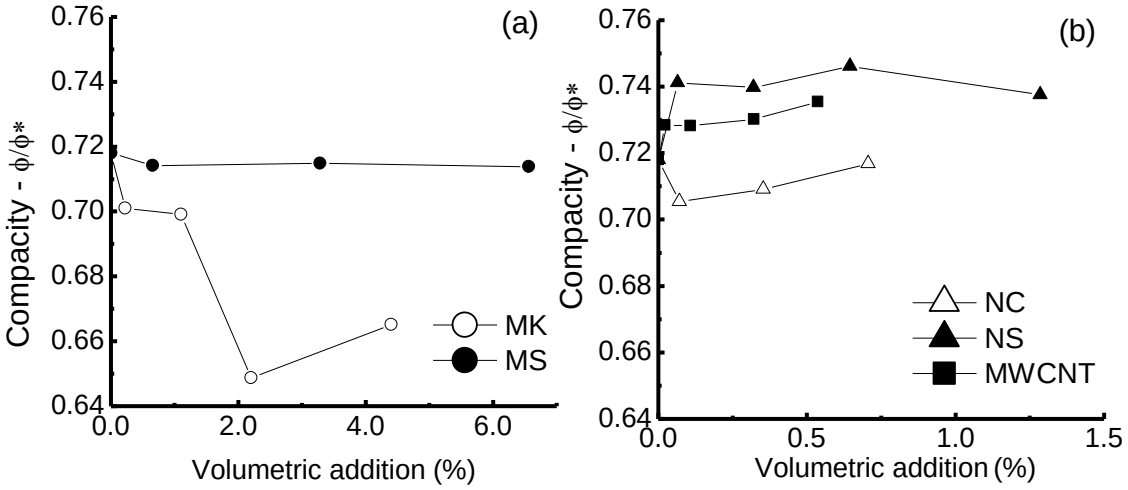

Figure 6.11 – Normalized solids concentration (Φ /Φ*) of cement blended with different volumetric additions of (a) MS and MK, and (b) NC, NS and MWCNT

6.8 Summary and conclusions

This work showed that, contrary to observations of micro- and macro- particle additions to cement pastes, compacity and normalized solids concentration do not explain the influence of nanoparticles on the rheological behavior of cement pastes. These are associated only with the volume that nanoparticles are capable of filling in the granular matrix, ignoring surface interactions between particles. Compacity results of the raw materials showed that nanoparticles are able to fill only a very small fraction of the total volume, demonstrating that factors beyond geometrical interference are at play, as expected; these factors are not captured by either compacity or solids concentration.

A compatibility of the effect on rheological behavior of cement pastes between nano- and micro- particles was identified through the specific surface area of the particles. This compatibility was only found for particles of similar chemical and mineralogical composition, regardless of their particle size, i.e. MS and NS. When interpreting the effect of nanoparticles prone to agglomeration or flocculation (NC and

MWCNT), not only their effective specific surface area but also their dispersion degree, which is directly related to their surface area, must be taken into account. Here, dispersion degree should be seen as the presence of individual nanoparticles of high surface area, rather than agglomerates of lower surface area. Additionally, the presence of chemical dispersing agents to improve the dispersion degree of MWCNT has the potential to further influence the rheology of the paste, masking the real effect of this type of nanoparticles and making more difficult to compare it to other types of micro- and nano- particles.

7. Commercial dispersion – Effect on mechanical properties an microstructure

Effect of a MWCT/surfactant aqueous dispersion on the rheological and mechanical properties of Portland cement pastes

Abstract

Multi walled carbon nanotubes (MWCNT) are expected to enhance the load transfer and increase the flexural strength of a MWCNT-cement composite by working as “bridges” for load across cracks. For this, an adequate dispersion degree of nanotubes throughout the matrix must be obtained, being surfactants one of the most used chemical dispersing aids to attain this goal. A commercial MWCNT/surfactant aqueous dispersion was used to produce cement pastes with MWCNT additions up to 0.25% by mass of cement. Rheological behavior and mechanical performance were used to characterize the influence of nanotubes on the cement paste. It was found that the MWCNT/surfactant dispersion studied decreased the workability and mechanical properties of the cement paste, regardless of micrographs showing that MWCNT acted as bridges across submicrometric cracks. This was due to a delay of the hydration reaction of cement and an increase of the amount of entrapped air caused by the presence of surfactant. It was concluded that the reinforcing effect of nanotubes was masked by the negative effects of the surfactant on the mechanical performance of the matrix.

Keywords: Carbon nanotubes, surfactant, cracking, strength, bridge effect

7.1 Introduction

Surfactants are commonly used as chemical dispersing aids for multi walled carbon nanotubes (MWCNT) in water [207], but little work has been done to identify if the molecules used to disperse the nanotubes are able to interact with the cement grains

and modify the hydration reaction and performance of the cement based nanocomposites. It has been reported in the literature that the surfactant contained in MWCNT/surfactant dispersions is able to modify the rheological behavior of polymer and cement based matrices [145]. Nevertheless, it is not clear how this affects the reinforcing efficiency of MWNCT in a cement based matrix.

It has been reported that MWCNT/surfactant dispersions can retard the hydration reaction of cement by delaying the end of the induction period [119], and that this effect can be associated to the adsorption of surfactant on cement grains [182]. Additionally, surfactants can increase the amount of entrapped air in the matrix by adsorbing on the liquid-air interface of air bubbles, stabilizing them within the matrix [31]. These two effects can modify the overall mechanical behavior of a cement matrix and interfere with the reinforcing efficiency of MWCNT. This work studies the reinforcing effect of MWCNT in a Portland cement paste using a commercial MWCNT/surfactant aqueous dispersion.

7.2 Materials and methods

The materials used in the experimental campaign were class G cement, a cellulose based viscosity modifying agent (VMA), and a commercial aqueous dispersion of Multi Walled Carbon Nanotubes (MWCNT) with a solids concentration of 1% by mass and an anionic surfactant as dispersing agent. The specific type of surfactant was not disclosed by the manufacturer.

Imaging from MWCNT was obtained using a scanning transmission electron microscope (STEM) in bright field transmission mode with a 75 kV acceleration. The MWCNT commercial dispersion was diluted by a 1:200 factor in deionized water and dropped in a copper #300 Formvar mesh. This was left to dry in a desiccator before imaging.

A reference paste was produced with a fixed water-to-cement ratio (w/c) of 0.45 and 0.60% of VMA, also by mass of cement. VMA was used to prevent segregation or settlement of the paste during rheological testing. VMA dosage was determined from static sedimentation tests according to API Recommended Practice 10B-2, and was kept constant for all pastes tested. Four additions of MWCNT by mass of cement were tested (0.01, 0.05, 0.15 and 0.25%). Pastes were produced in a 600 ml constant speed mixer. Water, VMA and MWCNT were mixed for 1 minute at 500 rpm, then cement

was added and speed was increased to 2070 rpm during 1 minute. Mixing was kept for 5 more minutes, and immediately after, pastes were conditioned in an atmospheric consistometer at 150 rpm for 20 minutes at room temperature.

Rheology of the pastes was tested using a rheometer equipped with a Vane spindle. Samples were sheared from rest to 0.2s-1 in 180 seconds. Then, a constant 0.2 s-1 shear rate was maintained for 60 seconds to ensure homogeneity of the sample, and finally a flow curve was obtained by increasing the shear rate from 0.2 s^{-1} to 45.2 s^{-1} and back to 0.2 s^{-1} in 20 steps of 30 seconds each.

Pastes were poured in 25.0 x 50.0 mm cylindrical molds for compressive strength testing, and in 6.0 x 8.0 x 90.0 mm prismatic molds for flexural strength testing. A set of samples from each paste were tested after 1, 3 and 9 days of curing. After 24 hours in the molds, the samples were demolded and submerged in lime saturated water until testing age. Compressive strength was measured in an axial testing machine equipped with a 100 kN load cell and a LVDT to measure stroke. The load application rate was varied to maintain a fixed 0.04 mm/min stroke rate throughout the test. Flexural strength was measured in a universal mechanical testing machine equipped with a 5 kN load cell with a four-point bending setup. A LVDT was placed under the beam at midspan to measure deflection; this value was used to control the load application rate to maintain a fixed 0.15%/min deflection rate. Images of the setups used for mechanical testing are presented in Figure 7.1.

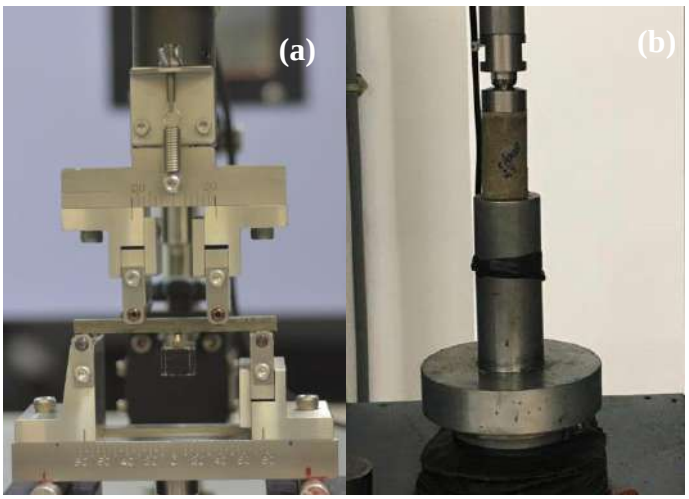

Figure 7.1 – Experimental setups used to measure (a) flexural and (b) compressive strength of pastes

Compressive strength was computed as the maximum load applied, divided by the cross section area of the cylinder. Flexural strength was computed according to the

ASTM C1161 standard using equation 7.1, while strain was computed using equation 7.2, which corresponds to the elastic beam equation for small deflections [208].

$$\sigma = \frac{3PL}{4bd^2} \quad (7.1)$$

$$\varepsilon = \frac{6d}{(L-a)(L+2a)} y \quad (7.2)$$

Where:

σ: Flexural strength (MPa)
P: Applied load (N)
b: Specimen width (8.0 mm)
d: Specimen thickness (6.0 mm)
L: Outer span (76.6 mm)
a: Inner span (30 mm)
y: Deflection of the beam at midspan (mm)

The remaining pieces of the prisms tested after 9 days of hydration were used for morphological characterization using electron microscopy. Fractured surfaces were coated with carbon and imaged in a STEM using 10 kV acceleration and a maximum magnification of 300.000X. The lower face of the prism, which was submitted to pure traction, was imaged using a low vacuum scanning electron microscope (SEM) with a15 kV acceleration and a 100X magnification.

7.3 Results and discussion

This section presents and discusses the morphological characterization of the MWCNT, as well as their influence on the rheological behavior and mechanical properties of cement paste.

7.3.1 MWCNT characterization

Imaging of an individual MWCNT is presented in Figure 7.2. It can be seen that the outer diameter of the nanotube is around 20 nm, while its length is approximately 2 µm, meaning that their aspect ratio is approximately 1000. No visible defects were found in its structure.

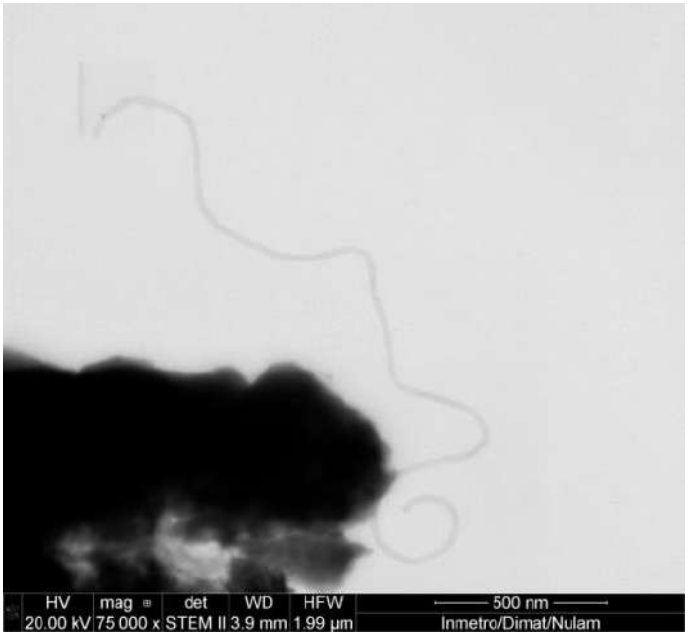

Figure 7.2 – TEM bright field image of a single MWCNT

7.3.2 Rheological behavior of MWCNT blended pastes

Four rheological parameters were used to characterize the influence of MWCNT on rheology of paste: static yield stress (τ_s), yield stress (τ_0), viscosity (μ_0) and hysteresis of the flow curve (H). Raw data, i.e. shear stress versus time and shear stress versus shear rate plots for the paste blended with 0.15% MWCNT are presented in Figure 7.3. The τ_s value is the shear stress required to make the paste flow from rest, and was obtained from the maximum shear value from the shear stress versus time plots (Figure 7.3(a)). The τ_0 and μ_0 values were obtained by fitting a Bingham model to the descending portion of the flow curve ($\gamma = \mu_0\tau + \tau_0$). The H value was the difference of area under the ascending and descending portions of the flow curves (Figure 7.3(b)). The rheological parameters of each paste versus the amount of MWCNT solid addition are presented in Figure 7.4. It was found that the commercial MWCNT aqueous dispersion modified all the rheological parameters of the paste, increasing them proportionally to the amount of nanotubes blended. This can be related with two main factors: the high surface area of MWCNT and the use of surfactants as dispersing agent in the aqueous dispersion. High surface area of nanoparticles blended in a cement matrix is expected to increase the water demand of the matrix [187]–[189], [191], [193], while surfactants can modify the rheological properties of the matrix [145] by adsorbing on the surface of cement grains [182].

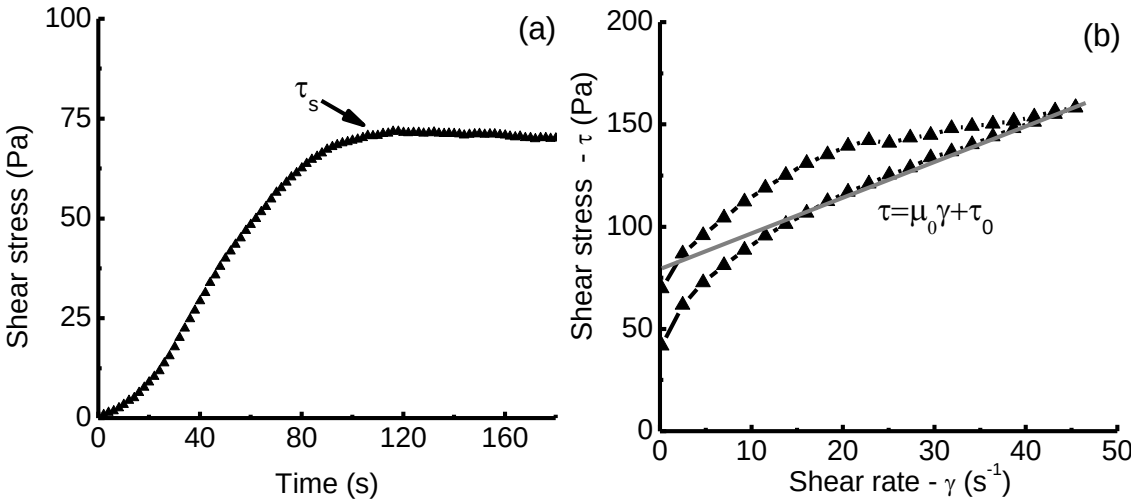

Figure 7.3 - Static yield stress (τ_s) and flow curves obtained for pastes blended with 0.15% MWCNT

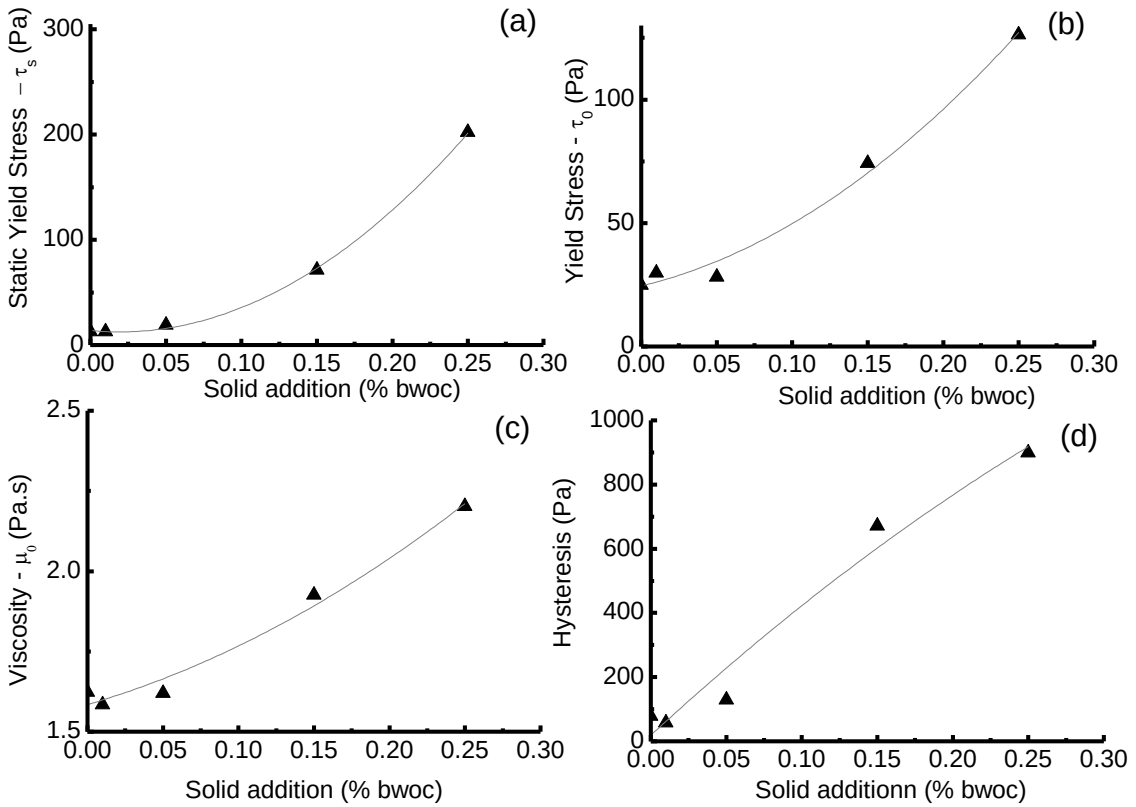

Figure 7.4 - (a) Static yield stress, (b) yield stress, (c) viscosity and (d) hysteresis of cement pastes blended with micro and nano particles versus percentage of solid substitution.

It should be noticed that hysteresis was the most influenced parameter, with an increase up to 1000% with respect to the reference paste. Hysteresis is indicative of thixotropic phenomena in the paste i.e. time dependent phenomena that modify the rheological behaviour of the paste in the time window from the beginning to the end of the measurement of the flow curve (approximately 23 minutes). It has been previously

demonstrated by the authors that the commercial MWNCT dispersion used in this work retards the hydration reaction of cement [119]; therefore, the increase in hysteresis cannot be associated with an acceleration of hydration kinetics and setting time of the paste. A similar behaviour has been reported for cement pastes blended with nanoclay and has been related to flocculation of the clay particles [203]. Similarly, for MWCNT the impact on thixotropy can be related to agglomeration phenomena of the dispersed nanotubes, induced by elevated pH values and by the presence of ionic species in the water [51].

7.3.3 Mechanical properties of MWCNT blended pastes

Two of the MWCNT amounts studied in the previous section (0.05 and 0.25%) were chosen to produce pastes and evaluate the influence of MWCNT on the mechanical behavior of the cement matrix, by comparing to the reference paste without MWCNT. Compressive strength results for pastes blended with 0, 0.05 and 0.25% MWCNT after 1, 3 and 9 days of curing are presented in Figure 7.5.

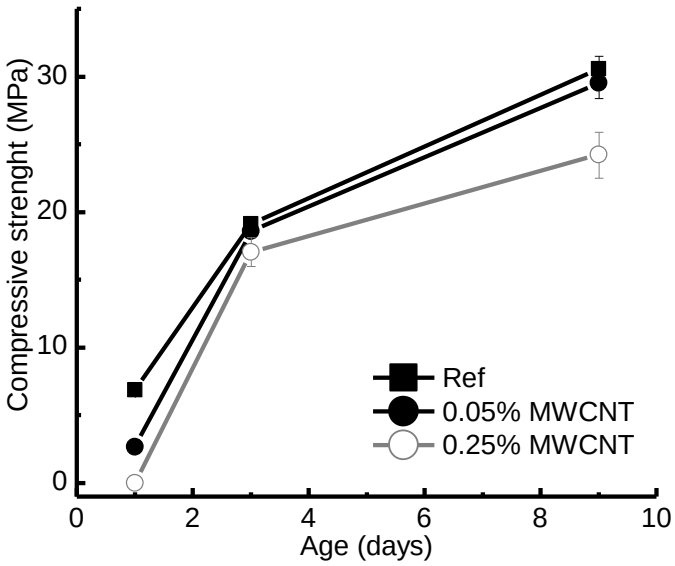

Figure 7.5 – Compressive strength results for pastes blended with 0, 0.05 and 0.25% MWCNT after 1, 3 and 9 days of curing.

It was found that compressive strength decreased with the increase in addition of MWCNT. This behavior was found to be consistent throughout all the curing ages tested. Additionally, the paste blended with 0.25% MWCNT did not set after 24 hours of curing in the mold, thus, its compressive strength was registered as zero. Even though the lower compressive strength after 1 day of hydration can be associated with a delay

of the hydration reaction induced by the adsorption of surfactants on cement grains, this has been found to be a temporary effect, after which hydration resumes normally [209]; therefore, surfactant adsorption on cement cannot be accounted for decreases in compressive strength after 3 and 9 days of hydration. Some authors have stated that nanotubes agglomerations can act as local stress concentration spots [77], decreasing the compressive strength of the matrix. While this could be the case, the porosity of the matrix has been identified to have an important role in the decrease of compressive strength. Images of the pastes blended with 0, 0.05 and 0.25% MWCNT after 9 days of curing, after compressive strength testing, are presented in Figure 7.6. Pores and air pockets with a size up to millimeters can be identified in the images of the MWCNT blended pastes. It is known that surfactants are able to stabilize air bubbles by adsorbing on the air-liquid interface [31]. These bubbles become entrapped in a cement matrix with increased yield stress and viscosity, which makes it more difficult to remove them by puddling or vibration. Both of these phenomena appear to be proportional to the amount of MWCNT blended, but it should be noticed that the surfactant-to-MWCNT ratio is always fixed and defined by the manufacturer of the MWCNT dispersion, therefore, the decrease of compressive strength can be also considered proportional to the surfactant concentration.

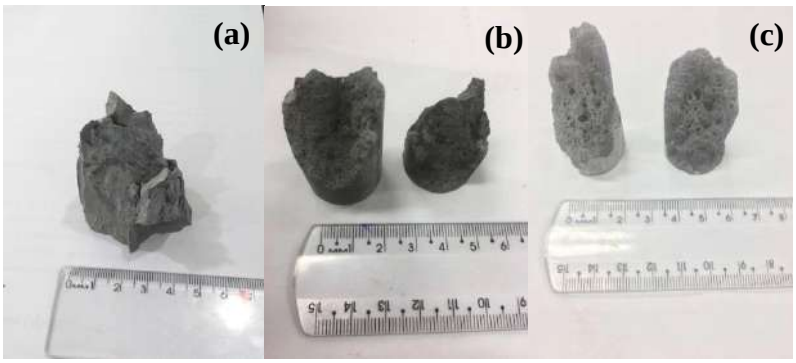

Figure 7.6 – Pastes blended with (a) 0%, (b) 0.05% and (c) 0.25% MWCNT with 9 days of curing, after compressive strength testing.

Flexural strength and elastic modulus results for pastes blended with 0, 0.05 and 0.25% MWCNT after 1, 3 and 9 days of curing are presented in Figure 7.7. A decrease in flexural strength and elastic modulus proportional to the MWCNT addition was found, similarly to the compressive strength results. No reinforcing effect of the MWCNT was identified at any age, thus, SEM imagining was carried out to verify the distribution of the MWCNT within the hydrated matrix.

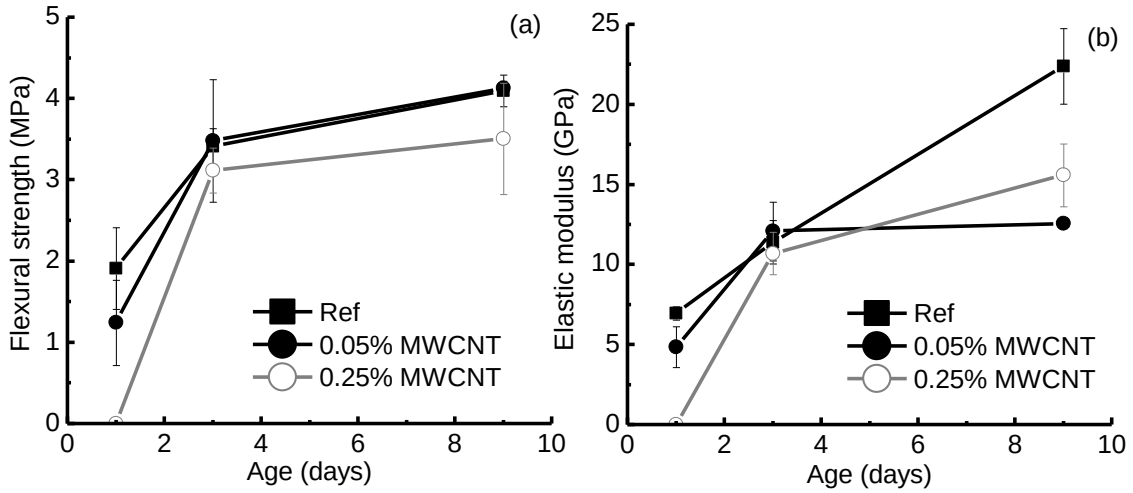

Figure 7.7 – (a) Flexural strength and (b) elastic modulus results for pastes blended with 0, 0.05 and 0.25% MWCNT after 1, 3 and 9 days of curing.

7.3.4 Microstructure of MWCNT blended pastes

SEM imaging from fractured surfaces of pastes with 0, 0.05 and 0.25% MWCNT are presented in Figure 7.8, Figure 7.9 and Figure 7.10 respectively. Images of the reference sample show the typical morphology of ettringite, which in some cases can be confused with MWCNT if no attention is given to scale, and calcium silicate hydrate (C-S-H) agglomerates along a microcrak. For the 0.05 and 0.25% MWCNT samples, nanotubes were found both as agglomerations within the matrix, as well as individual bridges across cracks of 1 μm width or less, which is compatible with their length. The presence of agglomerated nanotubes indicates that the commercial MWCNT/surfactant is probably sensitive to the highly alkaline environment generated by cement, meaning that a portion of the nanotubes will agglomerate and will not work as reinforcement in the composite. The individual nanotubes across the cracks were found in some cases with one long end outside the matrix, and in some others with both ends embedded in either side of the crack. This indicates that a portion of the nanotubes did act as reinforcement, probably modifying the load distribution within the composite. Nevertheless, the long ends indicate that most of the nanotubes suffered pull-out from the matrix, behavior characteristic of a poor interaction between the surface of the nanotubes and the hydrated cement matrix.

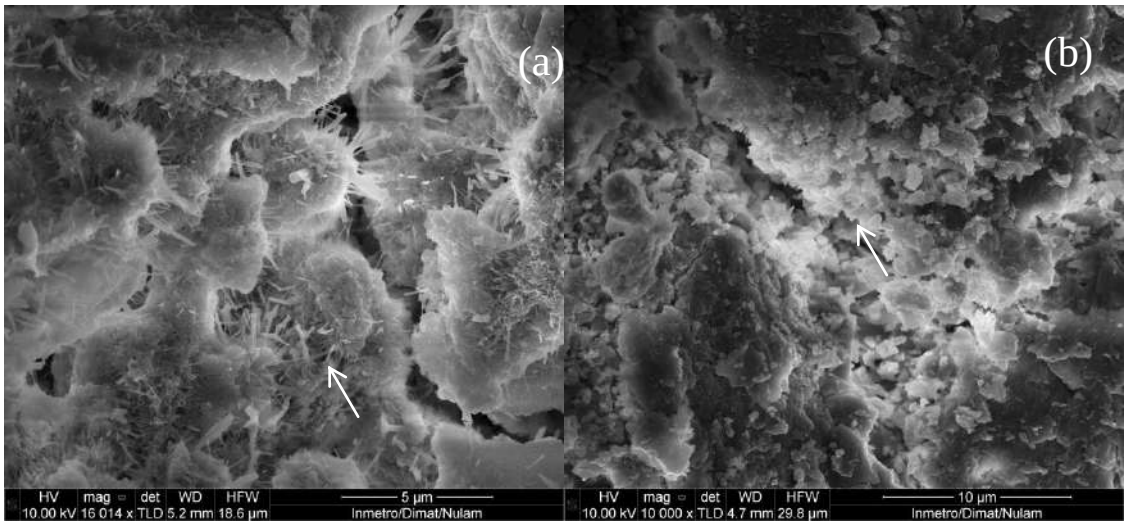

Figure 7.8 - SEM images of reference paste after 9 days of hydration. (a) ettringite clusters, and (b) C-S-H precipitations within a microcrack

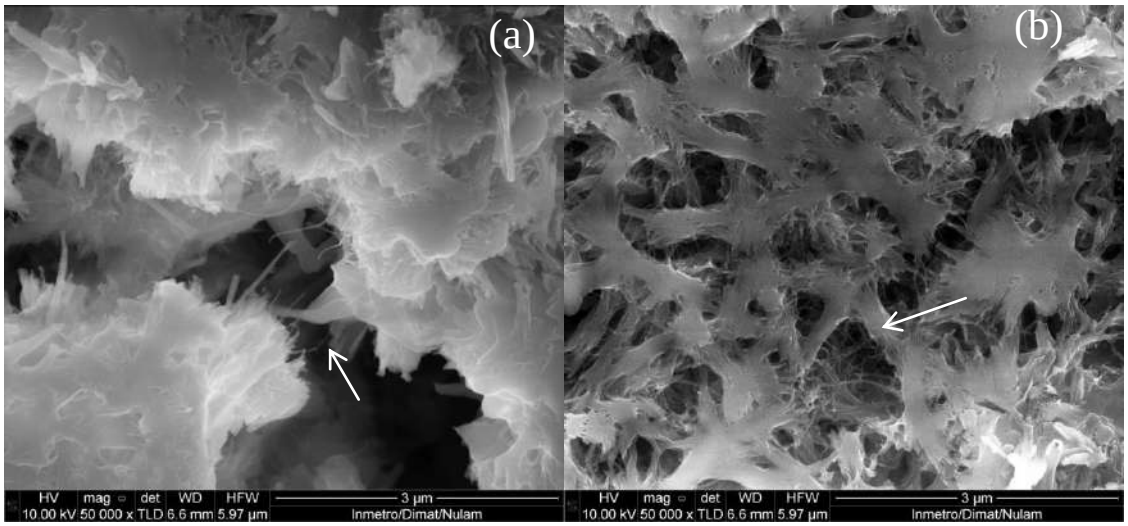

Figure 7.9 - SEM images of 0.15%MWCNT paste after 9 days of hydration. (a) individual MWCNT found in micro cracks, (b) agglomeration of MWCNT

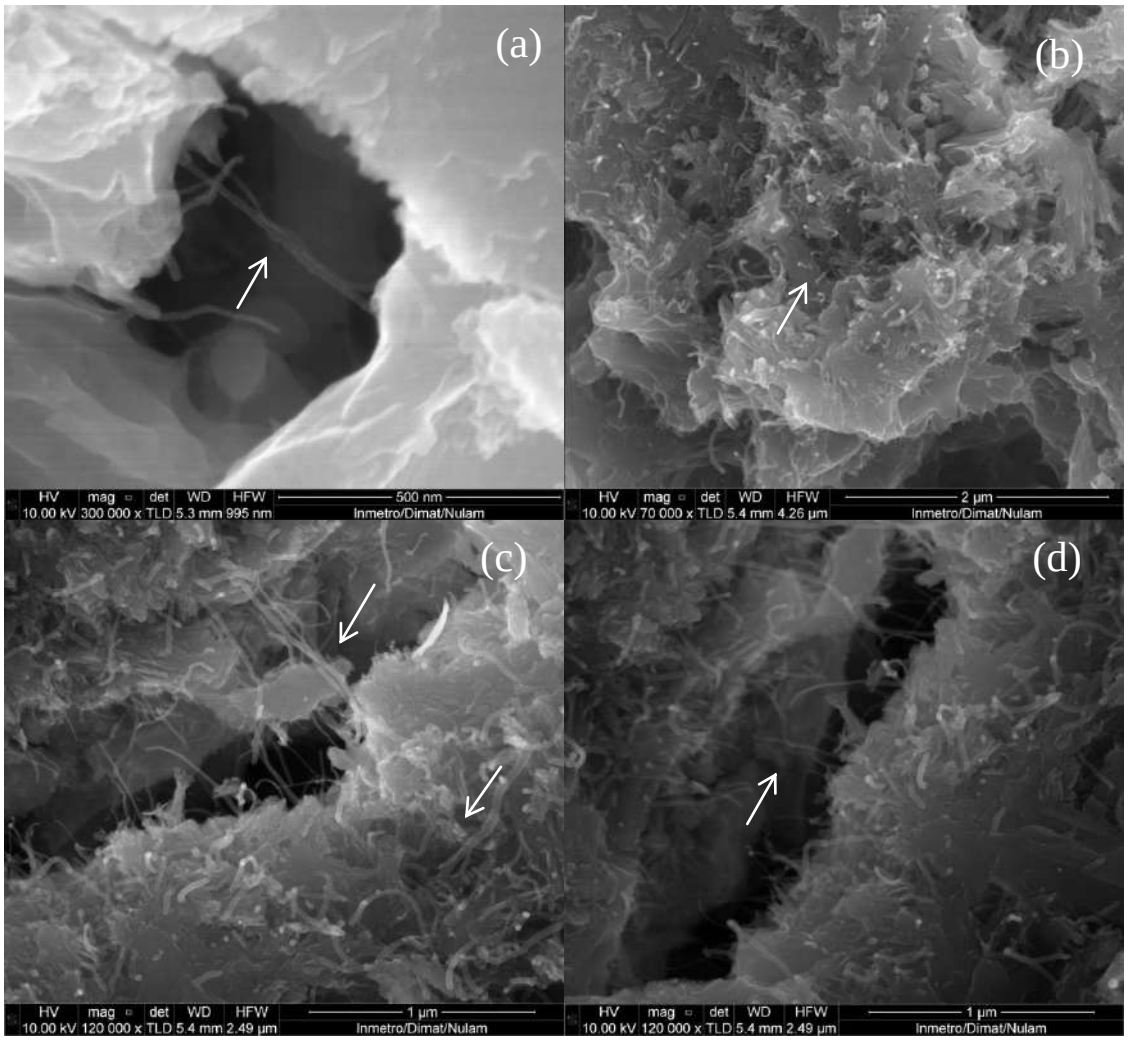

Figure 7.10- SEM images of 0.25%MWCNT paste after 9 days of hydration. (a) Individual MWCNT found in micro cracks, (b) agglomeration of MWCNT, (c) and (d) combination of individual MWCNT in micro cracks and agglomeration in the edges of the crack

Images of the bottom face of prisms tested in four-point bending after 9 days of curing, blended with 0 and 0.25% MWCNT are presented in Figure 7.11. A series of images were acquired at a 100X magnification, then a mosaic was assembled and all the cracks were highlighted in red using an image processing software. The goal of these images was to identify if MWCNT modified the cracking pattern of the prisms and induced multiple cracking, as other types of fibrous reinforcements do [210]. Two similar cracking patterns were found in the prisms, regardless of the presence of MWCNT. These patterns of connected cracks in the form of map, or map cracking, are characteristic of a superficial drying process. These cracks are not expected to be deep enough to modify the mechanical performance of the cement paste. The typical

thickness of the cracks was found to be around 10μm, as can be seen in Figure 7.12. In both cases, a single failure crack was found in the middle of the prism and no evidence of multiple parallel cracking that enhanced energy dissipation was found in the MWCNT blended sample. All cracks identified had a width of tens of micrometers, much wider than the length of the individual MWCNT.

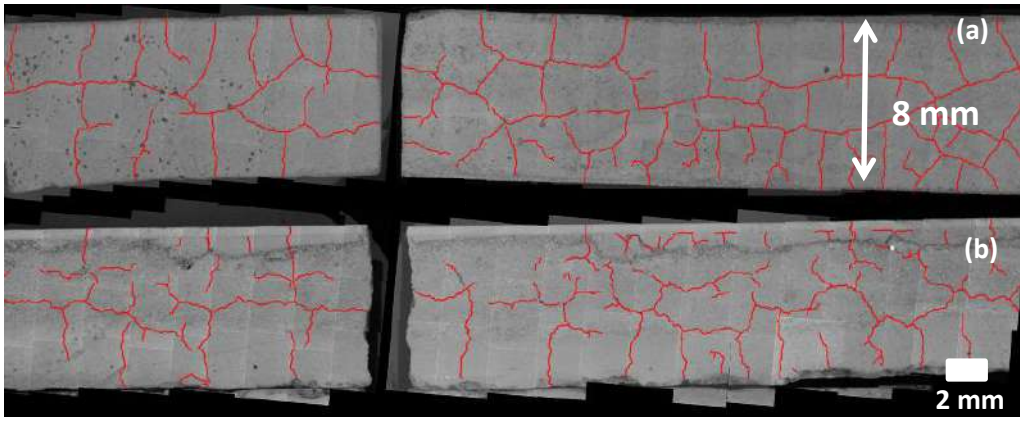

Figure 7.11 – SEM image of the bottom face of (a) 0 and (b) 0.25% MWCNT prisms submitted to flexural testing after 9 days of hydration. Cracks highlighted in red.

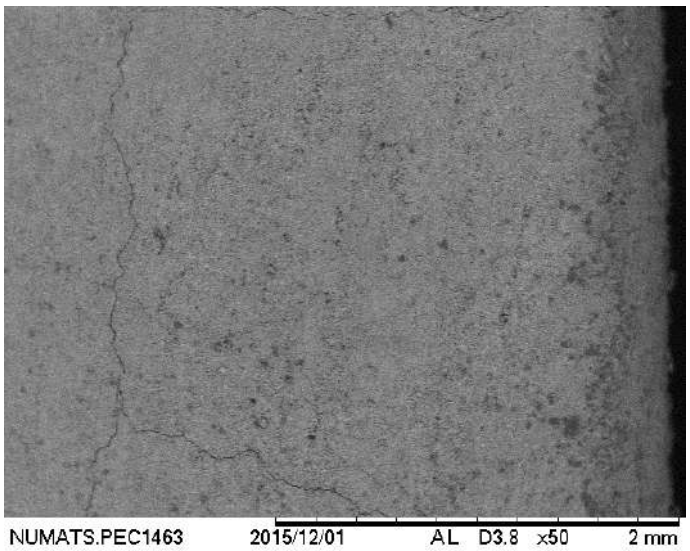

Figure 7.12 – Typical crack width found in imaged beams

7.4 General discussion

Blending MWCNT from a commercial MWCNT/surfactant dispersion induced an overall decrease of mechanical properties of the cement paste. The use of surfactant as chemical dispersing agent for MWCNT was identified as an important variable to take into account; this because it can delay the hydration reaction of cement and increase the

amount of entrapped air. SEM imaging of the different pastes studied showed that a portion of the MWCNT was able to bridge cracks and pores, but most of them suffered pull-out from the matrix. Also, no evidence of multiple parallel cracking was found in the prisms submitted to flexural testing.

The experimental evidence gathered in this work suggests that the negative effect of surfactants on the mechanical properties of the paste masks the reinforcing effect of MWCNT. Nevertheless, the use of chemical dispersing agents is necessary to guarantee an adequate degree of dispersion of MWCNT throughout the cement matrix; thus, compatibility between dispersing agent and cement is of prime importance to obtain a good performance in a nanotube-cement composite. All cracks identified in the bottom face of the prisms submitted to flexural load were much wider than the typical length of the individual MWCNT and were not affected by them. This raises the question of whether MWCNT are able to dissipate energy by inducing multiple cracking at submicron scale, or if their reinforcing mechanism is limited to control crack growth at the tip of the crack.

7.5 Conclusions

- The use of a commercial MWCNT/Surfactant dispersion induced a decrease of mechanical properties of a cement paste. No reinforcing effect from the MWCNT was identified in the matrix, regardless of the presence of a portion of nanotubes bridging submicrometric cracks.
- The reinforcing effect of MWCNT in the cement matrix was masked by the negative influence of surfactants on the mechanical behavior of the matrix.
- It is not clear if MWCNT generate multiple cracking at the submicron scale, or if their reinforcing mechanism is limited to control crack growth at the tip of the crack.

8. Commercial dispersion – Combination with nanosilica to mitigate retardation

Adsorption of surfactant by nanosilica particles in carbon nanotubes/water dispersions: application in a cement matrix

Abstract

This work studies how nanosilica particles interact with a commercial dispersion of non-functionalized carbon nanotubes rich in surfactant and how this combination affects the pozzolanic activity of the nanosilica in a cement paste. The materials used were multi walled carbon nanotubes (MWCNT) dispersed in water with an anionic surfactant as dispersing agent, colloidal silica nanoparticles (NS) dispersed in water, and Class G cement. Cement pastes with a water-to-cement ratio of 0.45 and additions of MWCNT and NS up to 0.50% by mass of cement were produced in two steps; the dispersions of nanoparticles were combined with the mixing water using an ultrasonic tip processor, and then the cement was added and hand mixed until a homogeneous paste was obtained.

Isothermal calorimetry results showed that when the pastes were blended only with MWCNT, the surfactant present in the dispersion acted as a retarding agent, delaying the heat release of the hydration reaction; whilst, when the pastes were blended with NS and MWCNT, this retardation effect was minimized. Transmission electron microscopy (TEM) and thermogravimetric analyses (TGA) results showed that in the first step of the mixing, the NS particles adsorbed the excess of surfactant present in the MWCNT dispersion, partially maintaining its pozzolanic activity.

Keywords: Carbon nanotubes, nanosilica, surfactant, retardation, pozzolanic effect

8.1 Introduction

Surfactants are commonly used as dispersing agents in colloid technology and have been identified as an effective dispersing agent for non-functionalized carbon nanotubes in water [45]. However, it is known that some surfactants molecules, such as

lignosulfonates or polyacrylates, adsorb onto the anhydrous surfaces of cement grains and retard its hydration reaction [183]; this poses a challenge when dispersing carbon nanotubes in a cement matrix using an excess of surfactant. Because adsorption is a surface area phenomenon, a novel approach to minimize this retardation effect is introducing an additional surface area onto which the excess surfactant molecules can adsorb, preventing them from adsorbing onto the surface of the cement grains and retarding the hydration. Nanosilica (NS) particles are an interesting option for this because since they have a dual functionality, high surface area for surfactant adsorption and high pozzolanic activity at early ages. This study focuses on how NS particles interact with a commercial dispersion of non-functionalized nanotubes rich in surfactant, and how this combination affects the pozzolanic activity of the NS.

8.2 Experimental

8.2.1 Raw Materials

The materials used in the experimental campaign were Class G cement produced by Holcim, AQUACYL 0302™ Multi Walled Carbon Nanotubes (MWCNT) produced by Nanocyl, and Cembinder W50 nanosilica produced by AkzoNobel. The MWCNT had an average diameter of 9.5 nm and an average length of 1.5 µm according to the manufacturer; the nanotubes came as an aqueous dispersion with a solids concentration of 3% and an anionic surfactant as the dispersing agent. A detailed characterization of the MWCNT has already been presented elsewhere [211]; therefore, only the characterization of the NS will be presented here.

The aqueous NS dispersion, which had a solids concentration of 15% by weight, was freeze dried and characterized using X-ray diffraction (XRD), energy dispersive X-ray spectroscopy (EDX), dynamic light scattering (DLS), and thermogravimetric analysis (TGA). XRD patterns were acquired with a D8 focus diffractometer from Bruker, equipped with a Cu radiation source (Kα 1.5418 Å); a 2Θ range from 10 to 60° was analyzed, using a step of 0.05° and an accumulation time of 1 second per step. EDX results were obtained using an EDX–720 equipment from Shimadzu. DLS results were performed with a Zetasizer Nano ZS from Malvern instruments. TGA were conducted using a platinum crucible in an atmosphere of N_2, with a gas flow of 100 mL/min and a heating rate of 10°C/min up to 1000°C; the equipment used was an SDT Q600 DSC-TGA from TA Instruments.

8.2.2 Experimental Procedures

A reference sample of pure cement was prepared using a water-to-cement ratio of 0.45, which was hand mixed for 90 seconds until a homogenous paste was obtained. Cement/MWCNT pastes were prepared by combining the MWCNT dispersion with the mixing water, maintaining the same water-to-cement ratio (w/c: 0.45) and a constant 0.25% addition of MWCNT by weight of cement, and then adding cement and hand mixing. Cement/MWCNT/NS were prepared first by adding the MWCNT and NS dispersions to the mixing water and then applying 500 J of ultrasonic energy with an ultrasonic tip processor to ensure homogeneity; the water content from the MWCNT and NS dispersions was taken into account to maintain constant water content of 18.63 g in each sonication procedure. The 0.25% addition of MWCNT was maintained and the amount of NS substitution was varied between 0.05 and 1.0%. After mixing the two dispersions, the cement was added and hand mixed.

A portion of 5 g of each paste was sealed in a glass ampoule and used immediately for isothermal calorimetry at 23°C. The rest of the paste was cured in 50 mL plastic airtight containers at room temperature for 80 hours. When testing age was reached, the hydration was stopped using a freeze dryer. TGA were performed using a platinum crucible in an N_2 inert atmosphere with a gas flow of 100 mL/min, measured up to 900°C with a heating rate of 10°C/min. Isothermal calorimetry results were obtained using a TAM Air isothermal calorimeter, with water as reference material.

8.3 Results and Discussion

8.3.1 Characterization of the NS

According to the EDX results presented in Table 8.1 and the XRD pattern presented in Figure 8.1, NS particles are composed mainly of amorphous silica. DLS results presented in Figure 8.2 show that the NS has an average particle size of 29.0 nm (d50) and a narrow size distribution. NS also presented a loss on ignition (LOI) of 9.0%, a TGA was performed to identify the source of this mass loss, and the results are presented in Figure 8.3. The total mass loss found in the thermogravimetric (TG) curve is compatible with that found in the LOI test. Most of it occurred under 100 °C, with a broad peak in the derivative thermogravimetric (DTG) curve at 42 °C, going almost up to 200 °C. This decomposition event can be associated with the evaporation of adsorbed

water onto the surface of the nanoparticles, combined with a dehydration of -OH groups present in the structure or on the surface of the silica as functional groups. According to the manufacturer, these functional groups were generated on the surface of the nanoparticles to enhance the stability of the aqueous dispersion over time.

Table 8.1 - Chemical compositions by EDX spectroscopy of NS /%

Composition	SiO_2	SO_3	Al_2O_3	P_2O_5	CaO	LOI
Content	87.2	1.8	1.0	0.8	0.2	9.0

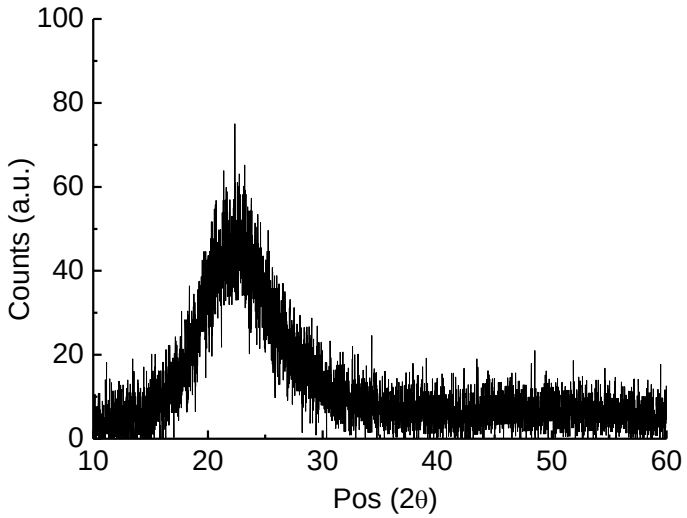

Figure 8.1 - XRD pattern of NS

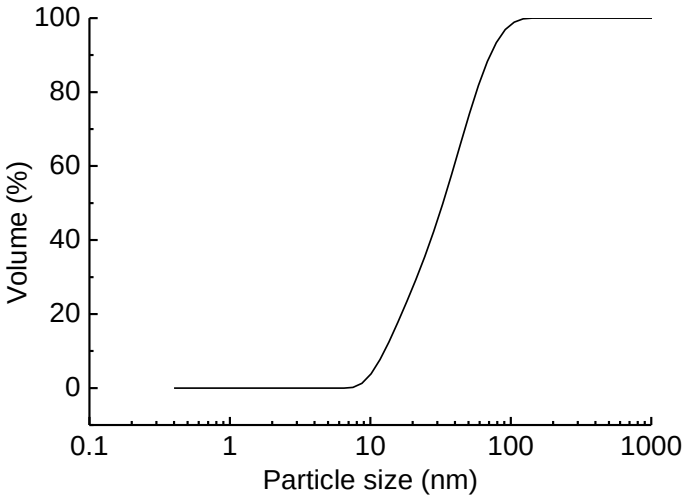

Figure 8.2 - Particle size distribution of NS

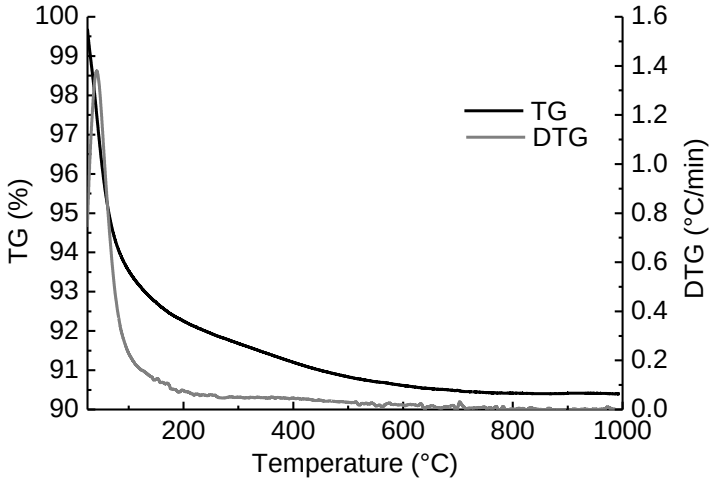

Figure 8.3 - Thermogravimetric analysis of NS

8.3.2 Transmission Electron Microscopy

After sonication and before adding the cement, a 5 µl aliquot of the 0.25%MWCNT/0.50%NS sample was taken and dropped in a No. 300 copper mesh. This was left to dry at room temperature and imaged by transmission electronic microscopy (TEM), both in bright field mode and in high-angle annular dark-field (HAADF) mode; the obtained images are presented in Figure 8.4. The bright field image, presented in Figure 8.4(a), shows an individual sphere of NS covered by a layer of a different material. The HAADF mode image, presented in Figure 8.4(b), shows that the layer around the NS particle is constituted of atoms of lower atomic weight than Si; this can be determined because the silica sphere appears brighter than its surroundings. According to the chemical composition of the NS dispersion, the presence of atoms lighter than Si is not sufficiently significant; therefore, this layer can be associated with the surfactant present in the MWCNT dispersion, which is composed mainly of C atoms, which are lighter than Si. This image suggests that the excess of surfactant from the MWCNT dispersion adsorbs on the free surface of the NS particles.

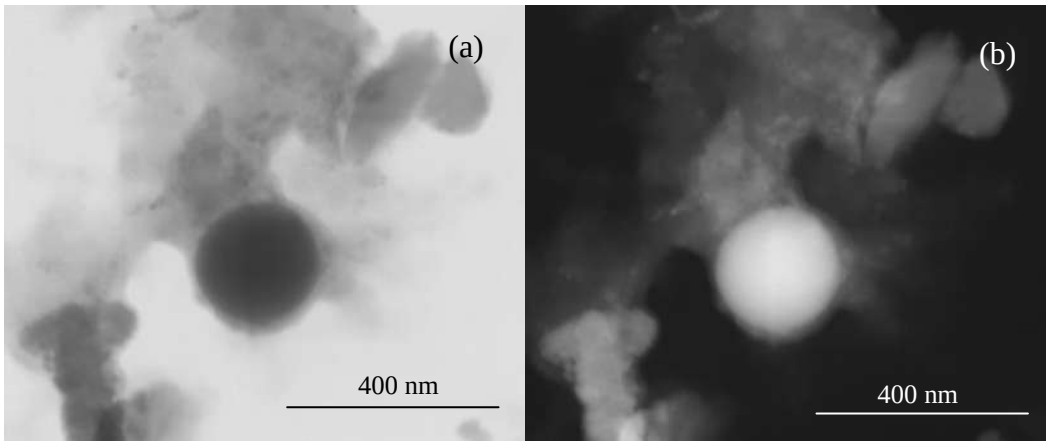

Figure 8.4 - TEM images of mixture of NS and MWCNT dispersions: (a) bright field mode and (b) HAADF mode

8.3.3 Isothermal Calorimetry Results

It has been previously demonstrated that an addition of 0.25% of AQUACYL 0302™ MWCNT widely retards the hydration reaction of Class G cement as result of an adsorption onto the surface of the cement grains of the excess surfactant present in the MWCNT [211]. This effect is presented in figure 5(a), where it can be observed that, if taking as a reference the time at which the maximum heat release occurs, the addition of 0.25% MWCNT retards the hydration reaction approximately 6 hours. This peak of heat release has been associated to the formation of calcium silicate hydrates (C-S-H) and $Ca(OH)_2$ [212]. In Figure 8.5(b), it can be observed that when adding NS to the MWCNT dispersion and before mixing with cement, the retardation effect becomes minimized. This is so effective that when using 1.0% NS, the hydration reaction becomes accelerated when compared to the control sample. To obtain a better visualization of the phenomena, the time to the maximum heat flow of the curves in Figure 8.5 (a) and Figure 8.5 (b) was plotted versus the amount of NS substitution; the result is presented in Figure 8.6. It can be observed that the time to the maximum heat flow is inversely proportional to the amount of NS introduced into the system and that these are not linearly correlated. Smaller amounts of NS more effectively minimize the effect of the surfactant; this probably because of the agglomeration phenomena of NS when higher concentrations of nanoparticles are used.

The cumulative heat curves of the studied samples are presented in Figure 8.7. Figure 8.7(a) shows how after the desorption of surfactant from the anhydrous cement grains, the total heat release of the sample blended with 0.25% MWCNT becomes

higher than the control sample. This was attributed to a nucleation effect of the MWCNT [211] or to the extension of the induction period. Figure 8.7 (b) shows that for a fixed amount of 0.25% MWCNT, the cumulative heat increases proportionally to the amount of NS. This indicates that despite having adsorbed the excess of surfactant, the NS particles still have pozzolanic activity and are probably also working as nucleation spots.

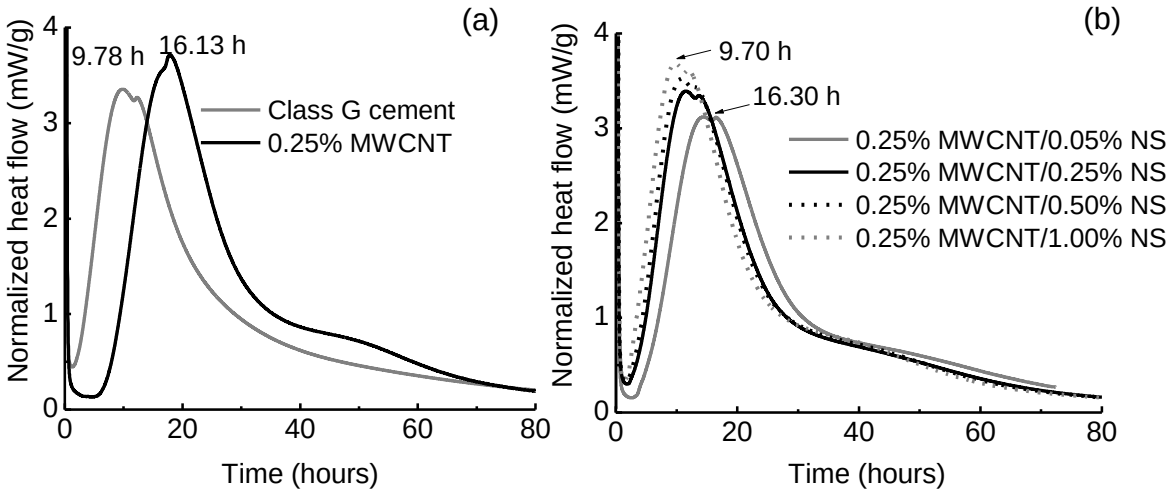

Figure 8.5 - Heat flow curves of (a) pure cement paste and cement paste combined with 0.25% MWCNT and (b) cement pastes combined with 0.25% MWCNT and different substitutions of NS

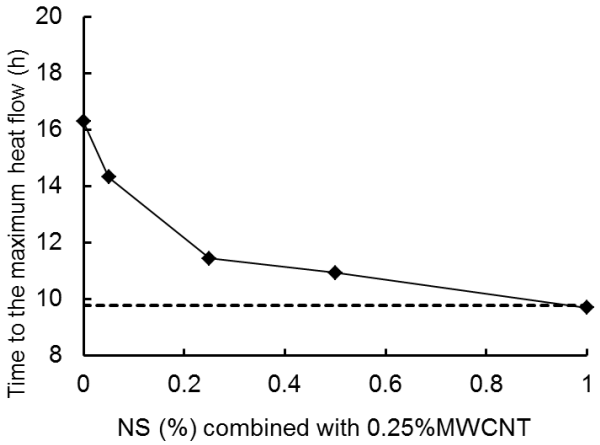

Figure 8.6 - Time at which appeared the maximum heat flow of cement pastes combined with 0.25% MWCNT and different substitutions of NS (dotted line: time to maximum heat flow of pure cement paste)

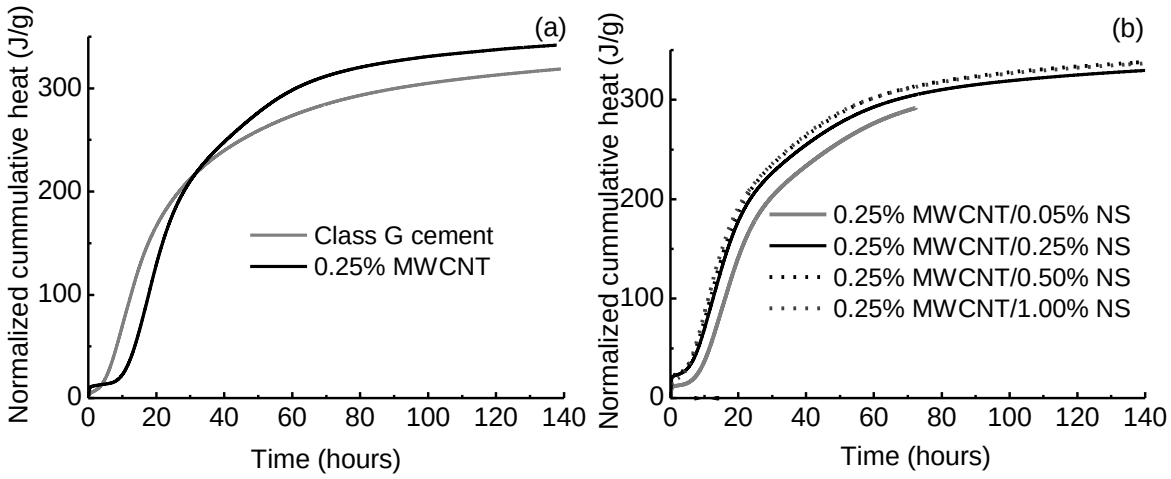

Figure 8.7 - Cumulative heat curves of (a) pure cement paste and cement paste combined with 0.25% MWCNT and (b) cement pastes combined with 0.25% MWCNT and different substitutions of NS

8.3.4 Thermogravimetric Analyses Results

TGA were performed to confirm if the NS particles still had pozzolanic activity after adsorbing the excess of surfactant present in the MWCNT dispersion. For this purpose, TG/DTG curves were obtained from samples blended with MWCNT and NS and compared with results from samples blended only with NS. Three main decomposition events were identified: (i) the dehydration of C-S-H, ettringite (AFt), monosulfoaluminate (AFm), and aluminate calcium hydrates (ACH and CASH) up to 200°C; (ii) the dehydroxilation of $Ca(OH)_2$ around 450°C, and (iii) the decarbonation of $CaCO_3$ around 600°C.

The effect of the pozzolanic reaction of NS was studied using the Total Combined Water (TCW), which corresponds to the sum of all mass loss associated with dehydration in the sample, i.e. the sum of the mass loss of C-S-H, AFt, AFm, ACH, CASH and $Ca(OH)_2$.This was presented as mass loss and not as weight fraction due to the non-stoichiometric structure of C-S-H and to the limitations of the conventional TGA experiment, which did not allowed to separate the mass loss corresponding to each mineral and calculate their proportions using stoichiometric balances. The individual mass loss of $Ca(OH)_2$ dehydration and $CaCO_3$ decarbonation were used to calculate their corresponding weight fraction. The $CaCO_3$ weight fractions were corrected by the initial carbonate content of the cement before hydration, and the $Ca(OH)_2$ weight fractions were corrected by the $CaCO_3$ from carbonation. The results are presented in

Figure 8.8 and Figure 8.9. Variations of TCW in each sample were calculated as a percentage of the TCW of a plain cement paste cured under the same conditions. The results are presented in Figure 8.10.

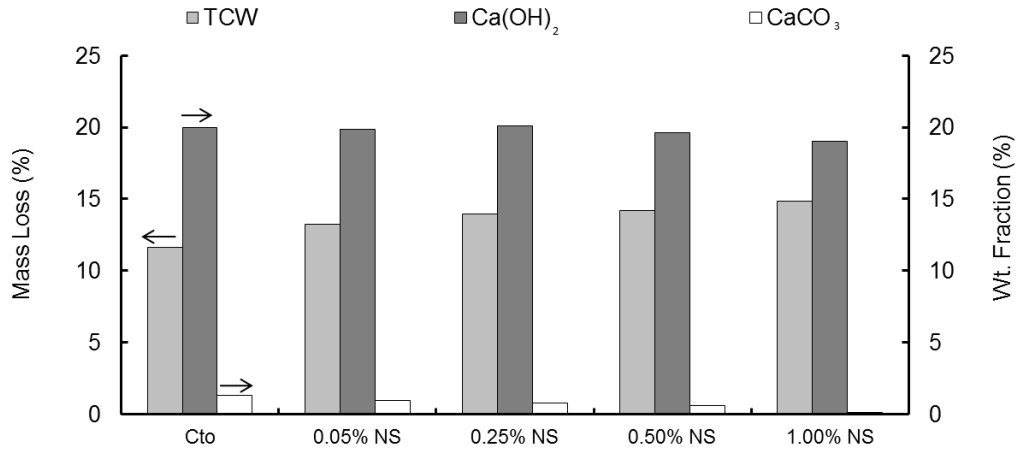

Figure 8.8 - TGA quantification results of pastes combined with different substitutions of NS and cured 80 hours (TCW: Total Combined Water)

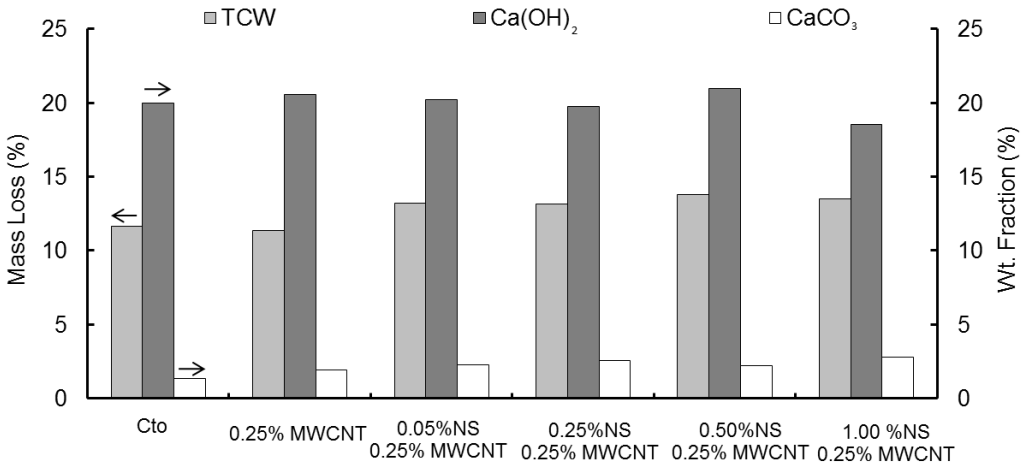

Figure 8.9 - TGA quantification results of pastes combined with 0.25% MWCNT and different substitutions of NS, cured 80 hours (TCW: Total Combined Water)

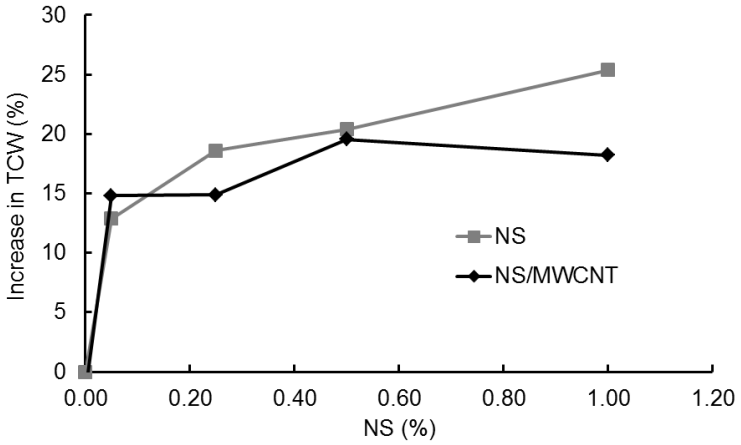

Figure 8.10 - Variation of TCW after 80 hours of curing, with respect to a plain cement paste, of pastes blended only with NS and with 0.25% MWCNT and NS

As expected, all the amounts of NS studied generated an increase of TCW as consequence of a higher formation of C-S-H, due to its pozzolanic activity and nucleation effect [7]. The extra C-S-H comes from two sources: from the pozzolanic reaction of NS that uses $Ca(OH)_2$ and water to form C-S-H, and from the acceleration of the C_3S hydration by the nucleation effect of NS. The acceleration of the C_3S hydration generates not only extra C-S-H. It was previously demonstrated that that even though the hydration is retarded, it is not completely hampered, and during this extra time additional $Ca(OH)_2$ is produced [119], this additional $Ca(OH)_2$ might be partially or totally consumed by the pozzolanic reaction, depending on the reactivity of the pozzolan. The NS particles consumed all this extra $Ca(OH)_2$,this was confirmed in figure 8, where it can be seen that the amount of $Ca(OH)_2$ in the sample remains fairly constant, while the TCW increases up to 30% with respect to plain cement for 1.0%NS. When using the combinations of NS with MWCNT, an increase of TCW was also identified in the pastes, but in a smaller magnitude. This indicates that after adsorbing the excess of surfactant, the NS particles still have pozzolanic activity, but this activity is limited by the presence of the surfactant molecules on its surface. For 0.25%MWCNT/1.0%NS, the increase of TCW was 18%, almost half of that obtained without the presence of MWCNT and surfactant in the media.

8.4 Final discussion

Experimental results obtained from TEM, isothermal calorimetry, and TGA techniques showed that the excess of surfactant present in the MWCNT aqueous

dispersion, which is used to disperse the nanotubes and maintain the colloid stability over time, widely retards the hydration reaction of cement. It was also found that if NS particles are previously mixed with the MWCNT dispersion, the retardation effect becomes completely minimized, depending on the amount of NS used. However, NS loses some of its pozzolanic activity. This effect is associated with adsorption/desorption phenomena; a schematic representation of the mechanism proposed to explain the effect of the NS particles is presented in figures 11 and 12.

The excess of surfactant present in the MWCNT adsorbs onto the surface of cement, maintaining the water molecules away from the cement and retarding its hydration until desorption occurs and the hydration reaction is resumed; this is presented in Figure 8.11. When the NS particles are previously mixed with the MWCNT dispersion, the excess of surfactant molecules becomes adsorbed onto their surface instead of the surface of the cement grains; this is presented in Figure 8.12. The adsorption of surfactant onto the surface of the NS particles causes a partial loss of its pozzolanic activity. Desorption of the surfactant from the surface of the NS should be carefully studied to confirm if the loss of pozzolanic activity is permanent or temporary.

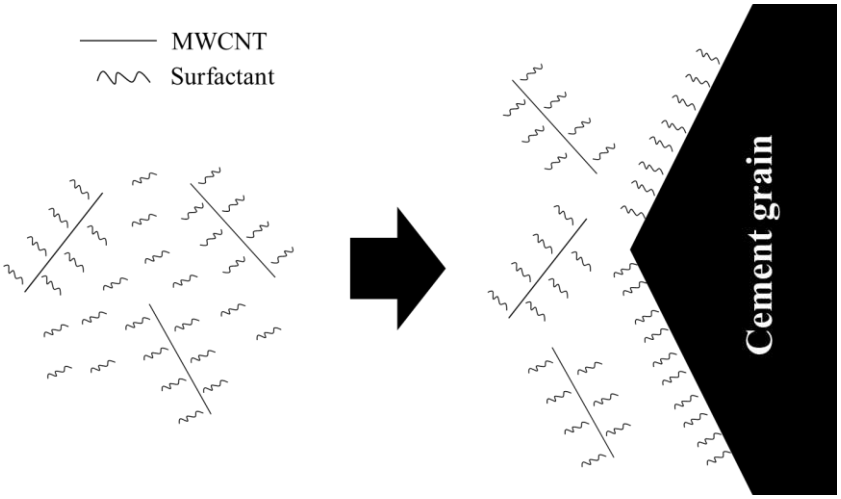

Figure 8.11 - Schematic representation of adsorption of surfactant molecules on anhydrous cement grains

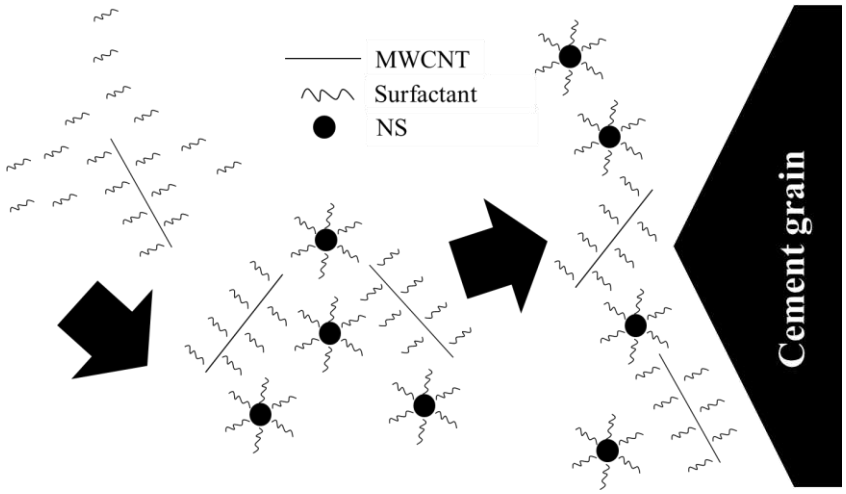

Figure 8.12 - Schematic representation of adsorption of surfactant molecules on NS particles instead of cement grains

8.5 Conclusions

The following conclusions are a result of this work:

- The excess surfactant used to disperse the MWCNT adsorbs onto the cement grains and retards its hydration reaction, which is only resumed when the surfactant desorbs from their surface.
- NS particles mixed with the MWCNT dispersion adsorb the excess of surfactant instead of the cement grains. This minimizes the retarding effect of the surfactant.
- The adsorption of surfactant onto the surface of NS particles causes a partial loss of its pozzolanic activity.
- Desorption of the surfactant from the surface of the NS should be carefully studied to confirm if this loss of pozzolanic activity is permanent or temporary.

9. Commercial dispersion – General two-step mixing process to mitigate retardation

Interaction of a carbon nanotube/surfactant/water dispersion with pozzolanic particles in Portland cement pastes

Abstract

Surfactants are used in carbon nanotube/water dispersions as dispersing agents to prevent nanotubes bundles. Nevertheless, when blended in a Portland cement paste, some of these dispersions can retard the hydration reaction of cement. A two-step mixing process is proposed to avoid or minimize this effect. A carbon nanotube dispersion containing surfactant was mixed with pozzolanic micro- and/or nano-particles (nanosilica, microsilica, metakaolin and nanolcay), then mixed with cement. Total organic carbon and UV-Vis spectroscopy were used to identify the interaction between the carbon nanotubes dispersion and cement grains. Isothermal calorimetry and ultrasonic pulse velocity tests were used to study the influence of the combinations of nanotubes and pozzolanic particles on the hydration kinetics and setting time of Portland cement pastes. Some surfactants can have a retarding effect on cement and that was observed when mixing the dispersion of nanotubes with cement in this study. It was observed that mixing pozzolans with the nanotube dispersion prior to mixing with cement minimizes the retardation effect of the dispersion regardless of the size of the pozzolans. It was also found that the effectiveness of pozzolans to prevent this retardation is not only proportional to the amount particles used and their specific surface area, but also dependent on their surface properties.

Keywords: Carbon nanotubes, surfactant, retardation, pozzolans, adsorption, surface area.

9.1 Introduction

Different strategies have been developed to incorporate carbon nanotubes into cement matrices, including dry mixing them with the cement in powder [86], growing them directly on cement grains [139], or dispersing them in the mixing water using ultrasonic waves and chemical dispersing agents [137]. When considering the use of nanotubes for field applications in the cement industry, the addition of carbon nanotubes to the matrix must be performed in a way that is efficient and that does not overcomplicate the production process. Dry mixing has low efficiency and is associated occupational hazards as a result of the inhalation risk of nanotubes [213]. Growing nanotubes on cement grains requires highly specialized infrastructure, and has the disadvantage of having a fixed percentage of nanotubes by mass of cement that cannot be modified should the production process requires it.

Dispersing nanotubes in water is a viable option to simplify field operations because this process can be performed previously off-site, stored, and transported. Maximizing the concentration of nanotubes dispersed in water minimizes the cost, time and polluting emissions associated with their transportation to the field or production plant [138]. This option, however, presents a challenge because a high degree of dispersion and a good level of stability over time must be ensured to obtain an efficient effect from the carbon nanotubes [11]. Surfactants are an effective dispersing agent for carbon nanotubes in water [45]; however, in high concentrations they can hamper the hydration reaction of cement because of steric hindrance caused by the adsorbed molecules of surfactant, generating a retardation of the hydration [183].

The surfactant present in a Multi Walled Carbon Nanotube (MWCNT) aqueous dispersion has been shown to retard the hydration reaction of cement pastes [211], this problem, however, is solved by combinig the nanosilica particles with the MWCNT dispersion before mixing them with cement [214]. The surfactant molecules are expected to adsorb onto the nanosilica, rather than the cement grains, not affecting the hydration of the anhydrous cement grains. Because adsorption is by nature a surface phenomenon, this methodology should not be limited only to nanosilica. Any particle with the appropriate surface properties should be able to adsorb surfactant to prevent its adsorption onto the cement grains, regardless of its size. Pozzolanic particles are well suited to fulfill this goal because they will provide a dual function: adsorb surfactant and fixate $Ca(OH)_2$ to produce calcium-silicate-hydrates (C-S-H) to increase

compressive strength of the matrix. This work studies the interaction of four different pozzolanic particles (microsilica (MS), nanosilica (NS), metakaolin (MK) and nanoclay (NC)) with class G Portland cement and a MWCNT aqueous dispersion containing surfactant as a dispersing agent.

9.2 Materials and methods

The materials used for this work were Class G cement, Multi Walled Carbon Nanotubes (MWCNT) aqueous dispersion, nanosilica (NS) aqueous dispersion, nanoclay - hydrophilic bentonite (NC), metakaolin (MK), and microsilica (MS). MWCNT had an average diameter of 9.5 nm and an average length of 1.5 μm according to the manufacturer; they were dispersed in water with a 3.0% solids concentration and 5.0% of anionic surfactant as dispersing agent. The manufacturer did not disclose the specific type of surfactant.

Raw materials were characterized by X-ray diffraction (XRD) and energy dispersive X-ray spectroscopy (EDX). XRD patterns were obtained in a 2Θ angle range from 8° to 60°, with a step of 0.01° and an accumulation time of 1 second. The equipment used had copper X-ray source (Cu Kα, λ = 1,5418 Å). Chemical composition of raw materials was obtained from EDX spectra using a X-ray fluorescence spectrometer. The equipment is capable of identifying elements from Na to U.

All the pozzolanic particles were combined with MWCNT as water based dispersions, except for NS, which was provided already dispersed in water and was used as received. MS, MK and NC were received in powder and had to be dispersed in deionized water using an ultrasonic tip processor. Sonication was performed in 20 seconds on/off cycles to prevent overheating the dispersions. Concentration of the dispersions and energy applied by the ultrasonic tip by mass of solids is presented in Table 9.1.

Table 9.1 - Concentration and energy used to produce dispersions of pozzolanic particles.

Pozzolanic particle	Solids concentration (wt %)	Dispersion energy (J/g)
MS	21.3	440
MK	21.3	440
NS	15.0	Pre-dispersed
NC	2.6	5320

Immediately after sonication, the particle size distribution of the dispersions was measured using dynamic light scattering for the nanoparticles and laser diffraction for the microparticles. NS and NC dispersions were measured by dynamic light scattering (DLS), and MS and MK dispersions were measured by laser diffraction. The specific surface area calculated with the Brunauer–Emmett–Teller (BET) theory of the dispersed pozzolanic particles was measured using N_2 adsorption isotherms. The dispersions were freeze dried to avoid any agglomeration of particles during the removal of water, and to obtain a powder with a surface area similar to that of the dispersion.

The interaction of the surfactant contained in the MWCNT dispersion with cement grains was studied using total organic carbon (TOC) and UV-Vis spectroscopy. TOC results were used to measure the amount of carbon adsorbed on the surface and entrapped between the grains of cement by the depletion method. Ultrapure water from was used for this experiment. Samples were stirred for 5 minutes and centrifuged at 4,000 rpm for 10 minutes. The supernatant was collected and diluted 1:10 (v/v) before measuring its TOC content. Each sample was prepared twice, and each test was repeated three times. In addition, the MWCNT content in the samples before and after centrifugation was measured using UV-Vis absorbance spectra with a UV-Vis spectrophotometer, from 200 to 800 nm in 0.2 nm steps.

The effect of the combination of MWCNT with pozzolanic particles on the kinetics of cement's hydration reaction was studied by isothermal calorimetry and ultrasonic pulse velocity tests. For the isothermal calorimetry tests, a 40.0 g reference sample of pure cement was prepared using a water-to-cement ratio of 0.45, which was hand mixed for 90 seconds until a homogenous paste was obtained. To prepare the cement pastes blended with the MWCNT and pozzolanic particles combinations, a two-step mixing process was adopted. First, the MWCNT dispersion was combined with the pozzolanic particles dispersions and the mixing water, and 500 J were applied with an ultrasonic tip processor to ensure homogeneity. Next, the cement was added and hand mixed for 90 seconds. Heat flow and cumulative heat curves were obtained at 23 °C using an isothermal calorimeter. The results were normalized by mass of cement.

For ultrasonic pulse velocity testing, 600 g pastes were prepared in a planetary mixer by first mixing the MWCNT and pozzolanic particles dispersions with the mixing water for 90 seconds at 350 rpm to ensure homogeneity. Next, the cement was added and mixed for 4 minutes at the same speed. A 60 second stop was included in the mixing process to scrape all material from the walls of the mixer. An ultrasonic cement

analyzer (UCA) was used for these tests. The samples were poured in the UCA container and puddled or densified to remove entrained air for 45 seconds with a glass rod. A hydrostatic pressure of 3.4 MPa (500 psi) was applied to ensure an adequate contact of the sample with the source and sensor of ultrasonic waves. This pressure was slowly released during a period of 4 hours. Samples were maintained at room temperature (23 °C ± 1 °C).

9.3 Results and discussion

In this section, the dispersion process of the pozzolanic particles is first characterized in terms of the particle size and specific surface area obtained at the end of the dispersion. Next, the interaction of the MWCNT dispersion with cement grains is identified. This information is followed by the study of the effect of the combinations of MWCNT with pozzolanic particles over the hydration kinetics and the setting time of cement pastes.

9.3.1 Raw materials characterization

Table 9.2 and Figure 9.1 present the chemical composition and XRD patterns of MS, NS, MK, NC, and MWCNT. The results show that both MS and NS consist primarily of amorphous SiO_2, with a purity of 91.97% for MS and 87.40% for NS. MK was found to consist of quartz, kaolinite, muscovite, and amorphous phase. The amorphous phase was identified by a broad reflection between 20° and 30° (2Θ) in the XRD pattern, which is typical of the aluminum silicates with pozzolanic activity from MK. This finding was confirmed by the chemical composition results, which showed high contents of SiO_2 and Al_2O_3. NC was found to consist of montmorillonite, aluminum silicate, and amorphous phase, which correlates with the SiO_2 and Al_2O_3 content found in the chemical composition. For MWCNT, 91.27% of the mass corresponded to loss on ignition, which is associated with the carbon content of the nanotubes. In addition, Al_2O_3 was identified in the sample, which could be a residue of the catalyst used during the production process of the MWCNT.

Table 9.2 - Chemical composition of pozzolanic by X-ray fluorescence of micro- and nano- particles (*LOI: Loss On Ignition)

	Percentage (%)				
Compound	MS	MK	NS	NC	MWCNT
SiO_2	91.97	47.57	87.24	48.28	0.53
Al_2O_3	1.16	40.69	1.02	19.01	7.01
Fe_2O_3	0.15	2.05	-	4.13	0.17
SO_3	1.74	1.46	1.72	1.81	0.46
MgO	-	-	-	3.28	-
CaO	0.83	0.51	0.22	1.19	0.11
K2O	0.88	1.76	-	-	-
P_2O_5	1.07	0.84	0.78	0.78	0.44
TiO_2	-	1.49	-	0.44	-
LOI*	2.27	3.62	9.01	1.09	91.27

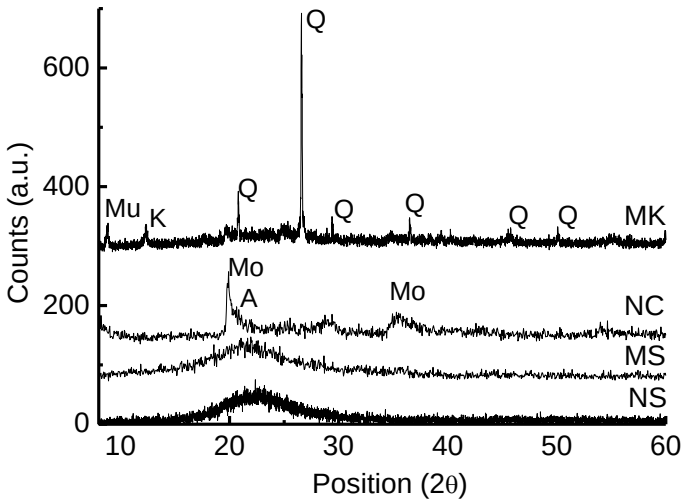

Figure 9.1 - X-Ray diffraction pattern of MK, NC, MS and NS (Mo: Montmorillonite - $AlSi_2O_6(OH)_2$, A: Aluminum silicate - $Al_2Si_4O_{10}$, Q: Quartz - SiO_2, K: Kaolinite - $Al_2Si_2O_5(OH)_4$, Mu: Muscovite - $KAl_2(AlSi_3O_{10})(OH)_2$)

9.3.2 Pozzolanic particle dispersions

Table 9.3 presents the specific surface area, average particle size, and specific mass of NS, MS, NC, and MK obtained after the dispersion process. MS and MK presented similar results, with values typical of microparticles. This similarity indicates that the dispersion process was equally effective for both cases. NS was found to have a high specific surface characteristic of a nanoparticle. NC is expected to have platelet morphology, with the thickness within tenths of nanometers and the width within hundredths of nanometers. The particle size value found for NC is expected to be

characteristic of the width of the particles. The specific surface area of NC was found to be low for a nanoparticle, which indicates that the dispersion process was not efficient enough to delaminate all of the clay platelets.

Table 9.3 - Specific surface area and average particle size of the pozzolanic particles after dispersion

Particle	Specific surface area (m^2/g)	Average particle size D_{50} (*µm - ** nm)
MS	18.1	9.6 *
MK	18.7	14.9 *
NS	219.9	32.6 **
NC	71.7	238.8 **

9.3.3 MWCNT dispersion/cement interaction

TOC and UV-Vis absorbance experiments were performed to determine whether or not the MWCNT aqueous dispersion interacts with the anhydrous cement grains. A cement paste with a water-to-cement ratio of 0.45 and 0.25 % MWCNT solids addition by mass of cement was adopted for these experiments. The components of the paste were tested in pairs, always maintaining the proportions of the original paste. The paste as a whole was also tested. First, water + cement were stirred, centrifuged, and tested to verify cement´s TOC contribution. Then, water + MWCNT were stirred and tested to measure the TOC corresponding to the total amount of carbon contained in the MWCNT dispersion. It was found that some amount of MWCNT can be segregated by centrifugation, corresponding to agglomerated nanotubes. Finally, water + cement + MWCNT were stirred, centrifuged, and tested to measure the amount of carbon remaining in the supernatant after centrifugation; Table 9.4 shows the results. It was found that the TOC contribution of water and cement was very low, whereas the primary TOC source was the MWCNT dispersion, as expected. After stirring and centrifuging the paste as a whole, TOC was found to be depleted by 94.0% (discounting the TOC contribution of water and cement). This decrease can be associated with the carbon adsorbed and entrapped on cement and segregation of agglomerated nanotubes, indicating that an interaction exists between the MWCNT dispersion and cement.

Table 9.4 - Total organic carbon results of a cement paste of w/c 4.0 and 0.25% MWCNT. (TOC: Total Organic Carbon, TC: Total Carbon, TIC: Total Inorganic Carbon).

Sample	TOC		TC		TIC	
	ppm	deviation	ppm	deviation	ppm	deviation
Water + Cement	1.583	0.018	2.74	0.047	1.161	0.029
Water + 0.25%MWCNT	77.245	2.235	77.800	2.140	0.554	0.100
Water + Cement + 0.25%MWCNT	6.095	1.607	7.547	1.857	1.452	0.250

UV-Vis absorption spectra of the same samples are presented in Figure 9.2. The water + MWCNT sample presented an intense absorption at approximately 200 nm, which is characteristic of dispersed MWCNT [61], whereas, the water + cement + MWCNT sample presented an absorption spectra similar to that of the water + cement sample. The MWCNT content in the supernatant was measured using the absorption value at 800 nm, which has been found to be linearly correlated to the MWCNT concentration in an aqueous media [215]. Most MWCNT was centrifuged out of solution with the cement during centrifugation, reaching depletion values similar to those obtained from TOC results. This outcome indicates that the surfactant and MWCNT do not separate during their interaction with cement.

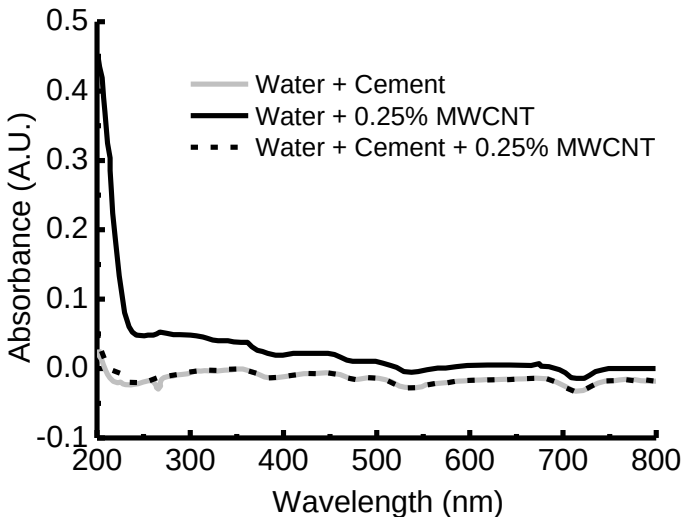

Figure 9.2 - UV-Vis absorbance spectra of a cement paste of w/c 4.0 and 0.25% MWCNT.

9.3.4 Hydration kinetics

Cement pastes were produced with a water-to-cement ratio of 0.45, an addition of 0.25% of solid MWCNT by mass of cement and different solid substitutions of pozzolanic particles by mass of cement. For the nanoparticles (NS and NC), the

substitutions ranged from 0.05 to 1.00%, and for the microparticles (MS and MK) from 0.25 to 10.0%. The water contained in the dispersions was taken into account to maintain a constant water-to-cement ratio of 0.45. Figure 9.3 through Figure 9.5 present the heat flow and cumulative heat curves obtained from the isothermal calorimetry experiments. All results were normalized by the mass of cement present in each sample.

Results for plain cement and 0.25% MWCNT pastes are presented in Figure 9.3. Four events were identified in the heat flow curves: (i) induction period, (ii) calcium silicate hydrates (C-S-H) and $Ca(OH)_2$ formation, (iii) a shoulder in the C-S-H peak denominated sulfate depletion, and (iv) the transformation of AFt into monosulfoaluminate (AFm) [216]. As expected, the MWCNT dispersion retarded the hydration reaction by prolonging the induction period, probably because of the adsorption of surfactant onto the cement grains [209]. This effect was not permanent because the hydration resumed and the heat release from C-S-H formation, sulfate depletion, and AFm formation became enhanced. The enhancement of the C-S-H peak can be attributed to a nucleation effect of the MWCNT [69] or to the extension of the induction period [184]. The enhancement of the sulfate depletion peak can be associated with a second ettringite (AFt) formation [212], possibly attributable to the Al_2O_3 content in the MWCNT. The enhancement of the AFm formation can be viewed as consequence of a higher formation of AFt, which is later transformed into AFm [217]. The cumulative heat curves show that the 0.25% MWCNT sample released a total amount of heat greater than that of the plain cement sample, surpassing it after 32 hours, which is approximately the time at which the second AFt formation ends and the transformation into AFm begins.

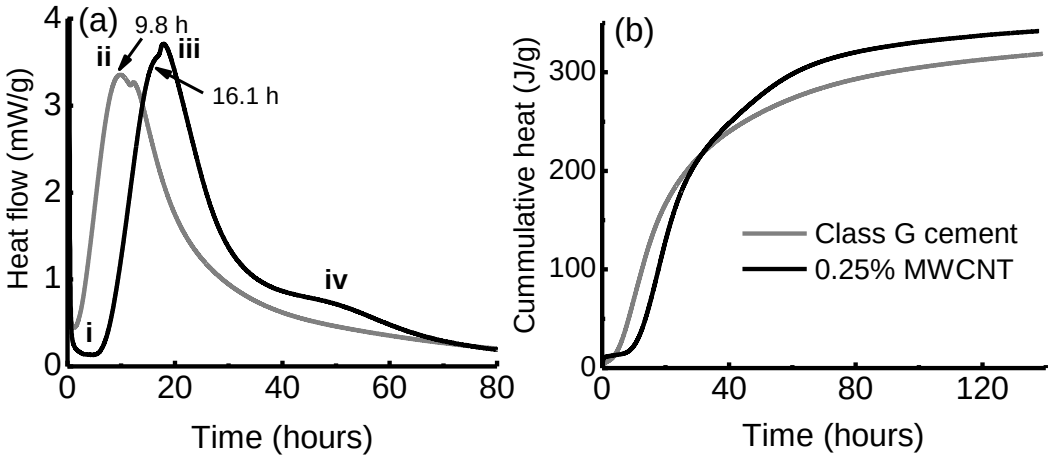

Figure 9.3 - (a) Heat flow and (b) cumulative heat curves of cement and cement/MWCNT pastes at 23°C

Heat flow and cumulative heat curves of the cement pastes with MWCNT/NS and MWCNT/MS combinations are presented in Figure 9.4 and Figure 9.5 respectively. The time at which the maximum heat flow occurred for the C-S-H formation was taken as a reference point to quantify the retardation effect of the MWCNT dispersion. For both NS and MS, the retardation of the hydration reaction decreased and the maximum value of heat flow increased, both proportionally to the amount of silica blended. In both cases, the higher percentages of silica surpassed the heat flow value of plain cement for the C-S-H formation peak, but did not have any effect in the sulfate depletion. This result indicates that the pozzolanic particles minimize the retardation effect of the MWCNT dispersion and maintain its pozzolanic activity at early ages to form C-S-H. The cumulative heat curves showed that after 140 hours of hydration, all combinations of MWCNT/NS and MWCNT/MS released a total amount of heat greater than that of plain cement, but did not surpass the 0.25% MWCNT sample. This result indicates that, at the latter ages, the pozzolanic activity of the silica particles is not significant, and the effects of the MWCNT dispersions control the hydration reaction. The combination 0.25% MWCNT/10.0% MS was the only combination that presented significant pozzolanic activity throughout the time tested.

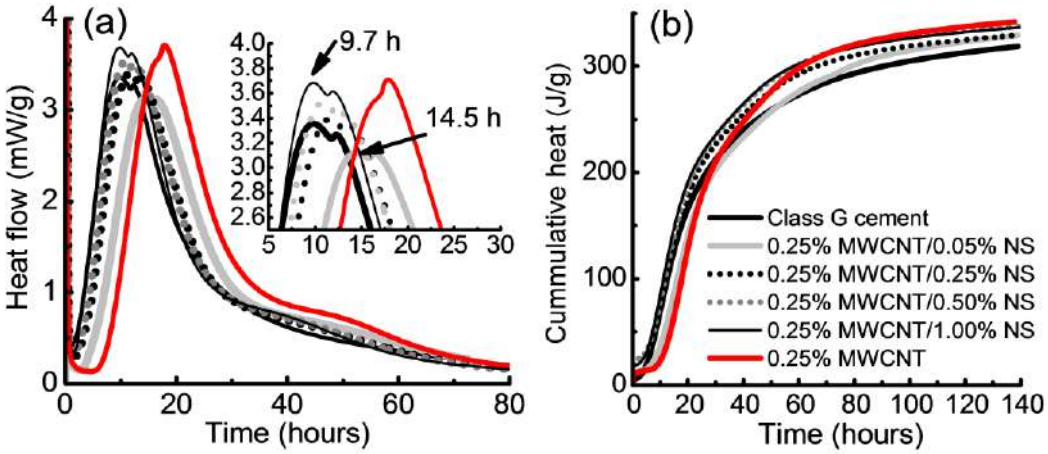

Figure 9.4 - (a) Heat flow and (b) cumulative heat curves of cement/MWCNT/NS pastes at 23 °C

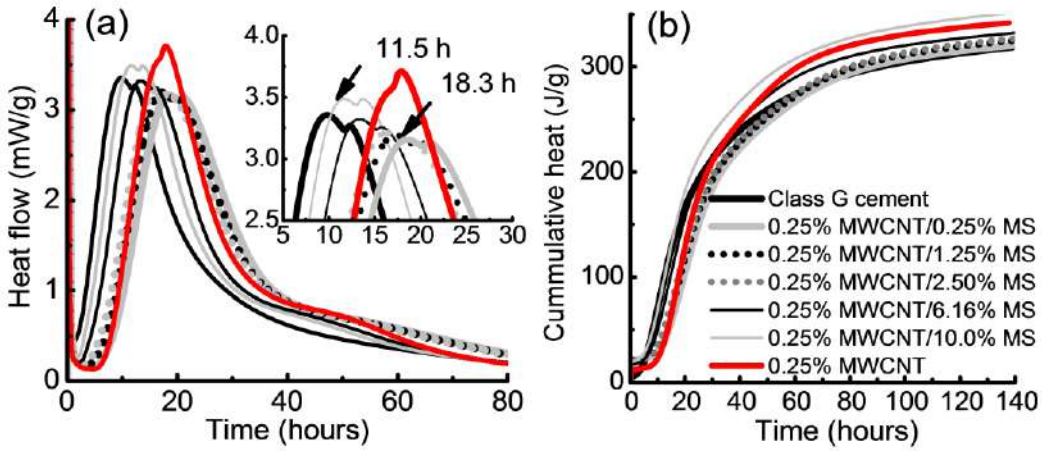

Figure 9.5 - (a) Heat flow and (b) cumulative heat curves of cement/MWCNT/MS pastes at 23 °C

Heat flow and cumulative heat curves of the cement pastes with MWCNT/NC and MWCNT/MK combinations are presented in Figure 9.6 and Figure 9.7 respectively. For NC and MK, the retardation of the hydration reaction also decreased, and the maximum value of heat flow increased proportionally to the amount of clay. In this case, the clay had a significant effect in the sulfate depletion peak, and almost no effect in the C-S-H formation peak. This outcome can be associated with the pozzolanic activity of the clay at early ages which, because of their mineralogical nature, produces C-S-H, C_2ASH_8 (gehlenite hydrate), and C_4AH_{13} (tetracalcium aluminate hydrate) [19]. MK was also found to increase the sulfate depletion peak as a result of enhancements of the dissolution of the anhydrous cement phases, which leads to additional exothermic reactions because of hydration of C_3A and pozzolanic reaction of MK [20]. Cumulative heat curves showed that after 140 hours of hydration, all combinations of MWCNT/NC and MWCNT/MK released a total amount of heat at least equal to or greater than that of plain cement, and less than or equal to that of the 0.25% MWCNT sample. As with silica particles, this result indicates that, at latter ages, the pozzolanic activity of the clay particles is not significant, and the effects of the MWCNT dispersions control the hydration reaction. The combination 0.25% MWCNT/10.0% MK was the only combination that presented significant pozzolanic activity throughout the time tested.

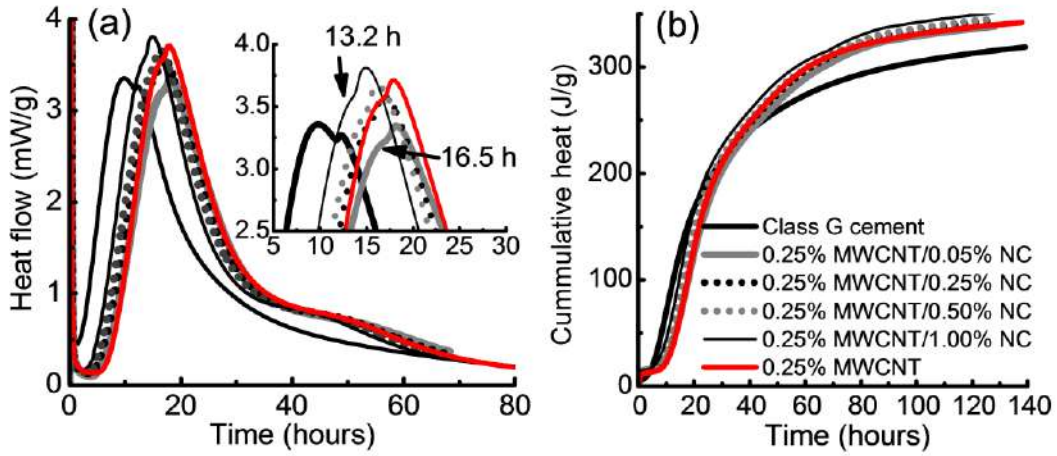

Figure 9.6 - (a) Heat flow and (b) cumulative heat curves of cement/MWCNT/NC pastes at 23 °C

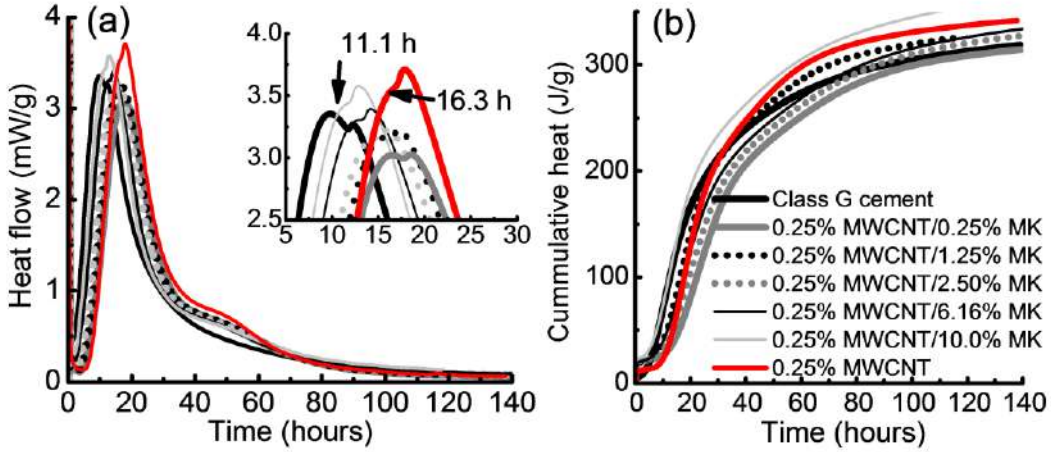

Figure 9.7 - (a) Heat flow and (b) cumulative heat curves of cement/MWCNT/MK pastes at 23 °C

To simplify the visualization of the effect of the pozzolanic particles over the retardation effect of the MWCNT dispersion, the time at which the maximum heat flow of the C-S-H formation occurs was plotted vs. the amount of pozzolanic particles combined with the MWCNT dispersion, as shown in Figure 9.8 and Figure 9.9. The time to the maximum heat flow for the C-S-H formation of plain cement is also plotted as a reference value, and any point over that value is considered to have suffered retardation. For the microparticles, the best results obtained were with a 10.0% substitution, presenting a minimum retardation of 1.72 hours. Of the substitutions studied, MK was more efficient than MS in terms of minimizing the retardation effect. Of the nanoparticles, NS was the most effective, capable of completely minimizing the retardation effect of the surfactant with a 1.00% substitution. The best result obtained

with NC has a retardation of 3.23 hours. The differences in effectiveness between MS and MK, and between NS and NC, can be attributed to the difference between their surface areas. The particles with greater surface areas available to adsorb surfactant were also found to be more effective in minimizing the retardation effect.

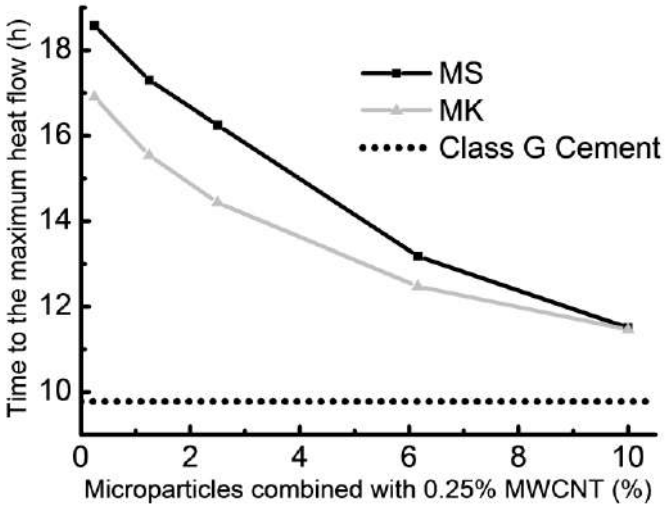

Figure 9.8 - Time to the maximum heat flow in cement/MWCNT/MS and cement/MWCNT/MK pastes (dotted line: time to the maximum heat flow of plain cement paste)

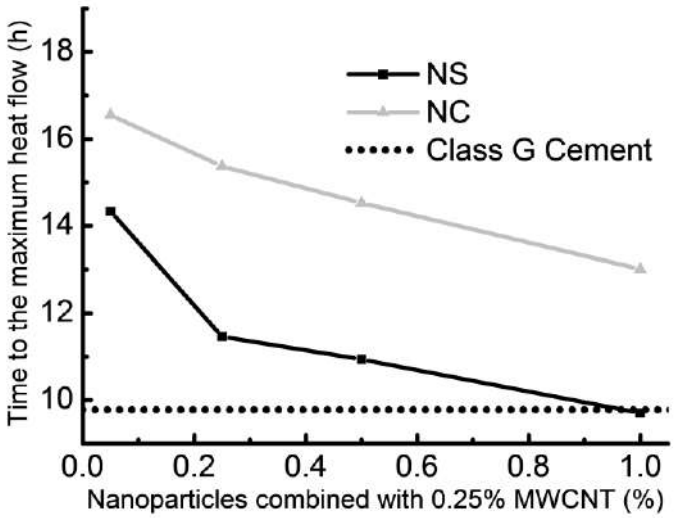

Figure 9.9 - Time to the maximum heat flow in cement/MWCNT/NS and cement/MWCNT/NC pastes (dotted line: time to the maximum heat flow of plain cement paste)

Knowing the specific surface area and the amount of solids in the pozzolanic particle dispersions, the total area of pozzolanic particles available for surfactant

adsorption in each 40.0 g sample can be calculated. This calculation enables a direct comparison of the effectiveness of the four types of particles studied. The retardation is calculated as the percent increase of time between the maximum heat flow of C-S-H formation of plain cement and each sample. Figure 9.10 shows the obtained results. The data for each type of particle was well adjusted by a decreasing segment of a parabola; this supports the fact that a proportional relation exists between the surface area of the pozzolanic particles and the retardation caused by the surfactant present in the MWCNT dispersion. For similar amounts of surface area in samples with different types of pozzolanic particles, different retardations are obtained. This result indicates that the effectiveness of the adsorption of surfactant does not depend only on the amount of surface area available, but that each type of particle has its own effectiveness, depending on its nature and electric surface properties.

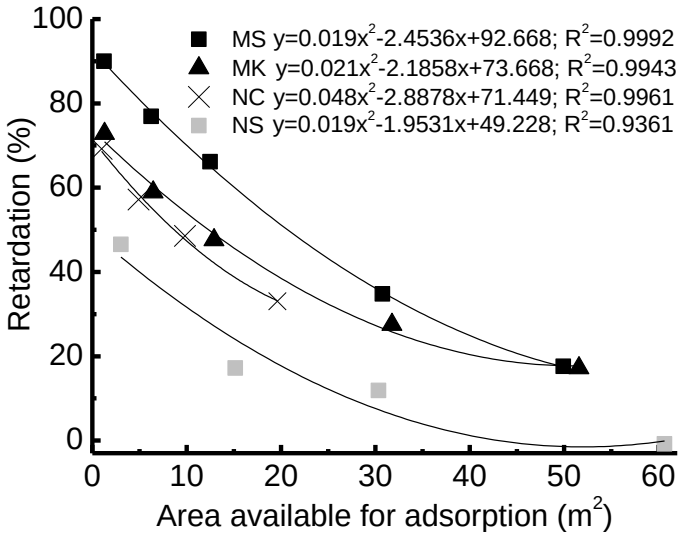

Figure 9.10 - Total surface area of pozzolanic particles versus retardation obtained when combined with MWCNT and cement

9.3.5 Setting time and strength development

To verify that the retardation effect of the MWCNT dispersion directly affects the setting time and strength development of the cement pastes, ultrasonic pulse velocity tests were performed. Plain cement pastes, pastes with only pozzolanic particles, and pastes with combinations of MWCNT dispersions and pozzolanic particles were studied. The 0.25% MWCNT addition was maintained, and only substitutions of 1.00% for NS and NC, and 10.0% for MS and MK were used. These substitutions are those that presented better results in minimizing the retardation effect. For each sample, the

transition from fluid to solid state was identified by its percolation threshold. This point indicates the moment at which the water in the paste ceases to be dominant, and a network of solid structures formed by the hydration products begins to govern the behavior of the material [218]. The percolation threshold was identified as the point of intersection of two linear segments in the wave velocity curves, before and after percolation occurred. Figure 9.11 provides an example of how the point was identified. The wave velocity curve for the plain cement paste presented one event associated with the percolation threshold at 6.8 hours, whereas the 0.25% MWCNT paste presented two events, one at 9.5 hours and one at 12.9 h. From this result, the MWCNT dispersions also retards the setting and strength evolution of the cement pastes.

The two percolation thresholds fall within the time range in which the heat flow peak of the C-S-H formation is increasing linearly, indicating that the MWCNT dispersion influences the kinetics of the hydration reaction, as well as the way the hydration products conform the solid phase at early ages. This result can mean a false setting or a refinement of the porous structure; further work is required to confirm this. At the end of the test, the wave velocity of the 0.25% MWCNT sample was shown to be greater than the plain cement sample. This result could be caused by an enhancement of the elastic moduli of the material [219], or by a refinement of the porous structure, which helps to transmit the ultrasonic waves more efficiently [220].

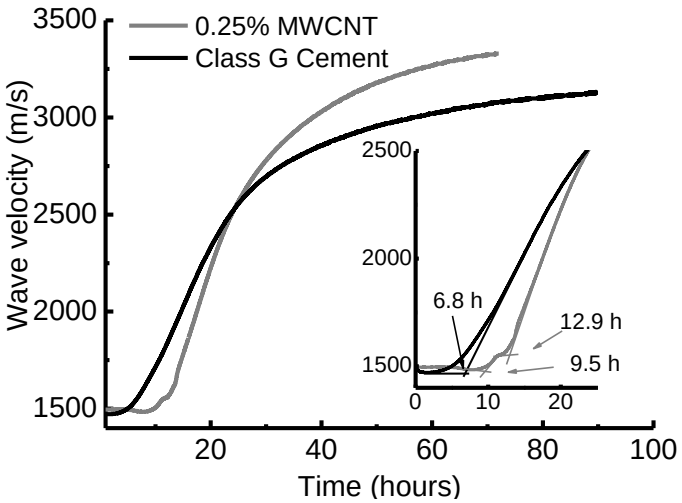

Figure 9.11 - Ultrasonic wave velocity curves of cement and cement/MWCNT pastes

Wave velocity curves for the different combinations of pozzolanic particles with MWCNT dispersions are presented in Figure 9.12 through Figure 9.15, and a summary

of the percolations thresholds of each sample is presented in Table 9.5. For all samples with only pozzolanic particles, regardless of the micrometric or nanometric nature of the pozzolan, the percolation threshold appeared earlier in comparison to the plain cement paste. This result is a consequence of the acceleration of the hydration reaction by the pozzolanic activity of the silica and clay particles. For samples with combinations of MWCNT dispersions and pozzolanic particles, only NS and MK generated a single percolation threshold that appeared earlier than the plain cement sample. NC and MS generated two percolation thresholds: one that appeared before that of the plain cement and one that appeared after. Regarding the wave velocity at the end of the test, all combinations of pozzolanic particles with MWCNT reached a wave velocity at least equal to that of plain cement, but less than that of the 0.25% MWCNT sample, indicating that all samples will have a different elastic moduli or porosity at later ages. This difference in behavior can be associated with the differences in rheology derived from each combination of nano- and micro- particles. It should be noticed that regardless of the lower final strength values with respect to the paste blended only with MWCNT, the nano- and micro-particle combinations were able to recover not only the setting time, but to enhance the strength development during the first hours of hydration to values even higher than the plain cement paste.

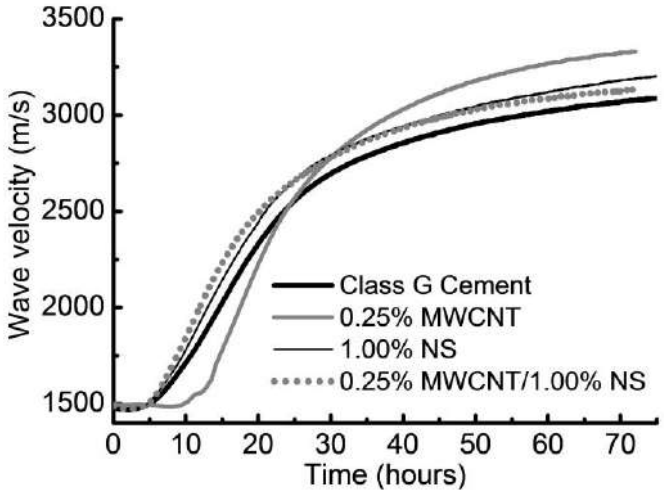

Figure 9.12 - Ultrasonic wave velocity curves of cement and cement/MWCNT/NS pastes

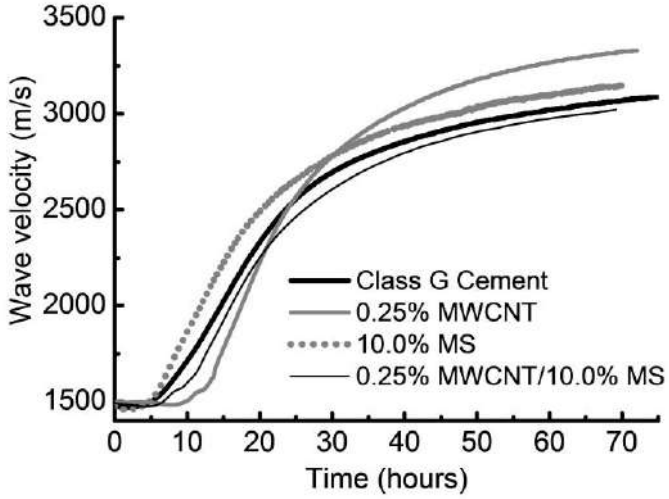

Figure 9.13 - Ultrasonic wave velocity curves of cement and cement/MWCNT/MS pastes

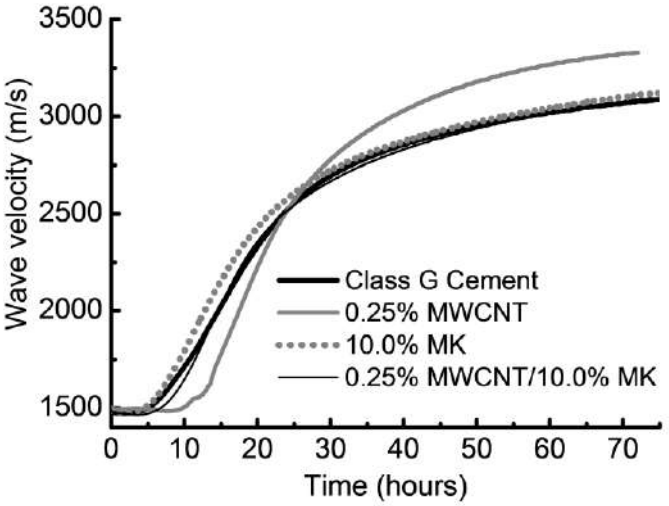

Figure 9.14 - Ultrasonic wave velocity curves of cement and cement/MWCNT/MK pastes

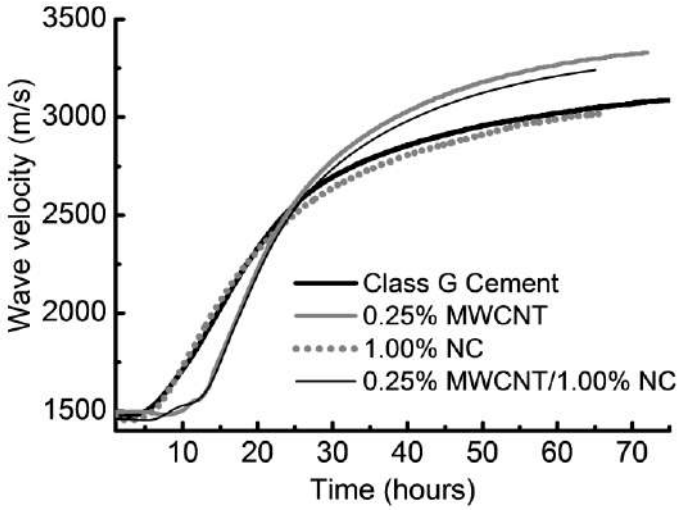

Figure 9.15 - Ultrasonic wave velocity curves of cement and cement/MWCNT/NC pastes

Table 9.5 - Time of the percolation threshold for all the samples studied by ultrasonic pulse

Sample	Percolation threshold (h)
Class G cement	6.8
0.25% MWCNT	9.5 – 12.9
1.00% NS	5.4
10.0% MS	4.7
10.0%MK	5.6
1.00%NC	5.5
0.25% MWCNT/1.00%NC	6.5 – 12.9
0.25% MWCNT/1.00%NS	5.2
0.25% MWCNT/10.0%MK	7.5
0.25% MWCNT/10.0%MS	5.6 – 10.2

9.4 General discussion

An interaction has been shown to exist between cement grains and a MWCNT aqueous dispersion with surfactant as a dispersing agent. Both carbon nanotubes and surfactant molecules are adsorbed or entrapped by cement grains during the first minutes of hydration; this phenomenon causes a retardation of the hydration reaction and setting time of class G cement. Evidence shows that the surfactant and MWCNT do not separate when mixed with cement; this result suggests that both surfactant molecules and carbon nanotubes prevent the water from reaching cement grains temporarily because of their hydrophobic properties, retarding the hydration reaction. This was evidenced by heat flow curves of cement pastes blended only with the MWCNT dispersion.

This retardation can be minimized by using pozzolanic micro or nanoparticles in a two-step mixing process in which the MWCNT dispersion interacts first with a pozzolanic particle dispersion, rather than interacting with cement. The retardation was found to be minimized proportionally to the amount of pozzolanic particles combined with the MWCNT dispersion; the effectiveness of each pozzolanic particle to minimize the retardation effect was different when comparing similar amounts of surface area of pozzolanic particles. This result indicates that the interaction between the MWCNT dispersion and the pozzolanic particles does not depend only on the amount of surface area of the nanoparticles, but also on the properties of such surface.

One potential issue the can be derived from this combination of MWCNT dispersion with pozzolanic particles is that the interaction of MWCNT dispersions with pozzolanic particles may cause a loss of stability of the MWCNT dispersion. The

electrostatic balance of the combinations and the stability of the MWCNT must be studied to confirm the severity of this issue and to determine how it influences the overall performance of the MWCNT in the cement matrix.

The effect of the combinations of MWCNT and pozzolanic particles was not only the minimization of the retardation. The AFt formation was enhanced by the Al2O3 present in the MWCNT as catalyst from their production and by the pozzolanic activity of the alumina based pozzolans; consequently, the amount of AFm formed from the transformation of AFt into AFm was also increased. The heat release associated with the formation of C-S-H and hydrated aluminates was also increased as consequence of the pozzolanic activity of the pozzolanic particles combined with the MWCNT.

The initial setting time and percolation threshold of the different cement pastes were also affected by the presence of surfactant in the MWCNT dispersion. These two parameters were retarded by the presence of the MWCNT dispersion, and accelerated by the presence of pozzolanic particles. In some cases, two percolation thresholds were identified; this outcome can be associated with a possible false setting or a possible rearrangement of the porous structure of the matrix. Further testing is required to identify the cause of this phenomenon.

9.5 Conclusions

- An interaction exists between cement grains and nanotubes dispersion that retards the hydration of cement; a two-step mixing procedure with different pozzolanic particles is capable of minimizing this retardation, regardless of the micrometric or nanometric nature of the pozzolan.
- The effectiveness of pozzolans to prevent this retardation is proportional to the amount particles used and their specific surface area, and depends on their surface properties. Further testing is required to identify the primary surface properties that control this phenomenon.
- The interaction of MWCNT dispersions with pozzolanic particles may cause a loss of stability of the MWCNT dispersion. The electrostatic balance of the combinations and the stability of the MWCNT must be studied to confirm the severity of this issue and determine how it influences the overall performance of the MWCNT in the cement matrix.

PHASE 2: IN-HOUSE MWCNT DISPERSION

10. In-house dispersion – Dispersion process and effect on hydration kinetics

Anionic, cationic and amphoteric surfactants used as dispersing agents for carbon nanotubes and their interaction with cement

Abstract

This work studies the hydration kinetics of Portland cement pastes blended with Multi Walled Carbon Nanotubes (MWCNT) aqueous dispersions. Anionic, cationic and amphoteric surfactants, i.e. surfactants that have different charged functional groups in their structure, were used as dispersing agents. MWCNT in powder form were dispersed in deionized water with sodium dodecyl sulfate, cetylpyridinium chloride and triton TX-100. Three concentrations of each surfactant (1, 10 and 100 mM) were tested, and all samples were sonicated until an adequate dispersion degree was obtained. Cement pastes blended with carbon nanotubes were prepared, and their hydration kinetics was studied using the Vicat needle and isothermal calorimetry tests. It was found that the surfactants used to disperse the MWCNT interacted with the surface of nanotubes, as well with the cement grains. Such triple interaction between MWCNT, surfactant and cement should be taken into account when interpreting the influence of MWCNT on the earl yage mechanical properties of cement materials.

Keywords: Carbon nanotubes, surfactant, retardation, pozzolans, adsorption

10.1 Introduction

Different methods, such as dry mixing with portland cement [86], sonication in acetone followed by evaporation [42], acid treatments combined with ultrasonic pulses [12], [61], [112], [130], growth of nanotubes directly onto cement grains [139], and use of chemical dispersing agents combined with ultrasonic pulses [47], [130], [131], [221]

have been studied to incorporate multi walled carbon nanotubes (MWCNT) in cement matrices. All these methods have a common goal, to break MWCNT bundles to obtain individual nanotubes that are evenly dispersed throughout the cement matrix; thus, maximizing their reinforcing efficiency. The most commonly used method in the literature is to disperse CNT in the mixing water using chemical dispersing agents, such as surfactants, in combination with ultrasonic pulses [48], [50], [51], [142]. Two mechanisms have been proposed to explain the dispersion of CNT by surfactants in water. The first mechanism is that surfactant molecules propagate through space formed in the MWCNT bundles by the ultrasonic pulse [131] and adsorb on their surface; these adsorbed molecules generate repulsion with other similarly charged molecules adsorbed on other MWCNT [181], hence separating the individual nanotubes. The second mechanism is that surfactants decrease surface tension of the mixing water, allowing a better wettability of the MWCNT [222], then adsorb onto their surface and generate repulsion between individual nanotubes. Dispersion efficiency of a surfactant depends on its polar nature and the length of the tail [133], [223], hydrophobic tails adsorb preferably on MWCNT due to super hydrophobic effect [181].

Both of these mechanisms have the potential to affect the hydration reaction of cement [182] through adsorption of the surfactant on the anhydrous cement grains. Nevertheless, literature reports show no consensus concerning the effect of MWCNT over the properties of cement-based composites. It is necessary to understand the triple interaction MWCNT/surfactant/cement, and how surfactants adsorbed onto MWCNT can affect the hydration of Portland cement. This information is important to build criteria to select dispersing agents for specific Portland cement-based composites applications. This work studies the triple interaction CNT/surfactant/cement, focusing on the difference of the effect on the hydration of cement of three differently charged surfactants: anionic, cationic and amphoteric.

10.2 Materials and methods

The materials used in this research were HE type hydraulic cement complying with ASTM C-1157, industrial grade MWCNT, laboratory grade Sodium Dodecyl Sulfate (SDS), Cetylpyridinium Chloride (CPC) and Triton X-100 (TX-100). Aqueous dispersions with 0.35% MWCNT were prepared using SDS, CPC and TX-100 in 1mM, 10mM and 100mM concentrations. Surfactant concentrations were chosen so that the

effect of surfactant could be evaluated near to and over their critical micelle concentration (CMC), which is the concentration at which micelles of surfactants start to form. MWCNT concentration was chosen from typical values from the literature. Surfactants were combined with water and stirred for 5 minutes using a magnetic stirrer; then, solid MWCNT were added to the mixture. Dispersions were sonicated using a 500 W ultrasonic processor set to 40 % amplitude in 20 seconds on/off cycles to avoid overheating the samples. When necessary, an ice bath was used to cool down the samples. A summary of the dispersions studied is presented in Table 10.1.

Table 10.1 – Summary of MWCNT/surfactant aqueous dispersions produced

Dispersion Name	Surfactant concentration (mM)	Surfactant type	MWCNT concentration (%)
SDS 1mM	1	SDS	0.35%
SDS 10 mM	10		
SDS 100 mM	100		
CPC 1mM	1	CPC	
CPC 10mM	10		
CPC 100 mM	100		
TX 100 1mM	1	TX 100	
TX 100 10mM	10		
TX 100 100mM	100		

The degree of dispersion of MWCNT/surfactant aqueous dispersions was measured by UV-Vis absorbance spectra. An aliquot was taken from each dispersion, diluted with deionized water by a 1:100 mass to mass factor, and placed in a 1.5 mL PMMA cuvette with a 10 mm optical pathway. A sample of deionized water and surfactant was sonicated and diluted to be used as a baseline before each test. Absorbance spectra were acquired from 250 to 800 nm in 0.2 nm steps. The best dispersion conditions, i.e. surfactant concentration and total amount of energy applied by the ultrasonic processor, were determined for each type of surfactant using UV-Vis spectroscopy. It is known that MWCNT aqueous dispersions present a peak in their absorbance spectra around 300 nm, which is related to the dispersion degree of the nanotubes [51]. This absorbance value (UV_{300}) was measured in aliquots taken from the dispersion process at evenly spaced energy intervals. Each aliquot was diluted by a 1:100 mass to mass factor and its absorbance spectra was measured from 190 to 850 nm, in 0.2 nm steps. A sample of water and surfactant was used as baseline for each test.

Stability of the dispersions produced in the best conditions determined earlier was characterized by ζ-potential measurements. Each sample was diluted by a 1:300 factor using water/surfactant dilutions with compatible concentrations. The test was carried out at 25 °C, with a 2 minutes thermal equilibrium wait and 100 readings per sample. The pH of the dispersions was raised from natural to 12.5 using $Ca(OH)_2$ dissolved in deionized water.

Cement pastes blended with MWCNT solid additions of 0.15%, by mass of cement, were produced in two steps. First, the MWCNT dispersions were combined with the mixing water; then, cement was added and mixed until a homogeneous paste was obtained. Plain cement pastes made without any MWCNT were produced by stirring the surfactant and water using a magnetic stirrer for 5 minutes; then, cement was added and mixed until a homogeneous paste was obtained. Setting time and hydration kinetics of the samples were studied by Vicat needle and isothermal calorimetry.

Setting time was measured using the Vicat needle test according to ASTM C 191 for two sets of samples. The first set (P1) was composed of plain pastes with surfactant and with the water-to-cement (w/c) ratio required for normal consistency of a hydraulic cement paste determined by ASTM C 187. The second set (B) was composed of pastes blended with MWCNT/surfactant dispersions with a fixed w/c of 0.55. Hydration kinetics of the pastes was evaluated using an isothermal calorimeter. The calorimeter was set to 27 °C, and 5.0 ± 0.2 g of paste was poured in glass ampoules. Water was used as the reference material. The obtained heat flow and cumulative heat curves were normalized by mass of cement present in the sample. Two sets of samples were also studied in this test. The first set (P2) was composed of plain paste with surfactant no MWCNT and a fixed w/c of 0.55. The second set (B) was the same used for setting time tests, which were pastes blended with MWCNT/surfactant dispersions with a fixed w/c of 0.55. A summary of the mixtures studied is presented in Table 10.2.

Table 10.2 – Summary of MWCNT/surfactant cement pastes studied

Past name			
Family	Surfactant and concentration	MWCNT solid addition (% bwoc)	w/c
P1	Reference	-	Amount necessary for normal consistency
	SDS 1mM		
	SDS 10 mM		
	SDS 100 mM		
	CPC 1mM		
	CPC 10mM		
	CPC 100 mM		
	TX 100 1mM		
	TX 100 10mM		
	TX 100 100mM		
P2	Reference	-	0.55
	SDS 1mM		
	SDS 10 mM		
	SDS 100 mM		
	CPC 1mM		
	CPC 10mM		
	CPC 100 mM		
	TX 100 1mM		
	TX 100 10mM		
	TX 100 100mM		
B	SDS 1mM	0.15	0.55
	SDS 10 mM		
	SDS 100 mM		
	CPC 1mM		
	CPC 10mM		
	CPC 100 mM		
	TX 100 1mM		
	TX 100 10mM		
	TX 100 100mM		

10.3 Results and discussion

This section presents the dispersion process adopted for the MWCNT/surfactant aqueous dispersions, characterizing the interactions among their components and discussing how they influence the time of setting and hydration kinetics of cement paste.

10.3.1 MWCNT imaging

The MWCNT used in this work were acquired in powder form and were expected to be agglomerated or entangled due to van der Waals interaction among them [44]. To obtain an image of the MWCNT agglomerates, a small amount of MWCNT was dispersed in deionized water without any dispersing agent using an ultrasonic bath

for 5 minutes, and then a drop of this dispersion was placed in a copper #300 Formvar mesh. This was left to dry in a desiccator before imaging using a scanning transmission electron microscope (STEM) in bright field transmission mode with a 75 kV acceleration. An image of a typical MWCNT entanglement is presented in Figure 10.1. It can be seen that even though the diameter of individual MWCNT is around 20 nm, their length is in the micrometric scale and the entanglements reach up to 500 nm in diameter. This image highlights the importance of an effective dispersion process to obtain individual nanotubes evenly dispersed.

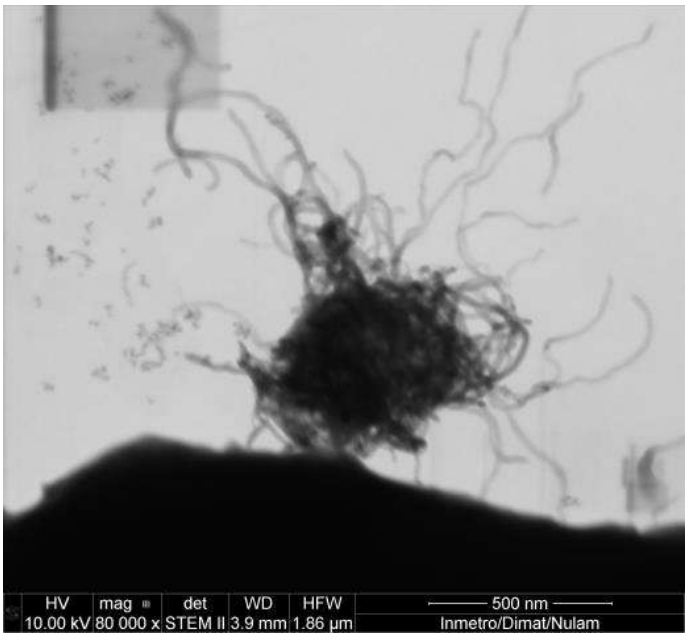

Figure 10.1 – TEM image of MWCNT agglomeration

10.3.2 Dispersion of MWCNT in water

The efficiency of the different surfactants as dispersing agents was characterized by the UV-Vis absorbance peak found between 250 and 300 nm (UV_{300}), which has been related to the presence of individual carbon nanotubes [47], [130], [131], [221]. The evolution of the UV_{300} value obtained for the three surfactants studied in the three concentrations is presented in Figure 10.2. The efficiency of each dispersant was found to be dependent on the surfactant concentration and amount of energy applied. For both SDS and CPC, it can be seen that the highest surfactant concentration (100 mM) yielded the best results; i.e. the highest UV_{300} value. For the TX 100 surfactant, the intermediate concentration (10 mM) not only yielded the best result among the three concentrations studied, but also among the three types of surfactants. Regarding dispersion energy, 390

J/g was chosen as the most adequate amount of energy to be applied to all the dispersions because at this energy value all dispersion exhibit a plateau, where increases of energy increase marginally the degree of dispersion. This energy value was chosen to preserve the integrity of MWCNT, since it has been reported in the literature that high amounts of energy applied can break and induce defects in the structure of MWCNT [51].

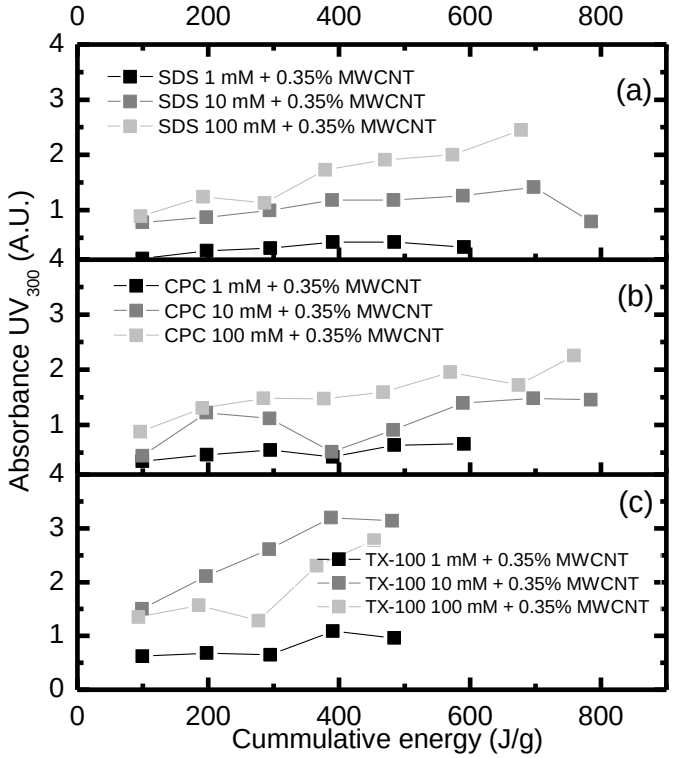

Figure 10.2 – Absorbance at 300 nm (UV_{300}) versus energy applied by ultrasonic processor of (a) SDS, (b) CPC, and (c) TX 100 at different concentrations (A.U.: Arbitrary units)

Absorbance spectra of the MWCNT/surfactant aqueous dispersions after applying 390 J/g using the ultrasonic processor are presented in Figure 10.3. These spectra represent the best dispersion conditions adopted for this work.

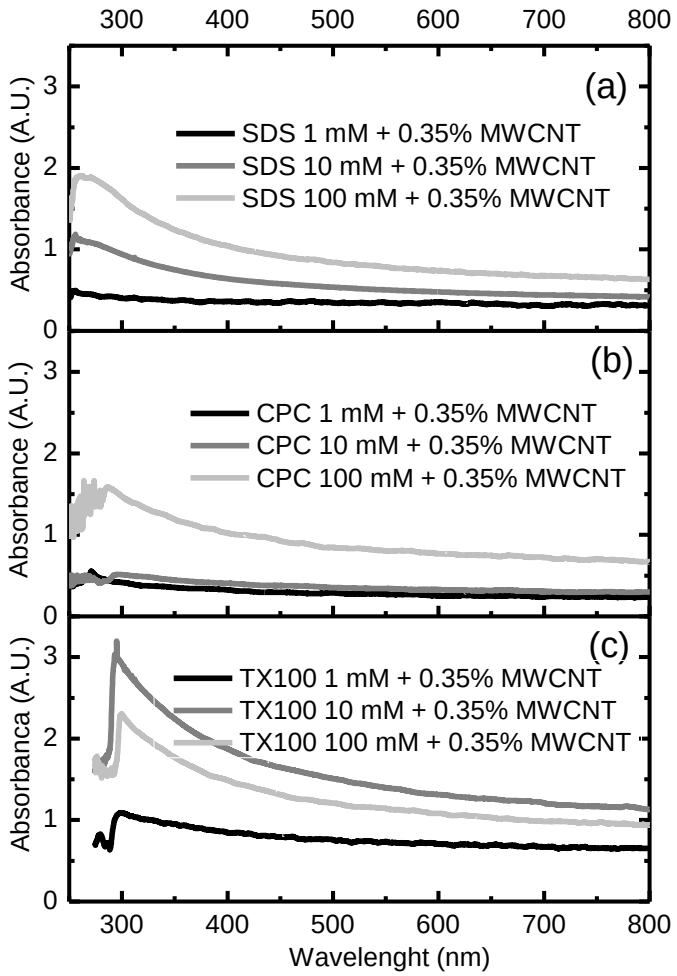

Figure 10.3 – Absorbance spectra of 0.35% MWCNT dispersions with (a) SDS, (b) CPC, and (c) TX 100 at different concentrations after applying 390 J/g by sonication. (A.U.: Arbitrary units)

The stability of the MWCNT/surfactant dispersions was characterized using ζ-potential measurements. These measurements were carried out for the three surfactant concentrations that yielded the best degree of dispersion after 390 J/g of sonication. The pH of the dispersions was increased with $Ca(OH)_2$ up to 12.5. $Ca(OH)_2$ was used as an alkaline agent instead of ammonia to better emulate the alkaline environment generated by cement during its hydration reaction, where $Ca(OH)_2$ is formed as an hydration product [31]. The obtained results are presented in Figure 10.4. The zone between +25 mV and -25 mV has an unstable electric potential for colloidal particles, which will have a tendency to agglomerate [224]. It was found that regardless of the nature of the surfactant used to disperse MWCNT, at high pH all the dispersions fell into the unstable zone. Nevertheless, this can be considered a satisfactory result when comparing to other types of dispersants such as superplasticizers. MWCNT/superplasticizer dispersions

have been reported to reach the isoelectric point for a similar pH value, exhibiting a complete destabilization of the colloid [51].

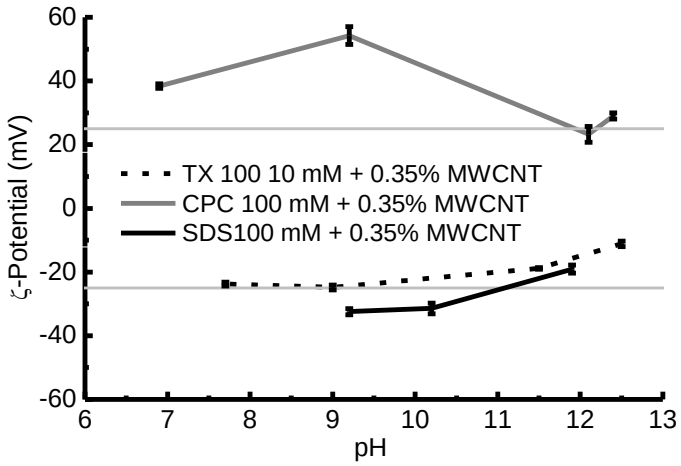

Figure 10.4 – ζ-potential versus pH of MWCNT/surfactant dispersions using the best dispersion conditions

10.3.3 Normal consistency and time of setting

After measuring the dispersion degree of the MWCNT/surfactant dispersions, these were used to prepare two sets of samples to evaluate time of setting. The first set (P1) was composed of pastes made of water, cement and surfactant. The objective of this set was to understand the individual effect of each type of surfactant on the setting time of Portland cement; i.e. the surfactant/cement interaction. Before measuring the time of setting, normal consistency tests were carried out to determine the w/c necessary to prepare each paste. The obtained results are presented in *Figure 10.5*. The reference sample reached normal consistency at w/c: 0.331. For SDS, CPC, and TX 100 at a 1 mM concentration, the amount of water required to obtain normal consistency was reduced to w/c: 0.293, 0.310 and 0.290 respectively. This can be associated with an adsorption of surfactant molecules on the cement grains with their hydrophobic chain towards water[182], which can generate steric repulsion between cement grains similarly to a plasticizer[225], thus decreasing the amount of water required to obtain a desired consistency. The increase in SDS concentration to 10 and 100 mM increased again the amount of water required to obtain normal consistency, while CPC and TX 100 decreased it marginally. It should be noticed that these concentrations are higher than CMC of SDS (8.2 mM), CPC (1.2 mM) and TX 100 (0.24 mM) according to the manufacturer data sheet. Both situations can reduce the efficiency of a surfactant as a

dispersant and limit its effect as a plasticizer. From these experiments, it cannot be concluded which phenomenon would govern the w/c variations due to different surfactant concentrations. Regarding the time of setting of the same set of pastes, it was found that all three types of surfactants increased both the initial and final setting times. These results are also presented in *Figure 10.5*. The increase in setting time was found to be proportional to the surfactant concentration, and is also a consequence of the adsorption of surfactant molecules on the cement grains[183] through different mechanisms, such as hydrophobic chains adsorbed towards water[182], steric repulsion[225], and hydrophobicity of cement grains[226] that retard the hydration process of cement. Some slight decrease in setting time was identified and associated with decreases in w/c rather than the effect of the surfactants.

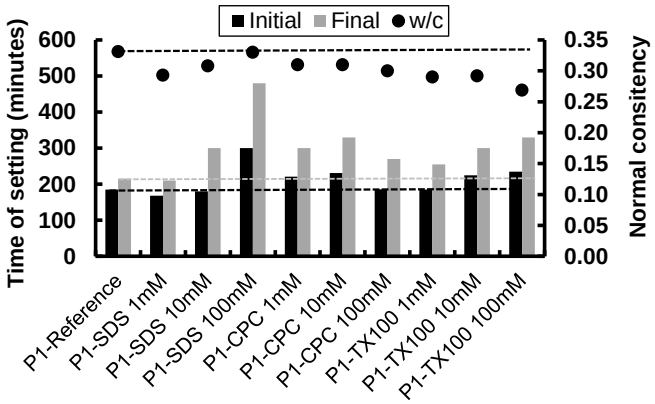

Figure 10.5 – Time of setting and normal consistency results of cement + surfactant pastes. Dotted lines are extensions of the P1-Reference sample.

The second set of samples tested in this section (B) was composed of pastes made of water, MWCNT/surfactant aqueous dispersions and cement. The objective of this set was to identify if surfactants used as dispersing agents in MWCNT aqueous dispersions are also capable of generating a retardation effect of the paste. Pastes were prepared with 0.15% MWCNT additions by weight of cement and a fixed w/c of 0.55. The results obtained are presented in *Figure 10.6*. For SDS at 1 and 10 mM concentrations, a decrease in final setting time of 30 and 60 minutes, respectively, was identified, while the 100mM concentration generated a 300 minute delay of the same. CPC at 1 mM generated a 60 minute decrease in final setting time, while 10 and 100 mM concentrations delayed final setting 36 and 370 minutes, respectively. TX 100 at 1 mM accelerated final setting by 60 minutes, while 10 and 100 mM retarded it by 60 and

360 minutes, respectively. This indicates that for the lower concentrations, some of the retardation effect induced by the surfactants was compensated by the presence of MWCNT, and that the role of surfactants in a MWCNT aqueous dispersion is not only limited to a dispersing agent, but there is a MWCNT/surfactant/cement triple interaction. Due to the low resolution and limited nature of the data obtained by the time of setting tests, it is not possible to infer the mechanism by which the presence of MWCNT can modify the effect of surfactants on cement grains.

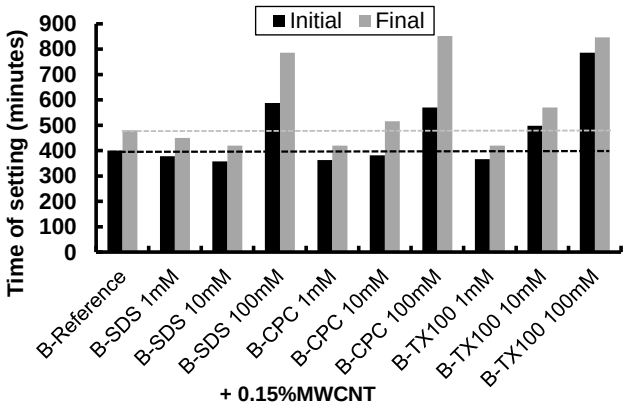

Figure 10.6 – Time of setting results of cement + surfactant + MWCNT's pastes. Dotted lines are extensions of the B-Reference sample for comparison purpose.

10.3.4 Isothermal calorimetry

To better understand the extent of the triple interaction of MWCNT/surfactant/cement, isothermal calorimetry tests were carried out using the P2 and B sets of samples. For each concentration and type of surfactant studied, heat flow and cumulative heat results of pastes made with only surfactant, and with MWCNT/surfactant dispersions were compared with the results of a reference sample of plain cement; all pastes had the same w/c of 0.55. In all cases, the induction period, the main heat release peak due to the calcium silicate hydrate (C-S-H) precipitation, the sulfate depletion, and the subsequent second ettringite (AFt) formation and monosulfoaluminate (AFm) transformation were clearly identified [216].

SDS heat flow and cumulative heat

Results for the sets of pastes made with SDS, with and without MWCNT, are presented in Figure 10.7. When compared to the reference sample, for all SDS

concentrations there is an overall decrease in the amount of energy released during hydration. In the heat flow curves a decrease the intensity of the heat release associated with C-S-H, $Ca(OH)_2$ and AFt formations was found. Additionally, for the P2-SDS 100 mM and B-SDS 100 mM + 0.15%MWCNT samples, a 1.5 hour increase of the induction period was identified, compatible with the increase of setting time found for the same samples. All three SDS concentrations presented a decrease of total heat release after 140 hours of hydration, as evidenced in the cumulative heat curves. This behavior can be considered consequence of the adsorption of surfactant molecules on the cement grains. When comparing results for samples with and without MWCNT for the same SDS concentration, it can be seen that there is a slight acceleration of the hydration kinetics of the pastes blended with MWCNT, with almost no effect on the total heat release. This acceleration is evidenced as a shift to the left of the heat flow curves, and can be associated with the nucleation effect of MWCNT **[69]** on C-S-H formation or with a portion of the surfactant that remained adsorbed on the MWCNT. The strongest shift to the left was found in the B-SDS 100 mM + 0.15%MWCNT sample, which was prepared with the highest dispersion degree among the three tested SDS concentrations.

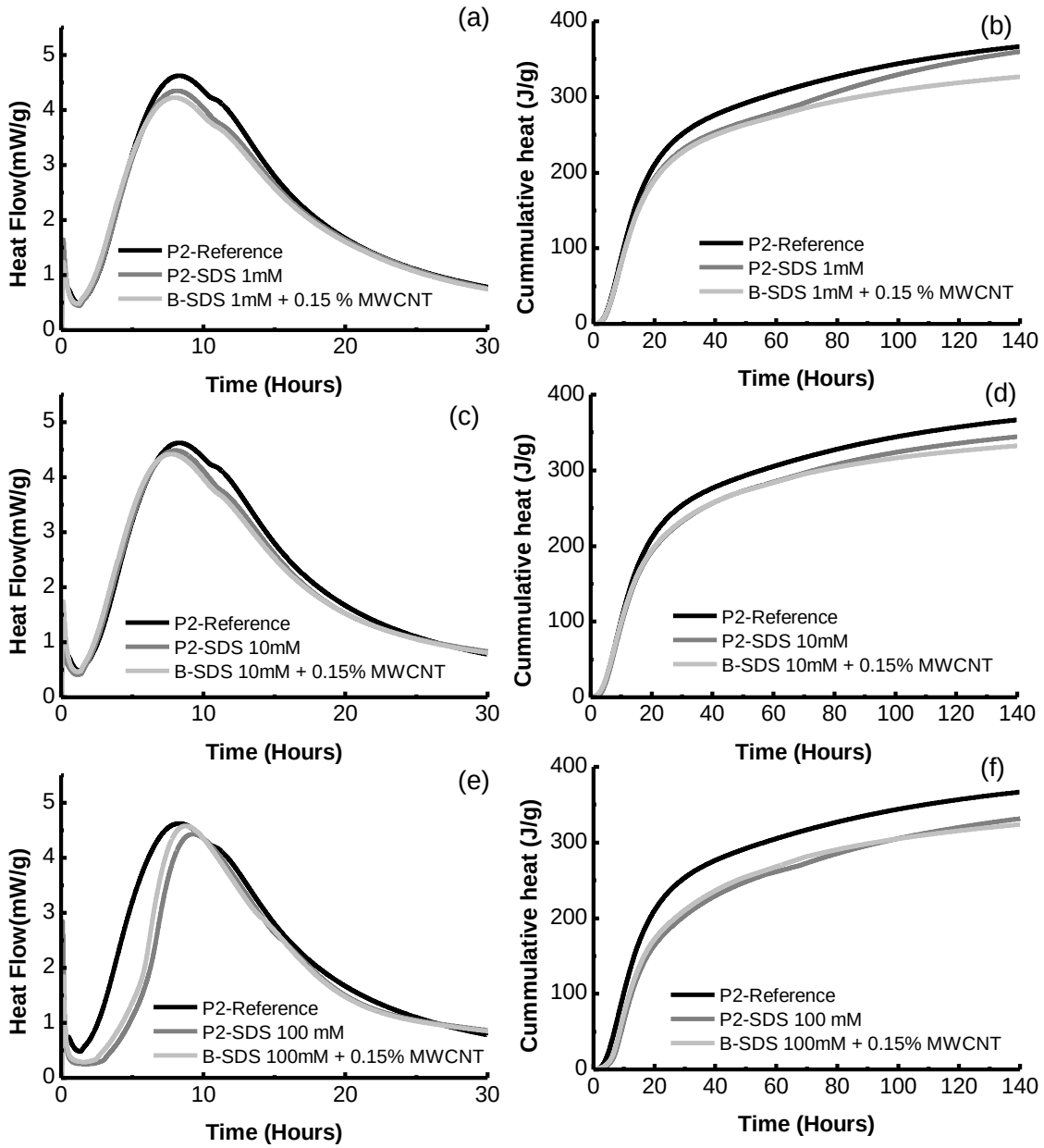

Figure 10.7 – Isothermal calorimetry results of cement pastes blended with and without 0.15% MWCNT using SDS as dispersing agent at (a-b) 1mM, (c-d) 10mM and (e-f) 100mM concentrations.

CPC heat flow and cumulative heat

Results for the sets of pastes with CPC, made with and without MWCNT, are presented in Figure 10.8. When compared to the reference sample, the B-CPC 1 mM and B-CPC 10 mM samples presented an increase of heat release in the heat flow peak associated with C-S-H, $Ca(OH)_2$ and AFt formations. The total heat release after 140 hours of hydration was also increased, as evidenced in the cumulative heat results. Heat release associated with C-S-H, $Ca(OH)_2$ and AFt formations returned to values similar

to that of the reference sample for the samples blended with MWCNT (B-CPC 1 mM + 0.15%MWCNT and B-CPC 10 mM + 0.15%MWCNT). After 140 hours of hydration, the total heat release also decreased by the presence of MWCNT. Additionally, a slight shift to the left in the heat flow curve was identified, which is compatible with the decrease in setting times found for the same samples. For the P2- CPC 100 mM sample, it was found that the surfactant decreased heat flow associated with AFt formation, and also decreased the total heat release after 140 hours. The 100 mM CPC + 0.15%MWCNT sample presented a further decrease in heat release. This is also compatible with the time of setting results, which presented a sensible retardation for this sample. From this set of results it can be said that the acceleration or retardation found can be associated with the interaction of CPC with cement grains [182]. The shift to the left found in the MWNCT blended samples can be associated either with nucleation effects induced by MWCNT [69], or with a portion of the surfactant that remained adsorbed on the MWCNT; thus, preventing it from affecting the hydration reaction and is related to the dispersion of the nanotubes.

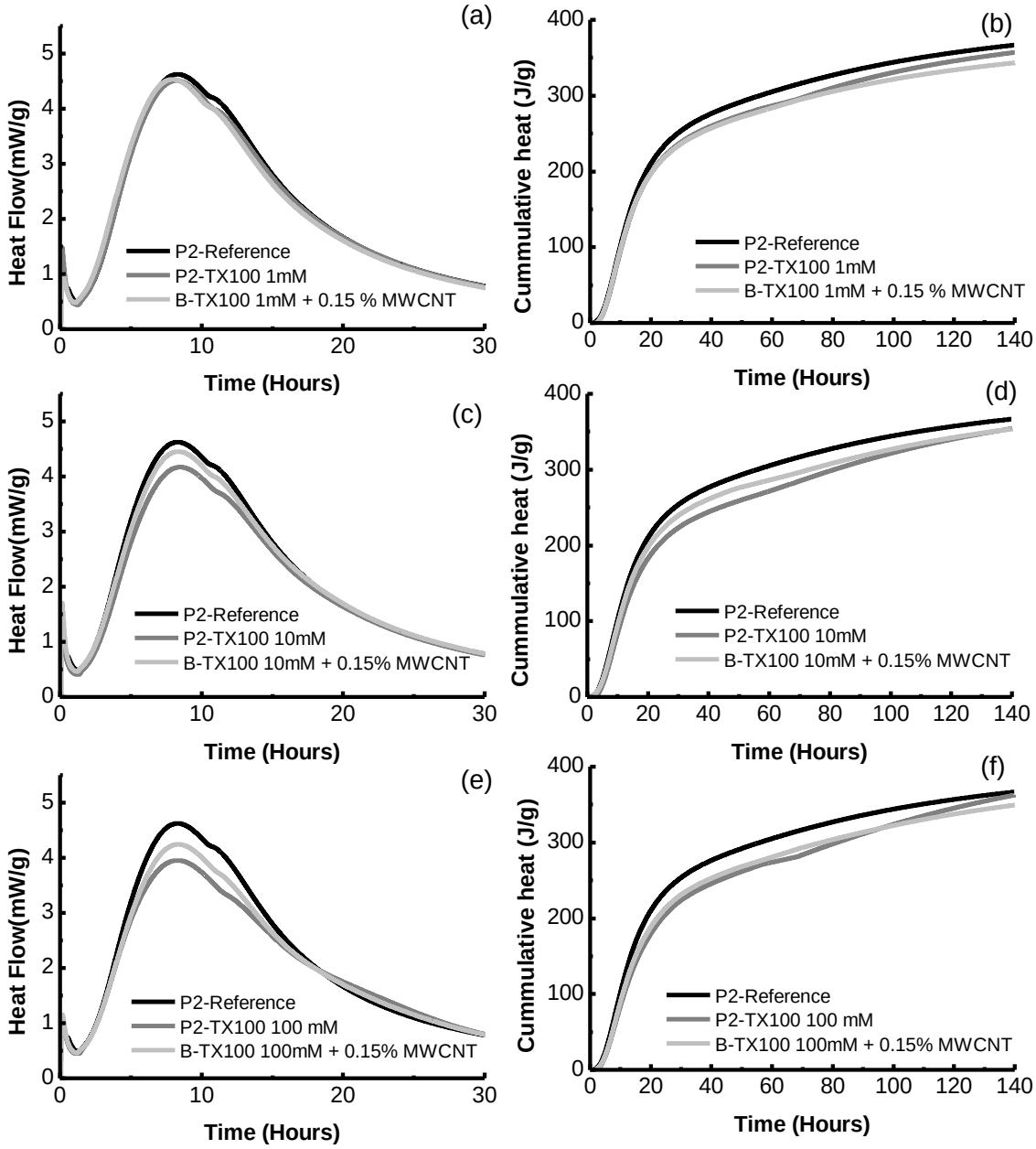

Figure 10.8 – Isothermal calorimetry results of cement pastes blended with and without 0.15% MWCNT using TX 100 as dispersing agent at (a-b) 1mM, (c-d) 10mM and (e-f) 100mM concentrations.

TX 100 heat flow and cumulative heat

Results for the sets of pastes with TX 100, made with and without MWCNT, are presented in Figure 10.9. A decrease in intensity of the heat release associated with C-S-H, $Ca(OH)_2$ and AFt formations was found with and without MWCNT. This decrease was found to be proportional to the TX 100 concentration and consistent up to 140 hours of hydration. This is compatible with the retardation effects found in the setting time experiments, and can be considered consequence of the adsorption of surfactant

molecules on cement grains [183]. When comparing results for samples with and without MWCNT for the same TX 100 concentration, it can be seen that the presence of MWCNT minimized or compensated for the heat release decrease associated with C-S-H, $Ca(OH)_2$ and AFt formations. This was found to be more effective for the B-TX 100 10 mM + 0.15%MWCNT sample, which was prepared with the dispersion with best dispersion degree among the three TX 100 concentrations. This is likely to be due to a portion of the surfactant that remained adsorbed on the MWCNT, since no shifts to the left were identified in the heat flow results for this set of samples.

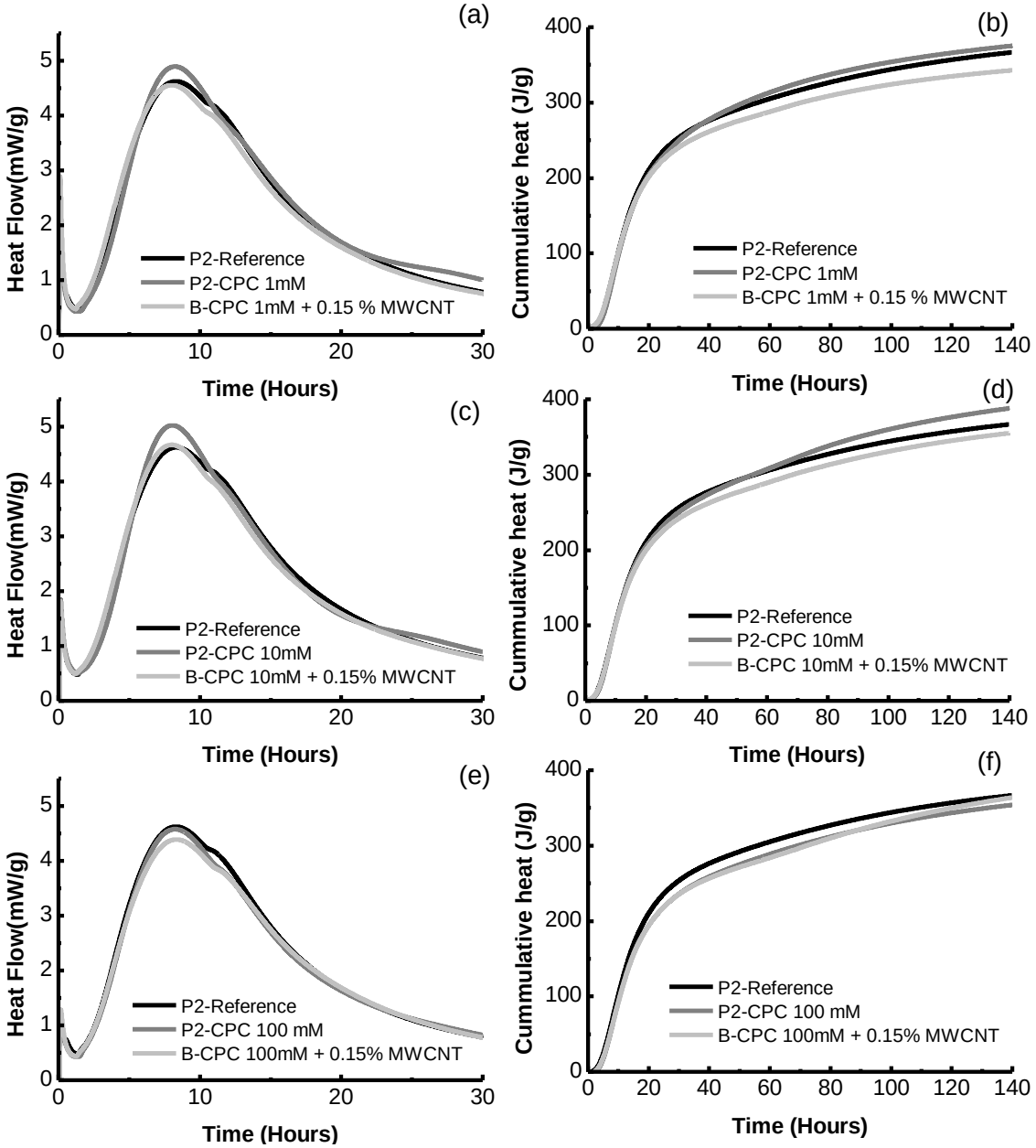

Figure 10.9 – Isothermal calorimetry results of cement pastes blended with and without 0.15% MWCNT using CPC as dispersing agent at (a-b) 1mM, (c-d) 10mM and (e-f) 100mM concentrations.

10.4 General discussion

As expected, each type of surfactant presented a different efficiency as dispersing agent for the MWCNT. This behavior is in accordance with the literature, where it has been reported that surfactants have a dispersability plateau for MWCNT, and that the concentration at which this plateau is reached depends on a number of factors such as nanotube diameter, pH, and nature of the surfactant [227]. Nevertheless, literature reports show that SDS[47], [131], [132], [221], [228], [229], CPC[182], [227] and TX 100[215], [229], [230] are suitable dispersing agents for MWCNT in water, regardless of their different efficiencies.

This research has characterized the triple interaction of MWCNT/surfactant/cement through the evaluation of the kinetics of hydration of cement and setting time of the paste. It was found that the use of surfactants can affect the hydration reaction of cement paste, ass expected; thus, retarding their time of setting and decreasing the heat release. This is due to different mechanisms clearly identified in the literature, such as hydrophobic chains adsorbed on cement grains towards water [182], steric repulsion between cement grains[225], and increased hydrophobicity of cement grains[226] due to the use of a dispersing agent. The need of a chemical dispersing agent for MWCNT is widely recognized, but this research showed that the real net effect of MWCNT on the hydration kinetics of Portland cement is widely surpassed or masked by the effect of surfactants used as dispersing agents for the nanotubes in the mixing water, regardless of the charge of the functional group in their structure. The net effect of MWCNT was identified as slight difference in the kinetics of hydration when comparing samples of the same surfactant concentration, in pastes made with and without MWCNT. These differences can be related with two sources, (i) nucleation effect of the MWCNT, or (ii) a portion of the surfactant molecules that remain adsorbed on the MWCNT; thus, preventing them to retard the hydration reaction. This was found to be strongly dependent on the dispersion degree obtained by the sonication process and the surfactant concentration. The mechanism that governs the triple interaction MWCNT/surfactant/cement was not completely identified and further work should be carried out to characterize it.

The nature of the surfactant used as dispersing aid for MWCNT in water was found to be of great importance in not only for the dispersion efficiency, but also to the performance of the cement paste in which they are blended. An amphoteric surfactant

was found to be more efficient to disperse MWCNT in water; its lack of electric charge might be associated with its higher efficiency, nevertheless, further work is required to confirm this hypothesis. A more efficient surfactant requires using a lower amount to obtain adequate dispersion, which in time means lower negative effects on the performance of the paste in both fresh and hardened states. This because the negative effects of surfactants on cement paste are directly proportional to the amount of surfactant present in the paste.

Studies of the effect of MWCNT aqueous dispersions with different types of surfactants on the mineralogical evolution, rheological behavior and strength development of cement based matrices should be conducted. The results of such studies will help to understand how the use of surfactants as dispersing agents for MWCNT affect the hydration of cement and lead to misinterpretations of the real effect of MWCNT on the properties of cement based composites.

10.5 Conclusions

From the experimental evidence gathered in this work, it can be concluded that the real net effect of MWCNT on the hydration kinetics of Portland cement is widely surpassed or masked by the effect of surfactants used as dispersing agents for the nanotubes in the mixing water, regardless of the charge of the functional group in their structure. The mechanism that governs the triple interaction of MWCNT/surfactant/cement was not completely identified, and further work should be carried out to characterize it.

11. In-house dispersion – Effect on rheology

Influence of MWCNT/surfactant dispersions on the rheology of Portland cement pastes

Abstract

Little work has been reported in the literature regarding the mechanisms by which multi walled carbon nanotubes (MWCNT) modify the rheology of cement based matrices. Surfactants are the most commonly used dispersing agents for MWCNT in water; however, it is necessary to understand if the triple interaction MWCNT-surfactant-cement has a direct impact on the rheological behavior of the cement matrix. This work studies the effect of MWCNT/surfactant aqueous dispersions on the rheology of cement pastes. Three types of surfactants (sodium dodecyl sulfate, cetylpyridinium chloride and triton TX-100) were used to prepare cement pastes with and without MWCNT. Three rheological parameters were determined for each sample: static yield stress, yield stress, and viscosity. The first was measured directly, while the other two were obtained by fitting a Bingham model to the descending portion of a flow curve. Additionally, X-ray diffraction and isothermal calorimetry were used to follow the hydration reaction of cement during the first hour. It was found that the MWCNT/surfactant dispersions generate an overall shift to higher yield stress values while maintaining viscosity, suggesting a modification of the interparticle attraction. It was concluded that the triple interaction MWCNT-surfactant-cement governs the rheology of cement pastes.

Keywords: Carbon nanotubes, surfactant, hydration, adsorption, rheology

11.1 Introduction

Different types of nanoparticles have been reported to decrease the workability of cement based matrices [187]–[189], [191], [193]. This effect is proportional to the amount of particles blended, and is related to a higher water demand due their

inherently higher specific surface area (SSA). This behavior has not been verified for multi walled carbon nanotubes (MWCNT). On the contrary, a decrease in viscosity has been found in cement pastes [145]; however, this decrease was related to a plasticizing effect from the surfactant used to disperse MWCNT in the mixing water, rather than to MWCNT themselves.

To obtain a good quality MWCNT dispersion in water, it is necessary to use high concentrations of dispersing agents in combination with a sonication process [207]. Surfactants are the most commonly used dispersing agent. They allow efficient dispersion by decreasing the surface tension of water [222] and by adsorbing on the surface of MWCNT through hydrophobic interactions [47]. Surfactant molecules adsorbed on the surface of MWCNT maintain the colloid stable through the electrostatic repulsion between the electric charges of their functional groups [231], and their dispersing efficiency depends on the tail length of the surfactant used [223].

When immersed in water, cement particles become flocculated or coagulated [232][233], and the rheological behavior of the matrix is governed interparticle interactions [185]. Surfactants can adsorb on the surface of cement grains through electrostatic interactions [182], increasing the hydrophobicity of the grains [226] and modifying the interparticle attraction [31]; thus, modifying the rheological behavior and hydration reaction of the matrix.

Given that surfactants are able to adsorb on both MWNCT and cement through different mechanisms, this work aims to verify if the influence of MWCNT/surfactant dispersions on the rheology of cement pastes depends only on the surface area of MWCNT, or if the presence of surfactants has an additional influence.

11.2 Materials and methods

The materials used were class G high sulfate resistance cement produced by Holcim, industrial grade NC7000 multi walled carbon nanotubes (MWCNT) produced by Nanocyl, sodium dodecyl sulfate (SDS) of 96% purity produced by J.T. Baker, cetylpyridinium chloride (CPC) 100% pure produced by Sigma Aldrich, triton X 100 (TX 100) of 98% purity produced by Sigma Aldrich, and Rheomac UW 410 viscosity modifying agent (VMA) produced by Basf Chemicals.

Specific surface area (SSA) of cement and MWCNT was measured using N_2 adsorption isotherms and BET theory in an ASAP 2020 Physisorption Analyzer from Micrometrics, and specific gravity was measured in a helium pycnometer from Micrometrics. All three surfactants were diluted in deionized water in 1mM, 10mM and 100mM concentrations and stirred for 5 minutes using a magnetic stirrer, surface tension measurements of these samples were carried out using the pendant drop method in a Dataphysics OCA 15EC equipment.

Aqueous dispersions containing 0.35% MWCNT were prepared using the three types of surfactants in 1mM, 10mM and 100mM concentrations. Surfactants were combined with deionized water and stirred for 5 minutes using a magnetic stirrer; the stirring magnet was removed and solid MWCNT were added to the mixture. Dispersions were then sonicated using an ultrasonic tip, which applied a total energy of 390 J/g to guarantee an adequate dispersion degree, as determined in a previous work by the authors [234]. Sonication was carried out in a 500 W ultrasonic processor set to 40 % amplitude in 20 seconds on/off cycles to avoid overheating the samples. When necessary, an ice bath was used to cool down the samples during sonication. These dispersions were used to produce MWCNT blended pastes.

Dispersion degree of the MWCNT/surfactant aqueous dispersions was measured by UV-Vis spectroscopy using a Genesys 10S UV-Vis spectrophotometer from Thermo Scientific. An aliquot was taken from each dispersion, diluted with deionized water by a 1:100 mass to mass factor, and placed in a 1.5 mL PMMA cuvette with a 10 mm optical pathway. A sample of deionized water and surfactant was stirred and diluted to be used as baseline before each test. Absorbance at 300 nm (UV_{300}) was measured for each dispersion.

Three families of pastes were produced for this work. The first, labeled as reference (Ref), was composed of water, cement and VMA; using a water-to-cement (w/c) ratio of 0.55. VMA was used to guarantee the stability of the pastes, i.e. avoid segregation and settling during rheological testing and curing of the samples. The most adequate VMA dosage was obtained from static sedimentation tests according to API Recommended Practice 10B-2 at room temperature. For this, pastes were prepared and poured in 25 mm by 100 mm cylindrical molds, sealed and cured at complete rest for 24 hours in a water bath at room temperature. After curing, samples were demolded and cut in four equal 25 mm height sections with a diamond saw. Density of each section was determined by Arquimedes principle and the static sedimentation ($\Delta\rho$) was

determined as the difference in density between the top and bottom quarters of each sample.

The second family of pastes, labeled as plain (P), was composed of water, surfactant, cement and VMA. The w/c and VMA dosage were maintained constant and equal to those of the reference paste, and only surfactant type and concentration were varied. The third family of pastes, labeled as blended (B), was composed of water, surfactant, MWCNT, cement and VMA. These pastes have the same proportion as the plain pastes, but are blended with 0.15% MWCNT by mass of cement. The MWCNT/surfactant dispersions previously sonicated were used to prepare these pastes. A summary of the proportions of the pastes studied is presented in Table 11.1.

Table 11.1. Proportions of cement pastes studied

Paste Name			w/c	VMA (% bwoc)
Family	Surfactant and concentration	MWCNT solid addition (% bwoc)		
Ref	-	-	0.55	1.00
P	SDS 1mM	-		
	SDS 10mM			
	SDS 100mM			
	CPC 1mM			
	CPC 10mM			
	CPC 100mM			
	TX 100 1mM			
	TX 100 10mM			
	TX 100 100mM			
B	SDS 1mM	0.15% MWCNT		
	SDS 10 mM			
	SDS 100 mM			
	CPC 1mM			
	CPC 10mM			
	CPC 100 mM			
	TX 100 1mM			
	TX 100 10mM			
	TX 100 100mM			

Pastes were mixed in a 600mL Chandler constant speed mixer by adding water, VMA and the MWCNT/surfactant dispersions when applicable. This was mixed at 500 rpm for 1 minute; then, cement was added and speed was increased to 2070 rpm during 1 minute and maintained constant for 5 more minutes. After this, pastes were transferred to an atmospheric consistometer set to room temperature, where were conditioned at

150 rpm for 20 minutes. Immediately after conditioning, bulk density (ρ) of the paste was measured using a mud balance following the API Recommended Practice 10B-2.

Hydration kinetics of the pastes was studied in a TAM Air Isothermal calorimeter. The calorimeter was set to 27.0 °C and 5.0 g of each paste were mixed for 90 seconds using an admix device inside the calorimeter to avoid any data loss at the beginning of the reaction. Water was used as reference material. Heat release was measured for one hour and the obtained heat flow curves were normalized by the mass of cement present in the sample. Immediately after removing from the calorimeter, pastes were mixed with isopropyl alcohol and oven dried at 60 °C for two hours to stop hydration. These samples were used for X-ray Diffraction (XRD) testing in a Bruker D8 diffractometer equipped with a Cu radiation source (Kα, λ = 1.5418 Å). Diffraction patterns were measured from 4 to 70° 2θ with a step size of 0.05 and an accumulation time of 30 seconds.

Rheology of the pastes was tested at room temperature using a Brookfield DVIII Ultra rheometer equipped with a V73 Vane spindle. Three rheological parameters were obtained from each paste: static yield stress (τ_s), yield stress (τ_0) and viscosity (μ_0). First, samples were sheared from rest to $0.2 s^{-1}$ in 180 seconds, from which τ_s was determined; then, a constant 0.2 s^{-1} shear rate was maintained for 60 seconds to ensure homogeneity of the sample, and finally a flow curve was obtained by increasing shear rate from 0.2 s^{-1} to 45.2 s^{-1} and back to 0.2 s^{-1} in 20 steps of 30 seconds each. This shear rate stepwise variation is presented in Figure 11.1. τ_0 and μ_0 were determined for each sample by fitting a Bingham model ($\tau = \tau_0 + \mu_0.\gamma$) to the linear descending portion of the flow curve. This testing method has been successfully applied before in a similar equipment for micro concrete [195].

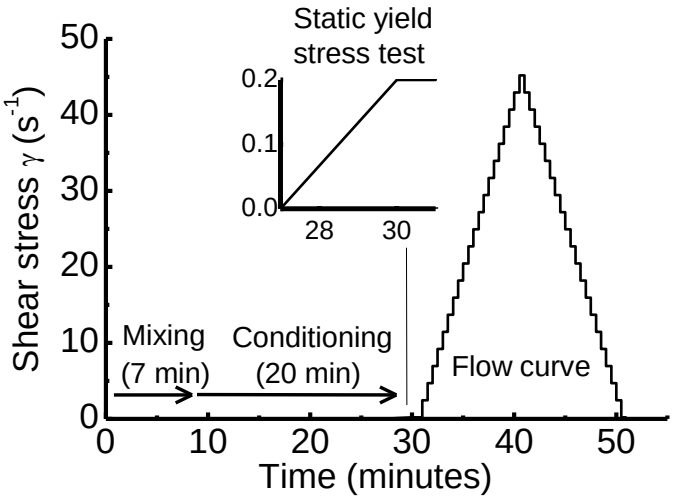

Figure 11.1 – Shear stress stepwise variation used for rheological testing

11.3 Results and discussion

This section presents and discusses the obtained results. First, characterization of the relevant parameters of the raw materials is presented, giving special attention to the stability to static sedimentation of the reference paste. Then, the influence of surfactant and MWCNT on the hydration kinetics and rheology of cement pastes is presented and discussed.

11.3.1 Raw materials characterization

Specific surface area and specific gravity results for cement and MWCNT are presented in Table 11.2. It was found that MWCNT have much higher surface area and lower density than cement, as expected for nanoparticles. Surface tension results of water with 1 mM, 10 mM and 100 mM surfactant concentrations are presented in Figure 11.2. It can be seen that of the three surfactants studied TX 100 was the most effective in lowering the surface tension of water, reaching its maximum effect at the 10 mM concentration, while CPC was the least effective.

Table 11.2 – Specific surface area and specific gravity results for cement and MWCNT

	SSA (m^2/g)	Specific gravity (g/cm^3)
Cement	0.84	3.26
MWCNT	208.0	1.50

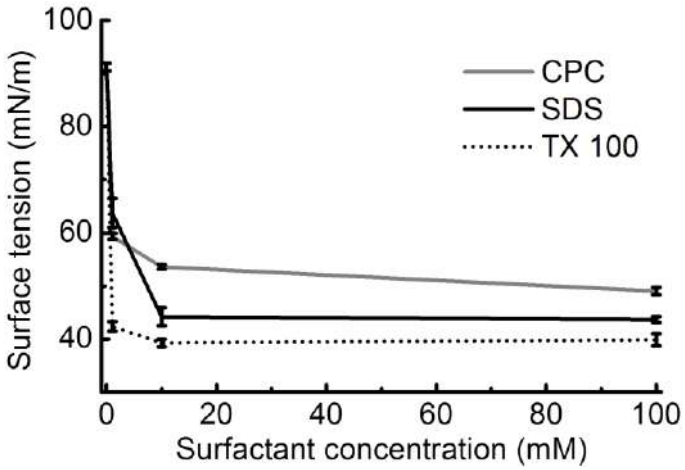

Figure 11.2 – Surface tension results of water with different concentrations of surfactants

The effectiveness of the sonication process of the MWCNT/surfactant aqueous dispersions was characterized using UV-Vis absorbance measurements at 300 nm (UV_{300}), which has been found to be proportional to the dispersion degree of MWNCT in water [51]. Obtained results are presented in Figure 11.3. It was found that each surfactant presented a different efficiency when acting as dispersing aid for MWCNT in water. These differences in efficiency are related to the decrease in surface tension of water, which allows a better wettability of the MWCNT [222], and to the different tail lengths of the surfactants [223]. TX 100 in a 10 mM concentration yielded the best dispersion degree of the 9 conditions studied, while CPC was the least efficient for al concentrations.

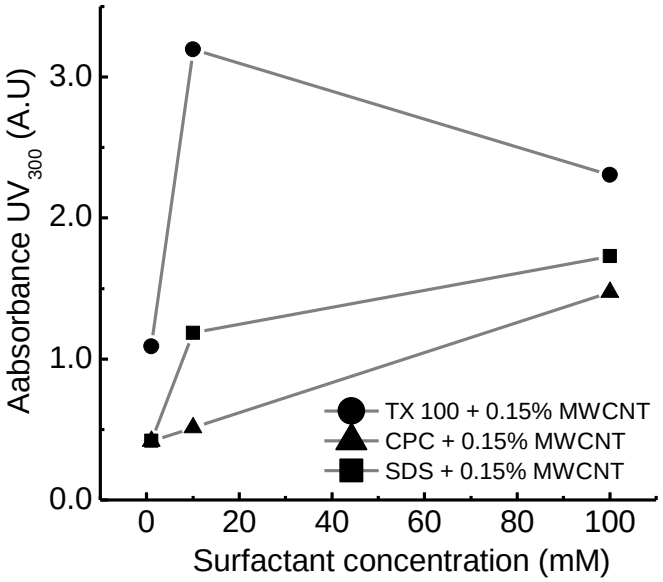

Figure 11.3 – Dispersion degree of the different MWCNT/surfactant dispersions measured by UV-Vis absorbance at 300 nm

11.3.2 Stability of the reference paste

All the pastes produced in this work are meant to be submitted to rheological testing; therefore, their stability becomes of great importance. Gravitational sedimentation can produce a vertical gradient of solids within the tested sample, causing overestimation of the yield stress and plastic viscosity results [185]; VMA was chosen as stabilizing agent to minimize this effect. Static sedimentation ($\Delta\rho$) of the reference paste was measured for different amounts of VMA in order to find the amount that minimized the density difference between the top and the bottom of the samples after 24 hours of curing at complete rest. Results are presented in Figure 11.4. It was found that 1.00% of VMA by mass of cement yielded the best results, bringing $\Delta\rho$ almost to zero. This amount of VMA was fixed for all the studied pastes.

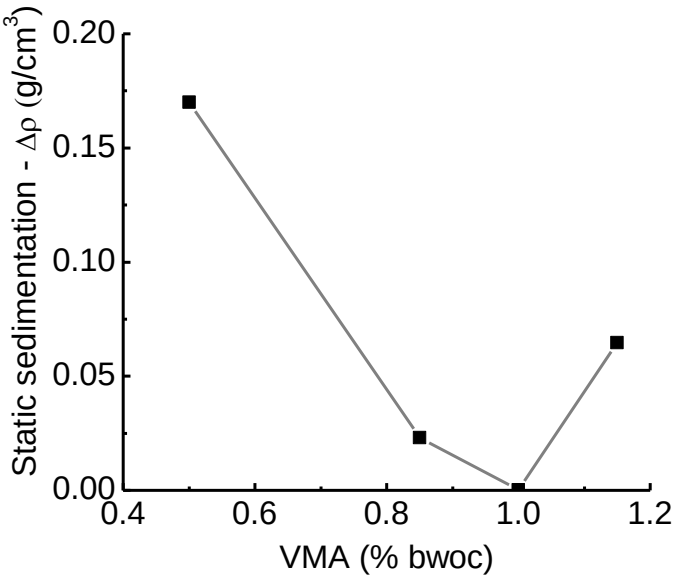

Figure 11.4 – Static sedimentation results of the reference paste for different amounts of VMA

11.3.3 Hydration kinetics during the first hour

The first hour of hydration, corresponding to the time window in which rheology was measured, was studied by isothermal calorimetry and XRD. The heat flow curves obtained for the reference paste and the P and B families of pastes are presented in Figure 11.5. It was found that during the first minutes upon contact with water, cement´s exothermic reaction was enhanced by the presence of surfactants in the mixing water. The geochemical theory for cement hydration states that hydration kinetics is governed by dissolution-precipitation processes [235], where the anhydrous phases of clinker dissolve upon contact with water at different rates while releasing heat.

Tricalcium aluminate (C_3A) is responsible for most of the heat released during the first minutes after contact with water, and its reaction is slowed down by the adsorption of sulfate ions (SO_4^{-2}) on reactive dissolution spots of C_3A [236]. Sulfate ions come mainly from gypsum [212], and are expected to yield ettringite (AFt), monosulfoaluminate (AFm), or amorphous hydroaluminates from its reaction with C_3A [237], [238]. XRD tests were performed to verify if such hydration products were formed after one hour of hydration.

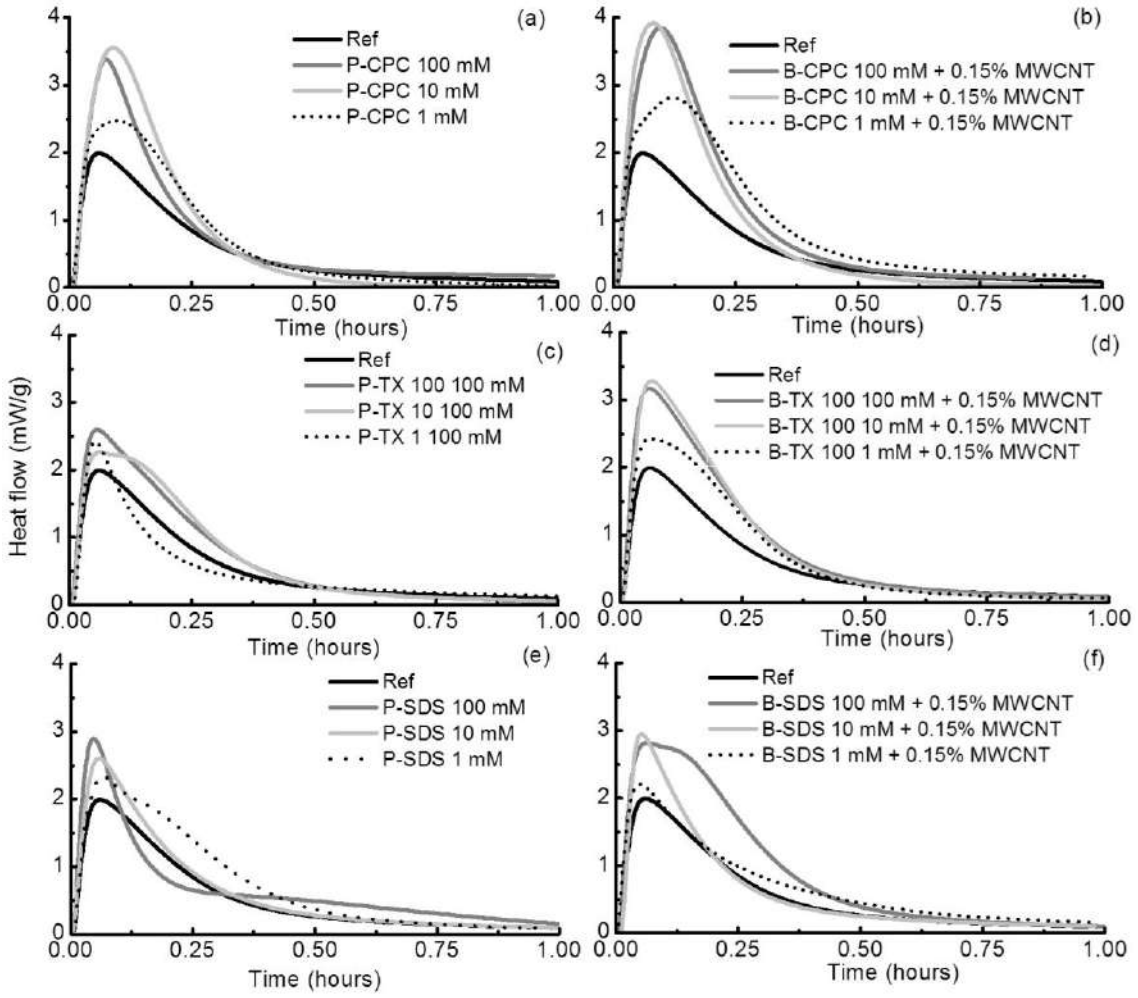

Figure 11.5 – Isothermal calorimetry heat flow results for pastes from the B and P families with (a) and (b) CPC, (c) and (d) TX 100, and (e) and (f) SDS in different concentrations

XRD patterns for pure cement and for the reference paste after 1 hour in contact with water are presented in Figure 11.6. It was found that the class G cement used contains anhydrite ($CaSO_4$), which can come from an uncontrolled temperature during grinding [212], or have been added as a thixotropic agent during production for oil well applications [31]. Regardless of its origin, it can be seen that after 1 hour of hydration

the diffraction peaks associated with anhydrite disappear, while the intensity of the diffraction peaks associated with gypsum ($CaSO_4 \cdot 2H_2O$) increases. This indicates that the anhydrite present in cement became hydrated, which is expected to happen when anhydrite is finely ground [239]. Additionally, no detectable amounts of AFt or AFm were found. This can be related to the short hydration time and the low C_3A content of the high sulfate resistant (HSR) class G cement used, which is maximum 3% according to API-10A specification, in contrast to a maximum of 15% for a typical ordinary Portland cement. Similar results were found for all the samples from the P family of pastes. These results are included as supplementary material.

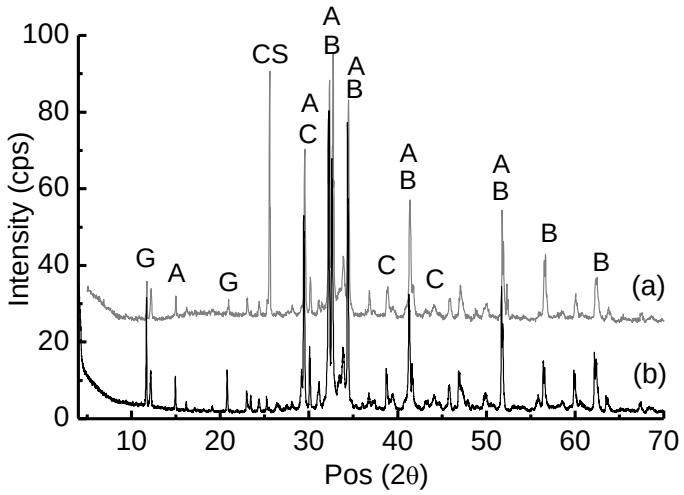

Figure 11.6 – XRD results for (a) pure cement and (b) reference paste after 1 hour in contact with water (G: Gypsum ($CaSO_4 \cdot 2H_2O$), CS: Anhydrite ($CaSO_4$), A; Alite, B: Belite, , C: Calcite, cps: counts per second)

The heat release enhancement due to the presence of surfactants can be explained in terms of the speed of clinker dissolution and anhydrite hydration, which depend on the amount of solid surface in contact with water. Surfactants are capable of lowering the surface tension of water and decreasing the contact angle in the liquid-solid interface. This enhances wettability of the powder [240] by deflocculation, exposing more solid surface to water and consequently increasing the heat release of cement during the first minutes of hydration. Since clinker dissolution and anhydrite hydration are both exothermic reactions [31], it is not possible with the experiments carried out in this work to separate the amount of heat release corresponding to each reaction.

Each type of surfactant studied presented a different effect on heat flow due to their different efficiencies to lower surface tension and due to their different molecular structures. It is known that the anhydrous phases present in clinker have different

charges on their surface [241], and that the adsorption of anionic and cationic surfactants depends on the surface charge of the solid surfaces; while most nonionic surfactants contain polar groups that form hydrogen bonds with the hydroxyl groups on the solid surface [226]. Additionally, the aqueous medium of cement paste makes it possible for surfactants to self-aggregate to from micelles as in a normal aqueous solution at high pH [242]. Some surfactant concentrations studied are above the critical micelle concentration (CMC) of SDS (8.2 mM), CPC (1.2 mM) and TX 100 (0.24 mM), according to the manufacturer data sheet. Any amount of surfactant above the CMC is expected to contribute only to micelle formation and not to adsorption density; additionally, high surfactant concentrations can modify the hydrophobicity of cement grains in a nonlinear way [226] and generate adsorptive micelles [182]. This is why in some cases the heat flow increase is not proportional to the amount of surfactant present in the sample.

11.3.4 Rheological measurements

The rheological parameters and bulk density in fresh state obtained for the reference and the B and P families of pastes are presented in Figure 11.7,

Figure 11.8 and Figure 11.9. Flow curves for each paste are presented in the supplementary material. It can be seen that MWCNT had a clear influence in all the rheological parameters measured when compared to the pastes with only surfactants and to the reference paste. The analysis of these results will be presented in two sections. First, the isolated effects of the different surfactants from the results obtained in the P family of pastes, and their mechanism of action will be presented. Then, the net effect of MWCNT will be discussed by comparing the B and P families of pastes.

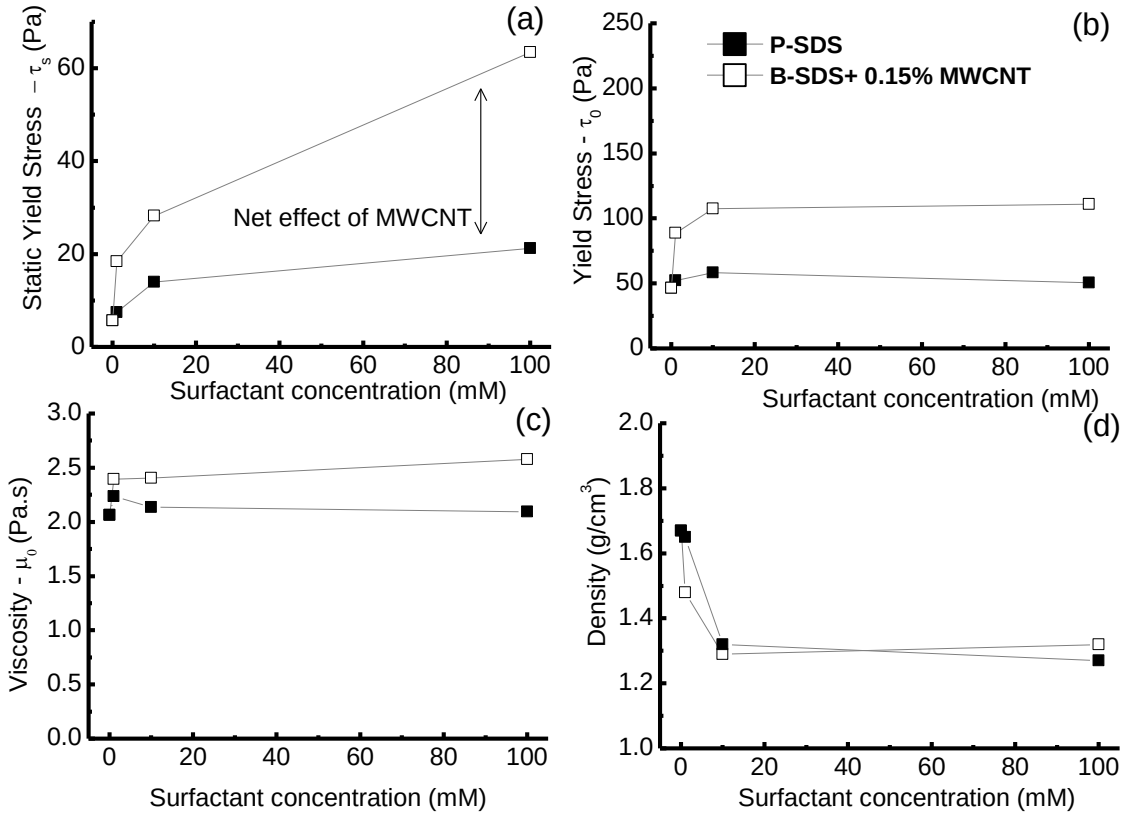

Figure 11.7 - (a) Static yield stress, (b) yield stress, (c) viscosity and (d) density of cement pastes blended different concentrations of SDS and 0.15% MWCNT

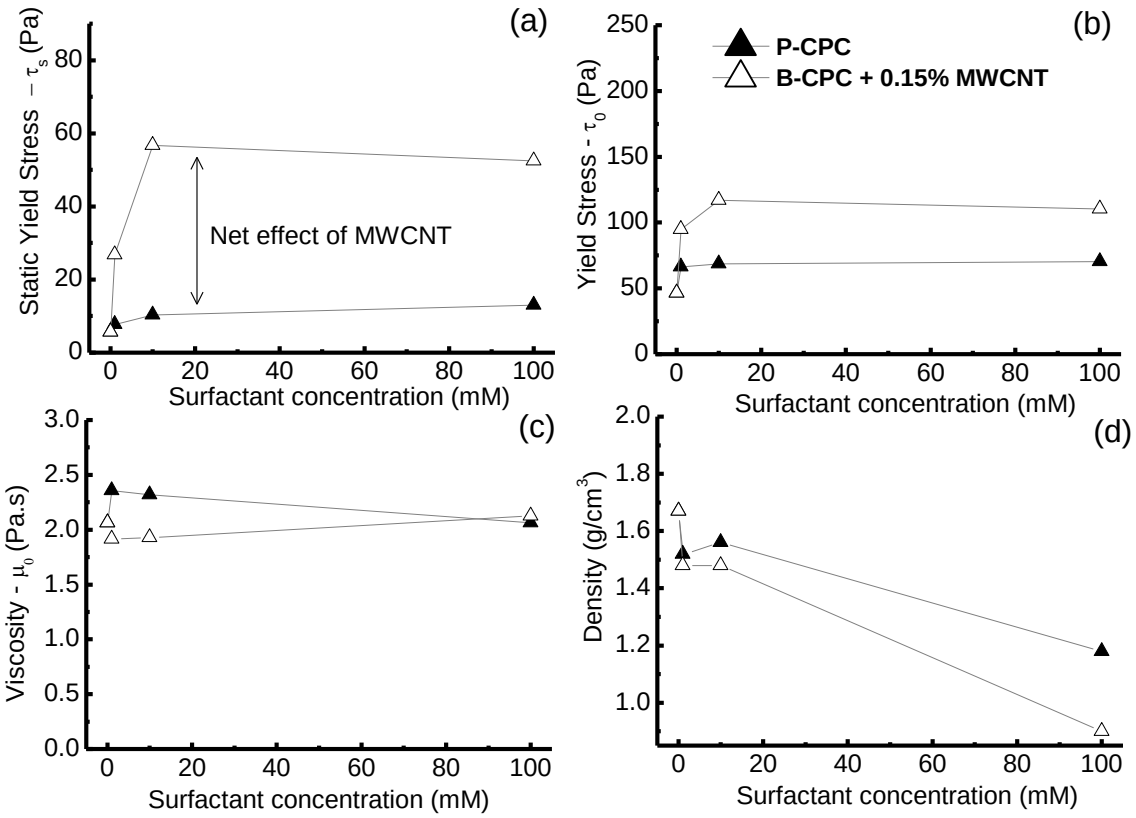

Figure 11.8 - (a) Static yield stress, (b) yield stress, (c) viscosity and (d) density of cement pastes blended different concentrations of CPC and 0.15% MWCNT

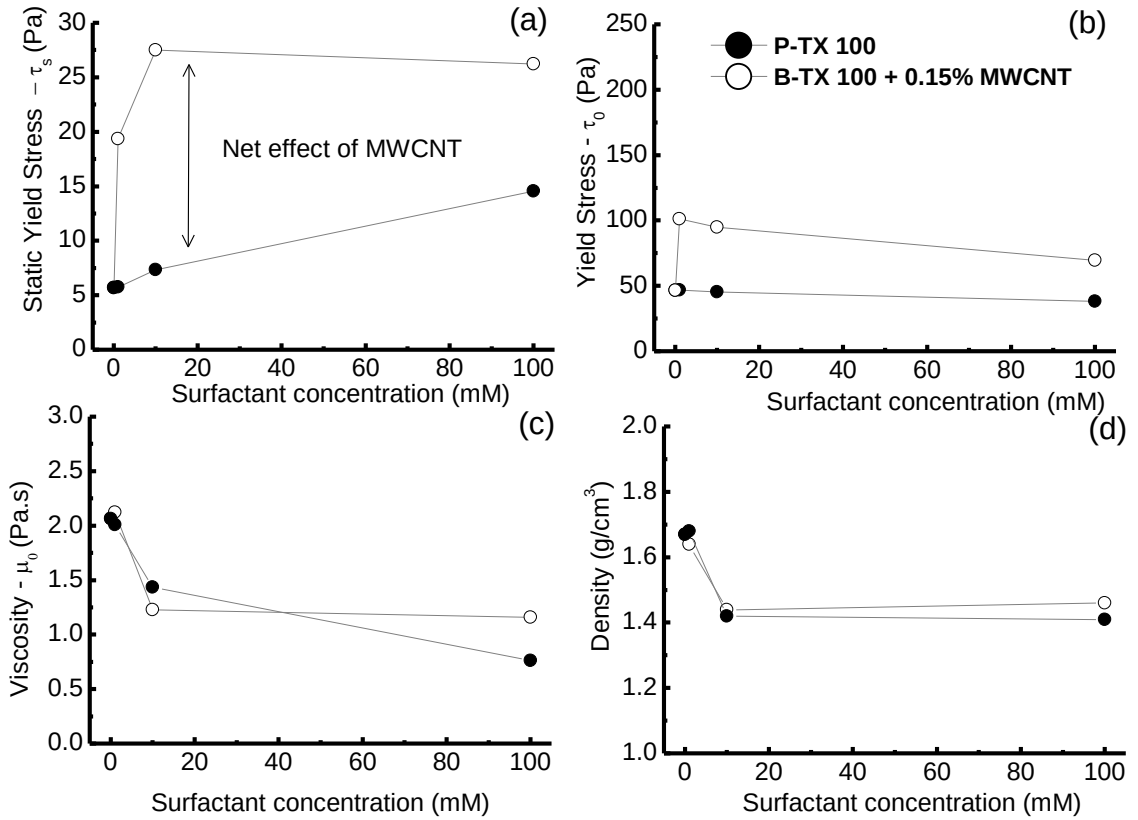

Figure 11.9 - (a) Static yield stress, (b) yield stress, (c) viscosity and (d) density of cement pastes blended different concentrations of TX 100 and 0.15% MWCNT

Effect of surfactants on the rheology of pastes

Regarding the isolated effect of surfactants it was found that the three types of surfactants, in the three concentrations studied, modified the flow properties of the pastes. The static yield stress (τ_s) was found to increase proportionally with the amount of surfactant, while the yield stress obtained from the Bingham model fitting (τ_o) varied differently according to the surfactant. Viscosity (μ_o) was only substantially modified by TX 100, and density (ρ) was found to decrease with the increase of surfactant.

For a better visualization of how surfactants modify the rheological behavior of the pastes, τ_s versus μ_o and τ_o versus μ_o plots were constructed and are presented in Figure 11.10. Two different trends were identified. For a decreasing μ_o, τ_s values were found to increase up to 270% with respect to the reference paste, while τ_o values presented variations from -17% for TX 100 to 52% for CPC when compared to the reference paste. TX 100 was the only surfactant that presented a substantial decrease of μ_o (63%), while SDS and CPC increased it up to 14% before returning to values similar to the reference paste.

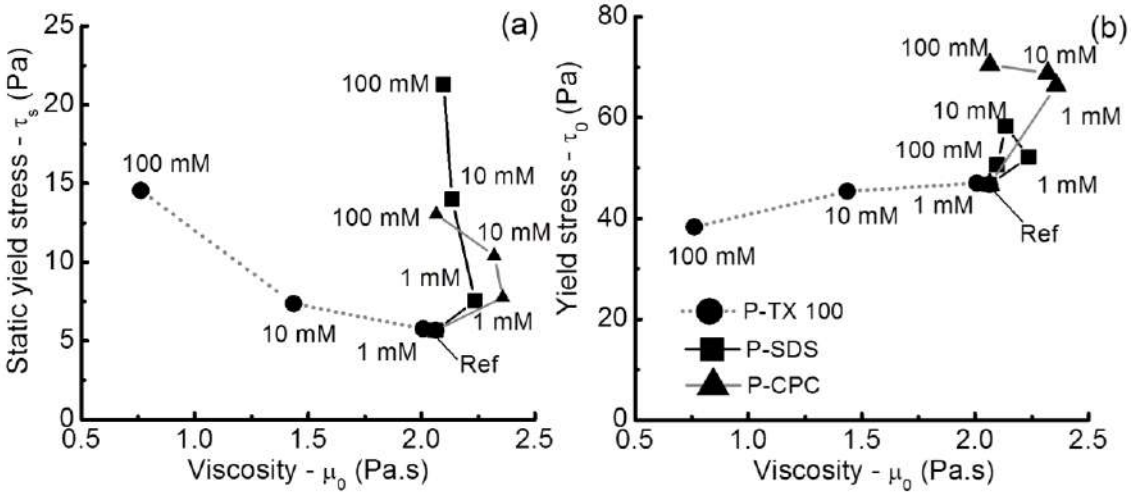

Figure 11.10 - (a) Static yield stress versus viscosity and (b) yield stress versus viscosity plots for plain cement pastes with different concentrations of SDS, CPC and TX 100

The increase in τ_s can be related to the enhancement in wettability of cement grains. It has been demonstrated in the previous sections that surfactants decrease the surface tension of water and expose more surface area of cement. This can affect the rheology of the pastes by one of the following mechanisms found in the literature:

(i) An increase of hydration products on the surface of cement grains can increase the interparticle locking [185]. Nevertheless, neither AFt nor AFm were detected in the XRD results after 1 hour of hydration. This is probably due to the low C_3A and high anhydrite content, which is less soluble than gypsum [243]. This leads to think that the effect of surfactants on the rheology of pastes does not rely on the formation of additional hydration products.

(ii) A portion of the water will be consumed by the hydration of anhydrite, significantly increasing the viscosity and yield stress of cement paste [232][244]. Nevertheless, XRD results showed that without the presence of surfactants (reference paste) all anhydrite was hydrated after one hour. Thus, there is no evidence of a link between the proportional increase of τ_s and surfactant concentration. This indicates that even though anhydrite plays an important role in the rheological properties of the reference paste, it has no role on the effects induced by surfactants.

(iii) Clinker particles in water are flocculated or coagulated [232][233], and the presence of surfactants helps to deffloculate clinker flocs and increase their surface area exposed to water. It is known that the rheology of pastes depends on the SSA of cement [245], where increasing SSA decreases workability of the matrix. Additionally, surfactant adsorption on the surface of cement can play an important role at this stage. In general, surfactants adsorb with their hydrophobic tails pointed towards water, increasing the hydrophobicity of cement grains, thus increasing interparticle attraction [31]. This will depend on the molecular structure of the surfactant and the surface charge of the different anhydrous phases in clinker. These mechanisms are believed to be most likely dominant in explaining the increase of τ_s.

The previously presented mechanisms cannot be directly extrapolated to the τ_0 results because yield stress depends on the shear history of the sample [185]. τ_0 is obtained from the descending portion of a flow curve, meaning that in this stage of the test the paste has been pre-sheared to the highest shear rate value used in the experiment, breaking the structures formed by interparticle interaction. This was true especially for TX 100, which presented a negative effect over τ_0, while SDS and CPC still presented some increase.

The decrease in μ_o and ρ can be related to the induction of air bubbles by surfactants. It has been previously reported that non-ionic [246] and ionic [68] surfactants can induce foam in cement matrices due to modifications in the surface tension of water [31]. Bubbles at as “ball bearings”, allowing cement particles to move past each other more easily [185], decreasing viscosity. Nevertheless, TX 100 presented the most significant reduction in viscosity but not the lowest density. Other amphoteric surfactants such as Pluronic F127 have exhibited similar behaviors [242][246]. Depending on the functional groups on the surfactant molecules, the hydrophobic backbone can be preferably adsorbed instead of the end group, causing dispersion of the grains by steric repulsion like a plasticizer [31], decreasing viscosity more effectively than air bubbles.

Net effect of MWCNT on the rheology of pastes

Regarding the net effect of MWCNT, increases both in τ_s and τ_0 were identified when compared to pastes from the P family, while μ_o did not appeared to be

substantially modified. τ_s versus μ_o and τ_0 versus μ_o plots were also constructed for this set of results and are presented in Figure 11.11. Similar trends to those of the P family of pastes were identified, but with an overall shift to higher τ_s and τ_0 values; such increase is expected to be related to the high surface area of MWCNT. This interpretation relays on the general fact that nanoparticles increase water demand, which does not apply to MWCNT because they are hydrophobic by nature [127]. Nevertheless, if surfactants are used to disperse MWCNT, the hydrophobic tails are adsorbed pointing inwards due to hydrophobic interactions, and the hydrophilic-charged end groups face outwards [181], allowing MWCNT to interact with water molecules [127] and cement grains depending on the nature of the surfactant used.

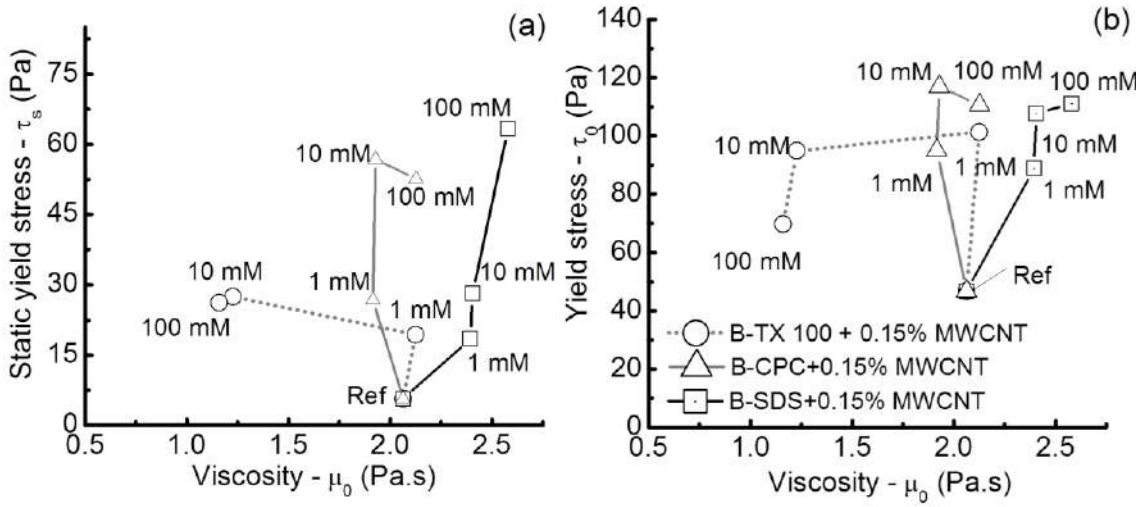

Figure 11.11 - (a) Static yield stress versus viscosity and (b) yield stress versus viscosity plots for plain cement pastes with different concentrations of SDS, CPC and TX 100 + 0.15% MWCNT

SSA, specific gravity and the proportions of the pastes were used to compute the total surface area of solids available in a unitary volume for each family of pastes prepared for rheological testing. It was found that the reference paste and the P family of pastes had a total surface area of solids of 0.963 m^2/cm^3, while the B family of pastes had a total surface area of solids of 1.323 m^2/cm^3. This means that a 0.15% addition of solid MWCNT by mass of cement increased 37% the total surface area of solids available in the paste. This additional surface area is enabled to interact with water and cement grains by the surfactants adsorbed on it. The overall shift to higher τ_s and τ_0 values while maintaining μ_o indicates that MWCNT modify the interparticle attraction, rather than interparticle locking or water demand. Increases in interparticle locking

would be seen as increases in μ_o, while increases in water demand would be seen as simultaneous modifications of τ_0 and μ_o [185].

It should be noted that the surface area of MWCNT was measured before any sonication or dispersion process. The goal of the sonication process in the presence of surfactants is to break MWCNT bundles to obtain individual nanotubes [54]. A direct consequence of this dispersion process is the increase of the surface area of MWCNT; therefore, dispersion degree must be closely related to the surface area of nanotubes after dispersion. Dispersion degree of the nanotubes was measured by absorbance measurements at 300 nm (UV_{300}), and in this work will be used as an indicative of changes in surface area. Even though there seems to be proportionality between the net effect of MWCNT and the UV_{300} value, it is not true that the condition that yielded the best dispersion degree also yielded the highest net effect. This indicates that the effect of MWCNT on the rheological behavior of the pastes does not depend solely on their SSA.

11.4 General discussion

The findings of this work show that MWCNT/surfactant dispersions have a considerable effect on the rheology of cement pastes. SSA of MWCNT seems to be the go-to feature to explain this effect, as with other nanoparticles, but a careful analysis of the results show that the presence of surfactants also plays an important role. Even though there seems to be a certain proportionality between the net effect of MWCNT on the rheological parameters of the cement pastes and the dispersion degree, it is not true that the condition that yielded the best dispersion degree (TX100 10 mM), and probably the highest MWCNT surface area, also presented the highest net effect, suggesting that more complex phenomena govern the effect of MWCNT/surfactant dispersions over cement pastes. Four key elements have been identified involving the influence of MWCNT/surfactant dispersions on the rheology of cement pastes:

(i) Surfactants increase the wettability of both cement and MWCNT by decreasing the surface tension of water. In the case of cement, this increase of wettability leads to an enhancement of heat release during the first minutes in contact with water, as evidenced by isothermal calorimetry results. In the case of MWCNT, it allows the dispersion of nanotube bundles in water to

obtain individual nanotubes, as evidenced by UV-Vis absorption experiments.

(ii) Surfactants adsorb both on cement and MWCNT. In the case of cement, surfactant molecules adsorb with their hydrophobic tails towards water, increasing hydrophobicity of cement grains. In the case of MWCNT, surfactants adsorb with their hydrophobic tails towards MWCNT surface and their hydrophilic groups towards water, giving them the capability of interacting with water and cement grains. This according to literature reports.

(iii) Surfactants induce bubbles in the paste, as evidenced by bulk density testing; these bubbles are stabilized by the adsorption of surfactants on their surface and are capable of working as "ball bearings" to decrease the viscosity of pastes, as evidenced by rheological testing.

(iv) Surfactants modify the surface properties of both cement and MWCNT, modifying the interparticle attractions, and consequently modifying the rheology of cement pastes, as evidenced by rheological testing.

An overall shift to higher τ_s and τ_0 values maintaining μ_o suggests that MWCNT/surfactant dispersions modify mainly the interparticle attraction rather than interparticle friction or water demand. Even though MWCNT have such a high SSA when compared to cement, the main source of solid surface area in the cement paste is cement. It is expected that when a MWCNT/surfactant dispersion is blended in a cement paste, some of the surfactant will remain adsorbed on the MWCNT, while another portion will adsorb on the cement grains. Therefore, the obtained results are probably also dependent on the four key elements cited above, which are inherent to the use of surfactants as a dispersing aid for MWCNT.

The nature and dispersion efficiency of the surfactant used was also found to be a critical factor depending on the application intended for the cement paste. While some surfactants were found to affect τ_s and τ_0, others were found to affect μ_o. Using a more efficient surfactant will imply a lower overall negative effect of the MWCNT/surfactant dispersion on the properties of the cement paste because such effects were found to be proportional to the amount of surfactant blended in the paste.

11.5 Conclusions

The following conclusions can be drawn from the results obtained in this work:

- MWCNT/surfactant dispersions are capable of affecting the rheological behavior of cement pastes by modifying the surface properties of both cement and MWCNT.
- Surfactants adsorption on the surface of MWCNT allows them to interact with water and cement particles, increasing the yield stress of cement pastes probably by increased interparticle attractions.
- Modification of rheological parameters by MWCNT should not be evaluated only as the consequence of the high SSA of nanotubes. Interactions of cement with the dispersing agent should also be taken into account.
- The amount of surfactant necessary to obtain an adequate dispersion degree of MWCNT in water seems to be incompatible with their use with cement matrices to obtain adequate rheological properties.
- The more efficient the surfactant used to disperse MWCNT in water, the lower the amount required to obtain an adequate dispersion degree, and therefore the lower the negative effects of the MWCNT/surfactant dispersion on the overall properties of cement paste.

11.6 Supplementary material

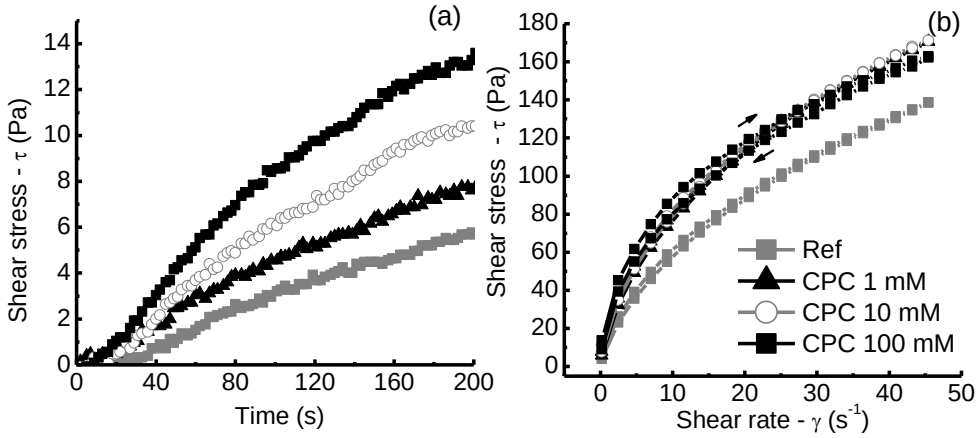

Figure S1 - (a) Static yield stress and (b) flow curves cement pastes blended different concentrations of CPC.

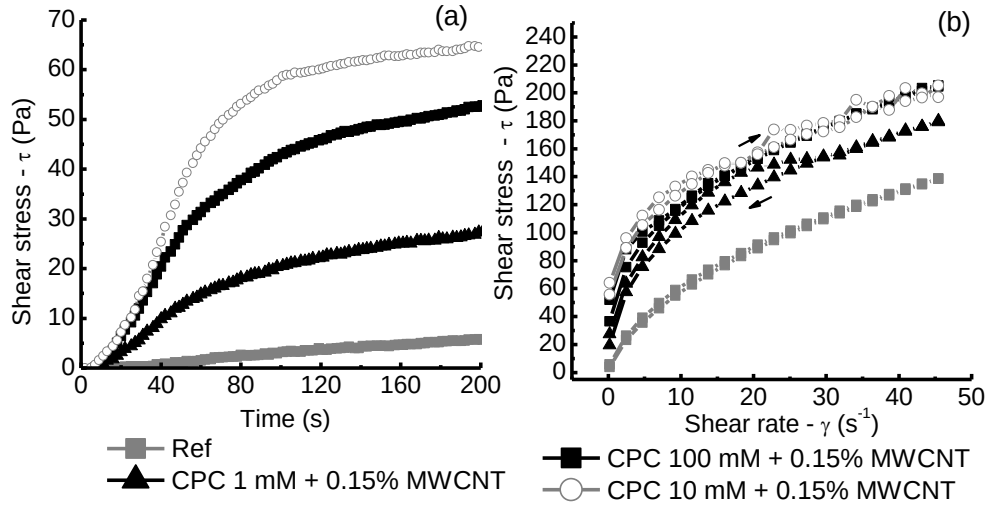

Figure S2 - (a) Static yield stress and (b) flow curves cement pastes blended different concentrations of CPC + 0.15%MWCNT.

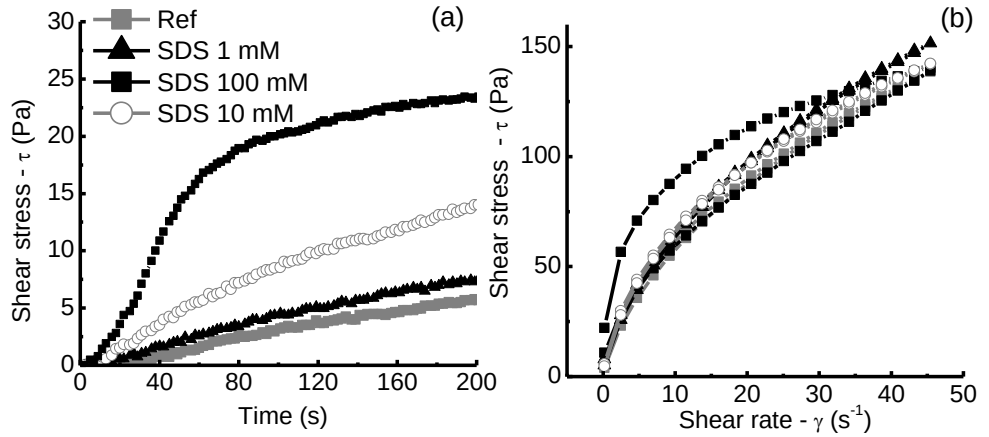

Figure S3 - (a) Static yield stress and (b) flow curves cement pastes blended different concentrations of SDS.

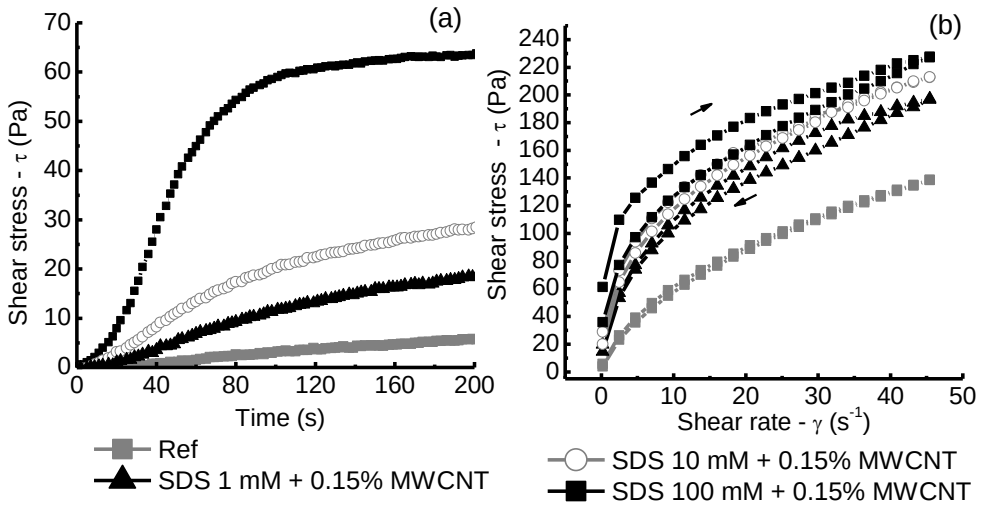

Figure S4 - (a) Static yield stress and (b) flow curves cement pastes blended different concentrations of SDS + 0.15%MWCNT.

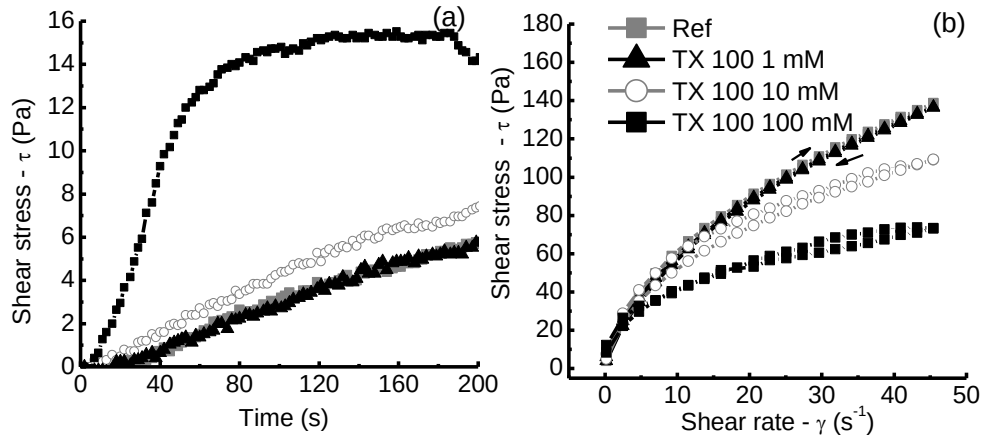

Figure S5 - (a) Static yield stress and (b) flow curves cement pastes blended different concentrations of TX 100.

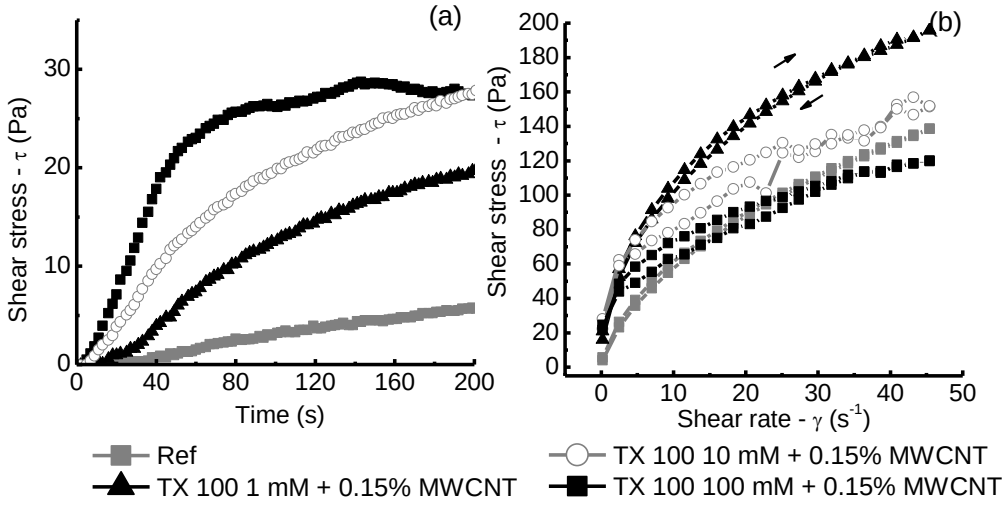

Figure S6 - (a) Static yield stress and (b) flow curves cement pastes blended different concentrations of SDS + 0.15%MWCNT.

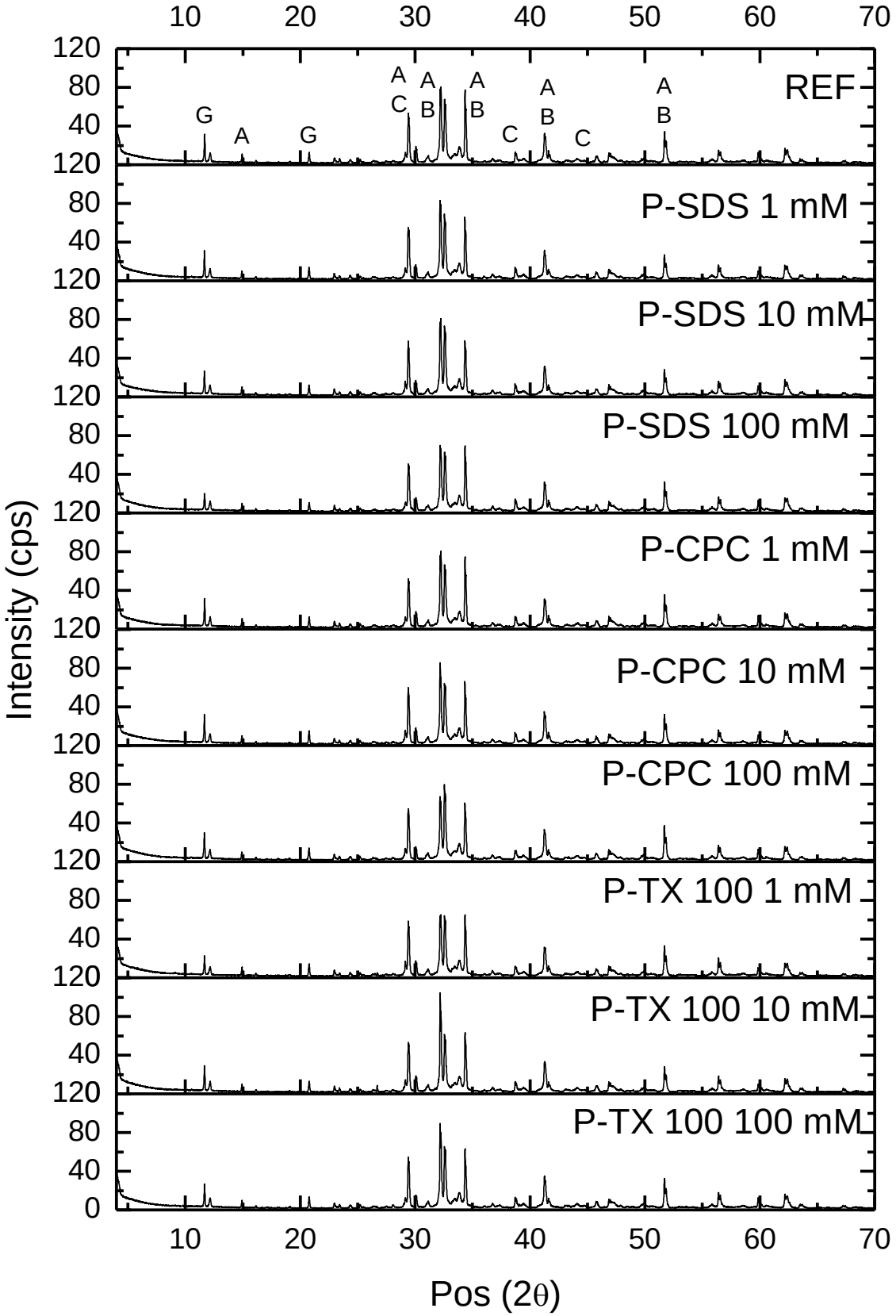

Figure S7 – XRD results for the P family of pastes after 1 hour of hydration (G: Gypsum ($CaSO_4 \cdot 2H_2O$), CS: Anhydrite ($CaSO_4$), A; Alite, B: Belite, , C: Calcite, cps: counts per second)

12. In house dispersion – Effect on mechanical properties

Reinforcing mechanism of MWCNT/surfactant dispersions in Portland cement pastes

Abstract

This work studies the reinforcing effect of Multi Walled Carbon Nanotubes (MWCNT) on cement pastes. MWCNT in powder were dispersed in deionized water using different surfactants as chemical dispersing agents in combination with an ultrasonic tip processor. Cement pastes with additions of carbon nanotubes of 0.15% by mass of cement were produced in two steps; first the dispersions of MWCNT were combined with the mixing water using an ultrasonic tip processor to guarantee homogeneity, then cement was added and mixed until a homogeneous paste was obtained. Mineralogical and mechanical properties of the pastes cured 7 days were measured and their facture behavior was characterized using linear elastic finite element simulations. It was found that even though the reinforcing effect of MWCNT was masked by the negative effect of the surfactants, nanotubes were capable of increasing both stress and strain capacity of the cement matrix by controlling the crack propagation process at the tip of the crack.

Keywords: Carbon nanotubes, surfactants, density, dispersion, adsorption, strength

12.1 Introduction

The mechanism by which multi walled carbon nanotubes (MWCNT) are able to enhance the mechanical properties of a cement matrix is called “bridge effect”. MWCNT are capable of creating a network of bridges that transmit load across cracks and pores [81], enhancing the load distribution within the matrix. This depends heavily on the length and aspect ratio of nanotubes [62]. Finite element modeling of beams

under flexural stress have proposed that MWCNT control crack propagation, allowing additional strain of the matrix by generating a sequential pull out of nanotubes while the crack develops, until complete pull out of the nanotubes is reached [50].

To guarantee and adequate crack propagation control, MWCNT must be well dispersed in the cement matrix [196] and bridging the correct phases. This means that if MWCNT agglomerate around individual hydrates instead of bridging neighboring ones, they will not have any effect on the load distribution in the matrix [68]. This is why the use of chemical dispersing agents, such as surfactants, is of prime importance to produce MWCNT reinforced cement based composites.

It is not clear what is the maximum extent of the reinforcing efficiency of MWCNT, but it has been found that small amounts of nanotubes increase the flexural strength of cement based matrices [22], identifying a correlation between their aspect ratio and reinforcing efficiency [45], [79], [247]. Additional parameters such as modulus of rupture [42], fracture energy and fracture toughness [87] have also been identified to increase with the presence of MWCNT in the matrix. This work aims to quantify the reinforcing efficiency of MWCNT/surfactant dispersions, separating the effects induced by surfactants in the mineralogical and mechanical properties of the matrix, from those induced by MWCNT.

12.2 Materials and methods

The materials used were class G high sulfate resistance (HSR) cement, industrial grade NC7000 multi walled carbon nanotubes (MWCNT), sodium dodecyl sulfate (SDS), cetylpyridinium chloride (CPC), triton X 100 (TX 100), and a viscosity modifying agent (VMA). Characterization of cement and VMA was performed by X-ray diffraction (XRD) and X-ray fluorescence (XRF). XRD tests were carried out in a diffractometer equipped with a Cu radiation source (Kα, λ = 1,5418 Å), from 4 to 70° 2θ with a step size of 0.05 and an accumulation time of 30 seconds. XRF test were carried out in a using a X-ray fluorescence spectrometer capable of identifying elements from Na to U. Morphological characterization of the MWCNT was carried out in a scanning transmission electron microscope (STEM) in transmission mode with a 20 kV acceleration and a 225,000X magnification. MWNCT were dispersed in deionized water using an ultrasonic bath; 1 ml of this dispersion was dropped in a #300 copper fomvar mesh and dried in a desiccator before imaging.

Deionized water was used to prepare MWCNT dispersions with 0.33% solid concentration of nanotubes using the three types of surfactants in 1mM, 10mM and 100mM concentrations. Surfactants were poured into the water stirred for 5 minutes, then solid MWCNT were added to the mixture. An ultrasonic tip was used to apply a total energy of 390 J/g in a 500 W ultrasonic processor set to 40 % amplitude in 20 seconds on/off cycles to avoid overheating the samples.

Three families of pastes were produced. A reference sample (Ref) composed of cement and VMA with water-to-cement ratio (w/c) of 0.55 and 1.0% VMA by mass of cement. VMA was used as a stabilizing agent to guarantee that there is no static sedimentation of the pastes during curing. The second family, named plain (P), maintained the same w/c and VMA amount, and was composed of water, surfactant, cement and VMA; surfactant type and concentration were varied. The third family, named blended (B), maintained the same proportion as the P family, but 0.15% MWCNT by mass of cement was blended into them.

Pastes were prepared by adding water, VMA and the MWCNT/surfactant dispersions to the mixer. A 500 rpm rotation was maintained for 1 minute, cement was added and rotation was increased to 2070 rpm during 1 minute and maintained constant for 5 minutes. Immediately after mixing, pastes were molded in 115x115x25 mm slabs, vibrated for 60 seconds in a vibrating table and cured in a high humidity environment for 7 days.

At testing age each slab was cut with a diamond saw to produce specimens for three-point bending. The obtained samples were 115x25x25 mm beams with one 5 mm notch placed at midspan in one of the 25 mm faces. Two metal plates were glued at the edge of the notch to couple a clip gauge to measure crack mouth opening displacement (CMOD). The load application rate was varied to maintain a constant deformation rate at the CMOD of 0.03%/min. Testing was carried out in a Shimadzu AGX 100 universal testing machine equipped with a 100 kN load cell. The experimental setup is presented in Figure 12.1. Flexural strength was calculated using equation 12.1.

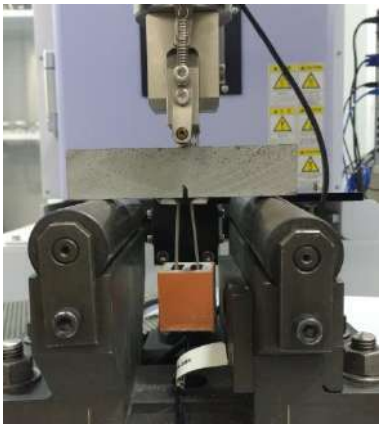

Figure 12.1 – Experimental setups used to measure flexural strength by three point bending

$$\sigma = \frac{3PS}{2B(W-a_0)^2} \quad (12.1)$$

Where:

P: applied load
S: span (90 mm)
B: beam width (25 mm)
W: beam height (25 mm)
a_0: notch depth (5 mm)

Changes in the energy adsorption capacity (D) of the paste induced by the presence of MWCNT were measured in the load versus deflection plots by adapting the procedure recommended by the RILEM technical committee 162 on test and design methods for steel fiber reinforced concrete [248]. A typical load versus deflection curve used for this procedure is presented in Figure 12.2. D was calculated as the area under the load-deflection curve after maximum load, and it consists of two components: the contribution from the cement paste (D1) and the contribution from the MWCNT (D2). D1 was approximated as a right triangle, and the slope of its hypotenuse was measured in pastes from the P family. This slope was then used to obtain D2 for the MWCNT blended pastes (B family) by subtracting D1 from D.

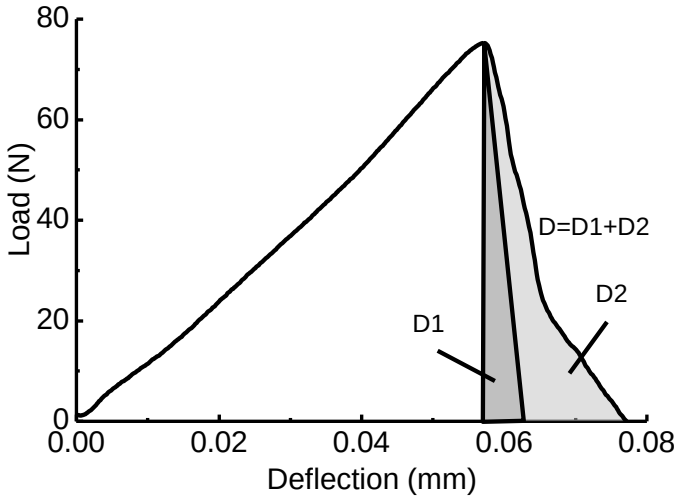

Figure 12.2 – Typical load versus deflection curve used to calculate energy absorption capacity

Linear elastic fracture mechanics was used to characterize the influence of MWCNT on the fracture behavior of the paste. This was achieved by employing a two parameter facture model for concrete [249] to interpret the results of three-point bending tests on notched beams of rectangular section. This model is based in the fact that the critical stress intensity factor (K_{Ic}) cannot be used to predict accurately the growth of a crack in a quasi-brittle material such as concrete, due to nonlinear slow crack growth before reaching the peak load [249]. The proposed model states that an effective crack extends before failure, which occurs only when the critical stress intensity factor K_I^S at the tip of the effective crack reaches a critical value (K_{Ic}^S) and, simultaneously, the crack tip opening displacement reaches its critical value ($CTOD_c$).

Compliance (C) was defined as $C = \frac{P}{CMOD}$. Two compliance parameters were used, initial compliance (C_i) and failure compliance (C_u), which corresponds to the compliance at the initial crack length and at failure respectively [250]. These parameters were obtained from experimental load versus CMOD plots, as the slope of two linear fits presented in Figure 12.3.

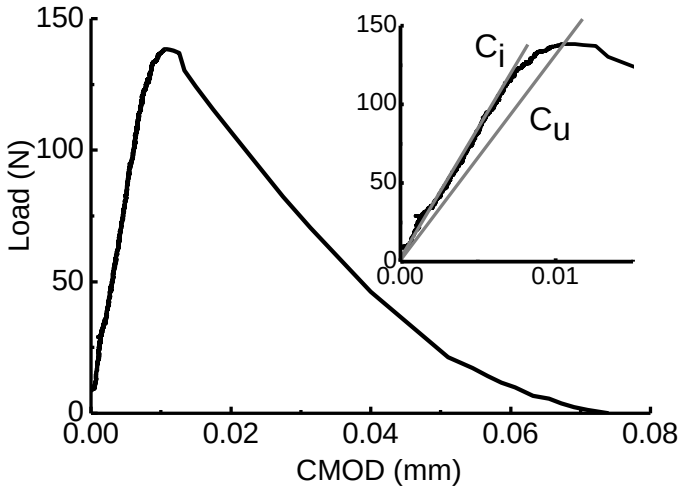

Figure 12.3 – Typical Load versus CMOD curve used to obtain C_i and C_u values

Linear elastic finite element simulations were used to obtain the K_{Ic}^{S}, $CTOD_c$ and E values from the two parameter model. The generic geometry used for the simulations is presented in Figure 12.4. The CMOD, CTOD and K_I curves for the actual notch beam geometries were obtained as a function of the effective crack extension (a_c-a_0), as shown in Figure 12.5. An initial simulation was performed applying P = 100 N and assuming E = 10 GPa. The Young's modulus (E) of the material was calculated by matching the observed C_i. The CMODc of the material was calculated by matching the observed C_u. The stress intensity factor was calculated using the energy release rate given by the J-integral. The effective crack length a_c was determined by matching the observed CMOD at failure in the CMOD versus a_c curve. The critical values $CTOD_c$ and K_{Ic}^{S} were obtained directly from the simulation results at $a = a_c$.

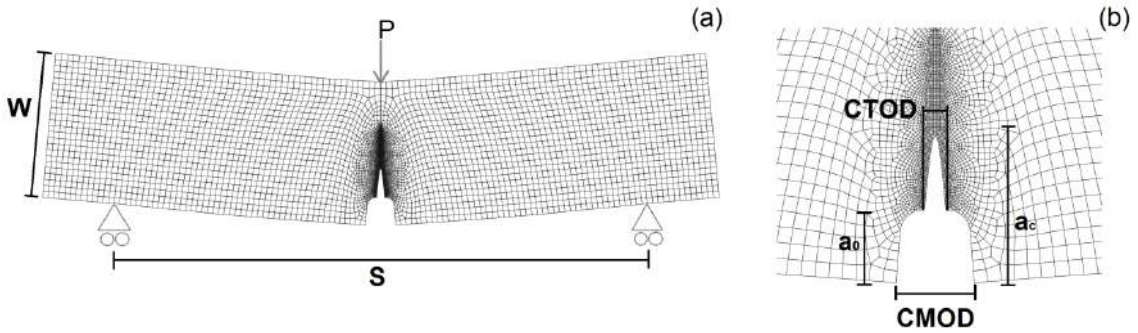

Figure 12.4 – (a) general geometry and (b) detail of the notch and crack used in the finite element simulations (scale factor: 200)

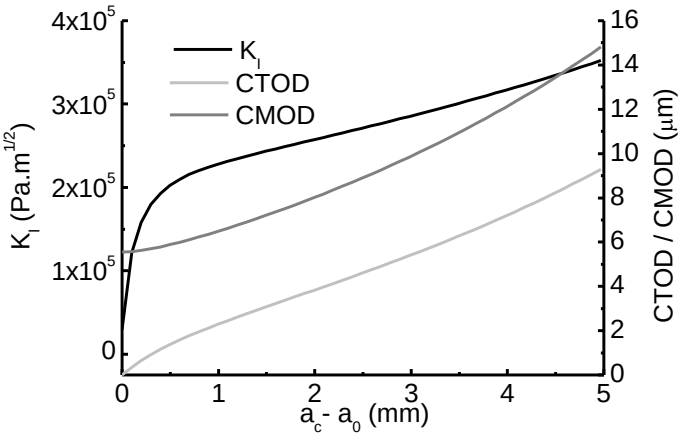

Figure 12.5 - Typical K_I, CTOD and CMOD versus effective crack extension plot

After mechanical testing, a portion of each slab was used to measure apparent density and open porosity by water absorption after 7 days of curing; another portion was ground with isopropanol and dried at 60 °C to stop hydration, this was used for mineralogical characterization. Thermogravimetric analyses (TGA) were performed in a a N_2 inert atmosphere with a gas flow of 100 ml/min, measured up to 900°C with a heating rate of 10°C/min. XRD tests were carried out in the same equipment and conditions as the characterization of raw materials.

12.3 Results and discussion

This section presents first the characterization of the raw materials used to produce cement pastes blended with MWCNT/surfactant dispersions; then, the individual effect of surfactants and MWCNT on the mineralogical and mechanical properties of the pastes are presented and discussed.

12.3.1 Materials characterization

Chemical and mineralogical composition of cement and VMA was characterized using XRD and XRF. The obtained results are presented in Figure 12.6 and Table 12.1. Regarding the cement, it was found that anhydrite ($CaSO_4$) was used as a setting time controller instead of gypsum ($CaSO_4 \cdot 2H_2O$). Regarding VMA, it was found that it is composed of cellulose mixed with calcium and sodium chloride. An image of individual MWCNT is presented in Figure 12.7. Nanotubes were found to have a diameter of approximately 20 nm and typical length between 1 and 2 μm.

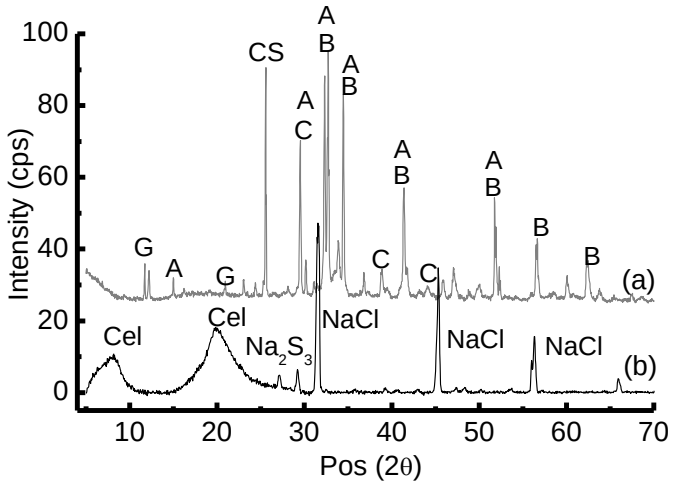

Figure 12.6 - X-Ray diffraction pattern of (a) cement and (b)VMA (Cel: Cellulose, G: Gypsum ($CaSO_4 \cdot 2H_2O$), CS: Anhydrite ($CaSO_4$), A; Alite, B: Belite, C: Calcite, cps: counts per second)

Table 12.1 - XRF chemical composition of cement and VMA (LOI: loss on ingnition)

	Cement	VMA
CaO	69.89	0.11
SiO_2	15.92	0.08
Fe_2O_3	5.33	-
Al_2O_3	3.94	0.01
SO_3	3.37	1.3
MgO	0.59	0.01
TiO_2	0.19	-
Na_2O	-	2.50
Cl	-	0.80
LOI	0.77	95.2

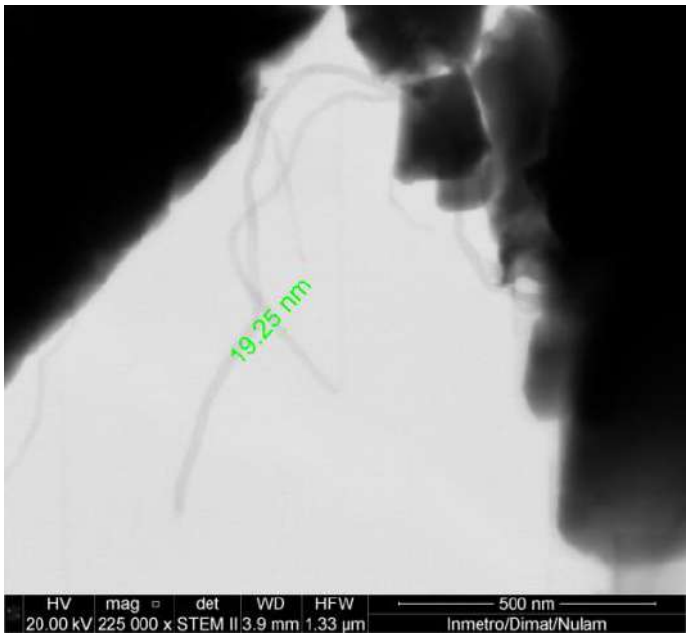

Figure 12.7 - TEM image of MWCNT

12.3.2 Mineralogical properties

The effect of the MWCNT/surfactant dispersions on the mineralogical properties of the pastes was studied using TGA and XRD. These tests were carried out only in the B family of pastes (blended with MWCNT), since MWCNT are not expected to interact chemically with the hydration reaction of cement [69]; therefore, results for the P and B families of pastes should not differ [209]. The TG curve and its first derivative (DTG) obtained for the reference sample is presented in Figure 12.8. Three main thermal events were found in these curves. The first with a DTG peak around 100°C and corresponding to the dehydration of all the hydrations products such as Calcium Silicate Hydrate (C-S-H), Ettringite (AFt), Monosulfoaluminate (AFm), and Calcium Aluminate Hydrates (ACH). The second with a DTG peak around 450°C corresponding to the dehydroxilation of $Ca(OH)_2$ which was formed as byproduct of the hydration of cement. The third DTG event which two overlapping peaks around 650°C corresponding to the decarbonation of $CaCO_3$, which was formed as two polymorphs [251].Weight fractions of $CaCO_3$ and $Ca(OH)_2$ were calculated as showed in equation 12.2. The amounts of C-S-H, AFt, AFm and ACH present in each sample were as the mass loss of Total Combined Water (TCW). The obtained results are presented in Figure 12.9.

$$WF\ (\%) = \frac{H}{MW_a} MW_b \quad (12.2)$$

Where:

H: mass loss corresponding to the thermal event being quantified

MW_a: molecular weight of the compound being lost by the sample

MW_b: molecular weight of the compound being decomposed in the sample

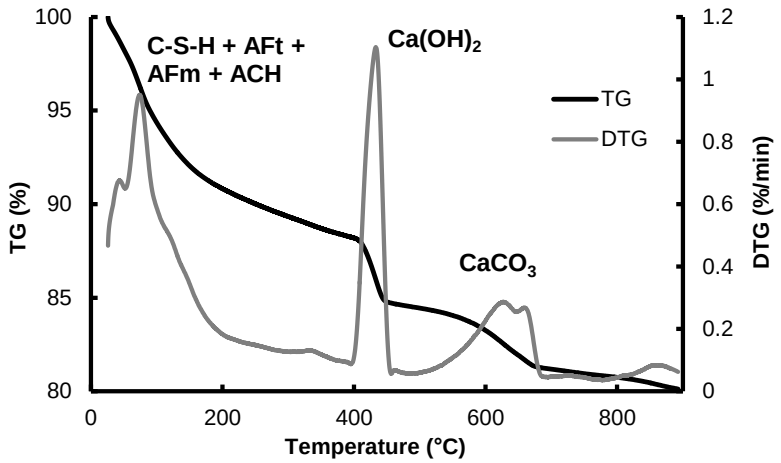

Figure 12.8 - TG and DTG curves of reference sample (C-S-H: calcium silicate hydrate, AFt: ettringite, AFm: monosulfoaluminate, ACH: calcium aluminate hydrates)

It was found that the MWCNT/surfactant dispersions did not have a substantial effect on the amount of $Ca(OH)_2$ or TCW after 7 days of hydration. Slight decreases (less than 1%) were observed for some of the MWCNT/surfactant dispersions, but were considered to be part of the dispersion of the measurement. Similar results were obtained in the XRD experiments, which showed no changes in the type of minerals present in the samples when compared to the reference paste. These results are presented in Figure 12.10. It is worth noticing that after 7 days of hydration some anhydrous cement was still found, but the hydration products were predominant.

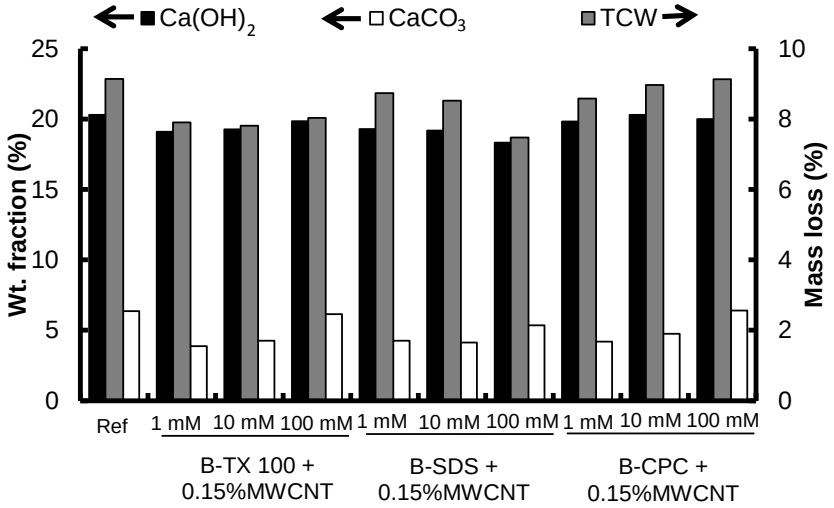

Figure 12.9 - TGA quantification results of pastes blended with 0.15%MWCNT and different concentrations of TX 100, SDS and CPC after 7 days of curing. (TCW: Total Combined Water)

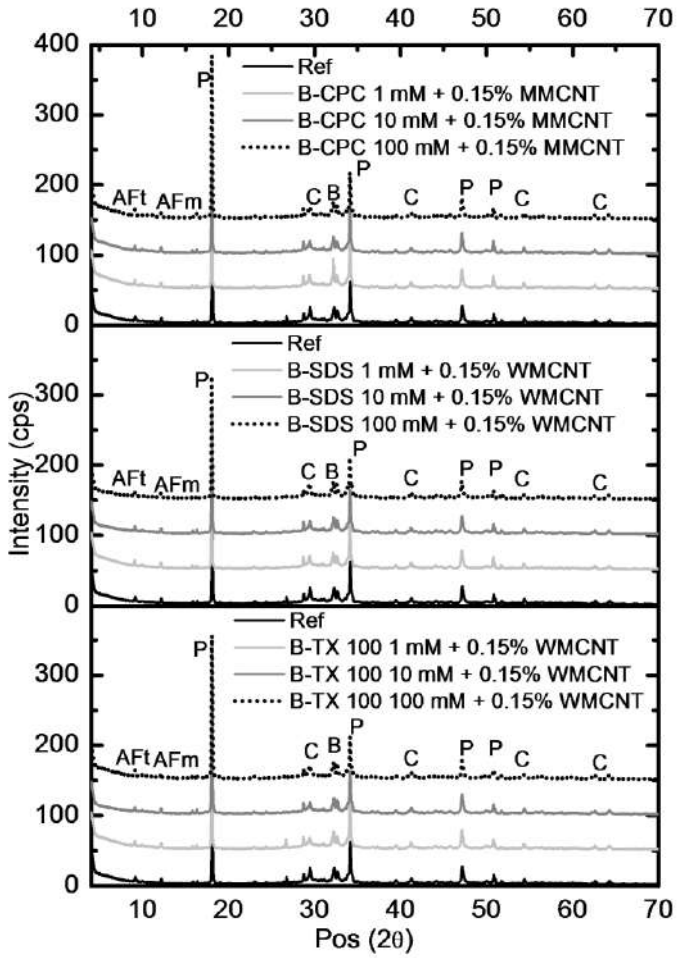

Figure 12.10 – XRD results of pastes blended with 0.15%MWCNT and different concentrations of TX 100, SDS and CPC after 7 days of curing (AFt: ettringite, AFm: monosulfoaluminate, P: $Ca(OH)_2$, B: belite, C: $CaCO_3$)

Apparent density was measured by water absorption for all the pastes from the B family after mechanical testing; the obtained results are presented in Figure 12.11. It was found that density was dependent on the surfactant concentration used to disperse the MWCNT. A higher surfactant concentration led to a lower density; decreasing from 1.29 g/cm^3 for the reference sample, down to 1.01 g/cm^3 for the 10mM SDS concentration. This behavior can be related to a decrease in surface tension of water caused by surfactants. Air bubbles are naturally entrapped during the mixing process, and surfactants are able to adsorb on the water-air interface of these bubbles with their hydrophobic tails towards air and their hydrophilic/polar groups towards water [31]. This stabilizes the bubbles and does not allow them to coalesce [31], which generates small non-connected bubbles in the paste. The volume of such bubbles is significant enough to lower the density of the paste.

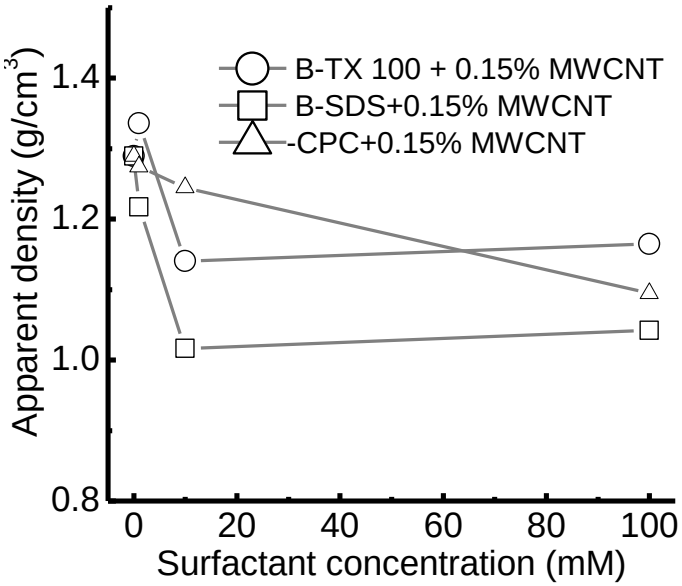

Figure 12.11 – Apparent density of pastes with different amounts of surfactant

12.3.3 Mechanical properties

Since surfactants play such an important role on the density of the pastes, three-point bending tests were carried out in pairs of pastes with the same surfactant concentration, with (B) and without (P) MWCNT. The goal of this experiment was to identify the individual effects of surfactants and MWCNT on the mechanical behavior of the matrix. Previous works by the authors have identified that for the sonication process described in the methodology, 10 mM, 100 mM and 100 mM are the most efficient surfactant concentrations to disperse MWCNT in water for TX100, SDS and CPC respectively; thus, only these concentrations were used to produce samples for mechanical testing. Flexural strength results for all pastes are presented in Figure 12.12. It was found that flexural strength decreased for all samples when compared to the reference, regardless of the presence of MWCNT in their composition. Nevertheless, when comparing pairs of pastes with the same surfactant type and concentration, it can be seen that MWCNT are able to improve the flexural strength of the matrix, increasing it up to 54% for the SDS case.

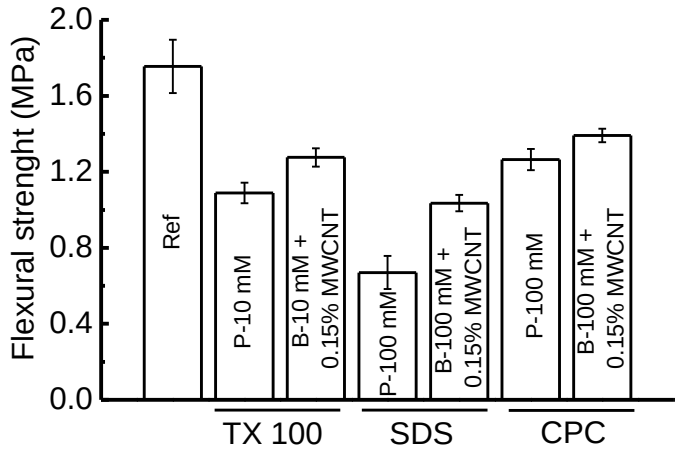

Figure 12.12 – Flexural strength results of pastes blended with and without MWCNT and TX 100, SDS and CPC after 7 days of curing

Apparent density and open porosity were also measured for the same pastes tested in three point bending. Results are presented in Figure 12.13. The expected or theoretical density of all pastes, obtained from the proportions and density of all materials used, was around 1.80 g/cm^3. The obtained densities are much lower than expected; this can be associated with the high open porosity obtained for each paste as consequence of the high energy mixing procedure and the usage of VMA. When taking into account this porosity values, the expected theoretical density drops to 1.19 g/cm^3, which agrees width the obtained experimental results. As previously found, the presence of surfactants decreased apparent density, but pastes blended with MWCNT (B) presented and increase in these parameters when compared to their plain homologous with the same surfactant type and concentration (P). This increase can be related to a lower surfactant availability to stabilize bubbles in the matrix, since a portion of the surfactant will adsorb on MWCNT during sonication [47] and will not be available to adsorb on the water-air interface to stabilize bubbles.

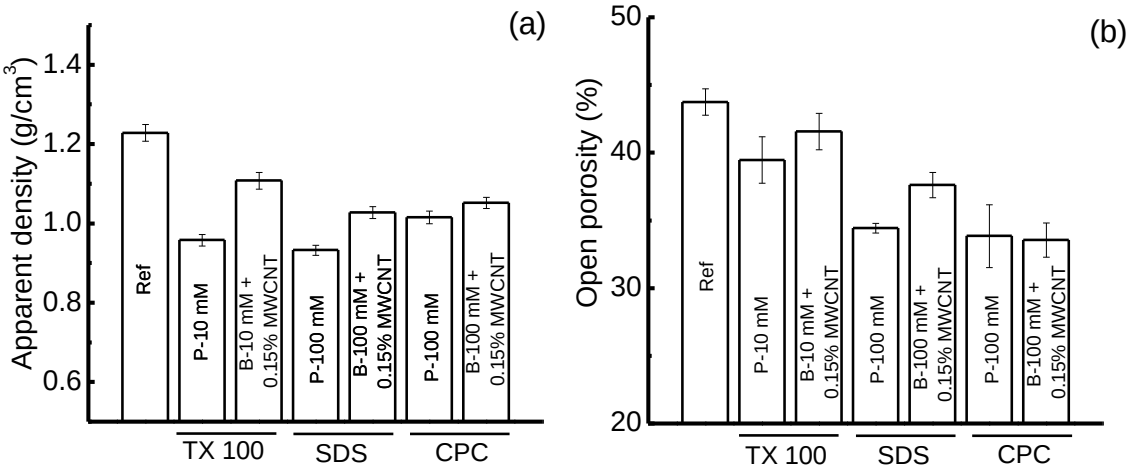

Figure 12.13 – (a) Apparent density and (b) open porosity of pastes tested in three point bending

A clear linear correlation between apparent density and flexural strength was found for each group of pastes with the same surfactant type and concentration, with and without MWCNT. This is presented in Figure 12.14. It can be seen that for each surfactant type, plain pastes always present the lowest density and the lowest flexural strength, while MWCNT blended pastes increase density, and proportionally increase flexural strength. This indicates that an apparent reinforcing effect from MWCNT can be partially related to changes in density of the paste, rather than to a better load transfer between cracks due to the MWCNT.

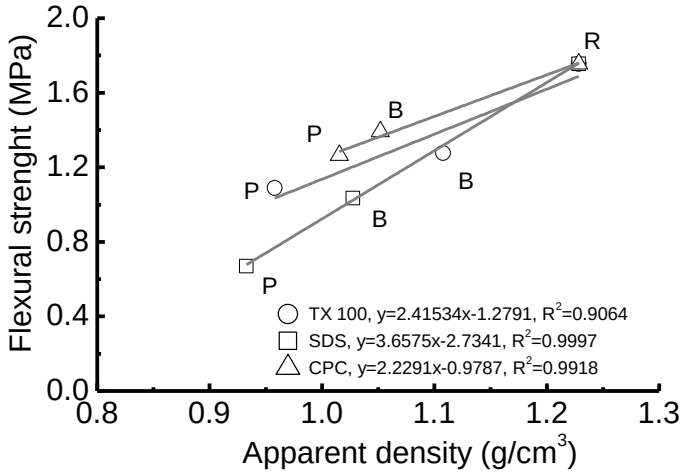

Figure 12.14 – Apparent density versus flexural strenght correlations for all pastes tested in three point bending (P: plain paste, B: blended paste)

Load versus CMOD plots for all samples tested in three point bending are presented in Figure 12.15. All samples showed the same general behavior. As load was applied, there was an elastic section where deformation varied linearly with load up to the maximum load where cracking begins. This was followed immediately by a

nonlinear crack growth process, and a strain softening behavior, where CMOD increases and load decreases until brakeage of the sample. No strain hardening behavior was found in any of the samples, meaning that no multiple cracking occurred due to the presence of MWCNT in the matrix. It can be seen that the deformation at which the elastic behavior ends remains roughly constant for all the samples, regardless of the presence of surfactant or MWCNT, while the maximum deformation of the sample was increased by MWCNT, as can be seen in Figure 12.15 (b). This indicates that the enhancement in deformation induced by MWCNT is mainly in the strain softening branch, affecting the crack opening and increasing ductility of the matrix.

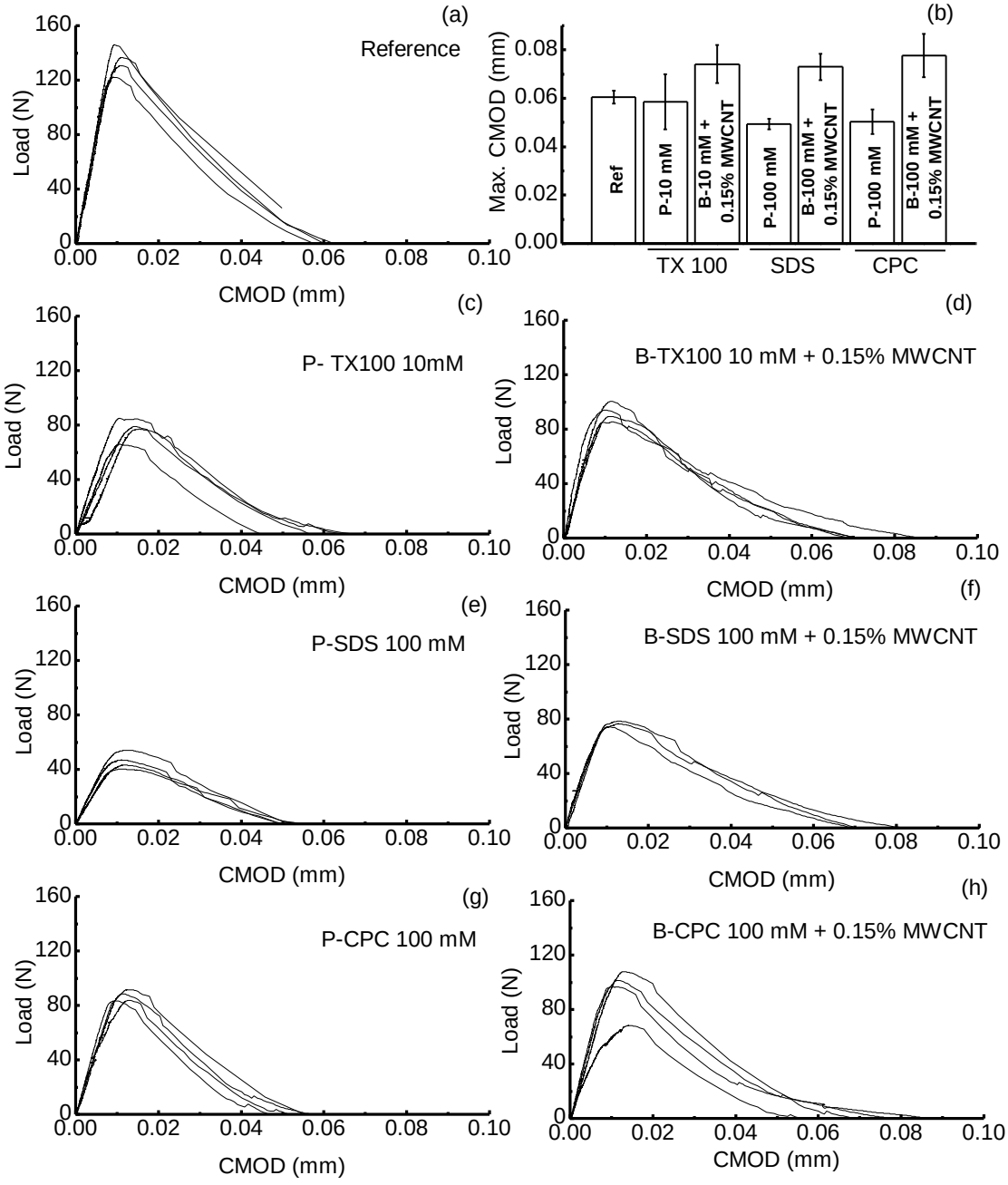

Figure 12.15 – Load versus CMOD for all pastes tested in three point bending

Energy absorption capacity results for the pastes blended with MWCNT are presented in Table 12.2. It was found that up to 80% of the energy absorption capacity after peak load was contributed by the MWCNT, while the contribution from the cement matrix (D1) remained approximately constant at 0.20 N.mm. The contribution from the MWCNT (D2) varied for each type surfactant due to their different dispersion efficiencies, which depend on the polar nature and the length of the molecule [133], [223]. The reinforcing effect of MWCNT is expected to depend strongly on the dispersion degree of the individual nanotubes throughout the cement matrix [196].

Table 12.2 – Energy absorption capacity results for MWCNT blended pastes

Sample	D (N.mm)	D1 (N.mm)	D2 (N.mm)
B-TX100 10 mM + CNT	0.82±0.07	0.18±0.02	0.64±0.09
B-SDS 100 mM + CNT	0.60±0.05	0.21±0.01	0.39±0.04
B-CPC 100 mM + CNT	0.57±0.15	0.20±0.07	0.37±0.22

Results obtained from the application of the two parameter fracture model are presented in Table 12.3. It was found that E and K_{Ic}^{S} decreased with the presence of surfactants (P family), but a portion of this decrease was recovered with the addition of MWCNT (B family). Similarly to the flexural strength results, the decrease in mechanical performance of the P family can be related to a lower density of the matrix, and the partial recovery to the reinforcing effect of MWCNT and to lower surfactant availability.

Critical crack length (a_c) and $CTOD_c$ were increased both by surfactants and MWCNT. The increase caused by surfactants can be related to a lower E, which allows a higher deformation of the material before rupture. The increase caused by MWCNT, when comparing results from P and B families of pastes, can be associated with their reinforcing effect. It should be noticed that MWCNT increased $CTOD_c$ by less than 1 µm, which is compatible with their typical length found in the TEM images.

Table 12.3 – Fracture mechanics analysis results

Sample	E (GPa)	a_c (mm)	a_c-a_0 (mm)	K_{Ic}^{S} ($Pa.m^{1/2} * 10^5$)	$CTOD_c$ (µm)
Ref	8.72±0.62	6.03±0.35	1.01±0.37	3.05±0.20	3.54±1.01
P-TX100 10 mM	4.44±0.50	6.00±0.06	0.93±0.09	1.97±0.09	4.37±0.84
B-TX100 10 mM + 0.15%MWCNT	6.66±0.89	6.65±0.47	1.54±0.57	2.45±0.16	4.67±0.61
P-SDS 100 mM	3.27±0.35	6.62±0.05	1.57±0.05	1.29±0.13	5.14±0.22
B-SDS 100 mM+ 0.15%MWCNT	4.84±0.09	6.76±0.46	1.73±0.46	1.95±0.15	5.57±1.26
P-CPC 100 mM	5.53±0.49	6.20±0.19	1.27±0.10	2.35±0.09	4.93±0.56
B-CPC 100 mM+ 0.15%MWCNT	5.76±1.12	6.54±0.42	1.56±0.43	2.48±0.23	5.72±1.52

In both the energy absorption capacity and fracture mechanics analysis results it can be seen that the samples blended with TX-100 presented a better performance when comparing within the pastes blended with the same type of surfactant, with and without MWCNT. This can be associated to better dispersion efficiency and a lower amount of surfactant required to reach such efficiency.

12.4 General discussion

The results found in this work showed that when using MWCNT/surfactant aqueous dispersions, surfactants decreased the density of the paste and consequently the mechanical performance of the composite. This decrease of mechanical performance was partially recovered by the presence of MWCNT, which were able to increase the strain and energy absorption capacities of the matrix, as evidenced by all the deformations measured and calculated, i.e. maximum CMOD, $CTOD_c$ and a_0.

When comparing all the results for pastes with the same surfactant type and concentration, with and without MWCNT, the reinforcing effect of nanotubes can be clearly identified. Such effect can be divided in three different moments: (i) during the elastic regime of the deformation, where it was found that MWCNT are capable of increasing the modulus of elasticity of the matrix due to a combination of their reinforcing effects and a lower availability of surfactant; (ii) during the crack propagation process, where it was found that MWCNT are capable of increasing the critical opening and therefore the effective length of the crack; and (iii) during the strain softening regime of the deformation, where it was found that MWCNT are capable of increasing the maximum deformation and energy absorption capacity of the matrix. No strain hardening behavior was found in any of the samples, meaning that no multiple cracking occurred due to the presence of MWCNT, probably due to a scale incompatibility between the nanotube length and the crack width.

The reinforcing effect of MWCNT on the mechanical behavior of the cement paste was much lower than the negative effect of surfactants; this is probably due to the lack of structures that transmit tensile load at the interfaces between MWCNT and hydration products [196]. This limits the reinforcing efficiency of MWCNT to the amount of load that the interfaces are capable of transmitting before suffering pull-out, regardless of the tensile strength of the nanotubes.

The type and amount of surfactant used to disperse MWCNT in the mixing water was also found to be an important factor because the more efficient the surfactant do disperse MWCNT in water, the lower the amount necessary to obtain an adequate dispersion degree, minimizing its negative effects on the properties of the cement paste.

12.5 Conclusions

It can be concluded that when using MWCNT/surfactant aqueous dispersions in a cement paste, the reinforcing effect of MWCNT is masked by the negative effect of the surfactants. An adequate comparison between pastes with the same type and amount of surfactant, with and without nanotubes, is necessary to identify the net reinforcing effect of MWCNT.

The increase in energy absorption capacity due to the presence of MWCNT in the matrix could not be related to strain hardening or multiple cracking behaviors, this due a scale incompatibility between the nanotube length and the crack width. Nevertheless, MWCNT are capable of increasing both stress and strain capacity of the cement matrix by controlling the crack propagation process at the tip of the crack.

13. Summary and final conclusions

After carrying out experimental campaigns using commercial and in-house prepared MWCNT/surfactant dispersions, their effect on the properties of a cement paste in fresh and hardened state can be divided in four sections: mineralogy, hydration kinetics and setting time, rheology, and mechanical properties.

13.1 Summary of phase 1 - commercial MWCNT/surfactant dispersion

The following overall effects of the commercial MWCNT/surfactant dispersion on cement paste were identified in Portland cement pastes:

- The hydration reaction of cement became widely retarded, while the amount of hydration products at a latter age was not affected.
- The rheological parameters of the paste increased drastically for low amounts of MWCNT blended, presenting even more pronounced effects than other types of micro- or nano- particles.
- The porosity of the paste in hardened state increased and its density decreased.
- The compressive and flexural strengths of the paste in hardened state decreased, both proportionally to the amount of MWCNT blended in the paste.

UCA experiments showed a potential increase in mechanical properties of the MWCNT blended pastes with respect to a plain cement paste after 24 hours of hydration; nevertheless, this was not confirmed by the mechanical testing and was considered and is not clear if this is consequence of the differences in rheology between samples for the UCA testing or consequence of the differences in porosity of the mechanical testing samples. Further work is required to decuple these variables.

Even though the retardation effect of surfactants was found to be a critical issue, two different strategies were identified to mitigate or overcome this effect: (i) elevating the temperature of the paste, and (ii) adding an additional surface area. From these two strategies, the first was found to accelerate the hydration reaction and mitigate partially the retardation effect of surfactant, while the second not only mitigated completely the retardation effect, but also enhanced the properties of the cement paste when compared to the control sample.

The commercial nature of the MWCNT/surfactant dispersion used made it impossible to identify the specific type of surfactant contained in its formulation and decouple its individual effects from those from MWCNT. This made necessary to start a second phase of work with a known surfactant and a controlled dispersion process.

13.2 Summary of phase 2 – In-house MWCNT/surfactant dispersion

This phase was able to produce aqueous MWCNT/surfactant dispersion using three different types of surfactants, finding that the amphoteric surfactant used (TX-100) was the most efficient to obtain an adequate degree of dispersion of MWCNT in water. The methodological approach used in this phase allowed decoupling the individual effects of surfactants and nanotubes on cement paste, finding that:

- Surfactants decrease the density of the cement paste in fresh state. This effect is proportional to the amount of surfactant present in the paste.
- Surfactants increase the setting time and modify the heat release kinetics of cement paste. This effect is partially compensated by the presence of MWCNT in the paste.
- Both surfactants and MWCNT decrease the workability of cement paste and worsen both its yield stress and viscosity.
- Surfactants increase the porosity of cement paste in hardened state, decreasing its mechanical performance. MWCNT are able to control the crack growth process at the tip of the crack and partially compensate the mechanical performance loss under flexural stress.

13.3 General Discussion – Dispersion process

The nature of the surfactant used as dispersing aid for MWCNT in water was found to be of great importance in both the dispersion efficiency and the performance of the cement paste in which they are blended. An amphoteric surfactant was found to be more efficient to disperse MWCNT in water; its lack of electric charge might be associated with its higher efficiency, nevertheless, further work is required to confirm this hypothesis. A more efficient surfactant requires using a lower amount to obtain adequate dispersion degree of MWCNT in water; this translates into lower negative

effects on the performance of the paste in both fresh and hardened states, which are directly linked to the amount of surfactant present in the paste.

13.4 General discussion - Effect on mineralogy

As expected, no significant effect of the MWCNT/surfactant dispersions on the mineralogical composition of the cement paste was found after several days of curing. This was evidenced by TGA and DRX testing after 1 hour and 7 days of curing, which showed no change in the type an amounts of minerals when comparing results for MWCNT bended pastes and plain pastes. This can be associated with the lack of chemical compatibility between the carbon structures of non-functionalized MWCNT and the hydration products of cement. Such lack of affinity can be considered positive, since it allows MWCNT to maintain their structural integrity and intrinsic properties when blended in cement paste.

13.5 General discussion - Effect on hydration kinetics and setting time

The use of surfactants as chemical dispersing aids for MWCNT in water affects the hydration reaction of cement paste, enhancing the dissolution of anhydrous cement, retarding its time of setting by prolonging its induction period. Such effects are due to different mechanisms such as decreased surface tension of water, surfactant chains adsorbed on cement grains with hydrophobic tails pointed towards water, and steric repulsion between charged surfactant chains adsorbed on cement grains. The net effect of MWCNT was identified as a slight difference in the kinetics of hydration of pastes with and without MWCNT. This difference can be considered a consequence either from the nucleation effect of the MWCNT, or from a portion of the surfactant molecules that remained adsorbed on the MWCNT and were prevented them to retard the hydration reaction. The evidence gathered in this work does not allow concluding in this regard.

The two-step mixing process proposed, in which the MWCNT/surfactant dispersion interact first with a pozzolanic particle dispersion rather than interacting with cement, was proven to be an effective method to mitigate the negative effects of surfactants on initial setting time and percolation threshold of cement paste. Pozzolanic micro- and nano- particles are a viable option for this purpose because they have a dual functionality, free surface area for surfactant adsorption and pozzolanic activity at later

ages. Their efficiency was found to depend not only on the specific surface area of the particles, but also on the properties of such surface.

13.6 General discussion - Effect on rheology

MWCNT/surfactant dispersions have a considerable effect on the rheology of cement pastes by modifying the interparticle attraction rather than interparticle friction or water demand. Both the specific surface area of MWCNT and the presence of surfactants were found to play an important role in such effects. Four key elements were identified involving the influence of MWCNT/surfactant dispersions on the rheology of cement pastes: surfactants increase the wettability of both cement and MWCNT by decreasing the surface tension of water, surfactants adsorb both on cement and MWCNT, surfactants induce and stabilize bubbles in the paste, and surfactants modify the surface properties of both cement and MWCNT.

13.7 General discussion - Effect on mechanical properties

Surfactants decrease the density of the cement paste, and consequently the mechanical performance of the composite. MWCNT partially recover this decrease in mechanical performance by increasing the strain and energy absorption capacities of the matrix through controlling the crack propagation process at the tip of the crack. The reinforcing mechanisms of MWCNT can be identified in three different moments: during the elastic regime of the deformation, where they increase the modulus of elasticity of the matrix; during the crack propagation process, where they increase the critical opening and effective length of the crack; and during the strain softening regime of the deformation, where they increase the maximum deformation and energy absorption capacity of the matrix. No multiple cracking was identified due to the presence of MWCNT, this due to a scale incompatibility between the nanotube length and the crack width. The lack of structures transmitting tensile load at the interfaces between MWCNT and hydration products limits the reinforcing efficiency of MWCNT to the amount of load that the interfaces are capable of transmitting before suffering pull-out, regardless of the tensile strength of the nanotubes.

13.8 Final conclusions and future perspective

MWCNT do have a beneficial effect on the mechanical properties of a cement based matrix. The cement/surfactant interaction, or in general the cement/dispersing agent interaction, can be considered an important source of variation regarding the overall effect of MWCNT on cement paste, the failure to consider such interaction has contributed to the lack of consensus identified in the literature regarding the beneficial effects of carbon nanotubes on cement based matrices.

The amount of the studied surfactants necessary to obtain an adequate degree of dispersion for MWCNT in water seems to be incompatible with an application in cement-based matrices. Nevertheless, the use of chemical dispersing agents is necessary to guarantee an adequate degree of dispersion of MWCNT throughout the cement matrix; thus, compatibility between dispersing agent and cement is of prime importance to obtain a good performance in a nanotube-cement composite.

The more efficient the surfactant used to disperse MWCNT in water, the lower the amount required to obtain an adequate dispersion degree, and therefore the lower the negative effects of the MWCNT/surfactant dispersion on the overall properties of cement paste.

Even though the beneficial effects of MWCNT as reinforcement for cement paste are masked by the presence of surfactants, this does not mean they don't exist. This masking effect may help to explain the mixed literature reports regarding the capabilities of MWCNT to improve the mechanical performance of cement-based composites.

The introduction of additional free surface area in a two-step mixing process is a viable solution for the detrimental effects of surfactants in cement composites when using MWCNT/surfactants aqueous dispersions. Nevertheless, the mechanism that governs the triple interaction MWCNT/surfactant/cement was not completely identified and further work should be carried out to characterize it.

One potential issue that can be derived from the combination of MWCNT/surfactant dispersions with pozzolanic particles is a loss of stability of the colloid. The electrostatic balance of the combinations and the stability of the MWCNT must be studied to confirm the severity of this issue and to determine how it influences the overall performance of the MWCNT in the cement matrix.

The adsorption of surfactant onto the surface pozzolanic particles may cause a partial loss of their pozzolanic activity. The adsorption/desorption process of the surfactant from the pozzolanic particles should be studied to confirm if the loss of pozzolanic activity is permanent or temporary.

So far, the exceptional properties of the individual MWCNT are being widely underused in cement matrixes. This is clearly evidenced in the fact that the beneficial effects of MWCNT over the mechanical properties of cement composites are comparable with the effects obtained with traditional fibers and pozzolanic particles. Novel functionalization and dispersion methods, specifically designed to target the dispersion and bond strength issues would provide the leap forward in knowledge necessary to exploit at its full the strengths of MWCNT. The use of the scale compatibility criteria is one of the tools that should be used to better understand the effects of the MWCNT; this means that the MWCNT must be used to target specific issues at their own scale, and not be expected to widely enhance the properties of the composite at all scales. The combined used of MWCNT with other larger fibers or pozzolanic particles will help to bring the effects of the MWCNT from the nanosacale, to the micro and macro scale, generating synergies of individual effects that bridge the scales as a cascade.

Publications obtained from this work

Book chapters

- **Oscar Mendoza Reales** and Romildo Dias Toledo Filho. *Nanotube-cement composites*. In Carbon Nanomaterials Sourcebook, *Volume II*, 1st ed., K. Sattler, Ed. Boca Raton: CRC Press, 2016, pp. 573–596.

Congress presentations

- **Oscar Mendoza Reales**, William Pearl, Maria Paiva, Christiane Miranda, and Romildo Toledo. 2015. *Effect of a Commercial Dispersion of Multi Walled Carbon Nanotubes on the Hydration of an Oil Well Cementing Paste*. In supplementary volume of: Fifth International Symposium on Nanotechnology in Construction (NICOM5), Chicago.
- **Oscar Mendoza Reales**, William Pearl, Maria Paiva, Christiane Miranda, and Romildo Toledo. 2015. *Adsorption of surfactant by nanosilica particles in carbon nanotubes/water dispersions: application in a cement matrix*. In proceedings of: 14th International Congress on the Chemistry of Cement (ICCC2015), Beijing.
- **Oscar A. Mendoza Reales,** Yhan Paul Arias Jaramillo, Carmen Delgado, Juan Carlos Ochoa Botero, Jorge Hernán Quintero and Romildo Dias Toledo Filho. 2017. *Surfactants as dispersants for carbon nanotubes in water: hydration of cement*. In supplementary volume of: 10th ACI/RILEM International conference on cementitious materials and alternative binders for sustainable concrete (ICCM 2017), Montreal.
- **Oscar A. Mendoza Reales**, Emílio C. C. M. Silva, Maria D. M. Paiva, Pedro Duda, and Romildo Dias Toledo Filho. 2017. *The role of surface area and compacity of nanoparticles on the rheology of cement paste*. In ACI Special Publication SP320: Proceedings of the 10th ACI/RILEM International conference on cementitious materials and alternative binders for sustainable concrete (ICCM 2017), Montreal.

Journal Articles

- **Oscar Mendoza Reales**, William Pearl, Maria Paiva, Christiane Miranda, and Romildo Toledo. 2016. *Effect of a Commercial Dispersion of Multi Walled Carbon Nanotubes on the Hydration of an Oil Well Cementing Paste*. Frontiers of Structural and Civil Engineering. Vol. 10, No. 2, pp. 147–179

- **Oscar Mendoza Reales** and Romildo Dias Toledo Filho. *A review on the chemical, mechanical and microstructural characterization of carbon nanotubes-cement based composites*. Construction and Building Materials. Vol. 154, pp. 697-710.
- **Oscar Aurelio Mendoza Reales**, Pedro Duda and Romildo Dias Toledo Filho. 2017. *Effect of a MWCT/surfactant aqueous dispersion on the rheological and mechanical properties of Portland cement pastes*. Submitted to Journal of Materials in Civil Engineering: Under Review.
- **Oscar A. Mendoza Reales**, Yhan Paul Arias Jaramillo, Juan Carlos Ochoa Botero, Jorge Hernán Quintero and Romildo Dias Toledo Filho. *Influence of MWCNT/surfactant dispersions on the rheology of Portland cement pastes*. Submitted to Cement and Concrete Research. Under review.
- **Oscar A. Mendoza Reales**, Yhan Paul Arias, Juan Carlos Ochoa Botero, Jorge Hernán Quintero, Emílio C. C. M. Silva and Romildo Dias Toledo Filho. *Reinforcing effect of MWCNT/surfactant dispersions in Portland cement pastes*. Submitted to Frontiers of Structural and Civil Engineering. Under Review.

Patents

- Pearl, Wiliam C., Ravi, Krishna, Toledo Filho, R.D., **Mendoza Reales, Oscar A**. *Overcoming the retardation of cement hydration from dispersing agents used in suspension of additives*. 2015. PCT deposit: PCT/US2015/020485 filed 13/03/2015 at United States Patent and Trademark Office. International Publication Number WO2016/148678 A1 in public domain: 22/09/2016.

14. Bibliography

[1] R. Feynman, “There is plenty of room at the bottom,” *Caltech Eng. Sci.*, vol. 23, no. 5, pp. 22–36, 1960.

[2] N. Taniguchi, “On the basic concept of Nano-technology,” *Proc. Int. Conf. Prod. Eng. Tokyo, Part II*, vol. 2, pp. 18–23, 1974.

[3] J. I. Tobón, “Evaluación del desempeño del cemento pórtland adicionado con nanopartículas de sílice,” Universidad Nacional de Colombia, 2011.

[4] F. Sanchez and K. Sobolev, “Nanotechnology in concrete – A review,” *Constr. Build. Mater.*, vol. 24, no. 11, pp. 2060–2071, Nov. 2010.

[5] F. Pacheco-Torgal, S. Miraldo, Y. Ding, and J. a. Labrincha, “Targeting HPC with the help of nanoparticles: An overview,” *Constr. Build. Mater.*, vol. 38, pp. 365–370, Jan. 2013.

[6] K. Sobolev, “Nanotechnology and nanoengineering of construction mateials,” in *Nanotechnology in Construction Proceedings of NICOM5*, 2015, pp. 3–13.

[7] L. P. Singh, S. R. Karade, S. K. Bhattacharyya, M. M. Yousuf, and S. Ahalawat, “Beneficial role of nanosilica in cement based materials – A review,” *Constr. Build. Mater.*, vol. 47, pp. 1069–1077, Oct. 2013.

[8] E. Mohseni, B. M. Miyandehi, J. Yang, and M. A. Yazdi, “Single and combined effects of nano-SiO2, nano-Al2O3 and nano-TiO2 on the mechanical, rheological and durability properties of self-compacting mortar containing fly ash,” *Constr. Build. Mater.*, vol. 84, pp. 331–340, 2015.

[9] R. Madandoust, E. Mohseni, S. Y. Mousavi, and M. Namnevis, “An experimental investigation on the durability of self-compacting mortar containing nano-SiO2, nano-Fe2O3 and nano-CuO,” *Constr. Build. Mater.*, vol. 86, pp. 44–50, 2015.

[10] A. Hakamy, F. U. A. Shaikh, and I. M. Low, “Characteristics of Nanoclay and Calcined Nanoclay-Cement Nanocomposites,” *Compos. Part B*, vol. 78, pp. 174–184, 2015.

[11] O. Mendoza, G. Sierra, and J. I. Tobón, “Effect of the reagglomeration process of multi-walled carbon nanotubes dispersions on the early activity of nanosilica in cement composites,” *Constr. Build. Mater.*, vol. 54, pp. 550–557, 2014.

[12] R. K. Abu Al-Rub, B. M. Tyson, A. Yazdanbakhsh, and Z. Grasley, “Mechanical Properties of Nanocomposite Cement Incorporating Surface-Treated and Untreated Carbon Nanotubes and Carbon Nanofibers,” *J. nanomechanics micromechanics*, vol. 2, no. March, pp. 3–8, 2012.

[13] S. Chuah, Z. Pan, J. G. Sanjayan, C. M. Wang, and W. H. Duan, “Nano reinforced cement and concrete composites and new perspective from graphene oxide,” *Constr. Build. Mater.*, vol. 73, pp. 113–124, Dec. 2014.

[14] S. Banerjee, D. D. Dionysiou, and S. C. Pillai, “Self-cleaning applications of TiO2 by photo-induced hydrophilicity and photocatalysis,” *Appl. Catal. B Environ.*, vol. 176–177, pp. 396–428, 2015.

[15] Y. Cao, P. Zavaterri, J. Youngblood, R. Moon, and J. Weiss, “The influence of cellulose nanocrystal additions on the performance of cement paste,” *Cem.*

Concr. Compos., vol. 56, pp. 73–83, Feb. 2015.

[16] J. J. Thomas, H. M. Jennings, and J. J. Chen, "Influence of nucleation seeding on the hydration mechanisms of tricalcium silicate and cement," *J. Phys. Chem. C*, vol. 113, no. 11, pp. 4327–4334, 2009.

[17] M. H. Hubler, J. J. Thomas, and H. M. Jennings, "Influence of nucleation seeding on the hydration kinetics and compressive strength of alkali activated slag paste," *Cem. Concr. Res.*, vol. 41, no. 8, pp. 842–846, Aug. 2011.

[18] H. Madani, A. Bagheri, and T. Parhizkar, "The pozzolanic reactivity of monodispersed nanosilica hydrosols and their in fl uence on the hydration characteristics of Portland cement," *Cem. Concr. Res.*, vol. 42, pp. 1563–1570, 2012.

[19] J. I. Tobón, J. J. Payá, M. V. Borrachero, and O. J. Restrepo, "Mineralogical evolution of Portland cement blended with silica nanoparticles and its effect on mechanical strength," *Constr. Build. Mater.*, vol. 36, pp. 736–742, Nov. 2012.

[20] Y. Fan, S. Zhang, S. Kawashima, and S. P. Shah, "Influence of kaolinite clay on the chloride diffusion property of cement-based materials," *Cem. Concr. Compos.*, vol. 45, pp. 117–124, 2014.

[21] A. R. Sakulich and V. C. Li, "Nanoscale characterization of engineered cementitious composites (ECC)," *Cem. Concr. Res.*, vol. 41, no. 2, pp. 169–175, Feb. 2011.

[22] S. Xu, J. Liu, and Q. Li, "Mechanical properties and microstructure of multi-walled carbon nanotube-reinforced cement paste," *Constr. Build. Mater.*, vol. 76, pp. 16–23, Feb. 2015.

[23] D. D. L. Chung, "Electrical Conduction Behavior of Cement-Matrix Composites," *J. Mater. Eng. Perform.*, vol. 11, no. April, pp. 194–204, 2002.

[24] D. D. L. Chung, "Electrically conductive cement-based materials," *Adv. Cem. Res.*, vol. 4, pp. 167–176, 2004.

[25] H. M. Jennings, J. J. Thomas, J. J. Chen, and D. Rothstein, "Cement Paste as a Porous Material," in *Handbook of Porous Solids*, F. Schuth, K. Sing, and J. Weitkamp, Eds. Weinheim: Wiley-VCH, 2002, pp. 2971–3028.

[26] I. G. Richardson, "The nature of C-S-H in hardened cements," *Cem. Concr. Res.*, vol. 29, no. July, pp. 1131–1147, 1999.

[27] J. J. Chen, J. J. Thomas, H. F. W. Taylor, and H. M. Jennings, "Solubility and structure of calcium silicate hydrate," *Cem. Concr. Res.*, vol. 34, no. 9, pp. 1499–1519, Sep. 2004.

[28] R. J.-M. Pellenq, A. Kushima, R. Shahsavari, K. J. Van Vliet, M. J. Buehler, S. Yip, and F.-J. Ulm, "A realistic molecular model of cement hydrates.," *Proc. Natl. Acad. Sci. U. S. A.*, vol. 106, no. 38, pp. 16102–7, Sep. 2009.

[29] J. J. Beaudoin, L. Raki, and R. Alizadeh, "A 29Si MAS NMR study of modified C–S–H nanostructures," *Cem. Concr. Compos.*, vol. 31, no. 8, pp. 585–590, Sep. 2009.

[30] G. Constantinides and F.-J. Ulm, "The nanogranular nature of C–S–H," *J. Mech. Phys. Solids*, vol. 55, no. 1, pp. 64–90, Jan. 2007.

[31] P. Hewlett, *Lea" s Chemistry of Cement and Concrete*, 4th ed., vol. 58, no. 10.

Oxford: Elsevier Science & Technology Books, 2004.

[32] A. J. Allen, J. J. Thomas, and H. M. Jennings, “Composition and density of nanoscale calcium-silicate-hydrate in cement.,” *Nat. Mater.*, vol. 6, no. 4, pp. 311–6, Apr. 2007.

[33] J. D. Bernal, J. W. Jeffrey, and H. F. W. Taylor, “Crystallographic research on the hydration of Portland cement. A first report on investigations in progress,” *Mag. Concr. Res.*, vol. 4, no. 11, pp. 49–54, 1952.

[34] I. Richardson, “Tobermorite/jennite- and tobermorite/calcium hydroxide-based models for the structure of C-S-H: applicability to hardened pastes of tricalcium silicate, ?-dicalcium silicate, Portland cement, and blends of Portland cement with blast-furnace slag, metakaol,” *Cem. Concr. Res.*, vol. 34, no. 9, pp. 1733–1777, Sep. 2004.

[35] R. J.-M. Pellenq, N. Lequeux, and H. van Damme, “Engineering the bonding scheme in C–S–H: The iono-covalent framework,” *Cem. Concr. Res.*, vol. 38, no. 2, pp. 159–174, Feb. 2008.

[36] X. Cong and R. J. Kirkpatrick, “29Si and 170 NMR Investigation of the Structure of Some Crystalline Calcium Silicate Hydrates,” *Advnced Cem. based Mater.*, vol. 3, pp. 133–143, 1996.

[37] G. Constantinides and F.-J. Ulm, “The effect of two types of C-S-H on the elasticity of cement-based materials: Results from nanoindentation and micromechanical modeling,” *Cem. Concr. Res.*, vol. 34, no. 1, pp. 67–80, Jan. 2004.

[38] M. Vandamme, F.-J. Ulm, and P. Fonollosa, “Nanogranular packing of C–S–H at substochiometric conditions,” *Cem. Concr. Res.*, vol. 40, no. 1, pp. 14–26, Jan. 2010.

[39] J. S. Dolado and K. van Breugel, “Recent advances in modeling for cementitious materials,” *Cem. Concr. Res.*, vol. 41, no. 7, pp. 711–726, Jul. 2011.

[40] H. M. Jennings, “Colloid model of C-S-H and implications to the problem of creep and shrinkage,” *Mater. Struct.*, vol. 37, no. February, pp. 59–70, 2004.

[41] Z. S. Metaxa, M. S. Konsta-Gdoutos, and S. P. Shah, “Carbon nanofiber cementitious composites: Effect of debulking procedure on dispersion and reinforcing efficiency,” *Cem. Concr. Compos.*, vol. 36, pp. 25–32, Feb. 2013.

[42] S. Musso, J.-M. Tulliani, G. Ferro, and A. Tagliaferro, “Influence of carbon nanotubes structure on the mechanical behavior of cement composites,” *Compos. Sci. Technol.*, vol. 69, no. 11–12, pp. 1985–1990, Sep. 2009.

[43] S. Sun, X. Yu, B. Han, and J. Ou, “In situ growth of carbon nanotubes/carbon nanofibers on cement/mineral admixture particles: A review,” *Constr. Build. Mater.*, vol. 49, pp. 835–840, Dec. 2013.

[44] S. Zhang, F. Lu, and L. Zheng, “Dispersion of multiwalled carbon nanotubes (MWCNTs) by ionic liquid-based Gemini pyrrolidinium surfactants in aqueous solution,” *Colloid Polym. Sci.*, vol. 289, no. 17–18, pp. 1815–1819, Sep. 2011.

[45] M. S. Konsta-Gdoutos, Z. S. Metaxa, and S. P. Shah, “Highly dispersed carbon nanotube reinforced cement based materials,” *Cem. Concr. Res.*, vol. 40, no. 7, pp. 1052–1059, Jul. 2010.

[46] P. Juilland, A. Kumar, E. Gallucci, R. J. Flatt, and K. L. Scrivener, “Effect of

mixing on the early hydration of alite and OPC systems," *Cem. Concr. Res.*, vol. 42, no. 9, pp. 1175–1188, Sep. 2012.

[47] L. Jiang, L. Gao, and J. Sun, "Production of aqueous colloidal dispersions of carbon nanotubes," *J. Colloid Interface Sci.*, vol. 260, no. 1, pp. 89–94, Apr. 2003.

[48] A. Cwirzen, K. Habermehl-Cwirzen, A. G. Nasibulin, E. I. Kaupinen, P. R. Mudimela, and V. Penttala, "SEM/AFM studies of cementitious binder modified by MWCNT and nano-sized Fe needles," *Mater. Charact.*, vol. 60, no. 7, pp. 735–740, Jul. 2009.

[49] X. Yu and E. Kwon, "A carbon nanotube/cement composite with piezoresistive properties," *Smart Mater. Struct.*, vol. 18, no. 5, pp. 1–5, May 2009.

[50] L. Y. Chan and B. Andrawes, "Finite element analysis of carbon nanotube/cement composite with degraded bond strength," *Comput. Mater. Sci.*, vol. 47, no. 4, pp. 994–1004, Feb. 2010.

[51] O. Mendoza, G. Sierra, and J. I. Tobón, "Influence of super plasticizer and $Ca(OH)_2$ on the stability of functionalized multi-walled carbon nanotubes dispersions for cement composites applications," *Constr. Build. Mater.*, vol. 47, pp. 771–778, 2013.

[52] X. Ouyang, Y. Guo, and X. Qiu, "The feasibility of synthetic surfactant as an air entraining agent for the cement matrix," *Constr. Build. Mater.*, vol. 22, no. 8, pp. 1774–1779, Aug. 2008.

[53] B. Łaźniewska-Piekarczyk, "The influence of chemical admixtures on cement hydration and mixture properties of very high performance self-compacting concrete," *Constr. Build. Mater.*, vol. 49, pp. 643–662, Dec. 2013.

[54] M. S. Strano, V. C. Moore, M. K. Miller, M. J. Allen, E. H. Haroz, C. Kittrell, R. H. Hauge, and R. Smalley, "The role of surfactan adsoption during ultrasonication in the dispersion of single walled carbon nanotubes." Journal of Nanoscience and Nanotechnology, pp. 81–86, 2003.

[55] G. Li, P. Wang, and X. Zhao, "Mechanical behavior and microstructure of cement composites incorporating surface-treated multi-walled carbon nanotubes," *Carbon N. Y.*, vol. 43, no. 6, pp. 1239–1245, May 2005.

[56] P.-C. Ma, N. a. Siddiqui, G. Marom, and J.-K. Kim, "Dispersion and functionalization of carbon nanotubes for polymer-based nanocomposites: A review," *Compos. Part A Appl. Sci. Manuf.*, vol. 41, no. 10, pp. 1345–1367, Oct. 2010.

[57] B. a. Kakade and V. K. Pillai, "An efficient route towards the covalent functionalization of single walled carbon nanotubes," *Appl. Surf. Sci.*, vol. 254, no. 16, pp. 4936–4943, Jun. 2008.

[58] M. Abdalla, D. Dean, P. Robinson, and E. Nyairo, "Cure behavior of epoxy MWCNT nanocomposites The effect of nanotube surface modification," *Polymer (Guildf).*, vol. 49, pp. 3310–3317, 2008.

[59] I. Madni, C.-Y. Hwang, S.-D. Park, Y.-H. Choa, and H.-T. Kim, "Mixed surfactant system for stable suspension of multiwalled carbon nanotubes," *Colloids Surfaces A Physicochem. Eng. Asp.*, vol. 358, no. 1–3, pp. 101–107, Apr. 2010.

[60] W. R. Jung, J. H. Choi, N. Lee, K. Shin, J.-H. Moon, and Y.-S. Seo, “Reduced damage to carbon nanotubes during ultrasound-assisted dispersion as a result of supercritical-fluid treatment,” *Carbon N. Y.*, vol. 50, no. 2, pp. 633–636, Feb. 2012.

[61] D.-Y. Kim, Y. S. Yun, H. Bak, S. Y. Cho, and H.-J. Jin, “Aspect ratio control of acid modified multiwalled carbon nanotubes,” *Curr. Appl. Phys.*, vol. 10, no. 4, pp. 1046–1052, Jul. 2010.

[62] R. K. Abu Al-Rub, A. I. Ashour, and B. M. Tyson, “On the aspect ratio effect of multi-walled carbon nanotube reinforcements on the mechanical properties of cementitious nanocomposites,” *Constr. Build. Mater.*, vol. 35, pp. 647–655, Oct. 2012.

[63] M. Sham and J. Kim, “Surface functionalities of multi-wall carbon nanotubes after UV/Ozone and TETA treatments,” *Carbon N. Y.*, vol. 44, no. 4, pp. 768–777, Apr. 2006.

[64] H. Gong, Y. Zhang, J. Quan, and S. Che, “Preparation and properties of cement based piezoelectric composites modified by CNTs,” *Curr. Appl. Phys.*, vol. 11, no. 3, pp. 653–656, May 2011.

[65] A. Yazdanbakhsh, Z. Grasley, B. Tyson, and R. K. Abu Al-Rub, “Dispersion quantification of inclusions in composites,” *Compos. Part A Appl. Sci. Manuf.*, vol. 42, no. 1, pp. 75–83, Jan. 2011.

[66] A. Yazdanbakhsh and Z. Grasley, “The theoretical maximum achievable dispersion of nanoinclusions in cement paste,” *Cem. Concr. Res.*, vol. 42, no. 6, pp. 798–804, Jun. 2012.

[67] A. Yazdanbakhsh, Z. Grasley, B. Tyson, and R. K. Abu Al-Rub, “Distribution of Carbon Nanofibers and Nanotubes in Cementitious Composites,” *Transp. Res. Rec. J. Transp. Res. Board*, vol. 2142, no. 1, pp. 89–95, Dec. 2010.

[68] A. Sobolkina, V. Mechtcherine, V. Khavrus, D. Maier, M. Mende, M. Ritschel, and A. Leonhardt, “Dispersion of carbon nanotubes and its influence on the mechanical properties of the cement matrix,” *Cem. Concr. Compos.*, vol. 34, no. 10, pp. 1104–1113, Nov. 2012.

[69] J. M. Makar and G. W. Chan, “Growth of Cement Hydration Products on Single-Walled Carbon Nanotubes,” *J. Am. Ceram. Soc.*, vol. 92, no. 6, pp. 1303–1310, Jun. 2009.

[70] M. Paillet, P. Poncharal, and A. Zahab, “Electrostatics of individual single-walled carbon nanotubes investigated by electrostatic force microscopy,” *Phys. Rev. Lett.*, vol. 94, no. 18, p. 186801, May 2005.

[71] F. Moulin, M. Devel, and S. Picaud, “Molecular dynamics simulations of polarizable nanotubes interacting with water,” *Phys. Rev. B*, vol. 71, pp. 1–7, 2005.

[72] Z.-C. Di, Y.-H. Li, Z.-K. Luan, and J. Liang, “Adsorption of chromium (VI) ions from water by carbon nanotubes,” *Adsorpt. Sci. Technol.*, vol. 22, no. 6, pp. 467–474, Jul. 2004.

[73] S. Wansom, N. Kidner, L. Woo, and T. Mason, “AC-impedance response of multi-walled carbon nanotube/cement composites,” *Cem. Concr. Compos.*, vol. 28, no. 6, pp. 509–519, Jul. 2006.

[74] B. Han, X. Yu, and J. Ou, “Effect of water content on the piezoresistivity of MWNT/cement composites,” *J. Mater. Sci.*, vol. 45, no. 14, pp. 3714–3719, Mar. 2010.

[75] S. Kawashima, P. Hou, D. J. Corr, and S. P. Shah, “Cement & Concrete Composites Modification of cement-based materials with nanoparticles,” *Cem. Concr. Compos.*, vol. 36, pp. 8–15, 2013.

[76] J. N. de Paula, J. M. Calixto, L. O. Ladeira, P. Ludvig, T. C. C. Souza, J. M. Rocha, and A. a. V. de Melo, “Mechanical and rheological behavior of oil-well cement slurries produced with clinker containing carbon nanotubes,” *J. Pet. Sci. Eng.*, vol. 122, pp. 274–279, Oct. 2014.

[77] F. Collins, J. Lambert, and W. H. Duan, “The influences of admixtures on the dispersion, workability, and strength of carbon nanotube–OPC paste mixtures,” *Cem. Concr. Compos.*, vol. 34, no. 2, pp. 201–207, Feb. 2012.

[78] R. Siddique and A. Mehta, “Effect of carbon nanotubes on properties of cement mortars,” *Constr. Build. Mater.*, vol. 50, pp. 116–129, Jan. 2014.

[79] M. S. Konsta-Gdoutos, Z. S. Metaxa, and S. P. Shah, “Multi-scale mechanical and fracture characteristics and early-age strain capacity of high performance carbon nanotube/cement nanocomposites,” *Cem. Concr. Compos.*, vol. 32, no. 2, pp. 110–115, Feb. 2010.

[80] L. Y. Chan and B. Andrawes, “Characterization of the uncertainties in the constitutive behavior of carbon nanotube/cement composites,” *Sci. Technol. Adv. Mater.*, vol. 10, no. 4, p. 45007, Aug. 2009.

[81] B. Wang, Y. Han, and S. Liu, “Effect of highly dispersed carbon nanotubes on the flexural toughness of cement-based composites,” *Constr. Build. Mater.*, vol. 46, pp. 8–12, Sep. 2013.

[82] M. Saafi, K. Andrew, P. L. Tang, D. McGhon, S. Taylor, M. Rahman, S. Yang, and X. Zhou, “Multifunctional properties of carbon nanotube/fly ash geopolymeric nanocomposites,” *Constr. Build. Mater.*, vol. 49, pp. 46–55, Dec. 2013.

[83] G. Yamamoto, S. Liu, N. Hu, T. Hashida, Y. Liu, C. Yan, Y. Li, H. Cui, H. Ning, and L. Wu, “Prediction of pull-out force of multi-walled carbon nanotube (MWCNT) in sword-in-sheath mode,” *Comput. Mater. Sci.*, vol. 60, pp. 7–12, 2012.

[84] O. Mendoza, G. Sierra, and J. I. Tobón, “Efecto híbrido de los nanotubos de carbono y la nanosilice sobre las propiedades mineralógicas y mecánicas de morteros de cemento Pórtland,” Universidad Nacional de Colombia, 2013.

[85] G. Y. Li, P. M. Wang, and X. Zhao, “Pressure-sensitive properties and microstructure of carbon nanotube reinforced cement composites,” *Cem. Concr. Compos.*, vol. 29, no. 5, pp. 377–382, May 2007.

[86] M. S. Morsy, S. H. Alsayed, and M. Aqel, “Hybrid effect of carbon nanotube and nano-clay on physico-mechanical properties of cement mortar,” *Constr. Build. Mater.*, vol. 25, no. 1, pp. 145–149, Jan. 2011.

[87] Y. Hu, D. Luo, P. Li, Q. Li, and G. Sun, “Fracture toughness enhancement of cement paste with multi-walled carbon nanotubes,” *Constr. Build. Mater.*, vol. 70, pp. 332–338, Nov. 2014.

[88] L. Sorelli, G. Constantinides, F. Ulm, and F. Toutlemonde, “The nano-mechanical signature of Ultra High Performance Concrete by statistical nanoindentation techniques,” *Cem. Concr. Res.*, vol. 38, no. 12, pp. 1447–1456, Dec. 2008.

[89] Q. Li, D. Tang, J. Tang, B. Su, J. Huang, and G. Chen, “Carbon nanotube-based symbiotic coaxial nanocables with nanosilica and nanogold particles as labels for electrochemical immunoassay of carcinoembryonic antigen in biological fluids.,” *Talanta*, vol. 84, no. 2, pp. 538–46, Apr. 2011.

[90] T.-W. Lin and H.-H. Shen, “The synthesis of silica nanotubes through chlorosilanization of single wall carbon nanotubes.,” *Nanotechnology*, vol. 21, no. 36, p. 365604, Sep. 2010.

[91] A. Chaipanich, T. Nochaiya, W. Wongkeo, and P. Torkittikul, “Compressive strength and microstructure of carbon nanotubes–fly ash cement composites,” *Mater. Sci. Eng. A*, vol. 527, no. 4–5, pp. 1063–1067, Feb. 2010.

[92] A. Sobolkina, V. Mechtcherine, C. Bellmann, V. Khavrus, S. Oswald, S. Hampel, and A. Leonhardt, “Surface properties of CNTs and their interaction with silica,” *J. Colloid Interface Sci.*, vol. 413, pp. 43–53, Jan. 2014.

[93] M. Kim, J. Hong, C. K. Hong, and S. E. Shim, “Preparation of silica-layered multi-walled carbon nanotubes activated by grafting of poly(4-vinylpyridine),” *Synth. Met.*, vol. 159, no. 1–2, pp. 62–68, Jan. 2009.

[94] I. W. Nam, H. K. Kim, and H. K. Lee, “Influence of silica fume additions on electromagnetic interference shielding effectiveness of multi-walled carbon nanotube/cement composites,” *Constr. Build. Mater.*, vol. 30, pp. 480–487, May 2012.

[95] H. K. Kim, I. W. Nam, and H. K. Lee, “Enhanced effect of carbon nanotube on mechanical and electrical properties of cement composites by incorporation of silica fume,” *Compos. Struct.*, vol. 107, pp. 60–69, Jan. 2014.

[96] R. Hamzaoui, S. Guessasma, B. Mecheri, A. M. Eshtiaghi, and A. Bennabi, “Microstructure and mechanical performance of modified mortar using hemp fibres and carbon nanotubes,” *Mater. Des.*, vol. 56, pp. 60–68, Apr. 2014.

[97] H. Y. Kordkheili, S. Hiziroglu, and M. Farsi, “Some of the physical and mechanical properties of cement composites manufactured from carbon nanotubes and bagasse fiber,” *Mater. Des.*, vol. 33, pp. 395–398, Jan. 2012.

[98] D. D. L. Chung, “Carbon materials for structural self-sensing, electromagnetic shielding and thermal interfacing,” *Carbon N. Y.*, vol. 50, no. 9, pp. 3342–3353, Aug. 2012.

[99] M. Sun, R. J. Y. Liew, M.-H. Zhang, and W. Li, “Development of cement-based strain sensor for health monitoring of ultra high strength concrete,” *Constr. Build. Mater.*, vol. 65, pp. 630–637, Aug. 2014.

[100] R. a MacDonald, C. M. Voge, M. Kariolis, and J. P. Stegemann, “Carbon nanotubes increase the electrical conductivity of fibroblast-seeded collagen hydrogels.,” *Acta Biomater.*, vol. 4, no. 6, pp. 1583–92, Nov. 2008.

[101] P. Xie, P. Gu, and J. J. Beaudoin, “Electrical percolation phenomena in cement composites containing conductive fibres,” *J. Mater. Sci.*, vol. 31, pp. 4093–4097, 1996.

[102] M. Sun, Q. Liu, Z. Li, and Y. Hu, “A study of piezoelectric properties of carbon fiber reinforced concrete and plain cement paste during dynamic loading,” *Cem. Concr. Res.*, vol. 30, pp. 1593–1595, 2000.

[103] M. S. Konsta-Gdoutos and C. A. Aza, “Self sensing carbon nanotube (CNT) and nanofiber (CNF) cementitious composites for real time damage assessment in smart structures,” *Cem. Concr. Compos.*, vol. 53, pp. 162–169, Oct. 2014.

[104] H. K. Kim, I. S. Park, and H. K. Lee, “Improved piezoresistive sensitivity and stability of CNT/cement mortar composites with low water–binder ratio,” *Compos. Struct.*, vol. 116, pp. 713–719, Sep. 2014.

[105] F. Azhari and N. Banthia, “Cement-based sensors with carbon fibers and carbon nanotubes for piezoresistive sensing,” *Cem. Concr. Compos.*, vol. 34, no. 7, pp. 866–873, Aug. 2012.

[106] B. Han, K. Zhang, X. Yu, E. Kwon, and J. Ou, “Electrical characteristics and pressure-sensitive response measurements of carboxyl MWNT/cement composites,” *Cem. Concr. Compos.*, vol. 34, no. 6, pp. 794–800, Jul. 2012.

[107] D. D. L. Chung, “Piezoresistive Cement-Based Materials for Strain Sensing,” *J. Intell. Mater. Syst. Struct.*, vol. 13, no. 1, pp. 599–609, 2002.

[108] D. Micheli, R. Pastore, a. Vricella, R. B. Morles, M. Marchetti, a. Delfini, F. Moglie, and V. M. Primiani, “Electromagnetic characterization and shielding effectiveness of concrete composite reinforced with carbon nanotubes in the mobile phones frequency band,” *Mater. Sci. Eng. B*, vol. 188, pp. 119–129, Oct. 2014.

[109] W. Supermolecules, “Lead to Super Construction,” no. November, 2008.

[110] B. Han, S. Sun, S. Ding, L. Zhang, X. Yu, and J. Ou, “Review of nanocarbon-engineered multifunctional cementitious composites,” *Compos. Part A Appl. Sci. Manuf.*, vol. 70, pp. 69–81, 2015.

[111] F. J. Baeza, O. Galao, E. Zornoza, and P. Garcés, “Effect of aspect ratio on strain sensing capacity of carbon fiber reinforced cement composites,” *Mater. Des.*, vol. 51, pp. 1085–1094, Oct. 2013.

[112] H. J. Park, M. Park, J. Y. Chang, and H. Lee, “The effect of pre-treatment methods on morphology and size distribution of multi-walled carbon nanotubes.,” *Nanotechnology*, vol. 19, no. 33, p. 335702, Aug. 2008.

[113] S. J. Chen, B. Zou, F. Collins, X. L. Zhao, M. Majumber, and W. H. Duan, “Predicting the influence of ultrasonication energy on the reinforcing efficiency of carbon nanotubes,” *Carbon N. Y.*, Apr. 2014.

[114] B. Krause, M. Mende, P. Pötschke, and G. Petzold, “Dispersability and particle size distribution of CNTs in an aqueous surfactant dispersion as a function of ultrasonic treatment time,” *Carbon N. Y.*, vol. 48, no. 10, pp. 2746–2754, Aug. 2010.

[115] G. Ferro, J. M. Tulliani, A. Lopez, and P. Jagdale, “New cementitious composite building material with enhanced toughness,” *Theor. Appl. Fract. Mech.*, vol. 76, pp. 67–74, 2015.

[116] M. K. Majumder, B. K. Kaushik, and S. K. Manhas, “Performance comparison between single wall carbon nanotube bundle and multiwall carbon nanotube for global interconnects,” *2011 Int. Conf. Emerg. Trends Networks Comput.*

Commun., pp. 104–109, 2011.

[117] B. Scheibe, E. Borowiak-Palen, and R. J. Kalenczuk, "Oxidation and reduction of multiwalled carbon nanotubes — preparation and characterization," *Mater. Charact.*, vol. 61, no. 2, pp. 185–191, Feb. 2010.

[118] H. M. Khater and H. A. Abd El Gawaad, "Characterization of alkali activated geopolymer mortar doped with MWCNT," *Constr. Build. Mater.*, vol. 102, pp. 329–337, 2016.

[119] O. Mendoza, W. Pearl, M. D. M. Paiva, C. Miranda, and R. Toledo Filho, "Effect of a commercial dispersion of multi walled carbon nanotubes on the hydration of an oil well cementing paste," *Front. Struct. Civ. Eng.*, vol. 10, no. 2, pp. 147–179, 2016.

[120] L.-C. Qin, "Determination of the chiral indices (n,m) of carbon nanotubes by electron diffraction.," *Phys. Chem. Chem. Phys.*, vol. 9, no. 1, pp. 31–48, 2007.

[121] P. R. Bandaru, "Electrical Properties and Applications of Carbon Nanotube Structures," *J. Nanosci. Nanotechnol.*, vol. 7, no. 4, pp. 1239–1267, 2007.

[122] N. Braidy, M. El Khakani, and G. Botton, "Single-wall carbon nanotubes synthesis by means of UV laser vaporization," *Chem. Phys. Lett.*, vol. 354, no. 1–2, pp. 88–92, 2002.

[123] Min Feng Yu, B. S., S. Arepalli, and R. S. Ruoff, "Tensile Loading of Ropes of Single Wall Carbon Nanotubes and their Mechanical Properties," *Phys. Rev. Lett.*, vol. 84, p. 5552, 2000.

[124] M. Yu, O. Lourie, M. Dyer, K. Moloni, T. Kelly, and R. R, "Strength and Breaking Mechanism of Multiwalled Carbon Nanotubes Under Tensile Load," *Science (80-.).*, vol. 287, no. 5453, pp. 637–640, 2000.

[125] Z. Tu and Z. Ou-Yang, "Single- and multi-walled carbon nanotubes viewed as elastic tubes with Young's moduli dependent on layer number," vol. 65, p. 4, 2001.

[126] J. Rausch, R.-C. Zhuang, and E. Mäder, "Surfactant assisted dispersion of functionalized multi-walled carbon nanotubes in aqueous media," *Compos. Part A Appl. Sci. Manuf.*, vol. 41, no. 9, pp. 1038–1046, Sep. 2010.

[127] A. Sobolkina, V. Mechtcherine, C. Bellmann, V. Khavrus, S. Oswald, S. Hampel, and A. Leonhardt, "Surface properties of CNTs and their interaction with silica," *J. Colloid Interface Sci.*, vol. 413, pp. 43–53, Jan. 2014.

[128] N. Grossiord, O. Regev, J. Loos, J. Meuldijk, and C. E. Koning, "Time-dependent study of the exfoliation process of carbon nanotubes in aqueous dispersions by using UV-visible spectroscopy.," *Anal. Chem.*, vol. 77, no. 16, pp. 5135–9, Aug. 2005.

[129] Y. Liu, L. Yu, S. Zhang, J. Yuan, L. Shi, and L. Zheng, "Dispersion of multiwalled carbon nanotubes by ionic liquid-type Gemini imidazolium surfactants in aqueous solution," *Colloids Surfaces A Physicochem. Eng. Asp.*, vol. 359, no. 1–3, pp. 66–70, Apr. 2010.

[130] X. Peng, J. Jia, X. Gong, Z. Luan, and B. Fan, "Aqueous stability of oxidized carbon nanotubes and the precipitation by salts," *J. Hazard. Mater.*, vol. 165, no. 1–3, pp. 1239–1242, Jun. 2009.

[131] J. Yu, N. Grossiord, C. Koning, and J. Loos, "Controlling the dispersion of multi-

wall carbon nanotubes in aqueous surfactant solution," *Carbon N. Y.*, vol. 45, no. 3, pp. 618–623, Mar. 2007.

[132] N. Grossiord, P. Van Der Schoot, J. Meuldijk, and C. E. Koning, "Determination of the surface coverage of exfoliated carbon nanotubes by surfactant molecules in aqueous solution.," *Langmuir*, vol. 23, no. 7, pp. 3646–53, Mar. 2007.

[133] Y. Tan and D. E. Resasco, "Dispersion of single-walled carbon nanotubes of narrow diameter distribution.," *J. Phys. Chem. B*, vol. 109, no. 30, pp. 14454–60, Aug. 2005.

[134] P. Alafogianni, K. Dassios, S. Farmaki, S. K. Antiohos, T. E. Matikas, and N.-M. Barkoula, "On the efficiency of UV-vis spectroscopy in assessing the dispersion quality in sonicated aqueous suspensions of carbon nanotubes," *Colloids Surfaces A Physicochem. Eng. Asp.*, 2016.

[135] S. J. Chen, C. Y. Qiu, A. H. Korayem, M. R. Barati, and W. H. Duan, "Agglomeration process of surfactant-dispersed carbon nanotubes in unstable dispersion: A two-stage agglomeration model and experimental evidence," *Powder Technol.*, vol. 301, pp. 412–420, 2016.

[136] B. Han, S. Ding, and X. Yu, "Intrinsic self-sensing concrete and structures: A review," *Measurement*, vol. 59, pp. 110–128, Jan. 2015.

[137] T. Nochaiya and A. Chaipanich, "Behavior of multi-walled carbon nanotubes on the porosity and microstructure of cement-based materials," *Appl. Surf. Sci.*, vol. 257, no. 6, pp. 1941–1945, Jan. 2011.

[138] Z. S. Metaxa, J.-W. T. Seo, M. S. Konsta-Gdoutos, M. C. Hersam, and S. P. Shah, "Highly concentrated carbon nanotube admixture for nano-fiber reinforced cementitious materials," *Cem. Concr. Compos.*, vol. 34, no. 5, pp. 612–617, May 2012.

[139] P. Ludvig, J. M. Calixto, L. O. Ladeira, and I. C. P. Gaspar, "Using Converter Dust to Produce Low Cost Cementitious Composites by in situ Carbon Nanotube and Nanofiber Synthesis," *Materials (Basel).*, vol. 4, no. 12, pp. 575–584, Mar. 2011.

[140] F. Yu, J. Chen, L. Chen, J. Huai, W. Gong, Z. Yuan, J. Wang, and J. Ma, "Magnetic carbon nanotubes synthesis by Fenton's reagent method and their potential application for removal of azo dye from aqueous solution.," *J. Colloid Interface Sci.*, vol. 378, no. 1, pp. 175–83, Jul. 2012.

[141] a Schierz and H. Zänker, "Aqueous suspensions of carbon nanotubes: surface oxidation, colloidal stability and uranium sorption.," *Environ. Pollut.*, vol. 157, no. 4, pp. 1088–94, Apr. 2009.

[142] V. S. Melo, J. M. F. Calixto, L. O. Ladeira, and A. P. Silva, "Macro- and Micro-Characterization of Mortars Produced with Carbon Nanotubes," *ACI Mater. J.*, no. 108, pp. 327–332, 2012.

[143] J. Keriene, M. Kligys, A. Laukaitis, G. Yakovlev, A. Špokauskas, and M. Aleknevičius, "The influence of multi-walled carbon nanotubes additive on properties of non-autoclaved and autoclaved aerated concretes," *Constr. Build. Mater.*, vol. 49, pp. 527–535, 2013.

[144] A. Cwirzen, K. Habermehl-Cwirzen, and V. Penttala, "Surface decoration of carbon nanotubes and mechanical properties of cement/carbon nanotube composites," *Adv. Cem. Res.*, vol. 20, no. 2, pp. 65–73, 2008.

[145] R. Nadiv, G. Vasilyev, M. Shtein, A. Peled, E. Zussman, and O. Regev, "The multiple roles of a dispersant in nanocomposite systems," *Compos. Sci. Technol.*, vol. 133, no. August, pp. 192–199, 2016.

[146] P. Zhao, S. Wang, A. Kadlec, Z. Li, and X. Wang, "Properties of cement–sand-based piezoelectric composites with carbon nanotubes modification," *Ceram. Int.*, 2016.

[147] a. M. Hunashyal, S. V. Tippa, S. S. Quadri, and N. R. Banapurmath, "Experimental Investigation on Effect of Carbon Nanotubes and Carbon Fibres on the Behavior of Plain Cement Mortar Composite Round Bars under Direct Tension," *ISRN Nanotechnol.*, vol. 2011, pp. 1–6, 2011.

[148] B. Zou, S. Jian, A. H. Korayem, F. Collins, and C. M. Wang, "Effect of ultrasonication energy on engineering properties of carbon nanotube reinforced cement pastes," *Carbon N. Y.*, vol. 85, pp. 212–220, 2014.

[149] Y. Yang, E. a. Grulke, Z. G. Zhang, and G. Wu, "Thermal and rheological properties of carbon nanotube-in-oil dispersions," *J. Appl. Phys.*, vol. 99, no. 11, 2006.

[150] M. a. Ahmed, Y. a. Hassanean, K. a. Assaf, S. I. EL-Dek, and M. a. Shawkey, "Piezoelectric response of MWCNTs/cement nanocomposites," *Microelectron. Eng.*, vol. 146, no. April, pp. 53–56, 2015.

[151] R. Nadiv, M. Shtein, M. Refaeli, A. Peled, and O. Regev, "The critical role of nanotube shape in cement composites," *Cem. Concr. Compos.*, vol. 71, no. August, pp. 166–174, 2016.

[152] Z. Chen, J. L. G. Lim, and E.-H. Yang, "Ultra high performance cement-based composites incorporating low dosage of plasma synthesized carbon nanotubes," *Mater. Des.*, vol. 108, pp. 479–487, 2016.

[153] A. Al-Dahawi, O. Öztürk, F. Emami, G. Yildirim, and M. Şahmaran, "Effect of mixing methods on the electrical properties of cementitious composites incorporating different carbon-based materials," *Constr. Build. Mater.*, vol. 104, pp. 160–168, 2016.

[154] G. Yakovlev, G. Yakovlev, J. Keriené, J. Keriené, A. Gailius, A. Gailius, I. Girnienė, and I. Girnienė, "Cement Based Foam Concrete Reinforced by Carbon Nanotubes," *Mater. Sci.*, vol. 12, no. 2, pp. 147–151, 2006.

[155] J. Kerienė, M. Kligys, A. Laukaitis, G. Yakovlev, A. Špokauskas, and M. Aleknevičius, "The influence of multi-walled carbon nanotubes additive on properties of non-autoclaved and autoclaved aerated concretes," *Constr. Build. Mater.*, vol. 49, pp. 527–535, Dec. 2013.

[156] I. K. Tragazikis, K. G. Dassios, D. A. Exarchos, P. T. Dalla, and T. E. Matikas, "Acoustic emission investigation of the mechanical performance of carbon nanotube-modified cement-based mortars," *Constr. Build. Mater.*, vol. 122, pp. 518–524, 2016.

[157] K. Bani-Hani, M. Irshidat, R. K. Abu Al-Rub, N. Al-Nuami, and A. Talleh, "Strength optimisation of mortar with CNTs and nanoclays," *ICE Proc. Struct. Build.*, no. JANUARY, 2016.

[158] J. Bharj, S. Singh, S. Chandler, and R. Singh, "Experimental Study on Compressive Strength of cement-CNT composite paste," *Indian J. Pure Appl. Phys.*, vol. 52, no. January, pp. 35–38, 2014.

[159] M. del C. Camacho, O. Galao, F. J. Baeza, E. Zornoza, and P. Garcés, "Mechanical properties and durability of CNT cement composites," *Materials (Basel).*, vol. 7, no. 3, pp. 1640–1651, 2014.

[160] P. Danoglidis, M. Falara, M. Katotriotou, M. S. Konsta-Gdoutos, and E. Gdoutos, "MWCNT and CNF Cementitious Nanocomposites for Enhanced Strength and Toughness," in *Proceedings of the 2015 SEM Conference on Experimental and Applied Mechanics*, 2015.

[161] P. Hlaváceck and V. Smilauer, "Fracture properties of cementitious composites reinforced with carbon nanofibers/nanotubes," *18th Int. Conf. Eng. Mech. 2012*, pp. 391–397, 2012.

[162] S. P. Shah, M. S. Konsta-Gdoutos, Z. S. Metaxa, and P. Mondal, "Nanoscale modification of cementitious materials," *Nanotechnol. Constr. 3*, pp. 125–130, 2009.

[163] J. Luo, Z. Duan, and H. Li, "The influence of surfactants on the processing of multi-walled carbon nanotubes in reinforced cement matrix composites," *Phys. Status Solidi Appl. Mater. Sci.*, vol. 206, no. 12, pp. 2783–2790, 2009.

[164] A. G. Nasibulin, S. D. Shandakov, L. I. Nasibulina, A. Cwirzen, P. R. Mudimela, K. Habermehl-Cwirzen, D. a. Grishin, Y. V. Gavrilov, J. E. M. Malm, U. Tapper, Y. Tian, V. Penttala, M. J. Karppinen, and E. I. Kauppinen, "A novel cement-based hybrid material," *New J. Phys.*, vol. 11, 2009.

[165] M. Eftekhari and S. Mohammadi, "Molecular dynamics simulation of the nonlinear behavior of the CNT-reinforced calcium silicate hydrate (C – S – H) composite," *Compos. Part A*, vol. 82, pp. 78–87, 2016.

[166] P. Trtik, B. Münch, and P. Lura, "A critical examination of statistical nanoindentation on model materials and hardened cement pastes based on virtual experiments," *Cem. Concr. Compos.*, vol. 31, no. 10, pp. 705–714, Nov. 2009.

[167] P. Lura, P. Trtik, and B. Münch, "Validity of recent approaches for statistical nanoindentation of cement pastes," *Cem. Concr. Compos.*, vol. 33, no. 4, pp. 457–465, Apr. 2011.

[168] Y. Sáez De Ibarra, J. J. Gaitero, E. Erkizia, and I. Campillo, "Atomic force microscopy and nanoindentation of cement pastes with nanotube dispersions," *Phys. Status Solidi Appl. Mater. Sci.*, vol. 203, no. 6, pp. 1076–1081, 2006.

[169] S. P. Shah, P. Hou, and X. Cheng, "Durability of Cement-Based Materials and Nano-particles: A Review," in *Nanotechnology in Construction Proceedings of NICOM5*, 2015, pp. 15–24.

[170] B. Han, Z. Yang, X. Shi, and X. Yu, "Transport properties of carbon-nanotube/cement composites," *J. Mater. Eng. Perform.*, vol. 22, no. 1, pp. 184–189, 2013.

[171] H. Kim, "Chloride penetration monitoring in reinforced concrete structure using carbon nanotube / cement composite," *Constr. Build. Mater.*, vol. 96, pp. 29–36, 2015.

[172] F. J. Baeza, O. Galao, E. Zornoza, and P. Garcés, "Multifunctional cement composites strain and damage sensors applied on reinforced concrete (RC) structural elements," *Materials (Basel).*, vol. 6, no. 3, pp. 841–855, 2013.

[173] D. D. Chung, "Dispersion of Short Fibers in Cement," *J. Mater. Civ. Eng.*, vol.

17, no. August, pp. 379–383, 2005.

[174] A. L. Materazzi, F. Ubertini, and A. D'Alessandro, "Carbon nanotube cement-based transducers for dynamic sensing of strain," *Cem. Concr. Compos.*, vol. 37, no. 1, pp. 2–11, 2013.

[175] J. Chen, D. Zhao, H. Ge, and J. Wang, "Graphene oxide-deposited carbon fiber/cement composites for electromagnetic interference shielding application," *Constr. Build. Mater.*, vol. 84, pp. 66–72, 2015.

[176] R. A. Khushnood, S. Ahmad, P. Savi, J.-M. Tulliani, M. Giorcelli, and G. A. Ferro, "Improvement in electromagnetic interference shielding effectiveness of cement composites using carbonaceous nano/micro inerts," *Constr. Build. Mater.*, vol. 85, pp. 208–216, 2015.

[177] A. D'Alessandro, M. Rallini, F. Ubertini, A. L. Materazzi, and J. M. Kenny, "Investigations on scalable fabrication procedures for self-sensing carbon nanotube cement-matrix composites for SHM applications," *Cem. Concr. Compos.*, vol. 65, pp. 200–213, 2016.

[178] B. Han, X. Yu, and E. Kwon, "A self-sensing carbon nanotube/cement composite for traffic monitoring," *Nanotechnology*, vol. 20, no. 44, p. 445501, 2009.

[179] B. Han, Y. Wang, S. Ding, X. Yu, L. Zhang, Z. Li, and J. Ou, "Self-sensing cementitious composites incorporated with botryoid hybrid nano-carbon materials for smart infrastructures," *J. Intell. Mater. Syst. Struct.*, pp. 1–29, 2016.

[180] M. Saafi, "Wireless and embedded carbon nanotube networks for damage detection in concrete structures.," *Nanotechnology*, vol. 20, no. 39, p. 395502, 2009.

[181] H. Wang, "Dispersing carbon nanotubes using surfactants," *Curr. Opin. Colloid Interface Sci.*, vol. 14, no. 5, pp. 364–371, Oct. 2009.

[182] T. Zhang, S. Shang, F. Yin, a. Aishah, a. Salmiah, and T. L. Ooi, "Adsorptive behavior of surfactants on surface of Portland cement," *Cem. Concr. Res.*, vol. 31, no. 7, pp. 1009–1015, 2001.

[183] Y. Li, H. Zhu, C. Yang, Y. Zhang, J. Xu, and M. Lu, "Synthesis and super retarding performance in cement production of diethanolamine modified lignin surfactant," *Constr. Build. Mater.*, vol. 52, pp. 116–121, 2014.

[184] X. Pang, P. Boontheung, and P. J. Boul, "Dynamic retarder exchange as a trigger for Portland cement hydration," *Cem. Concr. Res.*, vol. 63, pp. 20–28, 2014.

[185] P. F. G. Banfill, "Rheology of Fresh Cement and Concrete," *Rheol. Rev.*, vol. 2006, pp. 61–130, 2006.

[186] F. de Larrard, *Concrete mixture proportioning a scientific approach*, 1st ed. London: E. & F.N. Spon, 1999.

[187] L. Senff, R. C. E. Modolo, D. M. Tobaldi, G. Ascenção, D. Hotza, V. M. Ferreira, and J. A. Labrincha, "The influence of TiO2 nanoparticles and poliacrilonitrile fibers on the rheological behavior and hardened properties of mortars," *Constr. Build. Mater.*, vol. 75, pp. 315–330, 2015.

[188] A. Nazari and S. Riahi, "Al2O3 nanoparticles in concrete and different curing media," *Energy Build.*, vol. 43, no. 6, pp. 1480–1488, 2011.

[189] S. Riahi and A. Nazari, "Physical, mechanical and thermal properties of concrete

in different curing media containing ZnO2 nanoparticles," *Energy Build.*, vol. 43, no. 8, pp. 1977–1984, 2011.

[190] X. Sun, Q. Wu, J. Zhang, Y. Qing, Y. Wu, and S. Lee, "Rheology, curing temperature and mechanical performance of oil well cement: Combined effect of cellulose nanofibers and graphene nano-platelets," *Mater. Des.*, vol. 114, pp. 92–101, 2016.

[191] E. García-Taengua, M. Sonebi, K. M. A. Hossain, M. Lachemi, and J. Khatib, "Effects of the addition of nanosilica on the rheology, hydration and development of the compressive strength of cement mortars," *Compos. Part B Eng.*, vol. 81, pp. 120–129, 2015.

[192] L. Senff, J. A. Labrincha, V. M. Ferreira, D. Hotza, and W. L. Repette, "Effect of nano-silica on rheology and fresh properties of cement pastes and mortars," *Constr. Build. Mater.*, vol. 23, no. 7, pp. 2487–2491, 2009.

[193] S. Kawashima, P. Hou, D. J. Corr, and S. P. Shah, "Modification of cement-based materials with nanoparticles," *Cem. Concr. Compos.*, vol. 36, pp. 8–15, Feb. 2013.

[194] R. Y. Yang, A. B. Yu, S. K. Choi, M. S. Coates, and H. K. Chan, "Agglomeration of fine particles subjected to centripetal compaction," *Powder Technol.*, vol. 184, no. 1, pp. 122–129, 2008.

[195] G. C. Cordeiro, L. M. S. C. De Alvarenga, and C. A. A. Rocha, "Rheological and mechanical properties of concrete containing crushed granite fine aggregate," *Constr. Build. Mater.*, vol. 111, pp. 766–773, 2016.

[196] O. Mendoza and R. Toledo, "Nanotube–Cement Composites," in *Carbon Nanomaterials Sourcebook: Nanoparticles, Nanocapsules, Nanofibers, Nanoporous Structures, and Nanocomposites, VOlume II*, 1st ed., K. Sattler, Ed. Boca Raton: CRC Press, 2016, pp. 573–596.

[197] K. Vance, A. Kumar, G. Sant, and N. Neithalath, "The rheological properties of ternary binders containing Portland cement, limestone, and metakaolin or fly ash," *Cem. Concr. Res.*, vol. 52, pp. 196–207, 2013.

[198] I. Janotka, F. Puertas, M. Palacios, M. Kuliffayová, and C. Varga, "Metakaolin sand-blended-cement pastes: Rheology, hydration process and mechanical properties," *Constr. Build. Mater.*, vol. 24, no. 5, pp. 791–802, 2010.

[199] H. Paiva, A. Velosa, P. Cachim, and V. M. Ferreira, "Effect of metakaolin dispersion on the fresh and hardened state properties of concrete," *Cem. Concr. Res.*, vol. 42, no. 4, pp. 607–612, 2012.

[200] I. P. Sfikas, E. G. Badogiannis, and K. G. Trezos, "Rheology and mechanical characteristics of self-compacting concrete mixtures containing metakaolin," *Constr. Build. Mater.*, vol. 64, pp. 121–129, 2014.

[201] A. K. H. Kwan and Y. Li, "Effects of fly ash microsphere on rheology, adhesiveness and strength of mortar," *Constr. Build. Mater.*, vol. 42, pp. 137–145, 2013.

[202] D. Zheng, D. Wang, D. Li, C. Ren, and W. Tang, "Study of high volume circulating fluidized bed fly ash on rheological properties of the resulting cement paste," *Constr. Build. Mater.*, vol. 135, pp. 86–93, 2017.

[203] S. Kawashima, J. H. Kim, D. J. Corr, and S. P. Shah, "Study of the mechanisms

underlying the fresh-state response of cementitious materials modified with nanoclays," *Constr. Build. Mater.*, vol. 36, pp. 749–757, 2012.

[204] S. Kawashima, M. Chaouche, D. J. Corr, and S. P. Shah, "Rate of thixotropic rebuilding of cement pastes modified with highly purified attapulgite clays," *Cem. Concr. Res.*, vol. 53, pp. 112–118, 2013.

[205] N. a. Tregger, M. E. Pakula, and S. P. Shah, "Influence of clays on the rheology of cement pastes," *Cem. Concr. Res.*, vol. 40, no. 3, pp. 384–391, 2010.

[206] G. Quercia, G. Hüsken, and H. J. H. Brouwers, "Water demand of amorphous nano silica and its impact on the workability of cement paste," *Cem. Concr. Res.*, vol. 42, no. 2, pp. 344–357, Feb. 2012.

[207] O. Mendoza Reales and R. D. Toledo Filho, "Nanotube–Cement Composites," in *Carbon Nanomaterials Sourcebook Nanoparticles, Nanocapsules, Nanofibers, Nanoporous Structures, and Nanocomposites, Volume II*, 1st ed., K. Sattler, Ed. Boca Raton: CRC Press, 2016, pp. 573–596.

[208] G. W. HOLLENBERG, G. R. TERWILLIGER, and R. S. GORDON, "Calculation of Stresses and Strains in Four Point Bending Creep Tests," *J. Am. Ceram. Soc.*, vol. 54, no. 4, pp. 196–199, 1971.

[209] O. Mendoza, W. Pearl, M. D. M. Paiva, C. Miranda, and R. Toledo Filho, "Effect of a commercial dispersion of multi walled carbon nanotubes on the hydration of an oil well cementing paste," *Front. Struct. Civ. Eng.*, vol. In press, pp. 1–6, 2015.

[210] D. A. S. Rambo, Y. Yao, F. de Andrade Silva, R. D. Toledo Filho, and B. Mobasher, "Experimental investigation and modelling of the temperature effects on the tensile behavior of textile reinforced refractory concretes," *Cem. Concr. Compos.*, vol. 75, pp. 51–61, 2017.

[211] O. Mendoza, W. Pearl, M. Paiva, C. Miranda, and R. Toledo, "Effect of a commercial dispersion of multi walled carbon nanotubes on the hydration of an oil well cementing paste," in *Fifth International Symposium on Nanotechnology in Construction*, 2015, pp. 1–8.

[212] H. F. W. Taylor, *Cement chemistry*. London: Thomas Telford Services Ltd, 1997.

[213] C.-W. Lam, J. T. James, R. McCluskey, S. Arepalli, and R. L. Hunter, "A review of carbon nanotube toxicity and assessment of potential occupational and environmental health risks," *Crit. Rev. Toxicol.*, vol. 36, no. 3, pp. 189–217, 2006.

[214] O. Mendoza, W. Pearl, M. D. M. Paiva, C. R. Miranda, and R. Toledo Filho, "Adsorption of surfactant by nanosilica particles in carbon nanotubes / water dispersions : application in a cement matrix," in *Proceedings of the 14th International Congress on the Chemistry of Cement*, 2015, pp. 1–8.

[215] D. Lin, N. Liu, K. Yang, B. Xing, and F. Wu, "Different stabilities of multiwalled carbon nanotubes in fresh surface water samples," *Environ. Pollut.*, vol. 158, no. 5, pp. 1270–1274, 2010.

[216] K. L. Scrivener, P. Juilland, and P. J. M. Monteiro, "Advances in understanding hydration of Portland cement," *Cem. Concr. Res.*, vol. 78, pp. 38–56, 2015.

[217] H. Kuzel, "Initial Hvdration Reactions and Mechanisms of Delayed-Ettringite Formation in Portland Cements," *Cem. Concr. Compos.*, vol. 18, pp. 195–203,

1996.

[218] J. Zhang, L. Qin, and Z. Li, “Hydration monitoring of cement-based materials with resistivity and ultrasonic methods,” *Mater. Struct.*, vol. 42, no. 1, pp. 15–24, 2009.

[219] G. Sant, M. Dehadrai, D. Bentz, P. Lura, C. F. Ferraris, J. W. Bullard, and J. Weiss, “Detecting the fluid-to-solid transition in cement pastes,” *Concr. Int.*, vol. 236, no. june, pp. 53–58, 2009.

[220] J. Zhang, E. a. Weissinger, S. Peethamparan, and G. W. Scherer, “Early hydration and setting of oil well cement,” *Cem. Concr. Res.*, vol. 40, no. 7, pp. 1023–1033, 2010.

[221] J. Rausch, R.-C. Zhuang, and E. Mäder, “Surfactant assisted dispersion of functionalized multi-walled carbon nanotubes in aqueous media,” *Compos. Part A Appl. Sci. Manuf.*, vol. 41, no. 9, pp. 1038–1046, Sep. 2010.

[222] M. Liebscher, A. Lange, C. Schröfl, R. Fuge, V. Mechtcherine, J. Plank, and A. Leonhardt, “Impact of the molecular architecture of polycarboxylate superplasticizers on the dispersion of multi-walled carbon nanotubes in aqueous phase,” *J. Mater. Sci.*, vol. 52, no. 4, pp. 2296–2307, 2017.

[223] R. Rastogi, R. Kaushal, S. K. Tripathi, A. L. Sharma, I. Kaur, and L. M. Bharadwaj, “Comparative study of carbon nanotube dispersion using surfactants,” *J. Colloid Interface Sci.*, vol. 328, no. 2, pp. 421–428, 2008.

[224] S. Srinivasan, S. a. Barbhuiya, D. Charan, and S. P. Pandey, “Characterising cement–superplasticiser interaction using zeta potential measurements,” *Constr. Build. Mater.*, vol. 24, no. 12, pp. 2517–2521, Dec. 2010.

[225] H. Uchikawa, S. Hanehara, and D. Sawaki, “The role of steric repulsive force in the dispersion of cement particles in fresh paste prepared with organic admixture,” *Cem. Concr. Res.*, vol. 27, no. 1, pp. 37–50, 1997.

[226] R. Zhang and P. Somasundaran, “Advances in adsorption of surfactants and their mixtures at solid/solution interfaces,” *Adv. Colloid Interface Sci.*, vol. 123–126, no. SPEC. ISS., pp. 213–229, 2006.

[227] M. D. Clark, S. Subramanian, and R. Krishnamoorti, “Understanding surfactant aided aqueous dispersion of multi-walled carbon nanotubes,” *J. Colloid Interface Sci.*, vol. 354, no. 1, pp. 144–151, 2011.

[228] W. R. Jung, J. H. Choi, N. Lee, K. Shin, J.-H. Moon, and Y.-S. Seo, “Reduced damage to carbon nanotubes during ultrasound-assisted dispersion as a result of supercritical-fluid treatment,” *Carbon N. Y.*, vol. 50, no. 2, pp. 633–636, Feb. 2012.

[229] Y. Bai, I. S. Park, S. J. Lee, T. S. Bae, F. Watari, M. Uo, and M. H. Lee, “Aqueous dispersion of surfactant-modified multiwalled carbon nanotubes and their application as an antibacterial agent,” *Carbon N. Y.*, vol. 49, no. 11, pp. 3663–3671, Sep. 2011.

[230] P. Kumar and H. B. Bohidar, “Aqueous dispersion stability of multi-carbon nanoparticles in anionic, cationic, neutral, bile salt and pulmonary surfactant solutions,” *Colloids Surfaces A Physicochem. Eng. Asp.*, vol. 361, no. 1–3, pp. 13–24, May 2010.

[231] R. M. F. Fernandes, M. Buzaglo, M. Shtein, I. Pri Bar, O. Regev, E. F. Marques,

and I. Furó, “Lateral diffusion of dispersing molecules on nanotubes as probed by NMR,” *J. Phys. Chem. C*, vol. 118, no. 1, pp. 582–589, 2014.

[232] H. Hodne and A. Saasen, “Rheological Properties of the Silica phases in Clinker slurries,” *Annu. Trans. Nord. Rheol. Soc.*, vol. 11, no. 4068, pp. 2–5, 2003.

[233] C. M. Neubauer, M. Yang, and H. M. Jennings, “Interparticle Potential and Sedimentation Behavior of Cement Suspensions: Effects of Admixtures,” *Adv. Cem. Based Mater.*, vol. 8, no. 1, pp. 17–27, Jul. 1998.

[234] O. Mendoza, Y. Arias, C. Delgado, J. Ochoa, J. Quintero, and R. Toledo, “Dispersion of carbon nanotubes by anionic, cationic and amphoteric surfactants assited by ultrassound,” Rio de Janeiro, 2017.

[235] K. L. Scrivener and A. Nonat, “Hydration of cementitious materials, present and future,” *Cem. Concr. Res.*, vol. 41, no. 7, pp. 651–665, 2011.

[236] H. Minard, S. Garrault, L. Regnaud, and A. Nonat, “Mechanisms and parameters controlling the tricalcium aluminate reactivity in the presence of gypsum,” *Cem. Concr. Res.*, vol. 37, no. 10, pp. 1418–1426, 2007.

[237] T. Matschei, B. Lothenbach, and F. P. Glasser, “The AFm phase in Portland cement,” *Cem. Concr. Res.*, vol. 37, no. 2, pp. 118–130, 2007.

[238] A. Quennoz and K. L. Scrivener, “Cement and Concrete Research Hydration of C 3 A – gypsum systems,” *Cem. Concr. Res.*, vol. 42, no. 7, pp. 1032–1041, 2012.

[239] T. Sievert, A. Wolter, and N. B. Singh, “Hydration of anhydrite of gypsum (CaSO4.II) in a ball mill,” *Cem. Concr. Res.*, vol. 35, no. 4, pp. 623–630, 2005.

[240] T. Yuehua Yuan and R. Lee, “Contact Angle and Wetting Properties,” in *Springer Series in Surface Sciences*, 1st ed., vol. 51, no. 1, G. Bracco and B. Holst, Eds. Heidelberg: Springer Berlin Heidelberg, 2013.

[241] K. Yoshioka, E. Tazawa, K. Kawai, and T. Enohata, “Adsorption characteristics of superplasticizers on cement component minerals,” *Cem. Concr. Res.*, vol. 32, no. 10, pp. 1507–1513, Oct. 2002.

[242] R. Nadiv, G. Vasilyev, M. Shtein, A. Peled, E. Zussman, and O. Regev, “The multiple roles of a dispersant in nanocomposite systems,” *Compos. Sci. Technol.*, vol. 133, pp. 192–199, 2016.

[243] A. Saasen, J. O. Haugom, and E. Johansen, “The Effect of Gypsum and Anhydrite on Rheological Properties of Cement Slurries,” *Annual Transactions of the Nordic Rheology Society*, vol. 2. 1994.

[244] X. Zhang and J. Han, “The effect of ultra-fine admixture on the rheological property of cement paste,” *Cem. Concr. Res.*, vol. 30, no. 5, pp. 827–830, 2000.

[245] W. Berg, “Influence of specific surface and concentration of solids upon the flow behaviour of cement pastes,” *Mag. Concr. Res.*, vol. 31, no. 109, pp. 211–216, 1979.

[246] S. Parveen, S. Rana, R. Fangueiro, and M. C. Paiva, “Microstructure and mechanical properties of carbon nanotube reinforced cementitious composites developed using a novel dispersion technique,” *Cem. Concr. Res.*, vol. 73, pp. 215–227, 2015.

[247] F. Torabian Isfahani, W. Li, and E. Redaelli, “Dispersion of multi-walled carbon

nanotubes and its effects on the properties of cement composites," *Cem. Concr. Compos.*, vol. 74, no. October, pp. 154–163, 2016.

[248] RILEM TC 162-TDF, "Recommendations of RILEM TC 162-TDF: Test and design methods for steel fibre reinforced concrete: bending test," *Mater. Struct.*, vol. 35, no. 253, pp. 579–582, 2002.

[249] Y. Jenq and S. P. Shah, "Two parameter fracture model for concrete," *J. Eng. Mech.*, vol. 111, no. 10, pp. 1227–1241, 1985.

[250] A. Spagnoli, A. Carpinteri, and S. Vantadori, "Interpretin experimental fracture toughness results of quasi-brittle natural materials through multi-parameter approaches," *Frat. ed Integrità Strutt.*, vol. 33, pp. 80–88, 2015.

[251] A. Ramachandra, VS Paroli, RM Beaduoin, J Delgado, *Handbook of Thermal Analysis of Construction Materials*, 1st ed. New York: Noyes Publications, 2002.